Partially Composite Supersymmetry

a dissertation
submitted to the faculty of the
University of Minnesota
by

Andrew Stephen Miller

in partial fulfillment of the requirements
for the degree of
Doctor of Philosophy

Advisor: Tony Gherghetta

July 2020

Acknowledgments

In the list of those whose shoulders I have stood upon to write this dissertation, I place first my father, Stephen Miller, who instilled in me an early interest in science and gave me the tools to further it. Next come Professors Richard Olenick and Sally Hicks of the University of Dallas, who introduced me to physics as a discipline and whose deep love of their work and dedication to their students inspired me to pursue a graduate degree. And finally, I am grateful to my advisor, Professor Tony Gherghetta, for his generous support and patient encouragement during my time as a graduate student. It has been an honor to work with him, and I have invariably found his insight helpful, thoughtful, and wise. I could have asked for no better mentor. I have also profited greatly from my many interactions with the other members of the School of Physics and Astronomy of the University of Minnesota, in particular the faculty from whom I learned and with whom I taught and the graduate students and postdocs of the High Energy Theory Journal Club.

On the domestic front, I am greatly indebted to my parents, who have unhesitatingly provided support and encouragement to me throughout my education, and, most of all, to my wife, Chelsea, who embarked with me on this project when the end was not in sight, and helped me see it through regardless, admitting no impediments.

For Chelsea

Abstract

This dissertation presents the model of partially composite supersymmetry, constructed in a slice of five-dimensional anti-de Sitter spacetime (AdS_5). The Higgs fields are localized on the ultraviolet (UV) brane, while supersymmetry is broken on the infrared (IR) brane. The remainder of the field content of the minimal supersymmetric standard model (MSSM) is embedded into the five-dimensional (5D) bulk. The localizations of the bulk fields that are responsible for generating the fermion mass hierarchy simultaneously cause the first- and second-generation sfermions to be split from the lighter gauginos and third-generation sfermions. The sfermion mass scale is constrained by the observed 125 GeV Higgs boson, leading to stop masses and gauginos around 10–100 TeV and the first two generation sfermion masses around 100–1000 TeV. This gives rise to a splitlike supersymmetric model that explains the fermion mass hierarchy while simultaneously predicting an inverted sfermion mass spectrum consistent with direct-detection and flavor constraints. The lightest supersymmetric particle is a gravitino, in the keV to TeV range, which can play the role of dark matter. According to the AdS/CFT correspondence, this model has a dual description as a four-dimensional (4D) strongly coupled theory of supersymmetric partial compositeness.

The analytic portion of this dissertation concerns the detailed construction of the five-dimensional formalism. The effective four-dimensional Yukawa couplings are extracted from the 5D theory in the zero-mode approximation, and an analytic expansion for the fermion masses and mixing parameters in terms of the fermion zero-mode profiles is provided. In order to provide a full numeric solution, the fermion masses and mixing parameters are extracted from low-energy experimental data and evolved to the IR-brane scale, where the four-dimensional MSSM is matched to the five-dimensional theory. 5D Yukawa coupling matrix elements and bulk field localizations are determined by a numeric fit to the 4D parameters. The resulting flavor solutions dictate the structure of supersymmetry breaking on the IR brane for the sfermions, the Higgs sector, and the soft trilinear scalar couplings.

An analysis of supersymmetry breaking on the IR brane is given at tree level for the gravitino, the gauginos, and the sfermions. In order to construct a one-loop analysis, the propagators for bulk fields are constructed, both in the supersymmetric limit and in the presence of supersymmetry-breaking boundary conditions on the IR brane. In particular, the propagator matrix for a family of bulk scalar fields is obtained in the case that the IR-brane boundary mass term is not diagonal in the bulk mass basis. These results are used to calculate one-loop radiative corrections to bulk and boundary scalar fields as well as the Higgs b term and the soft trilinear scalar couplings arising from the supersymmetry

breaking on the IR brane. These corrections are shown to provide the dominant soft mass contributions for UV-localized scalars fields and transmit supersymmetry breaking to the Higgs sector, which is protected at tree-level by its finite separation from the IR brane.

In the phenomenological portion of this dissertation, constraints arising from dark matter cosmology, experimental limits on flavor-changing neutral currents and CP violation, and the 125 GeV Higgs mass and current lower bounds on sparticle masses from the Large Hadron Collider (LHC) are applied to the parameter space of the model. Additional theoretical considerations are developed, including an analysis of the tachyonic constraints on sfermion mass hierarchies induced by large radiative corrections in the bulk theory and in the MSSM. The viable parameter space of the model is then identified out of the collection of all constraints, and two benchmark parameter space points are selected for analysis.

The numeric portion of this dissertation presents a spectrum calculation and analysis for these points. This analysis gives the first results for the partially composite model of supersymmetry that are compatible with the 125 GeV, current LHC limits, and flavor constraints. This intricate connection between the fermion and sfermion mass spectrum can be tested at future experiments.

Contents

List of Figures

List of Tables

1 Introduction

The standard model of particle physics (SM) is the most fundamental theory of nature known to modern physics. It provides a framework for understanding the subatomic world, describing the interactions of all observed subatomic particles under all fundamental forces apart from gravity. As a theory, the standard model grew out of several separate research programs in the latter half of the twentieth century. Although its conceptual roots can easily be traced back to the beginning of the century in covariant construction of classical electrodynamics provided by the special theory of relativity and in the development of quantum theory, its more direct theoretical antecedents lie in the formulation of quantum electrodynamics (QED) as an abelian gauge theory and its extension to nonabelian groups, which allowed the unification of electromagnetism with the weak force [1–3]. This was supplemented by the discovery of strong interactions and asymptotic freedom [4–7], such that by the mid 1970s, the standard model attained its current theoretical structure as a theory of the electroweak and strong forces with three generations of leptons and quarks, although several of the particles it predicted still awaited empirical observation. There followed a concerted experimental effort, leading in its course to the discoveries of the bottom quark in 1977 [8], the top quark in 1995 [9, 10], the tau neutrino in 2000 [11], and, ultimately, in the Higgs boson in 2012 [12, 13].

The discovery of the Higgs boson is widely considered to have completed the standard model. Nevertheless, the theory as it stands is necessarily incomplete as a complete description of nature, as it leaves unexplained a variety of physical phenomena, most notably gravity, dark matter, and the origin of the neutrino masses, as well as several deep theoretical questions about the shape of physics at higher energies, such as the origin of the fermion mass hierarchy, the stabilization of the electroweak scale, and the prospect of grand unification. Among numerous possible extensions of the standard model, one of the more popular is supersymmetry (SUSY), which offers, among other advantages, a natural dark matter candidate, improved prospects of gauge coupling unification, a solution to the hierarchy problem, and the unification of gravity with the other forces. The recent discovery of the Higgs boson at the LHC has led to new constraints on supersymmetric theories. To explain

a 125 GeV Higgs mass, top quark superpartners (stops) must have masses on the order of 10–100 TeV. Further, the additional couplings and degrees of freedom introduced in supersymmetry can, in the absence of some additional suppression mechanism, generate flavor-changing neutral currents and CP-violation at levels above current experimental limits, unless the masses of the first- and second- generation sfermions are above 100 TeV. Simultaneously satisfying these two constraints most naturally results in a split sfermion mass spectrum with lighter stops and heavier selectrons that mirrors (inverts) the ordering of the spectrum of fermions in the standard model. This raises the question of whether the hierarchies in both spectra are related and can be explained by the same mechanism.

Precisely such a connection can be realized naturally in the context of theories of warped extra dimensions, which are able give a natural explanation for large hierarchies in scale, such as those arising in the structure of the standard model fermion masses and mixing angles [14–16]. In this dissertation, we investigate a model of supersymmetry in five dimensions, where the extra dimension is compactified on an orbifold, and the bulk geometry is a slice of anti-de Sitter (AdS_5) spacetime partially composite supersymmetry [17, 18]. Due to the curvature of the spacetime, the bulk fields have exponential wave function profiles over the extra dimension that can be used to explain the fermion mass hierarchy. In our supersymmetric context, generating the fermion mass hierarchy in this way simultaneously causes the first- and second-generation sfermions to be split from the lighter gauginos and third-generation sfermions. According to the AdS/CFT correspondence, this theory has a dual description as a four-dimensional strongly coupled large-N gauge theory. The gravitational background of the five-dimensional description models this strong dynamics. In light of the Higgs boson discovery, this enables us to obtain specific quantitative predictions for the sparticle spectrum that can then be used to help guide future experimental searches.

We structure this dissertation as follows. In Chapter 2, the standard model is outlined, and several of its shortcomings are discussed. This motivates a review of supersymmetry, with a focus on the minimal supersymmetric standard model (MSSM). The 125 GeV Higgs mass, the current superpartner mass limits from the Large Hadron Collider (LHC), and the supersymmetric flavor problem suggest a split supersymmetric spectrum. We locate the theory of partially composite supersymmetry within this context as a solution providing a deep connection between the flavor physics of the standard model and the breaking of supersymmetry, simultaneously able to explain the fermion mass hierarchy and generate a phenomenologically indicated sfermion mass hierarchy.

Chapter 3 then introduces the formalism of the five-dimensional (5D) model of partially

composite supersymmetry. We discuss extensions of the standard model to extra dimensions in general, before specializing to the warped background of a slice of AdS_5. After giving a construction of the MSSM in this spacetime, we turn to the AdS/CFT correspondence and give a review of the four-dimensional (4D) dual theory.

In order to make quantitative predictions from this model, we develop the theory of flavor physics in the extra dimension in Chapter 4. We work within the zero-mode approximation to provide matching relations between the fermion masses and mixings of the SM and MSSM and the Yukawa couplings and bulk field localizations of the 5D theory. We discuss the extraction of the four-dimensional flavor observables from low-energy experimental data and their evolution up to the IR-brane mass scale where the matching occurs. By means of a hierarchical approximation, analytic expressions for the 4D fermion masses and mixing parameters can be given in terms of the fermion zero-mode profiles. We supplement this with the procedure for a full numerical χ^2 fit of the 5D parameters to the 4D observables.

This is followed in Chapter 5 by a discussion of supersymmetry breaking on the IR brane, which we parametrize through the introduction of spurion. We give the tree-level results for the gravitino, the gauginos, and the sfermions, before presenting the full one-loop contributions from the bulk. Because the Higgs sector is localized on the UV brane, the Higgs soft terms and the soft trilinear scalar couplings are protected from supersymmetry breaking at tree level but receive soft masses at loop level. Additionally, the tree-level masses for UV-localized scalars are exponentially suppressed, so loop corrections cannot be neglected.

Chapters 6 and 7 provide the technical details that support the calculation of the one-loop radiative corrections to the sfermion soft masses, the Higgs soft masses, and the soft trilinear scalar couplings presented in Chapter 5. Chapter 6 is a catalog of the bulk propagators for the component fields matter hypermultiplets and vector supermultiplets. For the first time we calculate the propagator matrix for a family of bulk scalar fields with exact dependence on an IR-brane mass matrix. These expressions are used in Chapter 7, where we calculate one-loop radiative corrections to bulk and boundary scalar fields as well as the Higgs b term and the soft trilinear scalar couplings arising from the supersymmetry breaking on the IR brane.

Phenomenological implications from the results derived in Chapters 4 and 7 are discussed in Chapter 8. We investigate constraints arising from dark matter cosmology, experimental limits on flavor-changing neutral currents and CP violation, and the 125 GeV Higgs mass and current lower bounds on sparticle masses from the Large Hadron Collider (LHC), as

well as theoretical considerations such as gauge coupling unification and an analysis of the tachyonic constraints on sfermion mass hierarchies induced by large radiative corrections in the bulk theory and in the MSSM. We summarize the constraints on the parameter space for two cases, one in which the supersymmetry-breaking spurion is a singlet and another in which it is not a singlet, selecting two benchmark points for analysis.

These analyses are presented in Chapter 9, along with a description of the renormalization procedure within the MSSM which we use to calculate the pole mass spectra. The main results of this dissertation are summarized in the final section, Chapter 10, giving our outlook and conclusions.

In the appendices, we review some background material and establish notation. The structure of spinors is documented in Appendix A. Field theory in the AdS_5 bulk is discussed in some detail in Appendix B, for scalars, Dirac and symplectic Majorana spinors, gauge fields, and the graviton and gravitino. In Appendix C, we provide analytic approximations for the zero-mode masses for scalar and fermion bulk fields in the presence of arbitrary boundary mass terms, as well as two different approximation schemes for heavier Kaluza-Klein spectra. Finally, in Appendix D, we give an overview of the multiplet structure of $\mathcal{N} = 1$ 5D supersymmetry.

2 The Standard Model and Supersymmetry

In this chapter we present the basic formalism of the standard model of particle physics and identify several of the theoretical and observational issues that suggest the need for physics *beyond the standard model* (BSM) and give clues to the new structure that may arise at higher energies. We then discuss the minimal supersymmetry extension of the standard model and review the phenomenological arguments for a split superpartner spectrum and a connection between supersymmetry breaking and flavor. With this motivation, we introduce in the last section the theory of partially composite supersymmetry, which provides a natural explanation for the fermion mass hierarchy and generates as a consequence an inverted sfermion hierarchy.

2.1 The Standard Model and Its Discontents

2.1.1 The standard model of particle physics

We first give a brief overview of the structure of the standard model of particle physics. It is beyond the scope of the current discussion to give a thorough exploration of the subtleties of the theory, but a wide variety of pedagogical treatments of the topic are available. In particular, we recommend Ref. [19], which uses the same mostly positive metric signature convention that we employ here.[1]

[1] That is, we take the Minkowski metric to be defined

$$\eta^{\mu\nu} = \mathrm{diag}(-1, +1, +1, +1)\,. \tag{2.1}$$

Note that with this sign convention,

$$\partial_\mu \equiv \frac{\partial}{\partial x^\mu} = \left(+\frac{1}{c}\frac{\partial}{\partial t}, \nabla_i\right)\,, \tag{2.2a}$$

$$\partial^\mu \equiv \frac{\partial}{\partial x_\mu} = \left(-\frac{1}{c}\frac{\partial}{\partial t}, \nabla_i\right)\,, \tag{2.2b}$$

such that

$$\partial^2 \equiv g^{\mu\nu}\partial_\mu\partial_\nu = -\frac{1}{c^2}\frac{\partial^2}{\partial^2 t} + \nabla^2\,. \tag{2.3}$$

The standard model may be formulated as a gauge theory of the product group

$$\mathcal{G}_{\text{SM}} = \text{SU}(3)_c \times \text{SU}(2)_L \times \text{U}(1)_Y \tag{2.6}$$

with three generations of matter, spontaneously broken to $\text{SU}(3)_c \times \text{U}(1)_{\text{EM}}$ by the Higgs mechanism. Here, $\text{SU}(3)_c$ is the color gauge symmetry of quantum chromodynamics, while $\text{SU}(2)_L \times \text{U}(1)_Y$ is the weak isospin-hypercharge product group. After spontaneous symmetry breaking, the remaining $\text{U}(1)_{\text{EM}}$ is the gauge symmetry of electromagnetism. The field content of the standard model is shown in Table 2.1. Note that we use the convention in which all fermions are defined as left-handed Weyl spinors.

The gauge symmetry (2.6), together with the requirements of Poincaré invariance, unitarity, causality, stability, and renormalizability completely determine the standard model Lagrangian, which can be written in the form

$$\mathcal{L}_{\text{SM}} = \mathcal{L}_{\text{fermion}} + \mathcal{L}_{\text{gauge}} + \mathcal{L}_{\text{Higgs}} + \mathcal{L}_{\text{Yukawa}} \,. \tag{2.7}$$

Here, we briefly discuss each term.

Fermion sector

For the fermions, the different gauge eigenstates are referred to as *flavors*. They can be naturally organized in to three *families* or *generations*, which sort particles with the same quantum numbers in order of increasing mass, and divided into two classes, the *colorful* quarks and the *colorless* leptons, distinguished by their representations under the color group $\text{SU}(3)_c$. We also note that the standard model gauge theory is *chiral* theory: particles of difference handedness transform in different representations of the gauge group $\mathcal{G}_{\text{SM}}$. The

---

The momentum is defined in the quantum mechanical convention as

$$p_\mu \equiv -i\partial_\mu = (-E, p_i) \,, \tag{2.4a}$$

$$p^\mu \equiv -i\partial^\mu = (+E, p_i) \,, \tag{2.4b}$$

such that a massive particle has

$$p^2 = g^{\mu\nu} p_\mu p_\nu = -m^2 = -\partial^2 \,. \tag{2.5}$$

Table 2.1: Field content of the standard model.

		representation			
	field	$SU(3)_c$	$SU(2)_L$	$U(1)_Y$	spin
B	weak hypercharge gauge boson	**1**	**1**	0	1
W	weak isospin gauge bosons	**1**	**3**	0	1
g	gluons	**8**	**1**	0	1
Q_1	first-generation quark doublet	**3**	**2**	$+\frac{1}{6}$	$\frac{1}{2}$
$\bar{u}_R$	right-handed up antiquarks	$\overline{\mathbf{3}}$	**1**	$-\frac{2}{3}$	$\frac{1}{2}$
$\bar{d}_R$	right-handed down antiquarks	$\overline{\mathbf{3}}$	**1**	$+\frac{1}{3}$	$\frac{1}{2}$
L_1	first-generation lepton doublet	**1**	**2**	$-\frac{1}{2}$	$\frac{1}{2}$
$\bar{e}_R$	right-handed antielectron	**1**	**1**	$+1$	$\frac{1}{2}$
Q_2	second-generation quark doublet	**3**	**2**	$+\frac{1}{6}$	$\frac{1}{2}$
$\bar{c}_R$	right-handed charm antiquarks	$\overline{\mathbf{3}}$	**1**	$-\frac{2}{3}$	$\frac{1}{2}$
$\bar{s}_R$	right-handed strange antiquarks	$\overline{\mathbf{3}}$	**1**	$+\frac{1}{3}$	$\frac{1}{2}$
L_2	second-generation lepton doublet	**1**	**2**	$-\frac{1}{2}$	$\frac{1}{2}$
$\bar{\mu}_R$	right-handed antimuon	**1**	**1**	$+1$	$\frac{1}{2}$
Q_3	third-generation quark doublet	**3**	**2**	$+\frac{1}{6}$	$\frac{1}{2}$
$\bar{t}_R$	right-handed top antiquarks	$\overline{\mathbf{3}}$	**1**	$-\frac{2}{3}$	$\frac{1}{2}$
$\bar{b}_R$	right-handed bottom antiquarks	$\overline{\mathbf{3}}$	**1**	$+\frac{1}{3}$	$\frac{1}{2}$
L_3	third-generation lepton doublet	**1**	**2**	$-\frac{1}{2}$	$\frac{1}{2}$
$\bar{\tau}_R$	right-handed tau antilepton	**1**	**1**	$+1$	$\frac{1}{2}$
H	Higgs doublet	**1**	**2**	$+\frac{1}{2}$	0

left-handed components of the fermions transform as doublets under $\mathrm{SU}(2)_L$,

$$Q_1 = \begin{pmatrix} u_L \\ d_L \end{pmatrix}, \qquad Q_2 = \begin{pmatrix} c_L \\ s_L \end{pmatrix}, \qquad Q_3 = \begin{pmatrix} t_L \\ b_L \end{pmatrix}, \tag{2.8a}$$

$$L_1 = \begin{pmatrix} \nu_{eL} \\ e_L \end{pmatrix}, \qquad L_2 = \begin{pmatrix} \nu_{\mu L} \\ \mu_L \end{pmatrix}, \qquad L_3 = \begin{pmatrix} \nu_{\tau L} \\ \tau_L \end{pmatrix}, \tag{2.8b}$$

while the right-handed components transform as singlets. If right-handed neutrinos exist, they transform as singlets under the entire standard model gauge group.

The fermion Lagrangian contains kinetic terms of the form

$$\mathcal{L}_{\text{fermion}} = \sum_{\psi} i\psi^\dagger \bar{\sigma}^\mu D_\mu \psi \,, \tag{2.9}$$

where $\bar{\sigma}^\mu$ is defined in (A.16) and the sum is over all the fermion gauge multiplets. The covariant derivative is defined as

$$D_\mu = \partial_\mu - i g_s G_\mu^a \frac{t^a}{2} - i g\, W_\mu^i \frac{\sigma^i}{2} - i g' B_\mu Y \,, \tag{2.10}$$

where g_s, g, and g' are the coupling constants of the $\mathrm{SU}(3)_c$, $\mathrm{SU}(2)_L$, and $\mathrm{U}(1)_Y$ subgroups, respectively, and the associated group generators are given by the Gell-Mann matrices t^a, the Pauli matrices σ^i (A.17), and the hypercharge Y.

The fermions can be written as vectors in family space. This is already suggested by the notation for the doublets Q_i and L_i. For the singlets, we take

$$\overline{\boldsymbol{u}} = \begin{pmatrix} \bar{u}_R \\ \bar{c}_R \\ \bar{t}_R \end{pmatrix}, \qquad \overline{\boldsymbol{d}} = \begin{pmatrix} \bar{d}_R \\ \bar{s}_R \\ \bar{b}_R \end{pmatrix}, \qquad \overline{\boldsymbol{e}} = \begin{pmatrix} \bar{e}_R \\ \bar{\mu}_R \\ \bar{\tau}_R \end{pmatrix}, \tag{2.11}$$

in which case,

$$\begin{aligned} \mathcal{L}_{\text{fermion}} = {} & i Q_i^\dagger \bar{\sigma}^\mu \left(D_\mu\right)_{ij} Q_j \\ & + i \bar{u}_i^\dagger \bar{\sigma}^\mu \left(D_\mu\right)_{ij} \bar{u}_j + i \bar{d}_i^\dagger \bar{\sigma}^\mu \left(D_\mu\right)_{ij} \bar{d}_j \\ & + i L_i^\dagger \bar{\sigma}^\mu \left(D_\mu\right)_{ij} L_j + i \bar{e}_i^\dagger \bar{\sigma}^\mu \left(D_\mu\right)_{ij} \bar{e}_j \,. \end{aligned} \tag{2.12}$$

The basis in family space in which the covariant derivatives are diagonal defines the *gauge-eigenstate basis* or the *interaction basis*.

Gauge sector

The gauge sector Lagrangian contains the kinetic terms of the gauge bosons as well as gauge-fixing and Faddeev-Poppov ghost Lagrangians:

$$\mathcal{L}_{\text{gauge}} = -\frac{1}{4}G^a_{\mu\nu}G^{a\mu\nu} - \frac{1}{4}W^i_{\mu\nu}W^{i\mu\nu} - \frac{1}{4}B_{\mu\nu}B^{\mu\nu} + \mathcal{L}_{\text{GF}} + \mathcal{L}_{\text{FP}}\,, \tag{2.13}$$

where the field strength tensors of the gauge fields take the form in the interaction basis

$$G^a_{\mu\nu} = \partial_\mu G^a_\nu - \partial_\nu G^a_\mu + g_s f^{abc} G^b_\mu G^c_\nu\,, \tag{2.14a}$$

$$W^i_{\mu\nu} = \partial_\mu W^i_\nu - \partial_\nu W^i_\mu + g\,\varepsilon^{ijk} W^j_\mu W^k_\nu\,, \tag{2.14b}$$

$$B_{\mu\nu} = \partial_\mu B^i_\nu - \partial_\nu B^i_\mu\,. \tag{2.14c}$$

Here, the f^{abc} and ε^{ijk} are the structure constants of $\mathrm{SU}(3)_c$ and $\mathrm{SU}(2)_L$, respectively.

Higgs sector

The Higgs doublet contains two complex scalar fields, and can be decomposed as

$$H = \frac{1}{\sqrt{2}}\begin{pmatrix} \sqrt{2}\,h^+ \\ h^0 + ia^0 \end{pmatrix}\,, \tag{2.15}$$

where $h^\pm$ is a complex charged scalar field, h^0 is a neutral CP-even scalar field, and a^0 is a neutral CP-odd scalar field. The Higgs Lagrangian takes the form

$$\mathcal{L}_{\text{Higgs}} = -(D_\mu H)^\dagger\,(D^\mu H) - V(H)\,, \tag{2.16}$$

where

$$V(H) = m^2 H^\dagger H + \frac{1}{2}\lambda\left(H^\dagger H\right)^2\,, \tag{2.17}$$

is the most general renormalizable scalar potential. If the mass term is negative, $-m^2 \equiv \mu^2 > 0$, the (CP-even) neutral component of the Higgs doublet acquires a nonzero vacuum

expectation value (VEV)

$$\langle h^0 \rangle = v \tag{2.18}$$

that spontaneously breaks the standard model gauge symmetry $\mathcal{G}_{\text{SM}}$ into $\text{SU}(3)_c \times \text{U}(1)_{\text{EM}}$. Of the four generators of electroweak symmetry group $\text{SU}(2)_L \times \text{U}(1)_Y$, three are spontaneously broken, implying the presence of three massless Nambu-Goldstone bosons. These are identified as the charged and CP-odd neutral degrees of freedom of the Higgs doublet and are absorbed in the *Higgs mechanism* by the $W^\pm$ and Z bosons, respectively, which acquire masses

$$m_W^2 = \frac{1}{2} g^2 v^2 \,, \tag{2.19a}$$

$$m_Z^2 = \frac{1}{2} \left(g'^2 + g^2 \right) v^2 \,. \tag{2.19b}$$

After this *electroweak symmetry breaking* (EWSB), the remaining degree CP-even real scalar of freedom of the Higgs doublet

$$h \equiv h^0 - \sqrt{2} \langle h^0 \rangle \tag{2.20}$$

is the physical Higgs boson, with mass

$$m_h^2 = \lambda v^2 = \mu^2 \,. \tag{2.21}$$

The expectation value of the Higgs field is set by the Fermi decay constant:[2]

$$v = \frac{1}{\sqrt{2^{3/2} G_F}} \simeq 174 \,\text{GeV} \,. \tag{2.22}$$

The experimentally measured Higgs boson mass, $m_h = (125.18 \pm 0.16)\,\text{GeV}$ [20–22], thus implies that the Higgs quartic coupling is approximately

$$\lambda \simeq 0.52 \tag{2.23}$$

at the electroweak scale.

[2] Here, and in the rest of this work, natural units are used in which the speed of light and the reduced Planck constant are set to unity: $c = \hbar = 1$.

Yukawa sector

The fermions couple to the Higgs doublet via Yukawa couplings:

$$\mathcal{L}_{\text{Yukawa}} = (y_u)_{ij}\, \bar{u}_i H Q_j - (y_d)_{ij}\, \bar{d}_i \overline{H} Q_j - (y_e)_{ij}\, \bar{e}_i \overline{H} L_j + \text{H.c.} \tag{2.24}$$

where $\boldsymbol{y}_{u,d,e}$ are matrices in family space and $\overline{H} \equiv i\sigma_2 H^*$. The basis in which the Yukawa coupling matrices are diagonal defines the *mass basis*. This is not the same as the interaction basis either for the quarks, resulting in *flavor mixing*. The Yukawa matrices for the quarks can be brought into diagonal form by the singular value decompositions

$$\boldsymbol{y}_{u,d} = \boldsymbol{V}_R^{u,d}\, \boldsymbol{y}_{u,d}^{\text{diag}}\, (\boldsymbol{V}_L^{u,d})^\dagger\,, \tag{2.25}$$

where

$$\boldsymbol{y}_u^{\text{diag}} = \text{diag}(y_u, y_c, y_t)\,, \qquad \boldsymbol{y}_d^{\text{diag}} = \text{diag}(y_d, y_s, y_b)\,. \tag{2.26}$$

Since the matrices $bmV_L^{u,d}$ and $bmV_R^{u,d}$ are unitary, all interactions in the lepton sector and all neutral-current interactions in the quark sector (i.e., the couplings to the neutral gauge bosons are not affected by this rotation). The quark charged-current interaction, however, becomes in the mass basis

$$\mathcal{L}_{\text{fermion}} \supset \frac{g}{\sqrt{2}}\, u_{L,i}^\dagger \bar{\sigma}^\mu W_\mu^+\, (V_{\text{CKM}})_{ij}\, d_{L,j} + \text{H.c.}\,, \tag{2.27}$$

where $\boldsymbol{V}_{\text{CKM}} = (\boldsymbol{V}_L^u)^\dagger\, \boldsymbol{V}_L^d$ is the Cabibbo-Kobayashi-Maskawa (CKM) matrix (4.9). Since the fermion couplings to the neutral gauge bosons are diagonal at tree level in the mass basis, there are no tree-level flavor-changing neutral currents (FCNCs) in the standard model. Additionally, all standard model interactions have an accidental flavor symmetry, which is only broken by the Yukawa couplings, such that flavor-changing neutral currents are suppressed even at loop level.[3] CP-violation in the standard model also arises only as a flavor-mixing effect in the CKM matrix.

After the Higgs obtains a VEV in electroweak symmetry breaking, each mass basis eigenstate ψ receives a mass of the form $m_\psi = y_\psi v$. The values of the Yukawa couplings necessary to generate the observed fermion masses are given in Table 2.2, where they are grouped according to generation to emphasize the hierarchical structure. We note that they

[3] This is the origin of the unitarity of the CKM matrix that is necessary for the Glashow–Iliopoulos–Maiani mechanism [23].

Table 2.2: Running standard model Yukawa couplings and corresponding fermion masses at the scale $Q = 173.1\,\text{GeV}$ in the $\overline{\text{MS}}$ renormalization scheme. Values obtained with the procedure discussed in Sec. 4.2.

	y	$m\,[\text{GeV}]$
u	$6.7228(29) \times 10^{-6}$	$0.001\,172\,3(5)$
d	$1.4610(6) \times 10^{-5}$	$0.002\,547\,6(10)$
e	$2.792\,980(10) \times 10^{-6}$	$4.870\,21(9) \times 10^{-4}$
c	$0.003\,38(2\,0^{+15}_{-14})$	$0.589(73^{+26}_{-24})$
s	$0.000\,290\,(94^{+13}_{-12})$	$0.0507(32^{+23}_{-21})$
μ	$5.883\,800(2) \times 10^{-4}$	$0.102\,598(2)$
t	$0.934\,801^{+0.005\,564}_{-0.005\,562}$	$163.004(970)$
b	$0.015\,480(7)$	$2.6993(12)$
τ	$0.009\,994\,4(4^{+5}_{-4})$	$1.742\,76(3)$

span approximately six orders of magnitude, resulting in a *fermion mass hierarchy*. In the standard model, the origin of this hierarchy is not explained, for the Yukawa couplings are simply added to the theory as primitive parameters.

2.1.2 Physics beyond the standard model

As a theory of physics at the electroweak scale, the standard model has been extensively tested at the quantum level and has succeeded in explaining a wide variety of experimental results. However, we have good reason to believe that the standard model falls short of being a complete theory of fundamental interactions, and that accordingly it should be viewed as an effective theory, valid over a range of scales, but eventually requiring an *ultraviolet completion* to take over at high energy. Here, we examine a few chosen problems to motivate the search for new physics.

Gravity and cosmology

Perhaps the most notable deficiency in the standard model as a description of nature is its lack of an account of gravity. The (reduced) *Planck scale* is the energy for which the

gravitational interactions of particles become order-one:

$$M_{\rm P} = \frac{1}{\sqrt{8\pi G}} \simeq 2.435 \times 10^{18}\,{\rm GeV}\,, \tag{2.28}$$

where G here is the gravitational constant. At this scale, the classical description of general relativity is expected to break down as quantum gravitational effects become important. Hence, although the standard model can in principle be valid up to the Planck scale, it is reasonable to believe that at that scale it must be superseded by a more fundamental description providing the unification of quantum field theory and gravity. An additional complication arises due to the vacuum energy that generically arises in any quantum field theory, which contributes classically to the source of stress-energy tensor in Einstein's equations as a cosmological constant. Observations of the acceleration of the expansion of the universe constrain the cosmological constant to be finite, but small [24, 25], many orders of magnitude smaller than the value predicted by the standard model (see Refs. [26, 27] for a review). The incorporation of gravity into quantum field theory may therefore require nontrivial modifications to our understanding of both theories.

A wide range of more local astrophysical and cosmological observations—including measurements galactic rotation curves, the distribution and morphology of large-scale structure, gravitational lensing, and temperature anisotropy of the cosmic microwave background (CMB)—have provided indirect evidence of *dark matter* (DM), another gravitational contribution to the mass density of the universe that does not produce detectable electromagnetic radiation. While other solutions (such as modifications to general relativity at large scales) have been proposed, it is natural to speculate that the observed dark matter can be attributed to the presence of a massive, electrically neutral particle. However, a particle with the necessary quantum numbers and mass to act as dark matter does not exists in the standard model, and so new physics is required if dark matter is to be explained in this way.

Massive neutrinos

New physics is also required in order to explain the observation of neutrino oscillation (see Ref. [20] for a review), which indicates that at least two of the neutrinos are massive. If the neutrinos are fundamentally Dirac states, they may obtain masses in the usual way through a Yukawa coupling to the (yet-unobserved) right-handed components:

$$\mathcal{L}_{\rm Yukawa} \supset (y_\nu)_{ij}\, \overline{\nu}_i H L_j + {\rm H.c.}\,. \tag{2.29}$$

The right-handed neutrinos $\overline{\nu}_i$ are in this case necessarily *sterile*, i.e., singlets under $\mathcal{G}_{\text{SM}}$. Due to the smallness of the neutrino masses,[4] the Yukawa couplings required here are minuscule, at maximum $\mathcal{O}(10^{-12})$, greatly exacerbating the Yukawa coupling hierarchy.

The standard model neutrinos may also be Majorana particles. In this case, a tree-level mass term is forbidden by the electroweak gauge symmetry and can only be added as a higher-dimension operator arising from some new physics at a heavier scale. The simplest such operator is dimension-five and takes the form

$$\mathcal{L}_{\text{Majorana}} = -\frac{1}{2}\frac{(\kappa_\nu)_{ij}}{\Lambda_\nu}\,\nu_{L,i}H\nu_{L,j}H + \text{H.c.}\,, \tag{2.32}$$

where Λ_ν is the scale of new physics and $\boldsymbol{\kappa}_\nu$ is a complex symmetric matrix of dimensionless coefficients in family space. In order to give rise to neutrino masses of the correct order, the scale of new physics must he high, approximately $\Lambda_\nu \gtrsim 10^{14}\,\text{GeV}$. We note that the theory at this scale must violate total lepton number (which is an accidental global symmetry of the standard model) in order to give rise to the term (2.32).

The mass eigenbasis of the neutrinos is not aligned with the weak eigenbasis. Therefore, just as in the quark sector, flavor mixing is observed in the lepton charged-current interactions in the mass basis:

$$\mathcal{L}_{\text{fermion}} \supset \frac{g}{\sqrt{2}}\,\nu^\dagger_{L,i}\,(U^\dagger_{\text{PMNS}})_{ij}\,\overline{\sigma}^\mu W^+_\mu e_{L,j} + \text{H.c.}\,, \tag{2.33}$$

where $\boldsymbol{U}_{\text{PMNS}}$ is the Pontecorvo-Maki-Nakagawa-Sakata (PMNS) matrix, defined in (4.22) or (4.35), depending on the form of the neutrino mass operator.

[4] The absolute neutrino mass scale is currently unconstrained from below. The sum of the neutrino masses

$$m_\nu^{\text{tot}} = \sum_i \frac{g_{\nu_i}}{2} m_{\nu_i}\,, \tag{2.30}$$

where g_{ν_i} is the number of spin degrees of freedom for ν_i and $\overline{\nu}_i$ together (i.e., $g_{\nu_i} = 4$ for a Dirac neutrino and $g_{\nu_i} = 2$ for a Majorana neutrino), is constrained from a combination of observations of the cosmic microwave background (CMB), the amplitude of density fluctuations on smaller scales from the clustering of galaxies and the Lyman-α forest, baryon acoustic oscillations, and Hubble parameter data to (see Ref. [20])

$$m_\nu^{\text{tot}} < 0.2\,\text{eV}\,. \tag{2.31}$$

Grand unification

The observations of dark matter and of massive neutrinos suggest the possibility of new physics, but the constraints they offer on its structure are primarily phenomenological. A more theoretical motivation for the potential shape of new physics above the electroweak scale can be found by taking seriously the symmetry structure of the theory of the standard model itself, in particular the conceptual unification of electromagnetism and the weak nuclear force into a theory of electroweak symmetry.[5] The question can naturally be asked if the standard model product group itself can be incorporated into some greater symmetry group, spontaneously broken at a very high energy scale, that would therefore be responsible for explaining the origin of all three fundamental forces. The smallest simple Lie group that contains $\mathcal{G}_{\rm SM}$ as a subgroup is SU(5).[6] In this case, the three coupling constants of $\mathcal{G}_{\rm SM}$ must be related to the underlying SU(5) coupling g_5 at the scale of SU(5) breaking as

$$g_5 = g_s = g = \sqrt{\frac{5}{3}}\, g' \,. \tag{2.34}$$

We show the evolution of the inverse coupling strength $\alpha_a = 4\pi/g_a^2$ with energy for each of the standard model gauge groups. Under renormalization in the standard model, the couplings tend toward a similar value, but cannot be described to unify. It is well known that in the minimal supersymmetric standard model, the extra particle content introduced at the scale $m_{\rm SUSY}$ is exactly that needed to bring the coupling together at the scale $m_{\rm GUT} \sim 10^{16}\,\text{GeV}$. We discuss supersymmetry in the next section, Sec. 2.2.

Such *grand unification* necessarily introduces new physics at the scale of the spontaneous breaking of the *grand unified theory* (GUT) symmetry. Although the GUT scale is typically quite heavy (close enough to the Planck scale that is not unreasonable to speculate that grand unification might be related to a theory of quantum gravity), it can lead to distinctive experimental signature such as proton decay that can be used to constrain the new physics. For a review, see Ref. [20].

[5] This is the Glashow-Weinberg-Salam model [1–3].

[6] The next smallest such Lie group is SO(10) [which contains SU(5) as a subgroup], and there are also other, more exotic choices. The SU(5) embedding, the Georgi-Glashow model [28], leads to an economic structure in which the standard model quarks and leptons fit into an anomaly-free chiral representation. Right-handed neutrinos can also naturally be introduced with masses around the SU(5) symmetry-breaking scale.

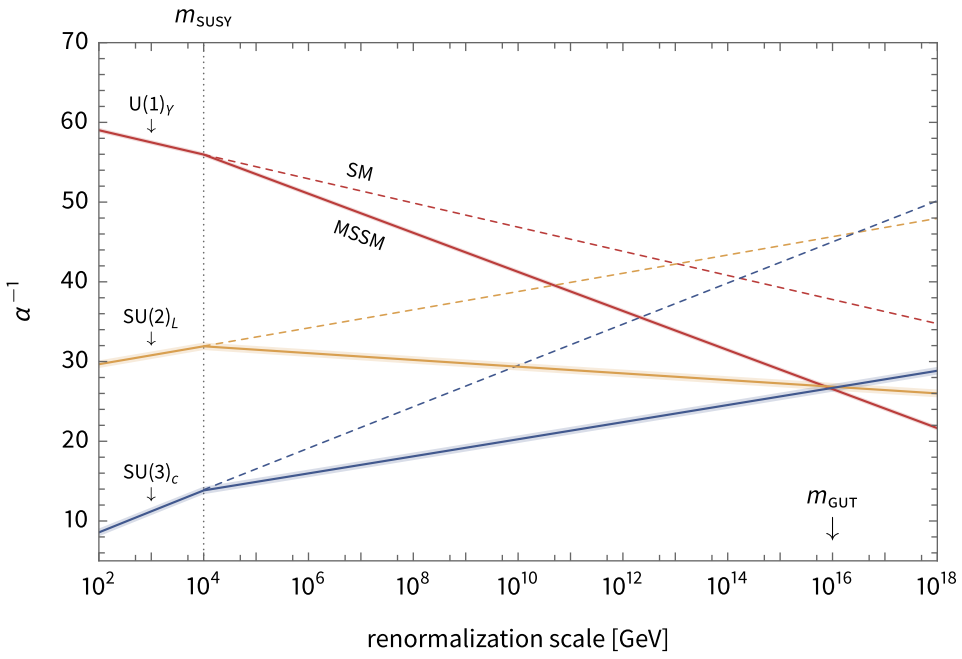

Figure 2.1: Plot of the running inverse coupling strengths of the standard model gauge groups in the SU(5) normalization as a function of renormalization scale in the standard model (dashed) and in the minimal supersymmetric standard model (solid). In the latter case, the shaded regions surrounding the lines give the uncertainty as calculated according to the renormalization procedure described in Sec. 4.2.

Stabilization of the electroweak scale

In the context of the standard model, the addition of new physics introduces an additional complication. In order to produce a VEV of the right size to give rise to the observed masses for W and Z bosons in EWSB, the Higgs scalar field must obtain a negative mass term of the scale

$$m^2 = -\mu^2 \sim -\left[\mathcal{O}(100)\,\mathrm{GeV}\right]^2 . \tag{2.35}$$

However, the mass of a scalar field receives additive renormalizations, and the scalar Higgs mass in the standard model is quadratically sensitive to the masses of any particle to which it couples (directly or indirectly). If there exists any new physics at higher energy (such as that suggested by a grand unified theory or a theory of quantum gravity), these masses are generically of the scale the ultraviolet cutoff Λ where the standard model is matched to the new theory. In this case, the Higgs mass at the electroweak scale can only be much smaller than Λ if the bare mass is of order $-\Lambda^2$ and this value is canceled down to $-\mu^2 \sim -\left[\mathcal{O}(100)\,\mathrm{GeV}\right]^2$

by radiative corrections. When the cutoff scale is large compared to the electroweak scale, this cancellation must be extremely precise [for instance, if we take Λ to be the Planck scale, the cancellation must be to approximately $(10^2\,\mathrm{GeV}/10^{19}\,\mathrm{GeV})^2 = 10^{-32}$].

The scale of electroweak symmetry breaking, which is determined by the Higgs mass, is therefore quadratically sensitive to the mass scale of heaviest particles that couple to the standard model, and, short of a dramatic cancellation, we expect it to be of the same order. Without a mechanism to stabilize the hierarchy between the scale of new physics and the electroweak scale, any extension of the standard model thus results in a *fine-tuning problem*, in which the parameters of the theory (in this case the Higgs bare mass) must take very particular values in order for the theory to be phenomenologically viable.[7] This defines a principle of *naturalness*, of which there are several formulations. The strongest version is originally due to Dirac [29, 30], which specifies that a theory is natural if all dimensionless coefficients are of order-one and the dimensionful parameters are of the same order of magnitude. This can be weakened by allowing small parameters to be natural if setting them to zero enhances the symmetry of the theory [31]. Technical naturalness requires only that none of the parameters receive radiative corrections that significantly exceed its magnitude.

In the presence of heavy new physics, the Higgs mass is not even technically natural unless the more fundamental theory includes a mechanism that protects the scale of electroweak symmetry breaking. Provided such a mechanism has been the focus of much of the model building for physics beyond the standard model. There are three main classes of solutions. The first is to propose a new bosonic symmetry that is spontaneously broken at higher energy scale. A composite Higgs boson in this case can arise, like the pion of QCD, as the pseudo-Nambu-Goldstone boson of some new strong dynamics.[8] The second option is to regulate the renormalization of the theory above the electroweak scale, which can be accomplished by introducing an approximate conformal invariance at higher energies [32, 33] or one or more extra dimensions with low-scale quantum gravity [14–16, 34].[9] The third possibility is an enhanced fermionic symmetry, namely supersymmetry, which we discuss in the next section.

The alternative to all of these solutions, of course, to accept a theory with tuning. Indeed,

[7] In the context of GUT models, the separation of the electroweak scale below the scale of grand unification is referred to as the *gauge hierarchy problem*; more generally, it is simply the *hierarchy problem*.

[8] Such theories typically present difficulties in their simplest forms, as the 125 GeV Higgs boson observed at the Large Hadron Collider (LHC) does appear to have properties consistent with a fundamental scalar field.

[9] According to the AdS/CFT correspondence (see Sec. 3.3), these two classes of ideas are related.

the current TeV-scale constraints on new physics at the LHC leaves many explanations of the hierarchy problem with at least a residual meso-tuning. If we take seriously the position that a fine-tuning mechanism exists in nature, it has famously been argued that this can be viewed as evidence that we live in a multiverse [35]. It is also not obvious that the principle of naturalness is justified in any way by the structure of nature (an unnatural theory certainly does not imply the presence of new physics, although it does suggest it), and there is accordingly some debate as to whether it is reasonable to view naturalness as a theoretical virtue or if tuning problems are merely unphysical artifacts of the way in which we construct our theories.

The fermion mass hierarchy and flavor mixing

Another hierarchy exists in the standard model even in the absence of new physics: namely, the fermion mass hierarchy. In order to generate the observed fermion masses after EWSB, the Yukawa couplings of the light fermions must be small parameters (see Table 2.2), which have no explanation within the theory.[10] In addition, the CKM matrix is mildly hierarchical, with the offdiagonal elements suppressed relative to the diagonal (see (4.10) for the Wolfenstein parametrization). To be consistent, an account of the hierarchies in the flavor sector should include not only an explanation of the spread in the fermion masses, but also of the specific structure of flavor mixing.[11]

In particular, as discussed in the previous section, flavor-changing processes and CP violation are highly suppressed in the standard model. The presence of new physics can, however, lead to tree-level FCNCs and CP violation and thus to large modifications of the standard model predictions for rare decays, neutral meson mixing, or other precision electroweak measurements. Within the standard model, these contributions can be parametrized as higher-dimension operators, suppressed by the scale of new physics Λ. In the absence of a mechanism to suppress such contributions, the current measurements set limits on the scale of new physics, roughly $\Lambda \gtrsim 10^4$–$10^5\,\text{GeV}$. This is in tension with a solution to the hierarchy problem, which prefers $\Lambda \lesssim 1\,\text{TeV}$ in order to preserve naturalness.

[10] If the neutrinos also obtain Dirac masses, the hierarchy is necessarily even larger.
[11] Note, however, that the PMNS matrix is not especially hierarchical.

2.2 Supersymmetry

In this section we discuss supersymmetry, a compelling theoretical paradigm that is able to successfully address many of the shortcomings of the standard model considered above. From a mathematical perspective, supersymmetry is one of the more natural extensions of the standard model. The Coleman-Mandula theorem states that under the assumptions of analyticity and nontriviality and in the presence of a mass gap, the most general Lie group symmetry of the S matrix is a local field theory is the direct product of the Poincaré group and an internal group [36]. According to the Haag–Łopuszański–Sohnius theorem [37], the only possible extension beyond this is the generalization of the Lie algebra of the internal symmetry group to include a $\mathbb{Z}_2$ grading (promoting it to a Lie superalgebra), introducing a set of additional generators (supercharges) that are fermionic rather than bosonic. The result is supersymmetry, which, due to the $\mathbb{Z}_2$ grading, enforces a relationship between fermions and bosons: it assigns to each bosonic degree of freedom a fermionic *superpartner*, differing in spin by $\frac{1}{2}$ unit, and vice versa. The single-particle states of a supersymmetric theory are organized into *supermultiplets*, irreducible representations of the supersymmetry algebra.

When supersymmetry is promoted to a local theory, the supersymmetry generators and the generators of the Poincaré algebra together form the Poincaré superalgebra. *Supergravity* (SUGRA), the gauge theory of this symmetry, combines the principles of supersymmetry and general relativity, thus providing a natural way to unify the theory gravity with the description of the other three fundamental forces. Besides the incorporation of gravity, the supersymmetrization of the standard model can provide a number of other phenomenologically and theoretically desirable features. Most famously, the supersymmetric symmetrization of the field content protects the mass terms of the theory against radiative corrections to all orders in perturbation theory (in diagrammatic terms, this amounts to an exact cancellation between the loop contributions of the members of a supermultiplet) [38, 39]. Supersymmetry thus removes the quadratic sensitivity of the Higgs mass to heavy mass scales, alleviating the hierarchy problem for the electroweak scale. Further, the additional particle content introduced by supersymmetry can provide improved prospects of gauge coupling unification (see Fig. 2.1) as well as number of suitable dark matter candidates. Here, we give a brief construction the minimal supersymmetric standard model. The quintessential review of this topic is Ref. [40].

2.2.1 The minimal supersymmetric standard model

In order to construct a minimal supersymmetric standard model, we locate each of the standard model fields inside a chiral supermultiplet or gauge supermultiplet. The field content of the MSSM is given in Tables 2.3 and 2.4. In supergravity, we additionally introduce a gravity supermultiplet, composed by graviton and its spin-$\frac{3}{2}$ superpartner, the *gravitino*. The superpartners of the gauge bosons are the spin-$\frac{1}{2}$ *gauginos*. The superpartners of the standard model chiral Weyl fermions are the complex scalar *sfermions*,[12] which are typically labeled according to the chirality of their superpartners. The left-handed sfermions are contained in $\mathrm{SU}(2)_L$ doublets

$$\widetilde{Q}_1 = \begin{pmatrix} \widetilde{u}_L \\ \widetilde{d}_L \end{pmatrix}, \qquad \widetilde{Q}_2 = \begin{pmatrix} \widetilde{c}_L \\ \widetilde{s}_L \end{pmatrix}, \qquad \widetilde{Q}_3 = \begin{pmatrix} \widetilde{t}_L \\ \widetilde{b}_L \end{pmatrix}, \tag{2.36a}$$

$$\widetilde{L}_1 = \begin{pmatrix} \widetilde{\nu}_{eL} \\ \widetilde{e}_L \end{pmatrix}, \qquad \widetilde{L}_2 = \begin{pmatrix} \widetilde{\nu}_{\mu L} \\ \widetilde{\mu}_L \end{pmatrix}, \qquad \widetilde{L}_3 = \begin{pmatrix} \widetilde{\nu}_{\tau L} \\ \widetilde{\tau}_L \end{pmatrix}. \tag{2.36b}$$

In order to ensure anomaly cancellation, the Higgs sector must be enlarged to two chiral multiplets, where the doublets take the form

$$H_u = \begin{pmatrix} H_u^+ \\ H_u^0 \end{pmatrix}, \qquad \widetilde{H}_u = \begin{pmatrix} \widetilde{H}^+ \\ \widetilde{H}^0 \end{pmatrix}, \tag{2.37a}$$

$$H_d = \begin{pmatrix} H_d^0 \\ H_d^- \end{pmatrix}, \qquad \widetilde{H}_d = \begin{pmatrix} \widetilde{H}^0 \\ \widetilde{H}^- \end{pmatrix}. \tag{2.37b}$$

The superpartners of the Higgs bosons are the spin-$\frac{1}{2}$ *higgsinos*. The scalar Higgs sector thus contains eight degrees of freedom. Three of these are absorbed by the gauge bosons as usual in EWSB, leaving five physical degrees of freedom: two charged scalars $H^\pm$, one pseudoscalar A, and two neutral scalars H and h. The last of these is identified as the 125 GeV resonance detected at the LHC.

In terms of these supermultiplets, the interactions between matter fields that are invariant

[12] The naming convention is as expected for the individual states: sup, sdown, scharm, sstrange, stop, sbottom, selectron, smuon, stau, and sneutrino.

Table 2.3: Chiral supermultiplets of the MSSM.

component fields				representation		
spin 0			spin $\frac{1}{2}$	$\mathrm{SU}(3)_c$	$\mathrm{SU}(2)_L$	$\mathrm{U}(1)_Y$
$\widetilde{Q}_i$	squark doublet	Q_i	quark doublet	$\mathbf{3}$	$\mathbf{2}$	$+\frac{1}{6}$
$\widetilde{u}_i^*$	up-squarks	$\bar{u}_i$	up-quarks	$\overline{\mathbf{3}}$	$\mathbf{1}$	$-\frac{2}{3}$
$\widetilde{d}_i^*$	down-squarks	$\bar{d}_i$	down-quarks	$\overline{\mathbf{3}}$	$\mathbf{1}$	$+\frac{1}{3}$
$\widetilde{L}_i$	slepton doublet	L_i	lepton doublet	$\mathbf{1}$	$\mathbf{2}$	$-\frac{1}{2}$
$\widetilde{e}_i^*$	selectrons	$\bar{e}_i$	electrons	$\mathbf{1}$	$\mathbf{1}$	$+1$
H_u	Higgs doublet	$\widetilde{H}_u$	higgsino doublet	$\mathbf{1}$	$\mathbf{2}$	$+\frac{1}{2}$
H_d	Higgs doublet	$\widetilde{H}_d$	higgsino doublet	$\mathbf{1}$	$\mathbf{2}$	$-\frac{1}{2}$

Table 2.4: Gauge supermultiplets of the MSSM.

component fields				representation		
	spin $\frac{1}{2}$		spin 1	$\mathrm{SU}(3)_c$	$\mathrm{SU}(2)_L$	$\mathrm{U}(1)_Y$
$\widetilde{B}$	bino	B	B boson	$\mathbf{1}$	$\mathbf{1}$	0
$\widetilde{W}$	winos	W	W boson	$\mathbf{1}$	$\mathbf{3}$	0
$\widetilde{g}$	gluinos	g	gluon	$\mathbf{8}$	$\mathbf{1}$	0

under supersymmetry transformations are given in the *superpotential*:

$$W_{\text{MSSM}} = -(y_u)_{ij}\,\bar{u}_i H_u Q_j + (y_d)_{ij}\,\bar{d}_i H_d Q_j + (y_e)_{ij}\,\bar{e}_i H_d L_j + \mu H_u H_d\,, \tag{2.38}$$

shown here in superfield notation. While this is the minimal superpotential, supersymmetry notably does not forbid terms giving rise to processes that violate baryon number B or total lepton number L at tree level. In the standard model, B and L are both accidental symmetries of the theory and processes such as proton decay that violate one or both are highly constrained by experiment. In order to forbid or suppress such terms in a

supersymmetric theory, a discrete R-parity can be introduced,[13] defined for each particle as

$$P_R = (-1)^{2(B-L)+2s}\,, \tag{2.39}$$

where s is the spin of the particle. Under this definition, supersymmetric particles have negative parity while the standard model particles and scalar Higgs bosons are positive. One consequence of this is that when R-parity is preserved the lightest supersymmetric particle (LSP) is stable. (Or, if the R-parity violation is small enough, the LSP can be metastable.) If the LSP is electrically neutral it can therefore fill the role of dark matter [47, 48]. In the MSSM, the suitable candidates are the gravitino and, after EWSB, the lightest neutralino (a linear combination of the bino, the neutral wino, and the neutral higgsinos).

Supersymmetry breaking

Due to the absence of superpartners at low energies, a realistic phenomenological model must contain supersymmetry breaking. From a theoretical perspective, we expect that supersymmetry, if it exists at all, should be an exact symmetry that is broken spontaneously. In order to maintain the stabilization of the electroweak scale that is provided by supersymmetry, this breaking must be *soft*, that is, all supersymmetry-breaking terms in the Lagrangian must be of positive mass dimension. In the MSSM the minimal soft supersymmetry breaking sector takes the form

$$\begin{aligned}
\mathcal{L}_{\text{soft}}^{\text{MSSM}} = &-\frac{1}{2}\left(M_3\widetilde{g}^a\widetilde{g}^a + M_2\widetilde{W}^i\widetilde{W}^i + M_1\widetilde{B}\widetilde{B} + \text{H.c.}\right) \\
&- \left((a_u)_{ij}\,\widetilde{u}_i^* H_u \widetilde{Q}_j - (a_d)_{ij}\,\widetilde{d}_i^* H_d \widetilde{Q}_j - (a_e)_{ij}\,\widetilde{e}_i^* H_d \widetilde{L}_j + \text{c.c.}\right) \\
&- (m_{\widetilde{Q}}^2)_{ij}\,\widetilde{Q}_i^*\widetilde{Q}_j - (m_{\widetilde{u}}^2)_{ij}\,\widetilde{u}_i\widetilde{u}_j^* - (m_{\widetilde{d}}^2)_{ij}\,\widetilde{d}_i\widetilde{d}_j^* - (m_{\widetilde{L}}^2)_{ij}\,\widetilde{L}_i^*\widetilde{L}_j - (m_{\widetilde{e}}^2)_{ij}\,\widetilde{e}_i\widetilde{e}_j^* \\
&- m_{H_u}^2 H_u^* H_u - m_{H_d}^2 H_d^* H_d - (b H_u H_d + \text{c.c.})\,,
\end{aligned} \tag{2.40}$$

where $M_{1,2,3}$ are soft gaugino masses, $\boldsymbol{a}_{u,d,e}$ are soft trilinear scalar coupling matrices, $\boldsymbol{m}^{\boldsymbol{2}}_{\widetilde{Q},\widetilde{u},\widetilde{d},\widetilde{L},\widetilde{e}}$ are soft sfermion mass matrices, $m_{H_{u,d}^2}$ are soft Higgs masses, and b is a soft Higgs scalar mixing. In total there are 105 unique parameters (masses, phases, and mixing angles).

The spontaneous breaking of supersymmetry itself requires the MSSM to be extended, as

[13] From a theoretical perspective this can be motivated by the introduction of a continuous $\mathrm{U}(1)_{B-L}$ symmetry as in Refs. [41–46].

the ultimate supersymmetry-breaking order parameter cannot belong to any of the MSSM supermultiplets. Schematically, supersymmetry must be broken in a *hidden sector* and communicated to the MSSM by a *messenger sector*. Allowing supersymmetry breaking in the hidden sector to be transmitted purely through gravitational interactions results in a model of *gravity-mediated supersymmetry breaking* or *Planck-scale-mediated supersymmetry breaking* [49–58]. Within this context, a minimal model assuming flavor-blindness (typically on purely phenomenological grounds) can be formulated that parametrizes the soft mass sector in terms of just four quantities: a common gaugino mass $m_{1/2}$, a common scalar mass m_0, a common trilinear scalar coupling A_0, and the Higgs soft mixing b. This is the *minimal supergravity* (MSUGRA) or *constrained minimal supersymmetric standard model* (CMSSM) scenario that has been the subject of the bulk of phenomenological and experimental studies of supersymmetry.

In *gauge-mediated supersymmetry breaking* (GMSB) models [59–65] (see Ref. [66] for a review), messenger chiral multiplets charged under the standard model gauge groups $\mathcal{G}_{\text{SM}}$ couple to the hidden supersymmetry-breaking sector. This has the effect of transmitting supersymmetry breaking to the MSSM indirectly and in a flavor-diagonal way. There is still gravitational communication between the MSSM and the hidden sector, but its contributions are typically subdominant compared to the gauge interaction effects.

A vital clue for determining the superpartner mass scale comes from the recent discovery of the 125 GeV Higgs boson [12, 13, 22]. To obtain this mass in minimal supersymmetry, the Higgs quartic coupling must receive sizable radiative corrections. These can arise from the top quark superpartners (or stops), provided that the lightest stop has mass of $\mathcal{O}(10)$ TeV. In the minimal framework there are no other significant contributions to the Higgs quartic coupling, and consequently the rest of the sparticle spectrum is not determined. The spectrum must only be compatible with the current LHC limits that require stop masses to be greater than $\mathcal{O}(1\text{–}2)$ TeV [67–72], gluino masses above $\mathcal{O}(2)$ TeV [68, 70–73], and neutralino masses above $\mathcal{O}(1)$ TeV [68, 72].[14]

The supersymmetric flavor problem

The sparticle spectrum is also constrained indirectly by precision electroweak experiments, as the additional degrees of freedom introduced by supersymmetry generically imply flavor-mixing and CP violation through the offdiagonal elements of the sfermion masses and the trilinear scalar couplings. In the absence of some suppressing mechanism the resulting

[14] These results are model-dependent.

FCNCs and CP-violating processes are too large to be compatible with current experimental limits. This is the *supersymmetric flavor problem*. There are several ways in which these dangerous FCNCs and CP-violating effects can be suppressed.

- **Soft supersymmetry-breaking universality**

  Large FCNCs and CP violation can be avoided if soft supersymmetry breaking is sufficiently universal. For the sfermion soft masses, a sufficient condition is flavor blindness (i.e., that the flavor symmetry of the standard model is respected, such that each mass matrix is proportional to the identity matrix in family space). Contributions from the trilinear scalar couplings can be suppressed if they are proportional to the corresponding Yukawa matrices, and CP-violating effects can be avoided by assuming that the soft parameters do not introduce any complex phases. This type of universality is frequently assumed (but not theoretically justified) in models with gravity-mediated supersymmetry breaking; in GMSB models it arises naturally as a consequence of the flavor-blindness of gauge interactions.

- **Alignment**

  In the alignment solution, the requirement that the sfermion soft mass matrices are flavor-blind is relaxed and replaced with the weaker requirement that they are arranged in flavor space to be aligned with the relevant Yukawa matrices [74, 75]. This can be motivated with the addition of some flavor symmetries.

- **Irrelevancy**

  Even if the sfermion masses and trilinear scalar couplings are fully anarchic, FCNCs and CP violation can be suppressed below current experimental constraints if the sfermions of the first and second generations are sufficiently heavy, $\mathcal{O}(100)$ TeV [76–79] or heavier [80–82]. This allows the flavor problem to be ameliorated without the addition of any extra structure. This leads to the scenario of *high-scale supersymmetry*, in which all of the superpartners are heavy, or *split supersymmetry* [35, 83] if the masses of the supersymmetric fermions (the gauginos and higgsinos) are loop-suppressed below the scalar mass scale. These maintain the successful features of supersymmetric models such as gauge coupling unification and the incorporation of gravity (and possibly a dark matter candidate) but push the sfermion spectrum firmly out of the realm of experimental relevance.[15]

[15]The Higgs mass is sensitive to the mass of the stop, and as the scale of supersymmetry breaking increases

Because the experimental limits involving FCNCs and CP violation among the third-generation standard model fermions are less restrictive, it is not necessary to push the entire sfermion spectrum up to high scales in order to solve the supersymmetric flavor problem. The scenario in which the masses of the third-generation sfermions are $\mathcal{O}(10)$ TeV, hierarchically lighter than those of the first and second generations which are least $\mathcal{O}(100)$ TeV, leads to a version of split supersymmetry [83] called *minisplit* [86, 87]. This has the advantage naturally explaining the 125 GeV Higgs and putting the third-generation sfermions within the reach of direct detection.

We note that the high mass scale of the spectra in these scenarios results is a degree of tuning for the electroweak scale. Due to the absence of low-energy supersymmetry at the LHC, however, we are forced to accept some tuning as a generic feature of supersymmetric models. This tuning could possibly be explained by a relaxion mechanism [88, 89].

All of these mechanisms suggest that supersymmetry breaking may have special relationship with flavor. In particular, in split supersymmetric models, the supersymmetry-breaking scale occurs near the PeV scale, with sfermion masses in the range 10–1000 TeV. Even though this hierarchy of sfermion masses seems prima facie unrelated to the fermion mass hierarchy, it begs the question as to whether these two hierarchies could in fact be explained by the same mechanism. In the following, we present a model of supersymmetry in a slice of five-dimensional anti-de Sitter spacetime that is naturally able to provide precisely such a connection.

2.3 Connecting Supersymmetry Breaking with Flavor

Here, we motivate a model of supersymmetry in a slice of five-dimensional anti-de Sitter space (AdS_5) [16]. The compactified extra dimension allows the supersymmetric Higgs sector, which we localized on the UV brane, to be physically separated from the supersymmetry-breaking sector, which we confine to the IR brane. The supersymmetric matter fields propagate in the bulk. Unlike other supersymmetric models, the theory does not need to rely on the

in these models, some tension arises with the observed 125 GeV Higgs boson (see Ref. [84] for historical context). If the stop is heavier than about $\mathcal{O}(10)$ TeV, obtaining a 125 GeV Higgs mass typically requires $\tan\beta$ to be low [85].

We also note that if the scale of supersymmetry breaking is high enough, radiative corrections to the Higgs soft masses can drive the Higgs scalar potential to a nontrivial minimum, providing *radiative electroweak symmetry breaking*.

Froggatt-Nielsen mechanism to explain the standard model fermion masses.[16] (Also note an alternative approach that radiatively generates fermion masses from a sfermion anarchy [92].) Instead, the overlap of fermion profiles [93] with the UV-localized Higgs fields explains the fermion mass hierarchy [94]. As we discuss in detail in Chapter 4, the standard model Yukawa couplings are used to constrain the bulk fermion profiles, determining localizations of the MSSM chiral multiplets in the bulk. Fields with large Yukawa couplings (such as the top quark and stop) must be localized near the UV, while fields with smaller Yukawa couplings must be IR-localized. Because of the curvature of the spacetime, fields in the bulk have exponential profiles in the extra dimension, such that fields that couple strongly to the Higgs fields necessarily have a weak coupling to the supersymmetry-breaking sector and vice versa. The fermion mass hierarchy therefore determines also determines the structure of supersymmetry breaking at the IR-brane scale, resulting in an inverted spectrum in which the UV-localized third-generation sfermions are lighter than those of the IR-localized first two generations. Both the Higgs-sector soft masses and the soft trilinear scalar couplings arise at loop order, due to radiative corrections from the bulk that transmit the breaking of

[16] One deficiency of the standard model that supersymmetry is not able to explain is the origin of the fermion mass hierarchy. Instead, this issue is typically addressed by recourse to the *Froggatt-Nielsen mechanism* [90] (see Ref. [91] for a review), which proposes a new $\mathrm{U}(1)_{\mathrm{F}}$ flavor symmetry under which the left-handed and right-handed components of the standard model fermions have different charges, while the Higgs is assumed to be a singlet. The Yukawa couplings in this case arise as higher-dimension operators of the form

$$\mathcal{L}_{\text{Yukawa}} \supset \left(\frac{S}{\Lambda_{\mathrm{F}}}\right)^{q_R+q_L} \psi_R H \psi_L \tag{2.41}$$

where $q_{L,R}$ are the flavor charges of the left- and right-handed fermions, S is a $\mathcal{G}_{\mathrm{SM}}$ singlet scalar *flavon* field with flavor charge -1, and Λ_{F} is the scale at which the heavier degrees of freedom are integrated out. Assuming that the flavor symmetry is spontaneously broken by a nonzero expectation value $\langle S \rangle$, a Yukawa coupling matrix is generated as

$$y_{ij} = g_{ij} \epsilon^{q_{R,i}+q_{L,j}} , \tag{2.42}$$

where $\boldsymbol{g}$ is a Hermitian matrix of complex coefficients, order-one in magnitude. Entries in the Yukawa matrix can be parametrically suppressed with order-one charges $q_{L,R}$ provided

$$\epsilon = \frac{\langle S \rangle}{\Lambda_{\mathrm{F}}} \tag{2.43}$$

is a sufficiently small number [perhaps $\mathcal{O}(0.1)$], allowing the fermion mass hierarchy and flavor structure of the standard model to be recovered.

We note that stripped of the context of the flavor symmetry, the structure of the Froggatt-Nielsen mechanism has a generic form, explaining the Yukawa couplings in terms of a small number ϵ, originating in a hierarchy of scales, raised to powers composed of two flavor-dependent, order-one numbers. This basic structure can arise quite naturally without the need for a new flavor symmetry (and its accompanying unknown high-scale theory) in the background of a warped extra dimension, as we discuss in detail in Chapter 4 (for a generic example, see Sec. 4.1.3), or through the strong dynamics of its four-dimensional dual theory of partial compositeness, which we consider in Sec. 3.3.

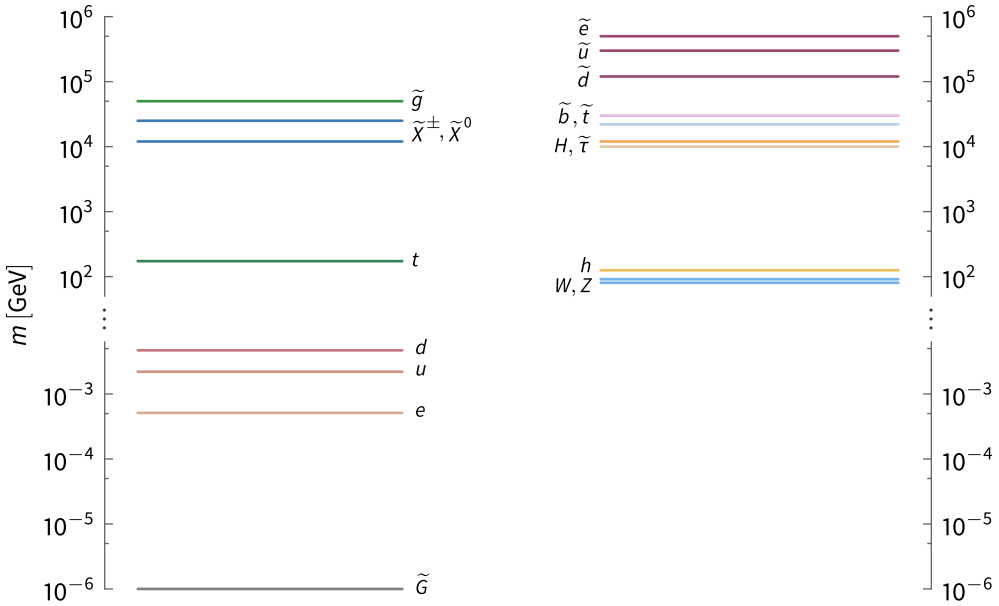

Figure 2.2: Schematic diagram depicting a possible particle spectrum of a model of supersymmetry in a slice of AdS_5. The left (right) column depicts the fermions (bosons). The sfermion mass hierarchy is inversely related to the fermion mass hierarchy and the LSP is the gravitino.

supersymmetry. Renormalization group evolution is then used to run the soft masses down to the electroweak scale and obtain superpartner mass spectrum. Using this procedure, in Chapter 9 we analyze two benchmark scenarios: one for the case that the gaugino masses arise from a singlet spurion and the other in nonsinglet spurion case. We find that the observed 125 GeV Higgs boson mass naturally accommodates sparticle spectra that hierarchically suppress the masses of the stops and the other third-generation sfermions below the mass scale of the first- and second-generation sfermions.

In particular, if the masses of the first- and second-generation sfermions are restricted to be above 100 TeV to solve the supersymmetric flavor problem, the stop masses lie in the range 20–100 TeV, while the mass of the lightest stau may be as low as 10 TeV. The lightest supersymmetric particle is the gravitino, with a mass in the approximate range 1 keV to 1 TeV, and it accordingly can play the role of dark matter. This differs from other split-supersymmetry models where the gravitino is usually the heaviest superpartner. The next-to-lightest supersymmetric particle (NLSP) is typically a bino, higgsino, or right-handed stau (10–25 TeV), whose decays to the gravitino could eventually be probed at a future 100 TeV collider. A schematic diagram of a possible mass spectrum of this five-dimensional

model is depicted in Fig. 2.2. We make this construction more precise in the following chapters.

According to the AdS/CFT correspondence, this five-dimensional model in a slice of AdS_5 has a dual description in four dimensions as *partially composite supersymmetry*. The five-dimensional model provides a calculable description of the strong dynamics that govern the dual theory, and in the following, we will refer to both the 4D and 5D descriptions by this name. Previous attempts to explain the sfermion mass hierarchy in a slice of AdS_5 before the Higgs boson mass was known were considered in Refs. [95, 96]. The results obtained in our analysis were first presented in Refs. [17, 18] and are the first predictions for the sfermion mass spectrum from partial compositeness that are compatible with a 125 GeV Higgs boson. In addition, they include, for the first time the full one-loop radiative corrections to the bulk scalar soft masses squared, the Higgs-sector soft terms, and the soft trilinear scalar couplings. For stops and other UV-localized sfermions, these corrections provide the dominant soft mass contributions, and accordingly have important phenomenological consequences. For the Higgs sector, they control the breaking of electroweak symmetry. In this work we generalize this structure to include flavor mixing effects through the CKM and PMNS matrices, as well as offdiagonal terms in the sfermion soft mass matrices the soft trilinear scalar coupling matrices.

3 Partially Composite Supersymmetry

In this chapter we construct the five-dimensional theory of partially composite supersymmetry. We first review the status of theories of spacetime with extra dimensions, before specializing to the geometry of five-dimensional AdS spacetime compactified over the $S^1/\mathbb{Z}_2$ orbifold. We then discuss supersymmetry in the slice of AdS_5, formulating a minimal model in which the MSSM arises as the effective four-dimensional theory below the compactification scale. Last, we present the strongly coupled theory that is dual to the five-dimensional model under the AdS/CFT correspondence and sketch an AdS/CFT dictionary connecting the two descriptions.

3.1 Theories in Five Dimensions

Theories proposing the extra dimensions of spacetime have a long history in the quest for a fundamental theory of nature in theoretical physics. In 1914, Nordström extended the classical Maxwellian theory of electromagnetism to five dimensions, noting that the five-dimensional vector potential could be contained both the four-dimensional electromagnetic vector potential and an additional four-dimensional scalar obeying field equations for what Nordström identified as a scalar theory of Newtonian gravity [97]. In 1921, a similar observation was made in the context of the newly developed general theory of relativity (GR) by Kaluza, who decomposed the structure of a five-dimensional theory of gravity[1] into a four-dimensional theory plus classical electromagnetism (and an additional four-dimensional scalar field). In 1926, Klein proposed the physical interpretation that the fifth dimension in Kaluza's theory is compact (periodic) and microscopic in size in order to explain its disappearance into four-dimensional structures at macroscopic scales [98].

From the modern perspective, the Kaluza-Klein theory (see Ref. [99] for a review) is the first example of a gauge-gravity duality, in this case the origination of a U(1) field, the electromagnetic vector potential, out of the fifth dimension. This idea was further

[1] Kaluza considered five-dimensional Lorentzian manifolds subject to a "cylinder condition" on the five-dimensional metric enforcing its independence from the coordinate of the extra dimension (equivalent to enforcing translation invariance along that direction).

developed when interest in enlarged spacetimes was revived with the advent of string theory in the 1980s, as it became known that theories of anomaly-free quantum gravity require additional spatial dimensions. In 1997, Maldacena's AdS/CFT conjecture formalized the duality between conformal field theories (i.e., SU(N) gauge theories in the large N limit) and higher-dimensional AdS spacetimes [100].

A more phenomenological approach was initiated in 1998 when Arkani-Hamed, Dimopoulos, and Dvali [14] proposed a solution to the relative weakness of gravity (i.e., the hierarchy problem) by localizing the standard model fields on a four-dimensional submanifold embedded in a spacetime with $d > 3$ spatial dimensions (see also [34]). A year later, in 1999, Randall and Sundrum [16] proposed a similar model in a nonfactorizable geometry, a slice of five-dimensional warped (anti-de Sitter) space. These models were soon expanded to include gauge and matter propagating in the bulk (see, for example, [94, 95, 101, 102]).

The necessary feature of modern approaches to theories of extra dimensions, is presence of compactification (or, alternatively, the localization of gravity [103, 104]) in order to recover a four-dimensional structure at macroscopic scales. The nature of this compactification is important. The original Kaluza-Klein theory itself is ultimately unsuccessful as a theory of nature due to the fact that its compactification does not permit chiral fermions to exist at low energies (see [105]). More recent theories have overcome this deficiency by considering compactifications that introduce mild singularities. We will discuss a simple orbifold compactification illustrating these features in the context of five-dimensional spacetime in Sec. 3.1.1.

In physical terms, the effect of compactification is to quantize the momenta of fields along the direction of the extra dimension. As a result, each field propagating in the bulk of an expanded spacetime may be decomposed in a Kaluza-Klein (KK) expansion into an infinite sum of four-dimensional fields convolved with eigenmodes along the extra dimension, resulting in a representation for the higher-dimensional field as an infinite tower of four-dimensional Kaluza-Klein states, each with increasing effective mass (but otherwise identical quantum numbers). The mass splittings between the KK states depend on the geometry of the spacetime as well as the specific boundary conditions of the field over the compactified space, which may or may not permit a massless mode (a zero mode).

Kaluza-Klein towers are the primary phenomenological signature of extra dimensions, and models containing them are subject to collider (direct production and virtual effects), astrophysical (supernova luminosity and neutron star cooling) and cosmological (relic density) constraints (see Ref. [20] for a review of extra dimension searches). If the standard model

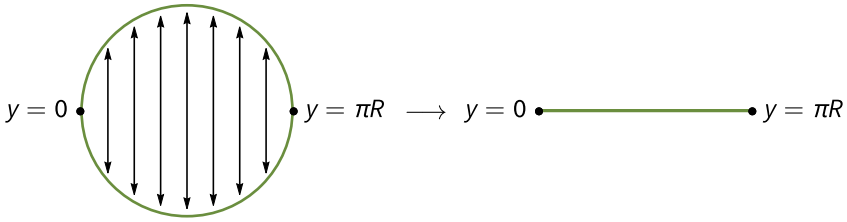

Figure 3.1: Visualization of the $S^1/\mathbb{Z}_2$ orbifold.

particles propagate in the bulk, the most stringent constraints are the direct-production bounds from the LHC at CERN, which are currently around the $\mathcal{O}(1\text{–}10)$ TeV scale. The graviton always probes the full extra-dimensional space and its KK modes additionally give rise to deviations from the Newtonian inverse-square-law behavior of the gravitational force at distances small enough compared to the size of the extra dimension which can be tested (see Refs. [106, 107] for reviews of recent experiments).

3.1.1 The orbifold compactification

We now specialize to theories with one compact extra dimension (Refs. [108–112] provide a variety of reviews of this subject). We consider a five-dimensional spacetime $x^M = (x^\mu, y)$, where x^μ are the usual four-dimensional coordinates and $x^5 = y$ is the coordinate of a compact spatial dimension. The simplest choice of compactification for the extra dimension is a periodic geometry such as S^1 (as in the original Kaluza-Klein model), such that

$$y \longleftrightarrow y + 2\pi R\,, \tag{3.1}$$

where R is the radius of the circle. Such a compactification breaks the translational symmetry of the fifth dimension, leading to the quantization of momentum in the extra dimension. The five-dimensional action must be invariant under the remaining discrete shift symmetry (3.1). Five-dimensional fields transforming with eigenvalue $+1$ (-1) of the shift symmetry operator T are classified as periodic (antiperiodic) functions over the extra dimension: schematically,

$$\Phi(x^\mu, y + 2\pi R) = T\Phi(x^\mu, y) = \pm\Phi(x^\mu, y)\,. \tag{3.2}$$

However, due to the expanded Clifford algebra in five dimensions (see Appendix A for a more precise discussion), a merely periodic compactification only permits vectorlike bulk fermions. Instead, the fifth dimension must be compactified on an interval, which can be

constructed by identifying opposite sides of the circle under the $\mathbb{Z}_2$ symmetry:

$$(x^\mu, y) \longleftrightarrow (x^\mu, -y) \tag{3.3}$$

This process is visualized in Fig. 3.1. The resulting structure is an $S^1/\mathbb{Z}_2$ orbifold, containing two fixed (singular) points, $y = 0, \pm\pi R$, which are the locations of effective 3-*branes* (submanifolds with three spatial dimensions and one time dimension) that form the boundary of the extra dimension and can support localized four-dimensional fields. The region between the branes we refer to as the *bulk*.

The five-dimensional action for the bulk is required to be invariant under the orbifold $\mathbb{Z}_2$ symmetry transformation (3.3). Fields propagating in the bulk need not be identified at $\pm y$, but may differ by the eigenvalues of the $\mathbb{Z}_2$ symmetry operator Z: schematically,

$$\Phi(x^\mu, -y) = Z\Phi(x^\mu, y) = \pm\Phi(x^\mu, y)\,, \tag{3.4}$$

for $Z^2 = \mathrm{id}$.[2] Bulk fields can therefore be assigned definite parity under Z; those transforming with eigenvalue $+1$ (-1) are classified as even (odd) functions over the orbifold. Once a choice is made, this also determines the field parity on the four-dimensional boundary at the orbifold fixed point $y = 0$, because

$$\Phi(x^\mu, 0) = \pm\Phi(x^\mu, 0)\,. \tag{3.5}$$

The parity on the boundary at the $y = \pm\pi R$ fixed point depends on the periodicity of the field. We identify four possible bulk parity profiles, which we delineate in Table 3.1. We note that in order to remain continuous, fields must vanish on fixed-point boundaries where they have odd $\mathbb{Z}_2$ parity.

3.1.2 Spacetime geometry

The orbifold construction specifies a spacetime topology for the extra dimension that is effectively an interval, parametrized by $y \in [0, \pi R]$ and possibly bounded by 3-branes. The gravitational background (the spacetime geometry) on which fields propagate is a solution of the five-dimensional Einstein equations. The gravitational action for this configuration

[2] Transformation rules for specific fields are extracted from the relevant bulk actions in the context of AdS_5 in Appendix B.

Table 3.1: Possible S^1-periodicity and $\mathbb{Z}_2$-parity assignments for bulk fields. The left (right) sign refers to the $\mathbb{Z}_2$ parity at the $y = 0$ ($y = \pm\pi R$) orbifold fixed point.

boundary parity	$\mathbb{Z}_2$ parity	S^1 periodicity
$(+,+)$	even	periodic
$(+,-)$	even	antiperiodic
$(-,+)$	odd	antiperiodic
$(-,-)$	odd	periodic

takes the form

$$S = -\int d^4x \int_{-\pi R}^{\pi R} dy\, \sqrt{-g} \left(\frac{1}{2} M_5^3 \mathcal{R}_5 + \Lambda_5 + \Lambda_{(0)}\, 2\delta(y) + \Lambda_{(\pi R)}\, 2\delta(y - \pi R) \right) , \tag{3.6}$$

where $\mathcal{R}_5$ is the five-dimensional Ricci scalar, constructed from the five-dimensional metric g_{MN}, M_5 is the five-dimensional reduced Planck mass, Λ_5 is a cosmological constant for the bulk, and $\Lambda_{(0)}$ and $\Lambda_{(\pi R)}$ are brane tensions on the boundaries. These latter are essentially free parameters, with the only constraint that the *effective* four-dimensional Planck mass and cosmological constant should be reduce to their observed values. In order for the spacetime to respect four-dimensional Poincaré invariance, the metric must take the general form

$$ds^2 = e^{-2A(y)} \eta_{\mu\nu}\, \mathrm{d}x^\mu \mathrm{d}x^\nu + \mathrm{d}y^2 \equiv g_{MN}(y)\, \mathrm{d}x^M \mathrm{d}x^N , \tag{3.7}$$

where $\eta_{\mu\nu} = \mathrm{diag}(-1, +1, +1, +1)$ is the four-dimensional Minkowski metric with maximally positive signature. The function $A(y)$ gives information about how the geometry of the space varies in the fifth dimension. If $A(y)$ is constant, we say the space is *flat*; otherwise the space is called *warped*.

3.1.3 Kaluza-Klein theory

For bulk fields, the effect of the physical consequences of their propagation in the extra dimension are determined through a generalized Kaluza-Klein theory, in which each five-dimensional field is expanded into an infinite tower of four-dimensional states. Here, we give a sketch of the general procedure. A detailed description of the Kaluza-Klein theory for scalars, fermions, and gauge bosons is presented in Appendix B in the context of AdS_5

[although many of the results are presented in terms of the generalized metric profile $A(y)$].

Starting with the five-dimensional action S_5 for each field, the classical equations of motion and the associated boundary conditions may be derived using the variational principle. In generic form, the variation of the action can be written as

$$\delta S_5 = \int d^5x\, \delta\Phi\, (\mathcal{D}\Phi) + \int d^4x\, \delta\Phi\, (\mathcal{B}\Phi)\,|_{y=0,\pi R}\,, \tag{3.8}$$

where Φ stands for a generic bulk field and $\mathcal{D}$ and $\mathcal{B}$ are differential operators acting on the field in the bulk and on the boundaries, respectively. In order for the variation δS_5 to vanish, we require both bulk and boundary terms in (3.8) to vanish separately. For the bulk term, this condition determines the *equations of motion* for the field:

$$\mathcal{D}\Phi = 0\,. \tag{3.9}$$

From the boundary terms,[3] we derive the *boundary conditions*, which must be satisfied by all solutions to the equations of motion. Typically, these may be either *Dirichlet* (D),

$$\delta\Phi\,|_{y=0,\pi R} = 0\,, \tag{3.10}$$

if the field has odd $\mathbb{Z}_2$ parity on a boundary, or *Neumann* (N),

$$\mathcal{B}\Phi\,|_{y=0,\pi R} = 0\,, \tag{3.11}$$

if the field has even $\mathbb{Z}_2$ parity. In general, there are thus four possible combinations of boundary conditions for each bulk field, corresponding to the four possible parity configurations detailed in Table 3.1.[4] We detail these in Table 3.2. The middle two combinations are commonly referred to as *twisted* boundary conditions. In the presence of additional operators on the branes, *mixed* boundary conditions may arise, involving both Neumann and Dirichlet terms.[5]

[3] The boundary terms for the four extended spacetime dimensions vanish, as we assume $\Phi \to 0$ as $x^\mu \to \pm\infty$.

[4] The difference between the orbifold and an interval compactification lies in the physical interpretation of the boundary conditions of bulk fields at the four-dimensional boundaries of the extra dimension. For an orbifold, the boundary conditions are related to the topology of the spacetime and the symmetries of the field: they imply certain quantum numbers for a bulk field. For an interval, this is not the case, although they still are constrained by the requirement that the solution to the equations of motion of a bulk field describes sensible physics.

[5] Examples of such boundary conditions may be seen in Appendix B, where we consider boundary mass terms for scalar and fermion fields. The presence of such boundary masses leads to the violation of five-dimensional momentum conservation on the branes.

Table 3.2: Correspondence between parity assignments and boundary conditions for bulk fields on the orbifold. The left (right) term in the tuples refers to the $\mathbb{Z}_2$ parity or type of boundary condition at the $y = 0$ ($y = \pm\pi R$) orbifold fixed point.

boundary parity	boundary conditions
$(+,+)$	(N,N)
$(+,-)$	(N,D)
$(-,+)$	(D,N)
$(-,-)$	(D,D)

In order to solve the five-dimensional equations of motion, we assume *Kaluza-Klein decompositions* (separation of variables) of the fields of the form

$$\Phi(x^\mu, y) = \sum_{n=0}^{\infty} \Phi^{(n)}(x^\mu)\, f_\Phi^{(n)}(y)\,, \tag{3.12}$$

where the *Kaluza-Klein eigenmodes* $\Phi^{(n)}$ are four-dimensional states obeying four-dimensional field equations with *mass eigenvalues* m_n. The series is indexed in order of increasing mass eigenvalues, such that the five-dimensional field can be viewed as an infinite *Kaluza-Klein tower* (in mass energy) of four-dimensional states, each with an associated *bulk profiles* $f_\Phi^{(n)}$. The bulk profiles obey orthonormality conditions of the form

$$\int_{-\pi R}^{\pi R} dy\, e^{2d_\Phi A(y)} f_\Phi^{(m)}(y) f_\Phi^{(n)}(y) = \delta_{mn} \tag{3.13}$$

where d_Φ is the mass dimension of the KK eigenmodes. When rescaled according to

$$\tilde{f}_\Phi^{(n)}(y) = e^{d_\Phi A(y)} f_\Phi^{(n)}(y)\,, \tag{3.14}$$

the bulk profiles give the *localization* of the KK eigenmodes along the extra dimension, specifying their *overlap* with other bulk fields and the boundary branes. Inserting the KK decomposition into the equation of motion and boundary conditions for the five-dimensional field gives rise to corresponding conditions on the profiles.

We note that the choice of orbifold parity assignments has consequences for the low-energy

spectrum of the theory. Fields with at least one Dirichlet boundary condition (i.e., fields with odd parity on at least on boundary) do not have a solution with zero mass eigenvalue. Massless Kaluza-Klein *zero modes* can only arise for fields with $(+,+)$ boundary parity, corresponding to (N,N) boundary conditions.

3.2 Supersymmetry in a Slice of AdS$_5$

We now consider the warped spacetime geometry of the Randall-Sundrum model [16] (RS1) compactified over an $S^1/\mathbb{Z}_2$ orbifold. The five-dimensional gravitational action takes the form (3.6). The classical anti-de Sitter solution, the solution to the five-dimensional Einstein equations with a negative bulk cosmological constant, is given by

$$A(y) = 2k\,|y|\ , \tag{3.15}$$

or

$$ds^2 = e^{-2k|y|}\eta_{\mu\nu}\,\mathrm{d}x^\mu \mathrm{d}x^\nu + dy^2 = g_{MN}\,\mathrm{d}x^M \mathrm{d}x^N\,, \tag{3.16}$$

where

$$k \equiv \sqrt{-\frac{\Lambda_5}{6M_5^3}} \tag{3.17}$$

is the AdS curvature scale (and $1/k$ is the curvature radius). This solution requires that the brane tensions are tuned against the bulk cosmological constant,

$$\Lambda_{(0)} = -\Lambda_{(\pi R)} = -\frac{\Lambda_5}{2k}\,, \tag{3.18}$$

as a consequence of four-dimensional Poincaré invariance (i.e., in order to ensure that the effective cosmological constant on each brane vanishes and the subspace geometry is Minkowski: see [113]). We do not specify a particular mechanism to stabilize the extra dimension in this configuration. One possibility is the Goldberger-Wise mechanism [114–116].

The four-dimensional reduced Planck mass is related to M_5 as

$$M_{\rm P}^2 = \frac{M_5^3}{k}\left(1 - e^{-2\pi kR}\right) \simeq \frac{M_5^3}{k}\,, \tag{3.19}$$

where we are assuming $\pi kR \gg 1$ in the latter approximation. In order for the classical metric solution to be valid, the AdS curvature must be small enough compared to the five-dimensional Planck scale so that higher-order curvature terms in the five-dimensional

gravitational action can be neglected. This requires $k/M_5 \lesssim 2$ [117], but, in the following, we have taken k to be generically smaller, choosing $k/M_5 = 0.1$. The resulting geometry is a slice of AdS_5, valid as an effective field theory description of spacetime at energies below the Planck scale. A possible ultraviolet completion for this configuration comes from string theory, where a five-dimensional "warped throat" geometry can arise in an enlarged spacetime after compactification on a six-dimensional manifold [118–122]. In these scenarios, one of the six dimensions of the internal space can become much large than the others (which are typically of order of the Planck length M_{P}^{-1}), resulting in a thin protuberance of AdS spacetime emerging from the internal manifold and terminating in an infrared singularity. With this account in mind, we interpret the 3-brane located at $y = 0$ in the extra dimension as an ultraviolet (UV) cutoff in our theory hiding the underlying Plank-scale dynamics and the 3-brane located at $y = \pi R$ as the infrared (IR) cutoff below which the extra dimension can no longer be resolved and spacetime is effectively four-dimensional. In the following, we will refer to these branes as the UV and IR branes, respectively. The cutoff scale of the UV brane is

$$\Lambda_{\mathrm{UV}} = M_5 \,, \tag{3.20}$$

while the scale of the IR brane is

$$\Lambda_{\mathrm{IR}} = \Lambda_{\mathrm{UV}} e^{-\pi k R} \,. \tag{3.21}$$

The curvature scale on the IR brane is

$$k_{\mathrm{IR}} = k e^{-\pi k R} \,. \tag{3.22}$$

The warped geometry thus naturally generates a separation of scales. The curvature of the bulk has the effect of suppressing the effective mass scale of the theory exponentially as a function of position of along the fifth dimension. We illustrate this behavior schematically in Fig. 3.2.

We note for future reference that the metric solution (3.7) with the AdS warp function (3.15) can be written in terms of a conformal coordinate along the fifth dimension:

$$ds^2 = \frac{1}{(kz)^2}\, \eta_{\mu\nu}\, \mathrm{d}x^\mu \mathrm{d}x^\nu + \mathrm{d}z^2 = g_{MN}\, \mathrm{d}x^M \mathrm{d}x^N \,, \tag{3.23}$$

where

$$z = \frac{e^A}{k} = \frac{e^{k|y|}}{k} \tag{3.24}$$

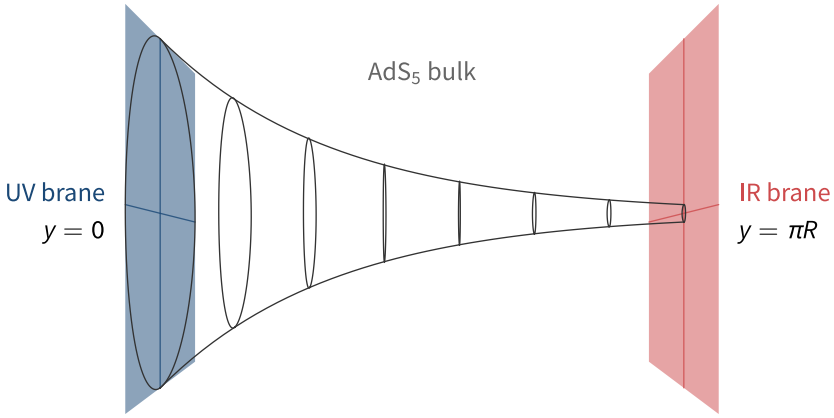

Figure 3.2: Visualization of a slice of AdS_5.

ranges from $z_{UV} = 1/k$ at the UV brane to $z_{IR} = 1/k_{IR}$ at the IR brane.[6]

3.2.1 The five-dimensional MSSM

Anti-de Sitter spacetime arises naturally in gauged supergravity as the maximally symmetric solution of Einstein equations with a negative cosmological constant. In five dimensions, the irreducible representation spin-$\frac{1}{2}$ of the Lorentz group SO(4,1) is a four-component Dirac spinor with eight real components (see Appendix A), which means there are a minimum of 8 supersymmetric charges (supercharges). The field content of a theory of minimal $\mathcal{N} = 1$ supersymmetry in five dimensions is thus the same as that of $\mathcal{N} = 2$ supersymmetry in four. [Although due to the curvature of anti-de Sitter spacetime, the momentum operator P_μ does not commute with supercharges and P^2 is not a Casimir operator (unlike in flat spacetime), such that fields belonging to the same supermultiplet will in general have different masses.] Compactification over the orbifold projects out half or all of the five-dimensional supercharges, leaving a residual $\mathcal{N} = 1$ or $\mathcal{N} = 0$ supersymmetry in four dimensions [94, 95].

The field theory of the AdS_5 bulk is developed in Appendix B, and in Appendix D we describe the multiplet structure of supersymmetry in a slice of AdS_5. Here, we construct a five-dimensional theory in which the minimal supersymmetric model survives as the effective 4D description below the scale of compactification. Based on the results outlined in Appendix D, it is clear that in order for the orbifold compactification to at least partially preserve supersymmetry it is necessary that the all bulk fields are periodic (as opposed

[6] Because z is restricted to positive values, it provides a double covering of the orbifold space.

to antiperiodic) over the orbifold. This corresponds to a choice of boundary parities that permits half of the bulk fields to have zero modes in their Kaluza-Klein decompositions, such that a four-dimensional $\mathcal{N} = 1$ supersymmetry remains at the massless level, while the massive Kaluza-Klein states form a tower of 4D $\mathcal{N} = 2$ supermultiplets with masses of order Λ_{IR}.

Thus, to obtain the MSSM field content at low energy, we embed the $\mathcal{N} = 1$ gravity, vector, and chiral matter superfields of the MSSM into periodic 5D $\mathcal{N} = 1$ gravity supermultiplets, vector supermultiplets, and hypermultiplets respectively, and identify the supermultiplets of the MSSM out of the resulting zero modes. For the gravity supermultiplet, we choose the vielbein and the left-handed component of the gravitino to have even orbifold parity, such that the massless theory contains the graviton and gravitino zero modes. The bulk profiles of the graviton and gravitino zero modes are UV-localized, taking the forms (B.178) and (B.151), respectively.

Besides gravity, we introduce the $\text{SU}(3)_c \times \text{SU}(2)_L \times \text{U}(1)_Y$ gauge content of the MSSM. In the context of a grand unified theory, this takes the form of a vector supermultiplet, charged under the GUT symmetry group (see below for further details), of which the gauge boson and one of the components of the gaugino are chosen to have even orbifold parity such that their zero modes are present in the massless theory as the MSSM gauge supermultiplet. The bulk profiles of the gauge boson and gaugino zero modes are conformally flat. The vector boson zero-mode profile is given in (B.123) while the gaugino zero-mode profile is that of a bulk Dirac fermion (B.65) with $c_L = \frac{1}{2}$.

We also introduce three generations of matter. Because of the vectorlike nature of the AdS_5 bulk, a full hypermultiplet must be added for each chiral multiplet of the MSSM, a chiral theory being recovered at the massless level. The orbifold parities of the matter fields are chosen so that the $\text{SU}(2)_L$ doublets Q and L are composed of left-handed zero-modes and the singlets $\bar{u}$, $\bar{d}$, and $\bar{e}$ (and $\bar{\nu}$ if Dirac neutrinos are included) of right-handed zero-modes. The bulk profiles of the left-handed and right-handed fermion zero modes take the forms (B.65) and (B.65), respectively, while the bulk profile for the scalar zero modes is given by (B.28). Due to the supersymmetric condition (D.13), the localizations of the fermion and scalar of a hypermultiplet are controlled by the same hypermultiplet localization parameter c. The zero modes of the matter hypermultiplets may thus be localized anywhere in the bulk.

The warped geometry naturally generates a separation of scales that can be used to explain the hierarchy between the scale of supersymmetry breaking and the Planck scale. The IR

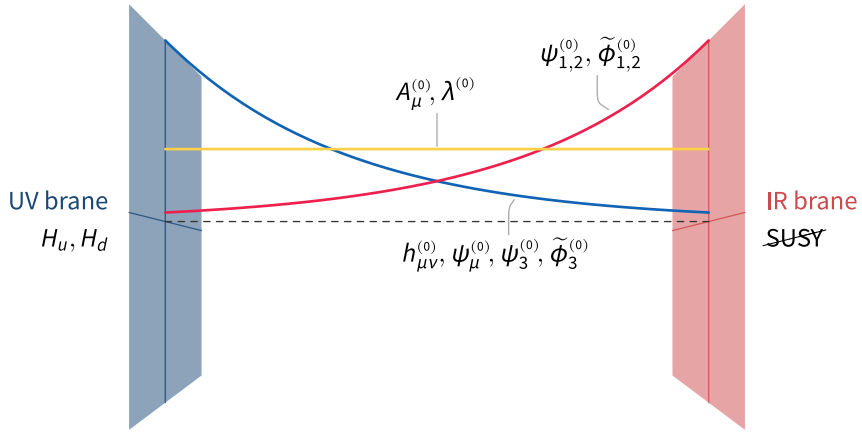

Figure 3.3: Schematic diagram of the localization structure of the MSSM field content in the 5D model.

brane is therefore identified with the scale where supersymmetry is broken; the bulk and UV brane remain supersymmetric. The $\mathcal{N} = 1$ Higgs supermultiplets are 4D fields confined to the UV brane. The MSSM chiral matter fields propagating in the bulk couple to the Higgs fields with brane-localized Yukawa couplings. As discussed in Chapter 4, the degree of overlap between a particular bulk fermion zero-mode profile and a UV-localized Higgs field determines its effective 4D Yukawa coupling and thus the size of the corresponding fermion mass after electroweak symmetry breaking. In this setup, third-generation fermion zero modes are therefore UV-localized, whereas the lighter first- and second-generation fermions have more IR-localized zero modes.

Because the localization of the fermion zero mode determines the localization of the entire hypermultiplet, the scalar zero modes share the fermion bulk geography: the third-generation sfermions are generally UV localized and the first- and second-generation sfermions are IR localized. Due to the properties of localization, the effective coupling strength of each superfield on the IR brane is inversely related to its coupling strength on the UV brane. Therefore, when supersymmetry is broken on the IR brane, the localization of the sfermions induced by the fermion mass spectrum results in an inverted scalar soft mass spectrum: light fermions have heavy superpartners, while heavy fermions have light superpartners. We give a detailed account of supersymmetry breaking in Chapter 5 and then explore the physics of this distinctive supersymmetric particle spectrum in Chapters 8 and 9. A schematic diagram of the localization structure of the 5D model is depicted in Fig. 3.3.

3.2.2 Grand unification and localized gauge symmetry breaking

In order to take advantage of the prospects of gauge unification offered by the addition of the supersymmetric particle content, we wish to embed the $\mathrm{SU}(3)_c \times \mathrm{SU}(2)_L \times \mathrm{U}(1)_Y$ gauge theory of the standard model into a larger GUT symmetry group such as SU(5). The supersymmetric gauge sector action therefore takes the form (D.25), where g_5 is the unified gauge coupling. Radiative corrections are expected to give rise to brane-localized kinetic terms (see Refs. [123–126]), introducing additional four-dimensional brane couplings:

$$S_5 \supset -\frac{1}{g_{\mathrm{UV}}^2} \int d^5x \, \sqrt{-g} \left(\frac{1}{4} F^a_{\mu\nu} F^{\mu\nu a} + \frac{1}{2} \bar{\lambda}^a_i \Gamma^\mu D_\mu \lambda^a_i \right) 2\delta(y) \,. \tag{3.25a}$$

and

$$S_5 \supset -\frac{1}{g_{\mathrm{IR}}^2} \int d^5x \, \sqrt{-g} \left(\frac{1}{4} F^a_{\mu\nu} F^{\mu\nu a} + \frac{1}{2} \bar{\lambda}^a_i \Gamma^\mu D_\mu \lambda^a_i \right) 2\delta(y - \pi R) \,. \tag{3.25b}$$

The evolution of gauge couplings in a slice of AdS_5 background is logarithmic [127–139]. Therefore, the unification of the standard model gauge coupling constants requires that the unifying symmetry is broken at a high scale $m_{\mathrm{GUT}} \sim 10^{16}\,\mathrm{GeV}$, which we assume is much greater than the compactification scale $\Lambda_{\mathrm{C}} = k_{\mathrm{IR}} \sim \Lambda_{\mathrm{IR}}$. Localizing the symmetry breaking to the UV brane, we introduce a Higgs field that is charged under the GUT gauge group. When the Higgs acquires a VEV $v_{\mathrm{GUT}} \sim m_{\mathrm{GUT}}$, the GUT symmetry is broken to $\mathcal{G}_{\mathrm{SM}}$. Below the scale m_{GUT}, the radiative contribution to the action on UV brane where the GUT symmetry is broken now takes the form

$$S_5 \supset -\frac{1}{g_{\mathrm{UV},a}^2} \int d^5x \, \sqrt{-g} \left(\frac{1}{4} F^a_{MN} F^{MNa} + \frac{1}{2} \bar{\lambda}^a_i \Gamma^M D_M \lambda^a_i \right) 2\delta(y) \,, \tag{3.26}$$

where the brane-localized gauge coupling is in general not the same for $\mathrm{SU}(3)_c$, $\mathrm{SU}(2)_L$, $\mathrm{U}(1)_Y$, and the quotient group of the GUT symmetry modulo the standard model groups (e.g., $\mathrm{SU}(5)/\mathcal{G}_{\mathrm{SM}}$), as indicated by the gauge index. The kinetic terms on the IR brane do not feel the effect of the breaking and remain symmetric under the GUT group.

The only surviving degrees of freedom in the low-energy theory (below Λ_{C}) are the zero modes of the vector supermultiplets of the standard model gauge groups. The relation between the four-dimensional gauge coupling g_a^2 and the fundamental parameters of the

theory takes the form [124–126]

$$\frac{1}{g_a^2} = \frac{\pi R}{g_5^2} + \frac{1}{g_{\mathrm{IR}}^2} + \frac{1}{g_{\mathrm{UV},a}^2}\,, \tag{3.27}$$

where the first two terms on the right-hand side are essentially GUT-symmetric, but the last one contains nonuniversal logarithms from loop effects.

3.2.3 Higgsino mass

Because the Higgs fields are confined to the UV-brane, they do not couple directly to the supersymmetry-breaking sector on the IR brane, and therefore the generation of a μ term via a Giudice-Masiero mechanism [140] is forbidden. Instead, to generate a sizable μ term, we consider the Kim-Nilles mechanism [141]. We first note that if $\mu = 0$, the MSSM has a global U(1) Peccei-Quinn symmetry, under which the charges of the chiral superfields of the theory take the values in Table 3.3.[7] If we introduce an $\mathrm{SU}(3)_c \times \mathrm{SU}(2)_L \times \mathrm{U}(1)_Y$ singlet chiral superfield on the UV brane with Peccei-Quinn charge -1, then a nonrenormalizable superpotential term

$$W_{\mathrm{KN}} = \frac{\kappa_\mu}{2\Lambda_{\mathrm{UV}}} S^2 H_u H_d\,, \tag{3.28}$$

where κ_μ is a dimensionless order-one coupling, is allowed on the UV brane. Assuming that the Peccei-Quinn symmetry is spontaneously broken by a nonzero vacuum expectation value $\langle S \rangle \sim f$, an effective μ term

$$\mu \simeq \frac{\kappa_\mu f^2}{2\Lambda_{\mathrm{UV}}} \tag{3.29}$$

is then generated. Because the global symmetry is anomalous (and assuming all other sources of breaking are small), the pseudo-Nambu-Goldstone boson associated with the spontaneous symmetry breaking can be identified with the axion. This axion is of the invisible Dine-Fischler-Srednicki-Zhitnitsky (DFSZ) type [142, 143], and is consistent with the present astrophysical constraints (see Ref. [20] for a review) provided that

$$10^9\,\mathrm{GeV} \lesssim f \lesssim 10^{12}\,\mathrm{GeV}\,. \tag{3.30}$$

[7] In the five-dimensional theory, the even bulk fields in the hypermultiplet take the MSSM charges, while the charges of the odd fields are opposite (one can see this by considering the bulk Dirac fermion mass, which mixes the even and odd components of the fermion).

Table 3.3: Peccei-Quinn charges of the MSSM chiral superfields, chosen to allow Yukawa interactions between Higgs superfields and the matter superfields. Also included is the Kim-Nilles singlet S, which has the charge necessary to allow the superpotential term (3.28). These charge assignments are not unique, as any multiple of weak hypercharge or $B - L$ may be added.

	Peccei-Quinn charge
$H_{u,d}$	$+1$
Q, L	-1
$\bar{u}, \bar{d}, \bar{e}$	0
S	-1

For this range of f, (3.29) implies

$$100\,\mathrm{GeV} \lesssim \mu \lesssim 100\,\mathrm{TeV}\,. \tag{3.31}$$

Thus, using the Kim-Nilles mechanism, we can solve the strong CP problem and generate the required values of the μ term.[8]

3.2.4 Numerical Kaluza-Klein Spectra

Approximate expressions for the Kaluza-Klein masses for bulk fields are given in Appendix C. A more exact determination of the Kaluza-Klein spectra can be achieved by solving the relevant quantization conditions numerically. Computationally, the roots of the combinations of Bessel function cross-products that comprise the quantization conditions (equivalently, the denominators of the associated propagator functions) are not difficult to extract. However, there are two complicating factors. The first is the potential for the root corresponding to

[8] We note that the Peccei-Quinn charge assignments also allow us to write a soft supersymmetry breaking term

$$S_5 \supset -\int d^5x\,\sqrt{-g}\left(\kappa_b S^2 H_u H_d + \text{c.c.}\right) 2\delta(y)\,, \tag{3.32}$$

where κ_b is a dimensionless order-one coupling. After S gets a VEV, a soft b term is induced as

$$b = \frac{\kappa_b f^2}{\Lambda_{\text{UV}}}\,. \tag{3.33}$$

Although this supersymmetry-breaking effect is a natural extension of the Kim-Nilles effect, we do not include it in our model, as we wish to confine the supersymmetry-breaking dynamics to the IR brane.

the zero-mode mass to be exponentially smaller than the roots of the massive states. This difference in scale can make the zero-mode root challenging for most root-finding algorithms to isolate unless the scale of the search is correctly specified. The analytic approximations for the zero-mode masses derived in Appendix C are useful in this instance, as they can be used to accurately locate a starting point for the search of the same scale as the desired root.[9]

The second complicating factor is the periodicity of the roots corresponding to the heavy Kaluza-Klein masses. Because any given interval will contain a number of roots, many of approximately the same scale, it can be difficult to determine precisely *which* root has been extracted from a given starting point by a given root-finding algorithm, especially as the particular numeric recipe of most algorithms is relatively opaque.[10] The analytic cross-product asymptotic expansion approximation (C.30) does become accurate enough for large n that it can likely be used as a starting point in a traditional root search with a good degree of confidence that the correct root will subsequently be returned. For smaller n, where the cross-product approximation is not a good, the large Bessel-zero asymptotic expansion approximation (C.36) may provide an alternative starting point estimation, but in general roots can only be correctly identified if the root-finder can resolve all of the roots in a given interval. This requires (as a sufficient condition) that the quantization condition be numerically constructed (sampled with sufficient density) over the entire interval. The execution of this exact process is a feature of another class of solutions to numeric problems, namely those involving differential equations. The algorithms used for numerically constructing the solutions to differential equations can therefore be naturally adapted to root-finding, particularly those packaged with an event-locator routine. The implementation used in this work is the Wolfram Language package NDRoot, which leverages the Wolfram Language numeric differential equation solver NDSolve to find function roots [144].[11]

[9] They are particularly useful in the intermediate region in which the zero-mode mass is no longer small, but not yet of the same scale as the heavier Kaluza-Klein masses. This is the upper range of the validity of the analytic approximation.

[10] For reference, we refer the reader to the FindRoot routine of the Wolfram Language. Although various different root-finding methods (such as various flavors of Newton's method and secant methods, Brent's method, etc.) can be specified, the behavior of the internal algorithms cannot be precisely controlled.

[11] The code is also available from the author upon request.

3.3 The Four-Dimensional Dual Theory

Remarkably, the five-dimensional theory in a slice AdS spacetime can be given a four-dimensional description as a strongly coupled large-N gauge theory. This is a result originating in the *AdS/CFT correspondence*, which conjectures a duality between type IIB string theory on $\mathrm{AdS}_5 \times S^5$ and a four-dimensional $\mathcal{N} = 4$ SU(N) gauge theory [100]. In part, the correspondence is motivated by the fact that the symmetries of these two theories are identical: the isometry of S^5 is the rotation group $\mathrm{SO}(6) \cong \mathrm{SU}(4)$, which is the same as the R-symmetry group of the supersymmetric gauge theory, and the isometry group of AdS_5 is precisely the conformal group in four dimensions, implying that the 4D gauge theory is a conformal field theory (CFT). The coupling g of the SU(N) Yang-Mills gauge theory is related to the string theory parameters as

$$4\pi g^2 N = \frac{R_{\mathrm{AdS}}}{l_s}\,, \tag{3.34}$$

where R_{AdS} is the curvature radius of AdS_5 and l_s is the string length. If the curvature scale of AdS_5 is much greater than the string length ($R_{\mathrm{AdS}} \gg l_s$), string corrections to the bulk gravity description can be neglected. For a classical AdS_5 background, the dual 4D CFT is therefore strongly coupled, as (3.34) implies $g^2 N \gg 1$. In this limit, therefore, the AdS/CFT correspondence is the holographic[12] duality between strong coupling in four dimensions and

[12]The relationship is holographic in the sense that the dynamics of field theory in four dimensions can be described by the geometry of a theory in one higher dimension. This can be made more precise by noting that the 5D bulk description is characterized by set of bulk fields, while a CFT is characterized by a set of operators. Therefore, for every 5D bulk field Φ there is an associated operator $\mathcal{O}$ of the CFT

$$\Phi \Longleftrightarrow \mathcal{O}\,, \tag{3.35}$$

where the boundary value of the bulk field

$$\Phi\,\big|_{\partial \mathrm{AdS}} \equiv \phi_0 \tag{3.36}$$

acts as a source field for the CFT operator $\mathcal{O}$. Then, the AdS/CFT correspondence can be quantified by define the generating functional [119, 145]

$$Z[\phi_0] = \int \mathcal{D}\phi_{\mathrm{CFT}}\, e^{-S[\phi_{\mathrm{CFT}}] - \int d^4x\, \phi_0 \mathcal{O}} = \int_{\phi_0} \mathcal{D}\phi\, e^{-S_{\mathrm{AdS}}[\phi]} \equiv e^{iS_{\mathrm{eff}}[\phi_0]}\,. \tag{3.37}$$

Here, S_{CFT} is the CFT action with ϕ_{CFT} generically denoting the CFT fields and S_{AdS} is the 5D bulk action. The effective action S_{eff} is obtained by integrating out the bulk degrees of freedom, and which, according to the correspondence, can be used to n-point functions (correlators) in the CFT: schematically,

$$\langle \mathcal{O} \cdots \mathcal{O} \rangle = \frac{\delta^n S_{\mathrm{eff}}}{\delta\phi_0 \cdots \delta\phi_0}\,. \tag{3.38}$$

weakly coupled gravity in five dimensions.

With this correspondence in mind, we construct here the four-dimensional partially composite model dual to supersymmetry in a slice of AdS_5. We note that because of the compactification of the extra dimension, the gravitational background has lower symmetry than pure AdS_5 spacetime, and instead corresponds to a truncation of the spacetime (a slice of AdS_5). The CFT of the partially composite model therefore must therefore also have lower symmetry than the full conformal group, with the conformal invariance broken by two mass scales: the UV cutoff of the theory Λ_{UV} and the confinement scale Λ_{IR}. While no rigorous proof of the AdS/CFT conjecture has yet been formulated, the correspondence is mathematically nontrivial, and an *AdS/CFT dictionary* to relate the two dual descriptions can be established [146]. We sketch the contents of such a dictionary for our partially composite model in Sec. 3.3.2

3.3.1 Supersymmetric partial compositeness

Partial compositeness [147] is a theory inspired by attempts such as (extended) technicolor [148–159] and the composite Higgs mechanism [160–165] to explain the origins of the standard model fermion masses and break electroweak symmetry by proposing new or extended strong dynamics, rather than by recourse to a fundamental Higgs boson.

In its modern formulation, a partially composite theory is composed of two sectors, an elementary sector defined at a high scale Λ_{UV}, and a composite sector, which arises at the lower scale Λ_{IR}, where the strong [SU(N)] dynamics that governs the theory confines. Operators in the composite sector mix with elementary fields with relevance that depends on their anomalous dimensions. Below the scale of confinement, the composite operators are each associated with a tower of massive resonances. Due to the elementary-composite mixing, the mass eigenstates of the theory are admixtures of elementary fields and composite resonances. The *degree of compositeness* of an eigenstate depends on the anomalous dimension of the associated composite operator (i.e., on the relevance of the elementary-composite mixing that gives rise to the state) and determines the interaction strength of the eigenstate with elements of the elementary and composite sectors and other mass eigenstates.

When partial compositeness is combined with supersymmetry, the resulting theory is the synthesis of the virtues of both explanatory paradigms. Notably, it can provide a mechanism that explains the origin of the inverted sfermion mass hierarchy and predicts the sparticle spectrum [17, 18]. Assuming that the Higgs fields are elementary, while the standard model

fields are admixtures arising from the linear mixing of elementary states with composite operators, the magnitudes of the corresponding Yukawa couplings then depend on the degree of compositeness of the standard model fermions. To obtain an order-one Yukawa coupling with the Higgs, the top quark must be mostly elementary, while, since the elementary and composite sectors mix with an irrelevant coupling, the smallness of the electron Yukawa coupling follows from assuming that the electron is mostly composite. The remainder of the standard model Yukawa couplings are generated by varying degrees of compositeness.

If one now further assumes that the strong dynamics is responsible for breaking supersymmetry, then an interesting correlation between fermion and sfermion masses results from partial compositeness. Supersymmetric operators that linearly mix with elementary fermions can now communicate supersymmetry breaking to the elementary sector. In this way, composite sfermions obtain large supersymmetry breaking masses, while elementary sfermions obtain hierarchically smaller soft masses. The fermion mass hierarchy is therefore inversely related to the sfermion mass hierarchy: light (elementary) stops correspond to heavy (elementary) top quarks, while heavy (composite) selectrons are related to the light (composite) electron. Together with the fact that gauginos and Higgsinos are predominantly elementary—and therefore lighter than the composite sfermions—a split supersymmetric spectrum arises where the fermion mass hierarchy is naturally explained. It is the anomalous dimensions of the corresponding supersymmetric operators that simultaneously controls the fermion and sfermion masses.

The details of the supersymmetric generalization of partial compositeness are given in Refs. [17, 18]. Here, to illustrate the mechanism of this model, we construct the theory for a single generation of chiral matter. In the elementary sector, chiral superfields take the usual form

$$\Phi = \phi + \sqrt{2}\,\theta\,\psi + \theta\theta\,F\,, \tag{3.39}$$

where ϕ is a complex scalar, ψ is a Weyl fermion, and F is an auxiliary field. The corresponding supersymmetric chiral operator is

$$\mathcal{O} = \mathcal{O}_\phi + \sqrt{2}\,\theta\,\mathcal{O}_\psi + \theta\theta\,\mathcal{O}_F\,, \tag{3.40}$$

where the scaling dimensions of the component operators are

$$\dim \mathcal{O}_\phi = 1 + \delta_\mathcal{O}\,, \tag{3.41a}$$

$$\dim \mathcal{O}_\psi = \tfrac{3}{2} + \delta_\mathcal{O}\,, \tag{3.41b}$$

$$\dim \mathcal{O}_F = 2 + \delta_{\mathcal{O}} \,, \tag{3.41c}$$

and $\delta_{\mathcal{O}} \geq 0$ is the anomalous dimension of the chiral operator [166]. The supersymmetric Lagrangian contains separate elementary and composite sectors, together with linear mixing terms of the form $[\Phi\mathcal{O}^c]_F$ for each chiral superfield Φ and charge-conjugate composite operator $\mathcal{O}^c$. At the UV cutoff scale $\Lambda_{\rm UV}$, it is given by

$$\mathcal{L}_\Phi = [\Phi^\dagger\Phi]_D + \frac{1}{\Lambda_{\rm UV}^{\delta-1}} \left([\Phi\mathcal{O}^c]_F + \text{H.c.}\right) \,, \tag{3.42}$$

where δ is the anomalous dimension of $\mathcal{O}^c$. We have taken order-one UV coefficients for the higher-dimension terms and omitted a kinetic mixing between the elementary and composite sectors in our minimal setup. The composite sector is assumed to confine at an infrared scale $\Lambda_{\rm IR}$.

In the limit of large N, the two-point function for the composite operator components can be written as a sum over one-particle states. For example, to leading order in $1/N$ for the scalar component,

$$\langle \mathcal{O}_\phi(p)\, \mathcal{O}_\phi(-p)\rangle = \sum_n \frac{a_n^2}{p^2 + m_n^2} \,, \tag{3.43}$$

where

$$a_n = \langle 0|\mathcal{O}_\phi|n\rangle \propto \frac{\sqrt{N}}{4\pi} \tag{3.44}$$

is the matrix element for $\mathcal{O}$ to create the nth state, with mass m_n, from the vacuum [167–169]. The elementary-composite mixing in the Lagrangian (3.42) mixes the elementary fields (ϕ, ψ) with the composite resonance states. Including for simplicity just the lowest-lying composite state $\Phi^{(1)} = (\phi^{(1)}, \psi^{(1)})$ with mass $m_\Phi^{(n)} = g_\Phi^{(1)}\Lambda_{\rm IR}$, the two-state system can be diagonalized to obtain the massless eigenstate $\Phi_0 = (\phi_0, \psi_0)$ [17]

$$|\Phi_0\rangle \simeq \mathcal{N}_\Phi \left\{ |\Phi\rangle - \frac{1}{\sqrt{\zeta_\Phi}\, g_\Phi^{(1)}} \sqrt{\frac{\delta - 1}{(\Lambda_{\rm IR}/\Lambda_{\rm UV})^{2(1-\delta)} - 1}}\, |\Phi^{(1)}\rangle \right\} \,, \tag{3.45}$$

where $g_\Phi^{(1)}$ and ζ_Φ are order-one constants, and $\mathcal{N}_\Phi$ is a normalization constant. Given that $\Lambda_{\rm IR} \ll \Lambda_{\rm UV}$, this expression shows that the massless eigenstates are mostly elementary for $\delta > 1$, whereas for $0 \leq \delta < 1$ they are an admixture of elementary and composite states.

This elementary-composite admixture of the massless eigenstate can be used to explain the fermion mass hierarchy [170], and then predict the sfermion mass spectrum. Consider elementary chiral fermions $\psi_{L,R}$ that are coupled to the elementary Higgs H via the

interaction

$$\mathcal{L} \supset \lambda\, \psi_L\, \psi_R\, H + \text{H.c.} \tag{3.46}$$

where λ is an order-one proto-Yukawa coupling (in this simplified model, we restrict to one fermion generation and ignore the distinction between H_u and H_d). Diagonalizing the fermion Lagrangian with the Higgs contribution gives the Yukawa coupling expression

$$y_\psi \simeq \begin{cases} \dfrac{\lambda}{\zeta_\Phi}\,(\delta-1)\,\dfrac{16\pi^2}{N} & \text{for } \delta \geq 1\,, \\ \dfrac{\lambda}{\zeta_\Phi}\,(1-\delta)\,\dfrac{16\pi^2}{N}\left(\dfrac{\Lambda_{\text{IR}}}{\Lambda_{\text{UV}}}\right)^{2(1-\delta)} & \text{for } 0 \leq \delta < 1\,, \end{cases} \tag{3.47}$$

where we have assumed that $\delta \equiv \delta_L = \delta_R$. We see that when $\delta \geq 1$ (corresponding to a mostly elementary fermion), the Yukawa coupling is of order one for sufficiently large N. Conversely, when $0 \leq \delta < 1$ (corresponding to a sizable composite admixture), the Yukawa coupling has a power-law suppression that depends on the degree of compositeness. This explains why composite fermions (identified with the first- and second-generation standard model fermions) have small Yukawa couplings, while elementary fermions (such as the top quark) have order-one Yukawa couplings.

The composite sector is also responsible for supersymmetry breaking. Soft scalar masses are generated only for the composite sector fields since there is no direct coupling of the supersymmetry breaking to elementary fields. For example, the massive scalar field, $\phi^{(1)}$ obtains a soft mass

$$\xi_4 \frac{(g_\Phi^{(1)})^2}{\Lambda_{\text{IR}}^2}\,[\mathcal{X}^\dagger \mathcal{X}\, \Phi^{(1)\dagger}\Phi^{(1)}]_D = \xi_4\,(g_\Phi^{(1)})^2\,\frac{|F_\mathcal{X}|^2}{\Lambda_{\text{IR}}^2}\,\phi^{(1)\dagger}\phi^{(1)}\,, \tag{3.48}$$

where $\mathcal{X} = \theta\theta\, F_\mathcal{X}$ is a composite-sector spurion and ξ_4 is a dimensionless parameter. Given the admixture (3.45), the soft mass for the lightest scalar state is

$$m_{\phi_0}^2 \simeq \begin{cases} \dfrac{(\delta-1)}{\zeta_\Phi}\dfrac{16\pi^2}{N}\dfrac{|F_\mathcal{X}|^2}{\Lambda_{\text{IR}}^2}\left(\dfrac{\Lambda_{\text{IR}}}{\Lambda_{\text{UV}}}\right)^{2(\delta-1)} & \text{for } \delta \geq 1\,, \\ \dfrac{(1-\delta)}{\zeta_\Phi}\dfrac{16\pi^2}{N}\dfrac{|F_\mathcal{X}|^2}{\Lambda_{\text{IR}}^2} & \text{for } 0 \leq \delta < 1\,, \end{cases} \tag{3.49}$$

where, for a large-N gauge theory, $\xi_4 \simeq 16\pi^2/N$ [169]. When the sfermion is mostly elementary ($\delta \geq 1$), the soft mass is power-law-suppressed since the supersymmetry breaking

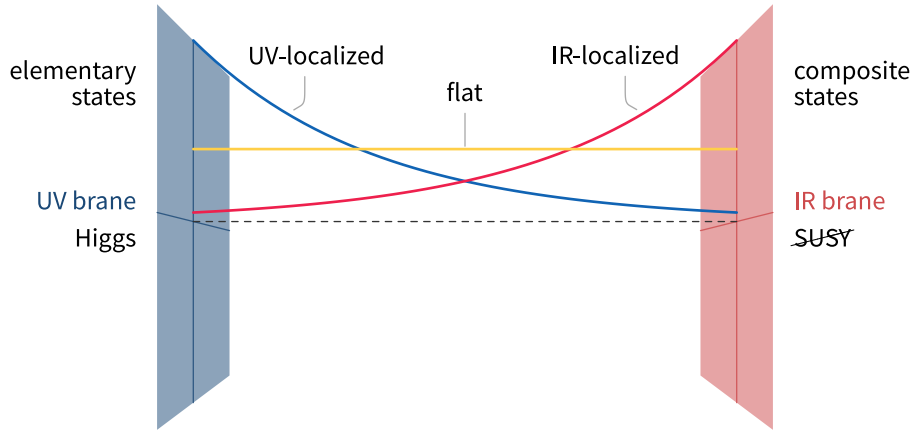

Figure 3.4: Visualization of the equivalence between localization in the AdS_5 bulk and degree of compositeness in the four-dimensional dual theory.

is transmitted via the elementary-composite mixing. (Note, however, that for sufficiently large δ, radiative corrections will become increasingly important. These corrections are calculated in Ref. [17]) This contrasts with the case $0 \leq \delta < 1$, where the mass eigenstate is mostly composite and there is no power-law suppression. Thus, elementary sfermions (identified with the stops) are much lighter than the composite sfermions (identified with the first- and second-generation sfermions), giving rise an inverted mass hierarchy.

A partially composite analysis can also be done for the vector and gravity supermultiplets. They lead to a mostly elementary gauge boson and gaugino, and an elementary graviton and gravitino [171]. Since supersymmetry breaking occurs in the composite sector, this implies that the gauginos are lighter than the mostly composite first- and second-generation sfermions and comparable in mass to the mostly elementary third-generation sfermions. On the other hand, since the gravitino has a tiny composite admixture, it is almost always the lightest supersymmetric particle. These are the qualitative features of the partially composite sparticle spectrum. Further details are presented in Ref. [17].

3.3.2 The AdS/CFT dictionary

The partially composite supersymmetric framework discussed above (with further details in Ref. [17]) relates the fermion and sfermion mass spectra that result from some unknown strong dynamics. The mechanism of partial compositeness is similar to single-sector models of supersymmetry breaking [95, 96, 172–176]. Even if the underlying gauge theory were completely known, however, quantitative predictions for the spectrum would be difficult to

obtain due to the nonperturbative dynamics.

The five-dimensional gravitational dual model provides a more transparent construction of this mechanism. The UV brane, which breaks the 5D Lorentz symmetry of the bulk theory, is associated in the 4D CFT with a UV mass scale $\Lambda_{\rm UV}$ that breaks the conformal symmetry, providing a UV cutoff for the theory. The IR brane, which compactifies the extra dimension and gives rise to the Kaluza-Klein quantization of bulk fields, is associated with the spontaneous breaking of the CFT by confinement at an IR mass scale $\Lambda_{\rm IR} = \Lambda_{\rm UV} e^{-\pi kR}$, causing particle bound states of the CFT to appear. The 4D field theory localized to the UV brane in the 5D theory thus corresponds to the elementary sector in the partially composite model and the theory on the IR brane to the composite sector. The UV-localized Higgs is therefore an elementary state, while the supersymmetry-breaking sector on the IR brane must be entirely governed by strong dynamics.

Fields in the bulk are dual to composite operators in the 4D CFT. The localization profile of a bulk field, which in the 5D theory controls the overlap of the field with the UV and IR branes and other fields in the bulk, is the analog of the anomalous dimension δ of the CFT operator, which controls the relevance of the its mixing with the elementary sector and therefore the degree of compositeness of the admixture in the low-energy theory. For example, in a hypermultiplet in the five-dimensional bulk, the fermion and scalar zero-mode profiles depend on the localization parameter c. The scaling dimensions of the fermionic and scalar operators in the 4D dual theory can in fact be parametrized directly in terms of the 5D hypermultiplet localization parameter:

$$\dim \mathcal{O}_{\psi_{L,R}} = \tfrac{3}{2} + \delta_{L,R} = \tfrac{3}{2} + \left|c \pm \tfrac{1}{2}\right|, \tag{3.50}$$

$$\dim \mathcal{O}_{\phi_{L,R}} = 1 + \delta_{L,R} = 1 + \left|c \pm \tfrac{1}{2}\right|, \tag{3.51}$$

Thus, there is direct relation

$$\delta_{L,R} = \left|c \pm \tfrac{1}{2}\right| \tag{3.52}$$

between the anomalous dimensions δ in the dual theory and the hypermultiplet localization parameter c.[13] This behavior is shown schematically in Fig. 3.4. As discussed in Sec. 3.3.1, the fermion and sfermion mass hierarchies in the four-dimensional theory critically depend on the values of the anomalous dimensions of the associated composite operators; a similar dependence on hypermultiplet localizations is evident as we develop the flavor structure and

[13] In the notation of Appendix B, there is an identity between the anomalous dimension and the Bessel function index of the bulk profiles: $\delta = |\alpha|$.

supersymmetry breaking sector of the five-dimensional model.

The Kaluza-Klein tower of a bulk field is precisely equivalent to the tower of composite states arising in the 4D CFT from the elementary-composite mixing. The advantage of the 5D description is that the KK mass matrix can be exactly diagonalized, whereas the spectrum of composite states in the CFT can only be approximately determined in the large N limit. In particular, this implies that correlators for the strongly-coupled CFT can be computed from 5D on-shell bulk action and hence radiative corrections involving loops of fields with composite admixtures can be calculated in terms of bulk propagators.

With this correspondence in mind, we work within the dual gravity model to construct a quantitative analysis of the standard model fermion mass hierarchy and flavor mixing in Chapter 4 and supersymmetry breaking in Chapter 5, before conducting a phenomenological survey of the model parameter space in Chapter 8 and calculating numeric spectra in Chapter 9.

4 Warped Space Flavor Physics

In this chapter, we consider the theory of flavor in the slice of AdS_5. We first construct the quark and lepton sectors in the five-dimensional theory. Next, we show how the flavor structure of the four-dimensional standard model can be recovered. And last, we discuss the numeric procedure we employ to obtain constraints on the five-dimensional model parameters from the standard model experimental flavor observables. Similar analyses have been performed in various contexts for the quark and lepton sectors (see Refs. [93, 177–185]) in nonsupersymmetric models, as well as in supersymmetric extensions [94, 96, 186]

4.1 The Brane-Localized Higgs Mechanism

Because the Higgs fields are localized to the UV brane, their Yukawa couplings to bulk matter fields are also brane-localized. In this section, we construct the formalism for these couplings to understand how the Yukawa coupling hierarchy and the structure of flavor mixing are explained by the localizations of the fermions in the bulk.

4.1.1 Quark sector

In the bulk mass basis (the basis in which the bulk mass terms of the 5D action are diagonal in flavor space),[1] Yukawa interactions between the quarks in the bulk with the Higgs fields on the UV brane take the form

$$\begin{aligned} S_5 &= \int d^5x\,\sqrt{-g}\,\Big[(Y_5^u)_{ij}\,\bar{u}_i(x^\mu,y)\,H_u(x^\mu)\,Q_j(x^\mu,y) \\ &\qquad\qquad - (Y_5^d)_{ij}\,\bar{d}_i(x^\mu,y)\,H_d(x^\mu)\,Q_j(x^\mu,y) + \text{H.c}\Big]\,2\delta(y) \\ &\equiv \int d^4x\,\Big[(y_u)_{ij}\,\bar{u}_i^{(0)}(x^\mu)\,H_u(x^\mu)\,Q_j^{(0)}(x^\mu) \\ &\qquad\qquad - (y_d)_{ij}\,\bar{d}_i^{(0)}(x^\mu)\,H_d(x^\mu)\,Q_j^{(0)}(x^\mu) + \text{H.c} + \cdots\Big]\,, \end{aligned} \tag{4.1}$$

[1] It is always possible to write the action in this basis [182].

where the ellipsis represents the couplings of the higher Kaluza-Klein states. Before electroweak symmetry breaking, the effective four-dimensional Yukawa couplings of the standard model quarks (corresponding to the zero modes of the five-dimensional fermion fields) are therefore

$$(y_u)_{ij} \equiv 2\,(Y_5^u)_{ij}\, f_{u_i}^{(0)}(y=0)\, f_{Q_j}^{(0)}(y=0) = 2\,(Y_u)_{ij}\, k\, N_{u_i}^{(0)} N_{Q_j}^{(0)}\,, \tag{4.2a}$$

$$(y_d)_{ij} \equiv 2\,(Y_5^d)_{ij}\, f_{d_i}^{(0)}(y=0)\, f_{Q_j}^{(0)}(y=0) = 2\,(Y_5^d)_{ij}\, k\, N_{d_i}^{(0)} N_{Q_j}^{(0)}\,. \tag{4.2b}$$

In terms of the hypermultiplet localization parameters, these are

$$(y_{u,d})_{ij} = (Y_{u,d})_{ij} \sqrt{\frac{4\,(1/2 + c_{u_i,d_i})\,(1/2 - c_{Q_j})}{\left(e^{2(1/2+c_{u_i,d_i})\pi kR} - 1\right)\left(e^{2(1/2-c_{Q_j})\pi kR} - 1\right)}}\,, \tag{4.3}$$

where we have defined the dimensionless quantities

$$(Y_{u,d})_{ij} \equiv (Y_5^{u,d})_{ij}\, k\,. \tag{4.4}$$

In general, these may be complex numbers which we expect to be order-one in magnitude.

After electroweak symmetry breaking, the neutral components of each MSSM Higgs doublet acquire VEVs,

$$v_u = \langle H_u^0 \rangle \equiv v \sin\beta\,, \tag{4.5a}$$

$$v_d = \langle H_d^0 \rangle \equiv v \cos\beta\,, \tag{4.5b}$$

where $v^2 \equiv v_u^2 + v_d^2 \simeq (174\,\mathrm{GeV})^2$. The boundary masses induced by the Higgs mechanism mix the right-handed and left-handed fields of the associated hypermultiplet, with the result that the associated Kaluza-Klein mass matrices are no longer diagonal and the orthogonality of the levels of the original massless ($v = 0$) decomposition is lost. Provided, however, that the additional boundary masses represent a small perturbation compared to the scale of the heavier Kaluza-Klein masses (that is, $v \ll m_{\mathrm{KK}} \sim \Lambda_{\mathrm{IR}}$) the offdiagonal entries that arise in the massless basis are small and can be safely neglected (cf. Ref. [182]). This is the *zero-mode approximation*, which corresponds to the first-order term in the expansion of the exact mass basis in powers of v^2/m_{KK}^2. The IR brane scales we consider for our model are heavy enough that the higher-order terms in this expansion are small. Working therefore in the zero-mode approximation, which offers the advantage of much greater simplicity than the exact solution

(expressions for the exact mass basis are derived in Ref. [182]), the four-dimensional quark Yukawa couplings after EWSB take the forms (4.2). The mass eigenvalues for the standard model quarks are then solutions to the equations

$$\det(m^2 \boldsymbol{I}_3 - v^2 \sin^2\beta\, \boldsymbol{y}_u^\dagger \boldsymbol{y}_u) = 0\,, \tag{4.6a}$$

$$\det(m^2 \boldsymbol{I}_3 - v^2 \cos^2\beta\, \boldsymbol{y}_d^\dagger \boldsymbol{y}_d) = 0\,, \tag{4.6b}$$

which may be obtained from the singular value decompositions

$$\frac{\boldsymbol{m}_u^{\text{diag}}}{v\sin\beta} = (\boldsymbol{V}_R^u)^\dagger \boldsymbol{y}_u \boldsymbol{V}_L^u \quad \Longleftrightarrow \quad v\sin\beta\, \boldsymbol{y}_u = \boldsymbol{V}_R^u\, \boldsymbol{m}_u^{\text{diag}} (\boldsymbol{V}_L^u)^\dagger\,, \tag{4.7a}$$

$$\frac{\boldsymbol{m}_d^{\text{diag}}}{v\cos\beta} = (\boldsymbol{V}_R^d)^\dagger \boldsymbol{y}_d \boldsymbol{V}_L^d \quad \Longleftrightarrow \quad v\cos\beta\, \boldsymbol{y}_d = \boldsymbol{V}_R^d\, \boldsymbol{m}_d^{\text{diag}} (\boldsymbol{V}_L^d)^\dagger\,, \tag{4.7b}$$

where

$$\boldsymbol{m}_u^{\text{diag}} = \text{diag}(m_u, m_c, m_t) \equiv v\sin\beta\, \text{diag}(y_u, y_c, y_t)\,, \tag{4.8a}$$

$$\boldsymbol{m}_d^{\text{diag}} = \text{diag}(m_d, m_s, m_b) \equiv v\cos\beta\, \text{diag}(y_d, y_s, y_b)\,, \tag{4.8b}$$

and

$$\boldsymbol{V}_{\text{CKM}} \equiv (\boldsymbol{V}_L^u)^\dagger \boldsymbol{V}_L^d = \begin{pmatrix} V_{ud} & V_{us} & V_{ub} \\ V_{cd} & V_{cs} & V_{cb} \\ V_{td} & V_{ts} & V_{tb} \end{pmatrix} \tag{4.9}$$

is the Cabibbo-Kobayashi-Maskawa matrix. In the Wolfenstein parametrization [187], we may write up to $\mathcal{O}(\lambda^5)$ [188] (compare to Ref. [189])

$$V_{ud} = 1 - \tfrac{1}{2}\lambda^2 - \tfrac{1}{8}\lambda^4\,, \tag{4.10a}$$

$$V_{us} = \lambda\,, \tag{4.10b}$$

$$V_{ub} = A\lambda^3 (\bar\rho - i\bar\eta)\,, \tag{4.10c}$$

$$V_{cd} = -\lambda + \tfrac{1}{2}A^2\lambda^5 (1 - 2\bar\rho - 2i\bar\eta)\,, \tag{4.10d}$$

$$V_{cs} = 1 - \tfrac{1}{2}\lambda^2 - \tfrac{1}{8}(1 + 4A^2)\lambda^4\,, \tag{4.10e}$$

$$V_{cb} = A\lambda^2\,, \tag{4.10f}$$

$$V_{td} = A\lambda^3 \left(1 - \bar{\rho} - i\bar{\eta}\right) , \tag{4.10g}$$

$$V_{ts} = -A\lambda^2 + \tfrac{1}{2}A\lambda^4 \left(1 - 2\bar{\rho} - 2i\bar{\eta}\right) , \tag{4.10h}$$

$$V_{ts} = 1 - \tfrac{1}{2}A^2\lambda^4 , \tag{4.10i}$$

where,

$$\lambda \equiv \frac{|V_{us}|}{\sqrt{|V_{ud}|^2 + |V_{us}|^2}} , \tag{4.11a}$$

$$A \equiv \frac{1}{\lambda}\frac{|V_{cb}|}{|V_{us}|} , \tag{4.11b}$$

$$\bar{\rho} + i\bar{\eta} \equiv -\frac{V_{ud}V_{ub}^*}{V_{cd}V_{cb}^*} = (\rho + i\eta)\left(1 - \frac{\lambda^2}{2} + \mathcal{O}(\lambda^4)\right) . \tag{4.11c}$$

A global fit of the standard model [190, 191] gives the best-fit values in Table 4.1 for these parameters. Also given is the value of the Jarlskog invariant J [192], a phase-convention-independent measure of CP violation defined

$$\mathrm{Im}\, V_{ij}V_{k\ell}V_{il}^*V_{kj}^* = J \sum_{m,n=1}^{3} \varepsilon_{ikm}\varepsilon_{jln} , \tag{4.12}$$

where ε_{ijk} is the Levi-Civita symbol. As a result of the unitarity of the CKM matrix, this definition results in nine distinct representations (for instance: $J = \mathrm{Im}\, V_{ud}V_{cs}V_{us}^*V_{cd}^*$). In terms of the Wolfenstein parameters,

$$J = A^2\lambda^6\bar{\eta} + \mathcal{O}(\lambda^8) . \tag{4.13}$$

The quark system in our five-dimensional model has 45 real parameters (18 each from $\boldsymbol{Y}_u$ and $\boldsymbol{Y}_d$ and nine from c_{Q_i}, c_{u_i}, and c_{d_i}) and ten constraints (six quark masses and four mixing angles from the CKM matrix). There are thus 35 free parameters, but not all of these are physical. Unlike the standard model, we are not free to make weak eigenbasis rotations to reduce the Yukawa matrices to a form specified by fewer unknown parameters (such as the standard non-Hermitian four-zero form) without simultaneously moving out of the basis in which the five-dimensional bulk mass matrices are diagonal. Therefore, in order to work in the bulk mass basis, we must generically assume anarchic five-dimensional

Table 4.1: Results of a global standard model fit for the CKM Wolfenstein parameters and Jarlskog invariant with 3σ uncertainty ranges [190, 191].

λ	$0.22475^{+0.00106}_{-0.000018}$
A	$0.840^{+0.016}_{-0.043}$
$\bar{\rho}$	$0.158^{+0.036}_{-0.020}$
$\bar{\eta}$	$0.349^{+0.029}_{-0.025}$
$J\,[10^{-5}]$	$3.17^{+0.29}_{-0.34}$

Yukawa couplings.[2] We will discuss the method we employ to determine these parameters and obtain fits to the standard model flavor observables in Sec. 4.4.

4.1.2 Lepton sector

A similar analysis can be performed for the lepton sector. In this case, we must first specify a model for the origin of the neutrino masses. We consider two scenarios: one in which the neutrinos are Dirac fermions and another in which lepton number is violated at high energy, generating an effective Majorana mass term for the standard model neutrinos via a dimension-five operator. This latter scenario is the generic low-energy effective theory corresponding to a wide variety of possible models of neutrino mass generation involving new heavy states, such as a Type I seesaw mechanism (see Refs. [179, 184]).

Dirac neutrinos

Here we introduce a family of right-handed neutrino fields $\overline{\nu}_i$ and assume that the right- and left-handed neutrinos obtain a Dirac mass via Yukawa couplings to the Higgs fields on the UV brane. In the bulk mass basis, this takes the form

$$S_5 = \int d^5x\,\sqrt{-g}\,\Big[-(Y_5^e)_{ij}\,\bar{e}_i(x^\mu,y)\,H_d(x^\mu)\,L_j(x^\mu,y) + (Y_5^\nu)_{ij}\,\overline{\nu}_i(x^\mu,y)\,H_u(x^\mu)\,L_j(x^\mu,y) + \text{H.c}\Big]\,2\delta(y)$$

[2] We also note that in the zero-mode approximation we are not allowed to make the simplifying assumption that all of the five-dimensional Yukawa couplings take the same value (i.e., $(Y_{u,d})_{ij} = Y$) unless we also assume the Yukawa matrices are diagonal in the bulk mass basis, as two of the three singular values of the corresponding four-dimensional Yukawa coupling matrix otherwise vanish.

$$\equiv \int d^4x \left[-(y_e)_{ij}\, \bar{e}_i^{(0)}(x^\mu)\, H_d(x^\mu)\, L_j^{(0)}(x^\mu) \right. \tag{4.14}$$
$$\left. + (y_\nu)_{ij}\, \bar{\nu}_i^{(0)}(x^\mu)\, H_u(x^\mu)\, L_j^{(0)}(x^\mu) + \text{H.c} + \cdots \right],$$

where, before electroweak symmetry breaking, the effective four-dimensional Yukawa couplings of the standard model leptons are

$$(y_e)_{ij} \equiv 2\,(Y_5^e)_{ij}\, f_{e_i}^{(0)}(y=0)\, f_{L_j}^{(0)}(y=0) = 2\,(Y_5^e)_{ij}\, k\, N_{e_i}^{(0)} N_{L_j}^{(0)}\,, \tag{4.15a}$$

$$(y_\nu)_{ij} \equiv 2\,(Y_5^\nu)_{ij}\, f_{\nu_i}^{(0)}(y=0)\, f_{L_j}^{(0)}(y=0) = 2\,(Y_5^\nu)_{ij}\, k\, N_{\nu_i}^{(0)} N_{L_j}^{(0)}\,. \tag{4.15b}$$

In terms of the hypermultiplet localization parameters, these are

$$(y_{e,\nu})_{ij} = (Y_{e,\nu})_{ij} \sqrt{\frac{4\,(1/2 + c_{e_i,\nu_i})\,(1/2 - c_{L_j})}{\left(e^{2(1/2+c_{e_i,\nu_i})\pi kR} - 1\right)\left(e^{2(1/2-c_{L_j})\pi kR} - 1\right)}}\,, \tag{4.16}$$

where we have defined the dimensionless quantities

$$(Y_{e,\nu})_{ij} \equiv (Y_5^{e,\nu})_{ij}\, k\,. \tag{4.17}$$

In general, these are complex numbers and order-one in magnitude.

In the zero-mode approximation, the four-dimensional lepton Yukawa couplings after electroweak symmetry-breaking also take the forms (4.15). The mass eigenvalues for the standard model leptons are then solutions to the equations

$$\det(m^2 \boldsymbol{I}_3 - v^2 \cos^2\beta\, \boldsymbol{y}_e^\dagger\, \boldsymbol{y}_e) = 0\,, \tag{4.18a}$$

$$\det(m^2 \boldsymbol{I}_3 - v^2 \sin^2\beta\, \boldsymbol{y}_\nu^\dagger\, \boldsymbol{y}_\nu) = 0\,, \tag{4.18b}$$

which may be obtained from the singular value decompositions

$$\frac{\boldsymbol{m}_e^{\text{diag}}}{v\cos\beta} = (\boldsymbol{V}_R^e)^\dagger \boldsymbol{y}_e \boldsymbol{V}_L^e \quad \Longleftrightarrow \quad v\cos\beta\, \boldsymbol{y}_e = \boldsymbol{V}_R^e\, \boldsymbol{m}_e^{\text{diag}} (\boldsymbol{V}_L^e)^\dagger\,, \tag{4.19a}$$

$$\frac{\boldsymbol{m}_\nu^{\text{diag}}}{v\sin\beta} = (\boldsymbol{V}_R^\nu)^\dagger \boldsymbol{y}_\nu \boldsymbol{V}_L^\nu \quad \Longleftrightarrow \quad v\sin\beta\, \boldsymbol{y}_\nu = \boldsymbol{V}_R^\nu\, \boldsymbol{m}_\nu^{\text{diag}} (\boldsymbol{V}_L^\nu)^\dagger\,, \tag{4.19b}$$

where

$$\boldsymbol{m}_e^{\rm diag} = {\rm diag}(m_e, m_\mu, m_\tau) = v\cos\beta\,{\rm diag}(y_e, y_\mu, y_\tau)\,, \tag{4.20a}$$

$$\boldsymbol{m}_\nu^{\rm diag} = {\rm diag}(m_1, m_2, m_3) = v\sin\beta\,{\rm diag}(y_1, y_2, y_3)\,, \tag{4.20b}$$

and

$$\boldsymbol{U}_{\rm PMNS}^{\rm (D)} \equiv (\boldsymbol{V}_L^e)^\dagger \boldsymbol{V}_L^\nu = \begin{pmatrix} U_{e1} & U_{e2} & U_{e3} \\ U_{\mu1} & U_{\mu2} & U_{\mu3} \\ U_{\tau1} & U_{\tau2} & U_{\tau3} \end{pmatrix} \tag{4.21}$$

is the Pontecorvo-Maki-Nakagawa-Sakata (PMNS) matrix. In the standard parametrization this takes the form

$$\boldsymbol{U}_{\rm PMNS}^{\rm (D)} = \begin{pmatrix} c_{12}c_{13} & s_{12}c_{13} & s_{13}e^{-i\delta} \\ -s_{12}c_{23} - c_{12}s_{23}s_{13}e^{i\delta} & c_{12}c_{23} - s_{12}s_{23}s_{13}e^{i\delta} & s_{23}c_{13} \\ s_{12}s_{23} - c_{12}c_{23}s_{13}e^{i\delta} & -c_{12}s_{23} - s_{12}c_{23}s_{13}e^{i\delta} & c_{23}c_{13} \end{pmatrix}, \tag{4.22}$$

where s_{ij} and c_{ij} denote $\sin\theta_{ij}$ and $\cos\theta_{ij}$, respectively. The standard mixing angles can be written in terms of phase-convention-invariant quantities as

$$\sin^2\theta_{12} = \frac{|U_{e2}|^2}{1-|U_{e3}|^2}\,, \tag{4.23a}$$

$$\sin^2\theta_{23} = \frac{|U_{\mu3}|^2}{1-|U_{e3}|^2}\,, \tag{4.23b}$$

$$\sin^2\theta_{13} = |U_{e3}|^2\,. \tag{4.23c}$$

The CP-violating phase δ may be determined jointly from the Jarlskog invariant [defined in the same way (4.12) as for the CKM matrix] and the magnitude of one of $U_{\mu1}$, $U_{\mu2}$, $U_{\tau1}$, or $U_{\tau2}$. For example,

$$J = {\rm Im}\, U_{\mu3}U_{e3}^* U_{e2}U_{\mu2}^* = \frac{1}{8}\cos\theta_{13}\sin 2\theta_{12}\sin 2\theta_{23}\sin 2\theta_{13}\,, \tag{4.24a}$$

$$\begin{aligned} |U_{\mu2}|^2 = {}& \cos^2\theta_{12}\cos^2\theta_{23} + \sin^2\theta_{12}\sin^2\theta_{23}\sin^2\theta_{13} \\ & - \frac{1}{2}\sin 2\theta_{12}\sin 2\theta_{23}\sin\theta_{13}\cos\delta\,, \end{aligned} \tag{4.24b}$$

such that

$$\sin\delta = \frac{8\,\mathrm{Im}\,U_{\mu3}U_{e3}^{*}U_{e2}U_{\mu2}^{*}}{\cos\theta_{13}\sin 2\theta_{12}\sin 2\theta_{23}\sin 2\theta_{13}}\,, \tag{4.25a}$$

$$\cos\delta = \frac{\cos^2\theta_{12}\cos^2\theta_{23} + \sin^2\theta_{12}\sin^2\theta_{23}\sin^2\theta_{13} - |U_{\mu2}|^2}{\frac{1}{2}\sin 2\theta_{12}\sin 2\theta_{23}\sin\theta_{13}}\,. \tag{4.25b}$$

The standard model global best-fit values [193, 194] (see also Ref. [195]) for these parameters as well as the neutrino mass differences are given in Table 4.2 for both neutrino mass hierarchy scenarios.

Table 4.2: Results of a global standard model fit for the PMNS mixing angles, Jarlskog invariant, and neutrino mass differences (including Super-Kamiokande atmospheric data) with 3σ uncertainties [193, 194].

	normal ordering	inverted ordering
$\sin^2\theta_{12}$	$0.310^{+0.040}_{-0.035}$	$0.310^{+0.040}_{-0.035}$
$\sin^2\theta_{23}$	$0.563^{+0.046}_{-0.130}$	$0.565^{+0.045}_{-0.129}$
$\sin^2\theta_{13}$	$0.022\,37^{+0.001\,98}_{-0.001\,93}$	$0.022\,59^{+0.001\,98}_{-0.001\,95}$
$\delta\,[\pi]$	$1.23^{+0.76}_{-0.43}$	$1.57^{+0.37}_{-0.43}$
J	$-0.022^{+0.061}_{-0.034}$ [a]	$-0.033^{+0.036}_{-0.042}$ [a]
$\Delta m^2_{21}\,[10^{-5}\,\mathrm{eV}^2]$	$7.39^{+0.62}_{-0.60}$	$7.39^{+0.62}_{-0.60}$
$\Delta m^2_{31}\,[10^{-3}\,\mathrm{eV}^2]$	$2.528^{+0.090}_{-0.092}$	$-2.436^{+0.091}_{-0.091}$ [a]
$\Delta m^2_{32}\,[10^{-3}\,\mathrm{eV}^2]$	$2.454^{+0.090}_{-0.092}$ [a]	$-2.510^{+0.091}_{-0.091}$

[a] Calculated from the fitted parameters.

The lepton system has 45 real parameters (18 each from $\boldsymbol{Y}_e$ and $\boldsymbol{Y}_\nu$ and nine from c_{L_i}, c_{e_i}, and c_{ν_i}) and nine constraints (three charged lepton masses, two neutrino mass differences, and four mixing angles from the PMNS matrix). There are thus 36 free parameters. As in the quark sector, we work in the bulk mass basis, where we generically assume anarchic five-dimensional Yukawa couplings.

Effective Majorana mass

If total lepton number is violated by new physics at higher energy, an effective Majorana mass is generated for the left-handed neutrinos that can be parametrized at low energy by the inclusion of a higher-dimension operator (Weinberg operator) on the UV brane:

$$\begin{aligned} S_5 = \int d^5x\,\sqrt{-g}\,\Big[& -(Y_5^e)_{ij}\,\bar{e}_i(x^\mu,y)\,H_d(x^\mu)\,L_j(x^\mu,y) \\ & - \frac{1}{2}\frac{(K_5^\nu)_{ij}}{\Lambda_{\rm UV}}\,L_i(x^\mu,y)\,H_u(x^\mu)\,L_j(x^\mu,y)\,H_u(x^\mu) + \text{H.c}\Big]\,2\delta(y) \\ \equiv \int d^4x\,\Big[& -(y_e)_{ij}\,\bar{e}_i^{(0)}(x^\mu)\,H_d(x^\mu)\,L_j^{(0)}(x^\mu) \\ & - \frac{1}{2}\frac{(\kappa_\nu)_{ij}}{\Lambda_\nu}\,L_i^{(0)}(x^\mu)\,H_u(x^\mu)\,L_j^{(0)}(x^\mu)\,H_u(x^\mu) + \text{H.c} + \cdots\Big] \end{aligned} \tag{4.26}$$

where $\boldsymbol{K}_5^\nu$ is a complex symmetric matrix of (inverse mass dimension) coefficients that include the effects of the heavy degrees of freedom integrating out at the mass scale Λ_ν. Before electroweak symmetry breaking, the effective four-dimensional Yukawa couplings of the standard model charged leptons take the same form (4.15a) as in the Dirac case, while the effective four-dimensional dimension-five operator coefficients (dimensionless) of the neutrinos are

$$(\kappa_\nu)_{ij} \equiv 2\,(K_5^\nu)_{ij}\,\frac{\Lambda_\nu}{\Lambda_{\rm UV}}\,f_{L_i}^{(0)}(y=0)\,f_{L_j}^{(0)}(y=0) \simeq 2\,(K_5^\nu)_{ij}\,\Lambda_\nu\,N_{L_i}^{(0)}N_{L_j}^{(0)}\,. \tag{4.27}$$

In terms of the hypermultiplet localization parameters, these are

$$(\kappa_\nu)_{ij} = (K_\nu)_{ij}\,\sqrt{\frac{4\,(1/2-c_{L_i})\,(1/2-c_{L_j})}{\left(e^{2(1/2-c_{L_i})\pi kR}-1\right)\left(e^{2(1/2-c_{L_j})\pi kR}-1\right)}}\,, \tag{4.28}$$

where have defined the dimensionless quantities

$$(K_\nu)_{ij} \equiv (K_5^\nu)_{ij}\Lambda_\nu\,. \tag{4.29}$$

In general, these are complex, and at most $\mathcal{O}(1)$ in magnitude, although typically we expect they may be significantly smaller, as they may include the effects of small couplings (such as neutrino Yukawa couplings in a Type I seesaw).

In the zero-mode approximation, the four-dimensional electron Yukawa couplings after

electroweak symmetry-breaking also take the forms (4.15a) and the dimension-five coefficients the forms (4.27). The mass eigenvalues for the standard model leptons are then solutions to the equations

$$\det(m^2 \boldsymbol{I}_3 - v^2 \cos^2\beta\, \boldsymbol{y}_e^\dagger\, \boldsymbol{y}_e) = 0\,, \tag{4.30a}$$

$$\det(m^2 \boldsymbol{I}_3 - v^4 \sin^4\beta\, \boldsymbol{\kappa}_\nu^\dagger\, \boldsymbol{\kappa}_\nu) = 0\,, \tag{4.30b}$$

which may be obtained from the factorizations[3]

$$\frac{\boldsymbol{m}_e^{\text{diag}}}{v\cos\beta} = (\boldsymbol{V}_R^e)^\dagger \boldsymbol{y}_e \boldsymbol{V}_L^e \quad \Longleftrightarrow \quad v\cos\beta\, \boldsymbol{y}_e = \boldsymbol{V}_R^e\, \boldsymbol{m}_e^{\text{diag}} (\boldsymbol{V}_L^e)^\dagger\,, \tag{4.33a}$$

$$\frac{\boldsymbol{m}_\nu^{\text{diag}}}{v^2\sin^2\beta} = \boldsymbol{V}_\nu^{\mathrm{T}} \boldsymbol{\kappa}_\nu \boldsymbol{V}_\nu \quad \Longleftrightarrow \quad v^2\sin^2\beta\, \boldsymbol{\kappa}_\nu = \boldsymbol{V}_\nu^*\, \boldsymbol{m}_\nu^{\text{diag}}\, \boldsymbol{V}_\nu^\dagger\,, \tag{4.33b}$$

where

$$\boldsymbol{m}_e^{\text{diag}} = \text{diag}(m_e, m_\mu, m_\tau) \equiv v\cos\beta\, \text{diag}(y_e, y_\mu, y_\tau)\,, \tag{4.34a}$$

$$\boldsymbol{m}_\nu^{\text{diag}} = \text{diag}(m_1, m_2, m_3) \equiv v^2\sin^2\beta\, \text{diag}(\kappa_1, \kappa_2, \kappa_3)\,. \tag{4.34b}$$

In this case, the PMNS matrix contains two extra Majorana CP-violating phases (here, in the PDG convention [20]):

$$\boldsymbol{U}_{\text{PMNS}}^{(\text{M})} \equiv (\boldsymbol{V}_L^e)^\dagger \boldsymbol{V}_\nu = \boldsymbol{U}_{\text{PMNS}}^{(\text{D})}\, \text{diag}(1, e^{i\alpha_{12}/2}, e^{i\alpha_{23}/2})\,. \tag{4.35}$$

The measured mixing angles (4.23) are independent of these phases. Due to the symmetry of the dimension-five operator, the lepton system has only 36 parameters (18 from $\boldsymbol{Y}_e$, 12 from $\boldsymbol{K}_\nu$, and six from c_{L_i} and c_{e_i}) and nine constraints (three charged lepton masses, two neutrino mass differences, and four mixing angles from the PMNS matrix). There are thus 27 free parameters.

[3] For a complex symmetric matrix $\boldsymbol{M}$, the Autonne-Takagi factorization $\boldsymbol{M} = \boldsymbol{U}^* \boldsymbol{\Sigma} \boldsymbol{U}^\dagger$ and the singular value decomposition $\boldsymbol{M} = \boldsymbol{V}_R\, \boldsymbol{\Sigma}\, \boldsymbol{V}_L^\dagger$ are related by the rephasings

$$\boldsymbol{U} = \boldsymbol{V}_L\, \text{diag}(e^{-i\phi_1}, e^{-i\phi_2}, \dots) = \boldsymbol{V}_R^*\, \text{diag}(e^{i\phi_1}, e^{i\phi_2}, \dots)\,, \tag{4.31}$$

where $\phi_n = \psi_n/2$ for

$$\boldsymbol{V}_L^{\mathrm{T}} \boldsymbol{M}\, \boldsymbol{V}_L = \boldsymbol{V}_R^{\mathrm{T}} \boldsymbol{M}^* \boldsymbol{V}_R = \boldsymbol{\Sigma}\, \text{diag}(e^{i\psi_1}, e^{i\psi_2}, \dots)\,. \tag{4.32}$$

4.1.3 Geometry and the Yukawa hierarchies

In the zero-mode approximation, the generic relation between a four-dimensional Yukawa coupling and the localization parameters of associated hypermultiplets (the bulk masses of the fermions) is given by

$$
\begin{aligned}
y_{ij} &= Y_{ij} \sqrt{\frac{4\,(1/2+c_{R,i})\,(1/2-c_{L,j})}{\left(e^{2(1/2+c_{R,i})\pi kR}-1\right)\left(e^{2(1/2-c_{L,j})\pi kR}-1\right)}} \\
&\sim \begin{cases} \sqrt{4\,(\frac{1}{2}+c_{R,i})\,(\frac{1}{2}-c_{L,j})}\,Y_{ij} & \text{for } -c_{R,i}, +c_{L,j} > \dfrac{1}{2} \\ \dfrac{1}{\pi kR}\,Y_{ij} & \text{for } -c_{R,i}, +c_{L,j} \sim \dfrac{1}{2} \\ \sqrt{4\,(\frac{1}{2}+c_{R,i})\,(\frac{1}{2}-c_{L,j})}\,Y_{ij}\,e^{-(1+c_{R,i}-c_{L,j})\pi kR} & \text{for } -c_{R,i}, +c_{L,j} < \dfrac{1}{2}\,. \end{cases}
\end{aligned}
\tag{4.36}
$$

Assuming that the five-dimensional couplings are order-one, we see that the strength of the four-dimensional couplings depends parametrically on the c parameters of the hypermultiplets, and the observed Yukawa hierarchies can therefore be generated by specifying localizations of the hypermultiplet fields in the bulk of the extra dimension. Recall that in the four-dimensional dual theory, this is equivalent to choosing the anomalous dimensions $\delta_{R,i}, \delta_{L,j}$.

To illustrate this, we consider a simplified model with Dirac neutrinos (normal mass ordering) in the zero-mode approximation that neglects quark and lepton mixing, such that the four-dimensional interaction basis coincides with the four-dimensional mass basis and the bulk mass basis. In this case, if we take a universal value for the five-dimensional Yukawa couplings, such that $(Y_{u,d,e,\nu})_{ii} = Y$, there is one parametric degree of freedom within each generation of leptons and within each generation of quarks, which we choose as the doublet c parameters c_{L_i,Q_i} without loss of generality.

The relations (4.2) and (4.15) hold for the running masses. Ultimately, we are interested in the hypermultiplet localization parameters at the IR-brane scale, where they are needed the soft masses received by the sfermions when supersymmetry is broken. Therefore, before we perform the 4D-5D Yukawa matching, we first evolve the four-dimensional Yukawa couplings to the IR-brane scale. We discuss the procedure we use to consistently perform the renormalization in Sec. 4.2. In Fig. 4.1, we give an example of the resulting matching, showing the allowed range of localization parameters of the standard model leptons and quarks. Generally, we see that the largeness of the third-generation Yukawa couplings

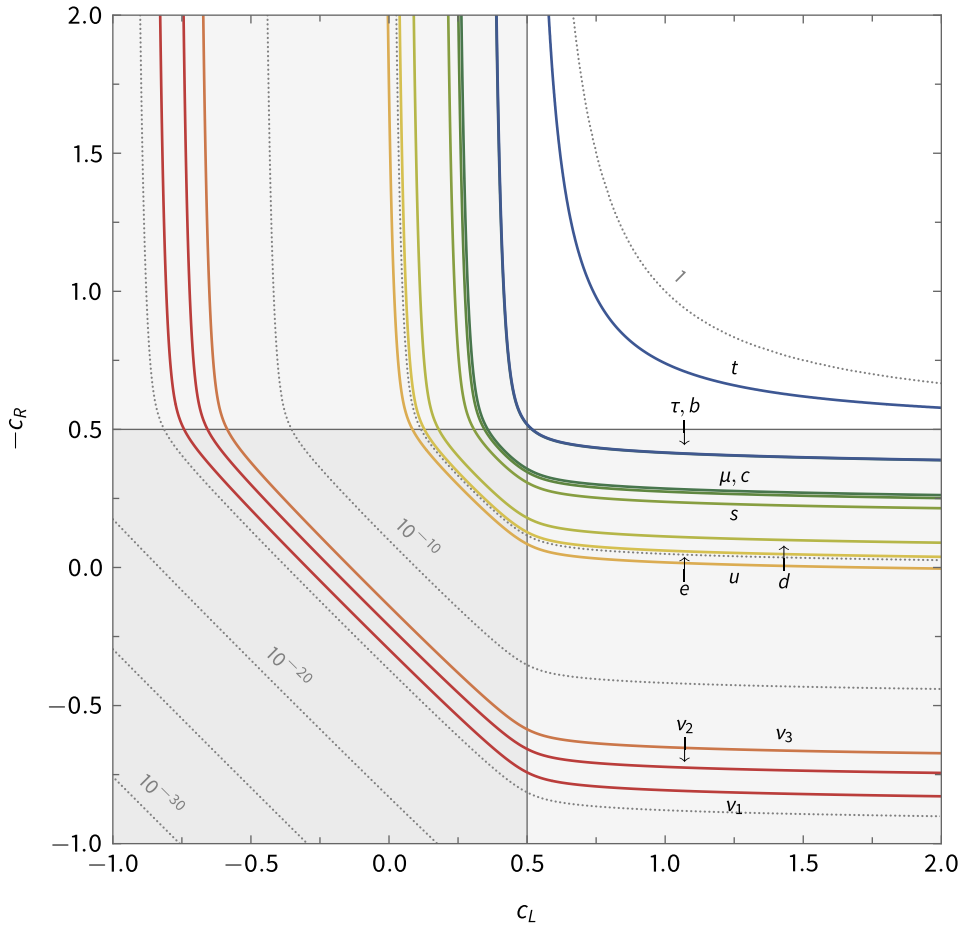

Figure 4.1: Plot of the dependence of the effective four-dimensional Yukawa couplings on the bulk fermion localization parameters c_L and c_R for a simplified model with Dirac neutrinos. We take $\Lambda_{\text{IR}} = 1 \times 10^7\,\text{GeV}$, $\tan\beta = 5$, and $Y = 1$. The neutrino masses have the normal hierarchy, with the lightest set at $m_{\nu_1} = 1\,\text{meV}$. The dotted lines give contours of the Yukawa coupling strength. The solid contour lines correspond to the coupling strengths of the standard model Yukawa couplings at the IR-brane scale. The region in which each field is IR-localized is shaded light gray and the region where both fields are IR-localized is darker gray.

requires the third-generation fermions for both leptons and quarks to be UV-localized (white region), while the smaller Yukawa couplings of the first and second generations lead to IR localization (darker gray region). Although it is always possible to make one of the chiral fermions in each generation UV-localized, only for the third generation can this be done without making at least one of the other chiral fermions IR-localized.

4.2 Renormalization of Flavor Observables

In the previous section we presented a tree-level analysis for the matching between Yukawa couplings and Weinberg operator in the zero-mode approximation, characterized by the matching relations (4.2), (4.15), and (4.27). The matching condition for the gauge couplings (3.27) is discussed in Sec. 3.2.2. The five-dimensional parameters in our model are relevant to the theory above the scale of compactification; below that scale, the theory is effectively four-dimensional. The matching between the two descriptions must therefore occur at the scale of compactification, i.e., at Λ_{IR}, and in hence in order to use the matching relations, the four-dimensional couplings and mixings must first be evolved to the IR-brane scale.

Here, we describe the numeric procedure we use to obtain an estimate of the renormalized four-dimensional couplings and mixings. It is necessary for the full flavor solution discussed in Sec. 4.4 to include the theoretical and experimental uncertainty in these parameters. The renormalization proceeds in three stages.

1. **Fitting to low-energy observables**

   As discussed in Sec. 2.1, the standard model as a field theory is defined by its field content and gauge group structure. This structure may be parametrized by a set of *theory parameters*, which for the standard model are the set of gauge couplings g', g, and g_3 (corresponding to $\text{SU}(3)_c$, $\text{SU}(2)_L$, and $\text{U}(1)_Y$, respectively);[4] the quark and charged lepton Yukawa couplings $y_{u,c,t}$, $y_{d,s,b}$, and $y_{e,\mu,\tau}$ (or equivalently the quark and charged lepton masses); the Higgs VEV v, mass term m, and quartic coupling λ; and the quark-sector mixing parameters (e.g., the CKM Wolfenstein parameters given in Table 4.1) and the neutrino mass differences and mixing parameters (given in Table 4.2). These theory parameters are defined at a specific renormalization scale within a specific renormalization scheme and may be evolved to other energy scales by solving the renormalization group equations (RGEs). In this formulation, the

[4] We can also include the hadronic light-quark contribution to the fine-structure constant as a parameter $\Delta\alpha^{(5)}_{\text{had}}(M_Z)$, essentially encoding the effect of nonperturbative physics in the low-energy theory.

standard model includes the tower of effective theories that arise at low energies as heavy particles are decoupled from the running.

The standard model theory parameters, however, are not directly observable. Experimental measurements are typically characterized by a set of on-shell *observable parameters*, given in Table 4.3.[5] The values of the theory parameters are determined by fitting the standard model to the observational data, matching the tower of effective theories as heavy particles are decoupled within the specified renormalization scheme.

We use the public computer code library SMDR (Standard Model in Dimensional Regularization) [196] to extract the values of the running theory parameters and their experimental and theoretical uncertainty ranges at the top quark mass scale $m_t^{\rm pole}$ (such that all six quarks are in the theory) in the modified minimal subtraction ($\overline{\rm MS}$) renormalization scheme. The values and uncertainties of the on-shell observable parameters used as input are given in Table 4.3.

2. Renormalization in the SM

The SMDR code does not incorporate Cabibbo-Kobayashi-Maskawa mixing or neutrino masses and mixing effects, so at the top quark mass scale we use the fitted CKM Wolfenstein parameters and Jarlskog invariant with 3σ uncertainty ranges given in Table 4.1 and the fitted PMNS parameters with 3σ uncertainty ranges given in Table 4.2 to construct the fermion mixing matrices. The neutrino mass differences (with 3σ uncertainty ranges) given in Table 4.2 are combined with a specification for the lightest neutrino mass to obtain either a set of neutrino Yukawa couplings or Weinberg operator coefficients.

The fermion Yukawa couplings (or, for Majorana neutrinos, Weinberg operator coefficients) form the diagonal entries of matrices in the mass basis. Before evolving the theory to higher scales, the mixing matrices are first used to rotate these coupling matrices into an interaction basis (specifically the one in which $\boldsymbol{y}_e$ and $\boldsymbol{y}_d$ are diagonal).

In addition, we convert to the SU(5) normalization for the gauge couplings:

$$g_1 = \sqrt{\frac{5}{3}}\, g' \qquad g_2 = g\,, \qquad g_3 = g_s\,. \tag{4.37}$$

[5] The CKM and PMNS mixing parameters and the neutrino mass differences are also considered fitted parameters, determined from the measurement of hadronic decay and neutrino oscillation data. For more information please see Ref. [20] for a review.

After this matching procedure, the parameters are then run to a specified renormalization scale by solving the SM beta functions at up to two loops.[6] At the final renormalization scale, the fermion coupling matrices are transformed into the mass basis and the CKM and PMNS mixing parameters recalculated. Parameter uncertainties are calculated by performing the renormalization with each input parameter individually varied across its uncertain range and summing the resulting deviations in quadrature (the central values are taken to be the result of the renormalization with all input parameters at their central values).

3. Renormalization in the MSSM

For renormalization in the MSSM, the SM parameters are first run to a specified scale m_{SUSY}, where they are matched to the MSSM parameters at tree level, and converted at one loop from $\overline{\text{MS}}$ into the dimensional reduction with modified minimal subtraction ($\overline{\text{DR}}$) renormalization scheme using the expressions of Ref. [197]. The parameters are then run to a specified renormalization scale by solving the MSSM beta functions at up to two loops. Parameter uncertainties are calculated as in the SM procedure. In addition, uncertainty due to neglected threshold corrections (the *MSSM uncertainty*) is estimated by varying the scale of supersymmetry over the interval $[m_{\text{SUSY}}/2, 2m_{\text{SUSY}}]$ and calculating the maximum resulting deviations, which are added linearly to the parameter uncertainties.

A new computer code automating this procedure is collected as the Wolfram Language package RunningCouplings [198].[7] The primary limitation of this method is the lack of supersymmetric threshold corrections from the decoupling of the sparticles. As noted above, we include as an additional SUSY uncertainty an estimate of the effect of a variation of the matching scale between the standard model and MSSM, but this estimate tends to dominate the other sources of uncertainty with origin in the fitting of the theory parameters to observational data at the electroweak scale (the *SM uncertainty*) in the high-scale parameters and may be insufficient if the spectrum of sparticles is highly hierarchical, as is the case in our model. To illustrate this, we show the relative sizes of the MSSM uncertainty (dotted lines) compared to the SM uncertainty (solid lines) in our renormalization procedure as a

[6] We use the convention in which the Higgs potential takes the form (2.17). The SMDR code uses the convention

$$V(H) = m^2 H^\dagger H + \lambda \left(H^\dagger H\right)^2 , \tag{4.38}$$

so we must make the additional conversion $\lambda \to 2\lambda$.

[7] The code is also available from the author upon request.

Table 4.3: Experimental observables in the low-energy standard model. Central values and uncertainties are taken from Ref. [20].

heavy particle pole masses	$m_W^{\text{Breit-Wigner}}$ [GeV]	80.379(12)
	$m_Z^{\text{Breit-Wigner}}$ [GeV]	91.1876(21)
	m_h^{pole} [GeV]	125.10(14)
	m_t^{pole} [GeV]	173.1(9)
running quark masses[a]	$m_u(2\,\text{GeV})$ [MeV]	$2.16^{+0.49}_{-0.26}$
	$m_d(2\,\text{GeV})$ [MeV]	$4.67^{+0.48}_{-0.17}$
	$m_s(2\,\text{GeV})$ [MeV]	93^{+11}_{-5}
	$m_c(m_c)$ [GeV]	$1.27^{+0.02}_{-0.02}$
	$m_b(m_b)$ [GeV]	$4.18^{+0.03}_{-0.02}$
lepton pole masses	m_e^{pole} [keV]	510.998 946 1(31)
	m_μ^{pole} [MeV]	105.658 374 5(24)
	m_τ^{pole} [MeV]	1776.86(12)
five-quark strong coupling[a]	$\alpha_s^{(5)}(M_Z)$	0.1181(11)
Fermi coupling constant	G_F [GeV^{-2}]	$1.166\,378\,7(6) \times 10^{-5}$
fine structure constant	α_0	137.035 999 139(31)
five-quark hadronic contribution to fine structure	$\Delta\alpha_{\text{had}}^{(5)}(M_Z)$	0.027 64(7)

[a] In the $\overline{\text{MS}}$ renormalization scheme.

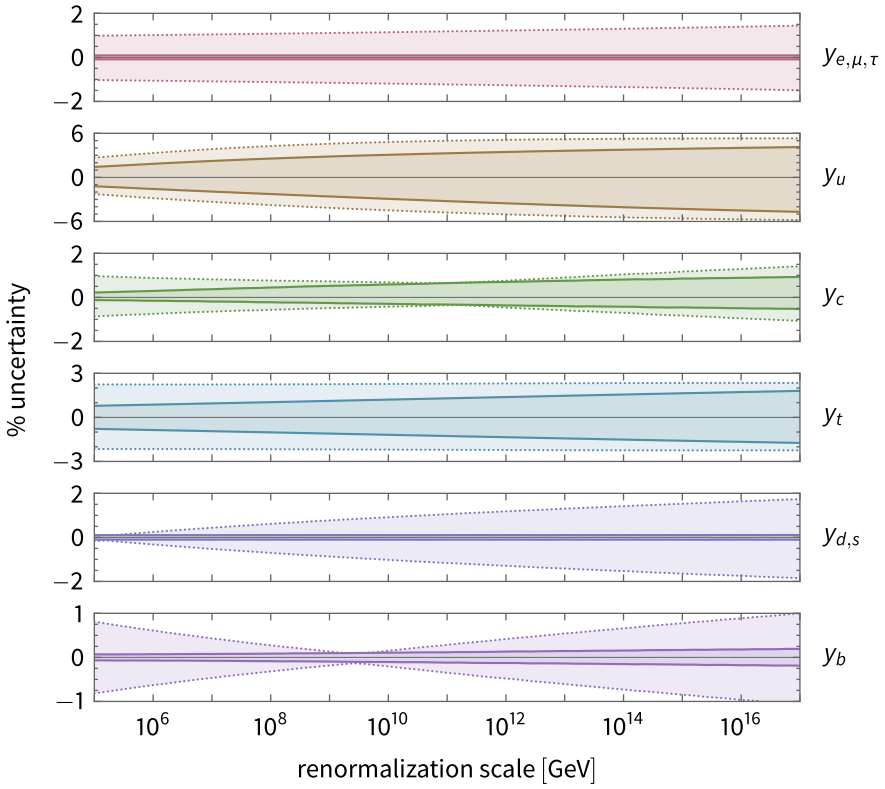

Figure 4.2: Plot of the estimated relative uncertainty of the charged lepton and quark Yukawa couplings in the MSSM as a function of renormalization scale for the matching and running procedure described in the text. The estimated MSSM uncertainty is given by the difference between the dotted (total uncertainty) and solid (SM uncertainty only) lines. We take $\tan\beta = 5$ and $m_{\text{SUSY}} = 10\,\text{TeV}$.

function of renormalization scale for the charged lepton and quark MSSM Yukawa couplings in Fig. 4.2. We note that overall the uncertainty is on the level of several percent and is indeed dominated by the MSSM uncertainty for the charged leptons and the down quarks; for the up quarks, the MSSM uncertainty is on the same order as the SM uncertainty. In this sense, we treat the renormalized values and uncertainties of the MSSM couplings and mixings as only a first-order estimate. Later, the estimate can be revised by the addition of threshold corrections from the MSSM sparticles once the pole mass spectrum is known. We describe a method for systematically incorporate these corrections in an iterative way such that the renormalization procedure can converge on a consistent spectrum in Sec. 9.1.

4.3 The Hierarchical Approximation

In order to match the five-dimensional theory to the flavor structure of the standard model, a large number of parameters must be specified in the five-dimensional model (summarized in Table 4.4), subject to only a relatively small number of experimental constraints. Most of the parameter degrees of freedom of the Yukawa matrices are nonphysical (only the fermion masses and mixing angles are physical) but must be defined in order to perform calculations in the interaction basis. This is no different than the usual situation in the standard model. But, whereas in the standard model it can be shown that in certain weak eigenbases some entries of the Yukawa matrices do not significantly affect the masses and mixing angle and can be set to zero (these are the *texture zeros*), the equivalent procedure cannot be performed in the 5D theory without moving out of the bulk mass basis for the fermions.

However, despite all of the nonphysical order-one Yukawa parameters that must be included in the parameter space of the theory, the localization geography of the 5D theory is still predictive of the standard model flavor structure (even in the case of the PMNS matrix, which is not especially hierarchical). We can estimate the main relationships between the fermion zero-mode localizations and their masses and mixings by exploiting the hierarchical structure of the Yukawa matrices evident in (4.2) and (4.15). If the hierarchies in the Yukawa couplings are explained by the structure of the overlaps of the standard model fermion zero modes with the UV brane,[8]

$$\left.\begin{array}{c} y_{u_1,d_1} \ll y_{u_2,d_2} \ll y_{u_3,d_3} \\ y_{e_1} \ll y_{e_2} \ll y_{e_3} \end{array}\right\} \Longrightarrow \left\{\begin{array}{c} N^{(0)}_{Q_1,u_1,d_1} \ll N^{(0)}_{Q_2,u_2,d_2} \ll N^{(0)}_{Q_3,u_3,d_3} \\ N^{(0)}_{L_1,e_1} \ll N^{(0)}_{L_2,e_2} \ll N^{(0)}_{L_3,e_3} \end{array}\right. , \tag{4.39}$$

the hierarchies in the zero-mode profiles provide a set of small parameters which can be used to expand the singular value decomposition of the Yukawa matrices.[9] This hierarchical profile expansion procedure (first applied to the quark sector in Ref. [182], and extended here to the lepton sector) is special instance of the more general systematic approximation scheme for the singular value decompositions of the Yukawa matrices detailed in Ref. [199]. Here,

[8] Note that these conditions are restrictive. Due to fact that two localization parameters enter into the matching equation for each four-dimensional Yukawa coupling element, the Yukawa hierarchies can be explained even if only one of the two families of fermions involved have hierarchical profile overlaps with the UV brane while those of the other remain order-one. In this case, the hierarchical approximation discussed here cannot be used.

[9] The hierarchies among the neutrino masses depend on the overall absolute mass scale as well as the ordering (see Fig. 4.5). Moderate hierarchies sufficient to permit an accurate expansion can be obtained for the normal hierarchy when $m_1 < \mathcal{O}(1)\,\text{meV}$.

we explicitly construct the first-order terms in the systematic approximation scheme detailed in Ref. [199] for the singular value decompositions of both the quark and lepton Yukawa matrices. We then use the matching relations (4.2) and (4.15) to write these approximations in terms of the fermion zero-mode profiles. In the case of the quark sector, we recover the hierarchical profile approximation of Ref. [182]. The results for the lepton sector are new.

4.3.1 Matrix conventions

First, we establish some notation. We consider an arbitrary complex 3×3 matrix $\boldsymbol{y}$. Under a singular value decomposition $\boldsymbol{y}$ can be written as

$$\boldsymbol{y} = \boldsymbol{V}_R \, \boldsymbol{y}_{\text{diag}} \boldsymbol{V}_L^\dagger, \tag{4.40}$$

where $\boldsymbol{V}_{L,R}$ are unitary matrices and $\boldsymbol{y}_{\text{diag}} = \text{diag}(y_1, y_2, y_3)$ is a diagonal matrix whose entries are the singular values of $\boldsymbol{y}$. The singular values are unique up to their phases, which we can be absorb into the definitions $\boldsymbol{V}_{L,R}$. Without loss of generality, we therefore assume that the singular values are real and non-negative and, further, that they are ordered $y_1 < y_2 < y_3$.[10] The products $\boldsymbol{m}_L = \boldsymbol{y}^\dagger \boldsymbol{y}$ and $\boldsymbol{m}_R = \boldsymbol{y}\, \boldsymbol{y}^\dagger$ are positive-semidefinite Hermitian matrices, which are diagonalized according to

$$\boldsymbol{m}_L = \boldsymbol{V}_L \, \boldsymbol{m}_{\text{diag}} \boldsymbol{V}_L^\dagger \,, \tag{4.41a}$$

$$\boldsymbol{m}_R = \boldsymbol{V}_R \, \boldsymbol{m}_{\text{diag}} \boldsymbol{V}_R^\dagger \,, \tag{4.41b}$$

where

$$\boldsymbol{m}_{\text{diag}} = \text{diag}(m_1, m_2, m_3) = \text{diag}(y_1^2, y_2^2, y_3^2) \,, \tag{4.42}$$

is a diagonal matrix whose entries are the eigenvalues of $\boldsymbol{m}_{L,R}$. The columns of $\boldsymbol{V}_{L(R)}$ are the eigenvectors of $\boldsymbol{m}_{L(R)}$.

For the special case that $\boldsymbol{y}$ is a complex symmetric matrix, it can also be decomposed according the Autonne-Takagi factorization:

$$\boldsymbol{y} = \boldsymbol{U}^* \boldsymbol{y}_{\text{diag}} \, \boldsymbol{U}^\dagger \,, \tag{4.43}$$

where $\boldsymbol{U}$ is unitary. This factorization is related to the singular value decomposition (4.40)

[10] This ordering assumption is not necessary but simplifies the succeeding discussion. For the more general case see Ref. [199].

by the rephasings

$$\boldsymbol{U} = \boldsymbol{V}_L \,\mathrm{diag}(e^{-i\phi_1}, e^{-i\phi_2}, e^{-i\phi_3}) = \boldsymbol{V}_R^* \,\mathrm{diag}(e^{i\phi_1}, e^{i\phi_2}, e^{i\phi_3})\,, \tag{4.44}$$

where $\phi_n = \psi_n/2$ for

$$\boldsymbol{V}_L^{\mathrm{T}} \boldsymbol{y}\, \boldsymbol{V}_L = \boldsymbol{V}_R^{\mathrm{T}}\, \boldsymbol{y}^* \boldsymbol{V}_R = \boldsymbol{y}_{\mathrm{diag}}\, \mathrm{diag}(e^{i\psi_1}, e^{i\psi_2}, e^{i\psi_3})\,. \tag{4.45}$$

Thus, in this case, the diagonalizations of the products $\boldsymbol{m}_L = \boldsymbol{m}_R^*$ take the forms:

$$\boldsymbol{m}_L = \boldsymbol{U}\boldsymbol{P}\, \boldsymbol{m}_{\mathrm{diag}}\, \boldsymbol{P}^* \boldsymbol{U}^\dagger = \boldsymbol{U} \boldsymbol{m}_{\mathrm{diag}}\, \boldsymbol{U}^\dagger\,, \tag{4.46a}$$

$$\boldsymbol{m}_R = \boldsymbol{U}^*\boldsymbol{P}\, \boldsymbol{m}_{\mathrm{diag}}\, \boldsymbol{P}^* \boldsymbol{U}^{\mathrm{T}} = \boldsymbol{U}^* \boldsymbol{m}_{\mathrm{diag}}\, \boldsymbol{U}^{\mathrm{T}}\,, \tag{4.46b}$$

where $\boldsymbol{P} = \mathrm{diag}(e^{i\phi_1}, e^{i\phi_2}, e^{i\psi_3})$.

4.3.2 Approximate diagonalization

Next, we summarize the main results of Ref. [199], although we employ a slightly modified formalism. We consider a positive-semidefinite 3×3 Hermitian matrix $\boldsymbol{m}$ of the form $\boldsymbol{m}_{L,R}$ defined in the previous section, where the diagonalization takes the form

$$\boldsymbol{m} = \boldsymbol{V} \boldsymbol{m}_{\mathrm{diag}} \boldsymbol{V}^\dagger\,. \tag{4.47}$$

The eigenvalues of $\boldsymbol{m}$ may be calculated

$$m_1^{(n)} = (\det \boldsymbol{m})\, (\mathrm{tr}\, \overline{\boldsymbol{m}}^n)^{-1/n} = m_1 \left[1 + \left(\frac{m_1}{m_2}\right)^n + \left(\frac{m_1}{m_3}\right)^n\right]^{-1/n}\,, \tag{4.48a}$$

$$m_2^{(n)} = \left(\frac{\mathrm{tr}\, \overline{\boldsymbol{m}}^n}{\mathrm{tr}\, \boldsymbol{m}^n}\right)^{1/n} = m_2 \left[\frac{1 + (m_1/m_2)^n + (m_1/m_3)^n}{1 + (m_1/m_3)^n + (m_2/m_3)^n}\right]^{1/n}\,, \tag{4.48b}$$

$$m_3^{(n)} = (\mathrm{tr}\, \boldsymbol{m}^n)^{1/n} = m_3 \left[1 + \left(\frac{m_1}{m_3}\right)^n + \left(\frac{m_2}{m_3}\right)^n\right]^{1/n}\,, \tag{4.48c}$$

where

$$\overline{\boldsymbol{m}} \equiv (\det \boldsymbol{m})(\boldsymbol{m}^{-1})^{\mathrm{T}} \tag{4.49}$$

is the cofactor matrix[11] of $\boldsymbol{m}$ and n is a positive integer.[12] At a given order n, the errors in this approximation are strictly bounded from above by the nth powers of the ratios of eigenvalues, $(m_1/m_2)^n$ or $(m_2/m_3)^n$, which therefore tend to zero as $n \to \infty$.

In order to approximate the unitary matrix $\boldsymbol{V}$ defining the diagonalization transformation, we first write it as (the *abc* parametrization of Ref. [199]):

$$\boldsymbol{V} = \begin{pmatrix} \frac{1}{n_1} & \frac{a - c^* \tilde{b}}{n_1 n_3} & \frac{b}{n_3} \\ -\frac{a^*}{n_1} & \frac{1 + b^* \tilde{b}}{n_1 n_3} & \frac{c}{n_3} \\ -\frac{\tilde{b}^*}{n_1} & -\frac{\tilde{c}^*}{n_1 n_3} & \frac{1}{n_3} \end{pmatrix} \begin{pmatrix} e^{i\alpha} & & \\ & e^{i\beta} & \\ & & e^{i\gamma} \end{pmatrix}, \tag{4.50}$$

where

$$a = -\frac{V_{21}^*}{V_{11}^*}, \qquad b = \frac{V_{31}}{V_{33}}, \qquad c = \frac{V_{32}}{V_{33}}, \tag{4.51}$$

are complex numbers and

$$\alpha = \arg V_{11}, \qquad \beta = \arg(\det \boldsymbol{V}) - \alpha - \gamma, \qquad \gamma = \arg V_{33}, \tag{4.52}$$

are phase angles. Together, these comprise the nine degrees of freedom of $\boldsymbol{V}$. The quantities

$$n_1^2 \equiv 1 + |a|^2 + |\tilde{b}|^2, \tag{4.53a}$$

$$n_3^2 \equiv 1 + |b|^2 + |c|^2. \tag{4.53b}$$

are normalization constants for the column vectors, and the notation

$$\tilde{b} \equiv b - ac = -\frac{V_{31}^*}{V_{11}^*}, \tag{4.54a}$$

$$\tilde{c} \equiv c + a^* b = -\frac{V_{32}^*}{V_{11}^* V_{33}^*}, \tag{4.54b}$$

[11] Note that this is defined for $m_1 = 0$.

[12] If $\boldsymbol{m}$ can be further factorized, such as $\boldsymbol{m}_L = \boldsymbol{y}^\dagger \boldsymbol{y}$ or $\boldsymbol{m}_R = \boldsymbol{y}\, \boldsymbol{y}^\dagger$ for a complex matrix $\boldsymbol{y}$ as discussed in the previous section, then n can take half-integer values. For example, $\boldsymbol{m}_L^{1/2} = \boldsymbol{y}^\dagger$ and $\boldsymbol{m}_L^{3/2} = \boldsymbol{y}^\dagger \boldsymbol{y}\, \boldsymbol{y}^\dagger$, etc.

is defined for convenience. The complex parameters can be approximated as

$$a^{(n)} = -\frac{(\overline{m}^n)_{21}}{(\overline{m}^n)_{11}}\,, \tag{4.55a}$$

$$b^{(n)} = \frac{(m^n)_{13}}{(m^n)_{33}}\,, \tag{4.55b}$$

$$c^{(n)} = \frac{(m^n)_{23}}{(m^n)_{33}}\,, \tag{4.55c}$$

$$\tilde{b}^{(n)} = -\frac{(\overline{m}^n)_{31}}{(\overline{m}^n)_{11}}\,. \tag{4.55d}$$

At a given order n, the errors are again of the order of the ratios $(m_1/m_2)^n$ or $(m_2/m_3)^n$, which therefore tend to zero as $n \to \infty$.[13]

Mixing matrices

In the quark and lepton sectors, the CKM and PMNS matrices are each composed as the product of two unitary matrices:

$$\boldsymbol{V}_{\text{CKM}} = (\boldsymbol{V}_L^u)^\dagger\, \boldsymbol{V}_L^d\,, \tag{4.56a}$$

$$\boldsymbol{U}_{\text{PMNS}} = (\boldsymbol{V}_L^e)^\dagger\, \boldsymbol{V}_L^\nu \tag{4.56b}$$

The Yukawa coupling decompositions (4.7) (for the quarks) and (4.19) (for the leptons with Dirac neutrinos) that define these matrices and the standard model fermion five-dimensional bulk mass matrices are both invariant under individual rotations of the fermion fields. We can use this freedom to choose the phases of the diagonal entries of the left-handed unitary matrices $\boldsymbol{V}_L^{u,d,e,\nu}$ to be real (pushing all residual phases in the decompositions into the right-handed matrices $\boldsymbol{V}_R^{u,d,e,\nu}$). In the *abc* parametrization (4.50), a particularly useful choice is $\alpha = \beta = \gamma = 0$. We note for future reference that given two unitary matrices $\boldsymbol{V}_{1,2}$ of this form, the elements of the product matrix $\boldsymbol{U} = \boldsymbol{V}_1^\dagger \boldsymbol{V}_2$ are written

$$U_{11} = \frac{1 + a_1 a_2^* + \tilde{b}_1 \tilde{b}_2^*}{n_{1,1}\, n_{1,2}}\,, \tag{4.57a}$$

[13] In fact, strict upper bounds on the errors depending on these ratios can be calculated. For further details, see Ref. [199].

$$U_{12} = \frac{a_2 - a_1}{n_{1,1}} + \frac{\tilde{b}_1 \tilde{c}_2 - \tilde{b}_2 \tilde{c}_{21}^*}{n_{1,1}\, n_{1,2}\, n_{3,2}}\,, \tag{4.57b}$$

$$U_{13} = \frac{\tilde{b}_{21} - \tilde{b}_1}{n_{1,1}\, n_{3,2}}\,, \tag{4.57c}$$

$$U_{21} = \frac{a_1^* - a_2^*}{n_{1,2}} + \frac{\tilde{b}_2^* \tilde{c}_1 - \tilde{b}_1^* \tilde{c}_{12}}{n_{1,1}\, n_{1,2}\, n_{3,1}}\,, \tag{4.57d}$$

$$U_{22} = 1 + a_1^* a_2 - \frac{\tilde{b}_1^* \tilde{b}_{12}}{n_{1,1}\, n_{3,1}} - \frac{\tilde{b}_2 \tilde{b}_{21}^*}{n_{1,2}, n_{3,2}} + \frac{\tilde{c}_1 \tilde{c}_2^* + (b_1 b_2^* + c_1 c_2^*)\, \tilde{b}_1^* \tilde{b}_2}{n_{1,1}\, n_{1,2}\, n_{3,1}\, n_{3,2}}\,, \tag{4.57e}$$

$$U_{23} = \frac{\tilde{c}_{21}}{n_{3,2}} - \frac{\tilde{c}_1 + (b_1 c_2 + b_2 c_1)\, \tilde{b}_u^*}{n_{1,1}\, n_{3,1}\, n_{3,2}}\,, \tag{4.57f}$$

$$U_{31} = \frac{\tilde{b}_{12}^* - \tilde{b}_2^*}{n_{1,2}\, n_{3,1}}\,, \tag{4.57g}$$

$$U_{32} = \frac{\tilde{c}_{12}^*}{n_{3,1}} - \frac{\tilde{c}_2^* + (b_1 c_2 + b_2 c_1)^*\, \tilde{b}_2}{n_{1,2}\, n_{3,1}\, n_{3,2}}\,, \tag{4.57h}$$

$$U_{33} = \frac{1 + b_1^* b_2 + c_1^* c_2}{n_{3,1}\, n_{3,2}}\,, \tag{4.57i}$$

where we have defined

$$\tilde{b}_{ij} = b_i + a_j c_i\,, \tag{4.58a}$$

$$\tilde{c}_{ij} = c_i - a_j^* b_i\,. \tag{4.58b}$$

4.3.3 Quark sector

We can reduce the complexity of the quark mass system somewhat by exploiting the hierarchical structure of the Yukawa matrices to expand the mass eigenvalues and eigenvectors. At the $n = 1$ order in the systematic approximation scheme discussed in the previous section the quark Yukawa couplings take the forms

$$y_{u,d}^2 = \frac{|\det \boldsymbol{y}_{u,d}|^2}{\operatorname{tr} \overline{\boldsymbol{y}}_{u,d}^\dagger\, \overline{\boldsymbol{y}}_{u,d}} + \mathcal{O}\left(\frac{y_{u,d}^4}{y_{c,s}^2}\right), \tag{4.59a}$$

$$y_{c,s}^2 = \frac{\operatorname{tr} \overline{\boldsymbol{y}}_{u,d}^\dagger\, \overline{\boldsymbol{y}}_{u,d}}{\operatorname{tr} \boldsymbol{y}_{u,d}^\dagger\, \boldsymbol{y}_{u,d}} + \mathcal{O}\left(\frac{y_{c,s}^4}{y_{t,b}^2}\right), \tag{4.59b}$$

$$y_{t,b}^2 = \operatorname{tr} \boldsymbol{y}_{u,d}^\dagger \boldsymbol{y}_{u,d} + \mathcal{O}(y_{c,s}^2)\,, \tag{4.59c}$$

where

$$\overline{\boldsymbol{y}}_{u,d} \equiv (\det \boldsymbol{y}_{u,d})\,(\boldsymbol{y}_{u,d}^{-1})^{\mathrm{T}} \tag{4.60}$$

is the cofactor matrix of $\boldsymbol{y}_{u,d}$.

In the zero-mode approximation discussed in Sec. 4.1.1, we can express the traces in terms of the five-dimensional Yukawa couplings and quark profiles as

$$\operatorname{tr} \boldsymbol{y}_{u,d}^\dagger \boldsymbol{y}_{u,d} = \sum_{ij} 4\,|(Y_{u,d})_{ij}|^2 \left(N_{u_i,d_i}^{(0)} N_{Q_j}^{(0)}\right)^2, \tag{4.61a}$$

$$\operatorname{tr} \overline{\boldsymbol{y}}_{u,d}^\dagger \overline{\boldsymbol{y}}_{u,d} = \sum_{ij} 4\,|(M_{u,d})_{ij}|^2 \prod_{m\neq i} \left(N_{u_m,d_m}^{(0)}\right)^2 \prod_{n\neq j} \left(N_{Q_n}^{(0)}\right)^2, \tag{4.61b}$$

where $(M_{u,d})_{ij}$ are the minors of the 5D Yukawa matrices, i.e., the determinants of the submatrices formed by removing the ith row and jth column of $\boldsymbol{Y}_{u,d}$. Up to a sign, they are equivalent to the entries of the cofactor matrix:

$$(M_{u,d})_{ij} = (-1)^{i+j} (\det \boldsymbol{Y}_{u,d}) \left(Y_{u,d}^{-1}\right)_{ji}. \tag{4.62}$$

The quark normalization factors arise from the quark profiles evaluated on the UV brane:

$$f_{Q_i,u_i,d_i}^{(0)}(y=0) = \sqrt{k}\, N_{Q_i,u_i,d_i}^{(0)}\,. \tag{4.63}$$

Using (4.61), we have

$$y_{u,d} = 2\,\frac{|\det \boldsymbol{Y}_{u,d}|}{|(M_{u,d})_{11}|}\, N_{Q_1}^{(0)} N_{u_1,d_1}^{(0)} \left[1 + \mathcal{O}\left(\frac{N_{Q_1}^{(0)}}{N_{Q_2}^{(0)}}, \frac{N_{u_1,d_1}^{(0)}}{N_{u_2,d_2}^{(0)}}\right)\right], \tag{4.64a}$$

$$y_{c,s} = 2\,\frac{|(M_{u,d})_{11}|}{|(Y_{u,d})_{33}|}\, N_{Q_2}^{(0)} N_{u_2,d_2}^{(0)} \left[1 + \mathcal{O}\left(\frac{N_{Q_1}^{(0)}}{N_{Q_2}^{(0)}}, \frac{N_{u_1,d_1}^{(0)}}{N_{u_2,d_2}^{(0)}}, \frac{N_{Q_2}^{(0)}}{N_{Q_3}^{(0)}}, \frac{N_{u_2,d_2}^{(0)}}{N_{u_3,d_3}^{(0)}}\right)\right], \tag{4.64b}$$

$$y_{t,b} = 2\,|(Y_{u,d})_{33}|\, N_{Q_3}^{(0)} N_{u_3,d_3}^{(0)} \left[1 + \mathcal{O}\left(\frac{N_{Q_2}^{(0)}}{N_{Q_3}^{(0)}}, \frac{N_{u_2,d_2}^{(0)}}{N_{u_3,d_3}^{(0)}}\right)\right], \tag{4.64c}$$

where we have assumed hierarchical profiles,

$$N_{Q_1,u_1,d_1}^{(0)} \ll N_{Q_2,u_2,d_2}^{(0)} \ll N_{Q_3,u_3,d_3}^{(0)}\,. \tag{4.65}$$

At first order in the profile hierarchies, we recover the expressions of Ref. [182].

Expressing the unitary matrices $\boldsymbol{V}_L^{u,d}$ in the *abc* parametrization (in the convention $\alpha = \beta = \gamma = 0$), we find in the $n = 1$ approximation:

$$a_{u,d} = -\frac{(\overline{\boldsymbol{y}}_{u,d}^{\dagger}\,\overline{\boldsymbol{y}}_{u,d})_{21}}{(\overline{\boldsymbol{y}}_{u,d}^{\dagger}\,\overline{\boldsymbol{y}}_{u,d})_{11}} + \mathcal{O}\!\left(\frac{y_{u,d}}{y_{c,s}}\right), \tag{4.66a}$$

$$b_{u,d} = \frac{(\boldsymbol{y}_{u,d}^{\dagger}\,\boldsymbol{y}_{u,d})_{13}}{(\boldsymbol{y}_{u,d}^{\dagger}\,\boldsymbol{y}_{u,d})_{33}} + \mathcal{O}\!\left(\frac{y_{u,d}}{y_{t,b}}\right), \tag{4.66b}$$

$$c_{u,d} = \frac{(\boldsymbol{y}_{u,d}^{\dagger}\,\boldsymbol{y}_{u,d})_{23}}{(\boldsymbol{y}_{u,d}^{\dagger}\,\boldsymbol{y}_{u,d})_{33}} + \mathcal{O}\!\left(\frac{y_{c,s}}{y_{t,b}}\right), \tag{4.66c}$$

$$\tilde{b}_{u,d} = -\frac{(\overline{\boldsymbol{y}}_{u,d}^{\dagger}\,\overline{\boldsymbol{y}}_{u,d})_{31}}{(\overline{\boldsymbol{y}}_{u,d}^{\dagger}\,\overline{\boldsymbol{y}}_{u,d})_{11}} + \mathcal{O}\!\left(\frac{y_{u,d}}{y_{t,b}}\right), \tag{4.66d}$$

which, in terms of the five-dimensional Yukawa couplings and quark profiles, take the forms

$$a_{u,d} = \frac{(M_{u,d})_{21}}{(M_{u,d})_{11}}\frac{N_{Q_1}^{(0)}}{N_{Q_2}^{(0)}}\left[1 + \mathcal{O}\!\left(\frac{N_{u_1,d_1}^{(0)}}{N_{u_2,d_2}^{(0)}}\right)\right], \tag{4.67a}$$

$$b_{u,d} = \frac{(Y_{u,d})_{13}}{(Y_{u,d})_{33}}\frac{N_{Q_1}^{(0)}}{N_{Q_3}^{(0)}}\left[1 + \mathcal{O}\!\left(\frac{N_{u_2,d_2}^{(0)}}{N_{u_3,d_3}^{(0)}}\right)\right], \tag{4.67b}$$

$$c_{u,d} = \frac{(Y_{u,d})_{23}}{(Y_{u,d})_{33}}\frac{N_{Q_2}^{(0)}}{N_{Q_3}^{(0)}}\left[1 + \mathcal{O}\!\left(\frac{N_{u_2,d_2}^{(0)}}{N_{u_3,d_3}^{(0)}}\right)\right], \tag{4.67c}$$

$$\tilde{b}_{u,d} = -\frac{(M_{u,d})_{31}}{(M_{u,d})_{11}}\frac{N_{Q_1}^{(0)}}{N_{Q_3}^{(0)}}\left[1 + \mathcal{O}\!\left(\frac{N_{u_1,d_1}^{(0)}}{N_{u_2,d_2}^{(0)}}\right)\right]. \tag{4.67d}$$

At first order in the hierarchies, we recover the expressions of Ref. [182]:

$$\boldsymbol{V}_L^{u,d} \simeq \begin{pmatrix} 1 & \dfrac{(M_{u,d})_{21}}{(M_{u,d})_{11}}\dfrac{N_{Q_1}^{(0)}}{N_{Q_2}^{(0)}} & \dfrac{(Y_{u,d})_{13}}{(Y_{u,d})_{33}}\dfrac{N_{Q_1}^{(0)}}{N_{Q_3}^{(0)}} \\ -\dfrac{(M_{u,d})_{21}^*}{(M_{u,d})_{11}^*}\dfrac{N_{Q_1}^{(0)}}{N_{Q_2}^{(0)}} & 1 & \dfrac{(Y_{u,d})_{23}}{(Y_{u,d})_{33}}\dfrac{N_{Q_2}^{(0)}}{N_{Q_3}^{(0)}} \\ \dfrac{(M_{u,d})_{31}^*}{(M_{u,d})_{11}^*}\dfrac{N_{Q_1}^{(0)}}{N_{Q_3}^{(0)}} & -\dfrac{(Y_{u,d})_{23}^*}{(Y_{u,d})_{33}^*}\dfrac{N_{Q_2}^{(0)}}{N_{Q_3}^{(0)}} & 1 \end{pmatrix}. \tag{4.68}$$

The CKM matrix elements are of the form (4.57), with $\boldsymbol{V}_{1,2} = \boldsymbol{V}_L^{u,d}$. In the $n = 1$ approximation, we find

$$V_{ud} = 1 + \mathcal{O}\left(\frac{y_d}{y_s}\right), \tag{4.69a}$$

$$V_{us} = \frac{(\overline{\boldsymbol{y}}_d^\dagger\, \overline{\boldsymbol{y}}_d)_{21}}{(\overline{\boldsymbol{y}}_d^\dagger\, \overline{\boldsymbol{y}}_d)_{11}} - \frac{(\overline{\boldsymbol{y}}_u^\dagger\, \overline{\boldsymbol{y}}_u)_{21}}{(\overline{\boldsymbol{y}}_u^\dagger\, \overline{\boldsymbol{y}}_u)_{11}} + \mathcal{O}\left(\frac{y_d}{y_s}\right), \tag{4.69b}$$

$$V_{ub} = \frac{(\overline{\boldsymbol{y}}_u^\dagger\, \overline{\boldsymbol{y}}_u)_{31}}{(\overline{\boldsymbol{y}}_u^\dagger\, \overline{\boldsymbol{y}}_u)_{11}} + \frac{(\boldsymbol{y}_d^\dagger\, \boldsymbol{y}_d)_{13}}{(\boldsymbol{y}_d^\dagger\, \boldsymbol{y}_d)_{33}} + \mathcal{O}\left(\frac{y_d}{y_b}\right), \tag{4.69c}$$

$$V_{cd} = \frac{(\overline{\boldsymbol{y}}_u^\dagger\, \overline{\boldsymbol{y}}_u)_{21}^*}{(\overline{\boldsymbol{y}}_u^\dagger\, \overline{\boldsymbol{y}}_u)_{11}^*} - \frac{(\overline{\boldsymbol{y}}_d^\dagger\, \overline{\boldsymbol{y}}_d)_{21}^*}{(\overline{\boldsymbol{y}}_d^\dagger\, \overline{\boldsymbol{y}}_d)_{11}^*} + \mathcal{O}\left(\frac{y_d}{y_s}\right), \tag{4.69d}$$

$$V_{cs} = 1 + \mathcal{O}\left(\frac{y_d}{y_s}\right), \tag{4.69e}$$

$$V_{cb} = \frac{(\boldsymbol{y}_d^\dagger\, \boldsymbol{y}_d)_{23}}{(\boldsymbol{y}_d^\dagger\, \boldsymbol{y}_d)_{33}} - \frac{(\boldsymbol{y}_u^\dagger\, \boldsymbol{y}_u)_{23}}{(\boldsymbol{y}_u^\dagger\, \boldsymbol{y}_u)_{33}} + \mathcal{O}\left(\frac{y_s}{y_b}\right), \tag{4.69f}$$

$$V_{td} = \frac{(\boldsymbol{y}_u^\dagger\, \boldsymbol{y}_u)_{13}^*}{(\boldsymbol{y}_u^\dagger\, \boldsymbol{y}_u)_{33}^*} + \frac{(\overline{\boldsymbol{y}}_d^\dagger\, \overline{\boldsymbol{y}}_d)_{31}^*}{(\overline{\boldsymbol{y}}_d^\dagger\, \overline{\boldsymbol{y}}_d)_{11}^*} + \mathcal{O}\left(\frac{y_d}{y_b}\right), \tag{4.69g}$$

$$V_{ts} = \frac{(\boldsymbol{y}_u^\dagger\, \boldsymbol{y}_u)_{23}^*}{(\boldsymbol{y}_u^\dagger\, \boldsymbol{y}_u)_{33}^*} - \frac{(\boldsymbol{y}_d^\dagger\, \boldsymbol{y}_d)_{23}^*}{(\boldsymbol{y}_d^\dagger\, \boldsymbol{y}_d)_{33}^*} + \mathcal{O}\left(\frac{y_s}{y_b}\right), \tag{4.69h}$$

$$V_{tb} = 1 + \mathcal{O}\left(\frac{y_s}{y_b}\right), \tag{4.69i}$$

such that the Wolfenstein parameters are written

$$\lambda = \left| \frac{(\overline{\boldsymbol{y}}_d^\dagger \, \overline{\boldsymbol{y}}_d)_{21}}{(\overline{\boldsymbol{y}}_d^\dagger \, \overline{\boldsymbol{y}}_d)_{11}} - \frac{(\overline{\boldsymbol{y}}_u^\dagger \, \overline{\boldsymbol{y}}_u)_{21}}{(\overline{\boldsymbol{y}}_u^\dagger \, \overline{\boldsymbol{y}}_u)_{11}} \right| + \mathcal{O}\left(\frac{y_d}{y_s}\right), \tag{4.70a}$$

$$A = \left| \frac{(\boldsymbol{y}_d^\dagger \, \boldsymbol{y}_d)_{23}}{(\boldsymbol{y}_d^\dagger \, \boldsymbol{y}_d)_{33}} - \frac{(\boldsymbol{y}_u^\dagger \, \boldsymbol{y}_u)_{23}}{(\boldsymbol{y}_u^\dagger \, \boldsymbol{y}_u)_{33}} \right| \left| \frac{(\overline{\boldsymbol{y}}_d^\dagger \, \overline{\boldsymbol{y}}_d)_{21}}{(\overline{\boldsymbol{y}}_d^\dagger \, \overline{\boldsymbol{y}}_d)_{11}} - \frac{(\overline{\boldsymbol{y}}_u^\dagger \, \overline{\boldsymbol{y}}_u)_{21}}{(\overline{\boldsymbol{y}}_u^\dagger \, \overline{\boldsymbol{y}}_u)_{11}} \right|^{-2} + \mathcal{O}\left(\frac{y_d}{y_s}\right), \tag{4.70b}$$

$$\bar{\rho} - i\bar{\eta} = -\frac{\frac{(\overline{\boldsymbol{y}}_u^\dagger \, \overline{\boldsymbol{y}}_u)_{31}}{(\overline{\boldsymbol{y}}_u^\dagger \, \overline{\boldsymbol{y}}_u)_{11}} + \frac{(\boldsymbol{y}_d^\dagger \, \boldsymbol{y}_d)_{13}}{(\boldsymbol{y}_d^\dagger \, \boldsymbol{y}_d)_{33}}}{\left[\frac{(\overline{\boldsymbol{y}}_u^\dagger \, \overline{\boldsymbol{y}}_u)_{21}}{(\overline{\boldsymbol{y}}_u^\dagger \, \overline{\boldsymbol{y}}_u)_{11}} - \frac{(\overline{\boldsymbol{y}}_d^\dagger \, \overline{\boldsymbol{y}}_d)_{21}}{(\overline{\boldsymbol{y}}_d^\dagger \, \overline{\boldsymbol{y}}_d)_{11}}\right] \left[\frac{(\boldsymbol{y}_d^\dagger \, \boldsymbol{y}_d)_{23}}{(\boldsymbol{y}_d^\dagger \, \boldsymbol{y}_d)_{33}} - \frac{(\boldsymbol{y}_u^\dagger \, \boldsymbol{y}_u)_{23}}{(\boldsymbol{y}_u^\dagger \, \boldsymbol{y}_u)_{33}}\right]} + \mathcal{O}\left(\frac{y_d}{y_b}\right). \tag{4.70c}$$

In terms of the profiles, we find

$$V_{ud} = 1 + \mathcal{O}\left(\frac{N_{Q_1}^{(0)}}{N_{Q_2}^{(0)}} \frac{N_{Q_1,u_1,d_1}^{(0)}}{N_{Q_2,u_2,d_2}^{(0)}}, \frac{N_{Q_2}^{(0)}}{N_{Q_3}^{(0)}} \frac{N_{Q_2,u_2,d_2}^{(0)}}{N_{Q_3,u_3,d_3}^{(0)}}\right), \tag{4.71a}$$

$$V_{us} = \left[\frac{(M_d)_{21}}{(M_d)_{11}} - \frac{(M_u)_{21}}{(M_u)_{11}}\right] \frac{N_{Q_1}^{(0)}}{N_{Q_2}^{(0)}} \left[1 + \mathcal{O}\left(\frac{N_{u_1,d_1}^{(0)}}{N_{u_2,d_2}^{(0)}}\right)\right], \tag{4.71b}$$

$$V_{ub} = \left[\frac{(Y_d)_{13}}{(Y_d)_{33}} - \frac{(M_u)_{21}}{(M_u)_{11}} \frac{(Y_d)_{23}}{(Y_d)_{33}} + \frac{(M_u)_{31}}{(M_u)_{11}}\right] \frac{N_{Q_1}^{(0)}}{N_{Q_3}^{(0)}} \left[1 + \mathcal{O}\left(\frac{N_{u_1}^{(0)}}{N_{u_2}^{(0)}}, \frac{N_{d_2}^{(0)}}{N_{d_3}^{(0)}}\right)\right], \tag{4.71c}$$

$$V_{cd} = \left[\frac{(M_u)_{21}^*}{(M_u)_{11}^*} - \frac{(M_d)_{21}^*}{(M_d)_{11}^*}\right] \frac{N_{Q_1}^{(0)}}{N_{Q_2}^{(0)}} \left[1 + \mathcal{O}\left(\frac{N_{u_1,d_1}^{(0)}}{N_{u_2,d_2}^{(0)}}\right)\right], \tag{4.71d}$$

$$V_{cs} = 1 + \mathcal{O}\left(\frac{N_{Q_1}^{(0)}}{N_{Q_2}^{(0)}} \frac{N_{Q_1,u_1,d_1}^{(0)}}{N_{Q_2,u_2,d_2}^{(0)}}\right), \tag{4.71e}$$

$$V_{cb} = \left[\frac{(Y_d)_{23}}{(Y_d)_{33}} - \frac{(Y_u)_{23}}{(Y_u)_{33}}\right] \frac{N_{Q_2}^{(0)}}{N_{Q_3}^{(0)}} \left[1 + \mathcal{O}\left(\frac{N_{u_2,d_2}^{(0)}}{N_{u_3,d_3}^{(0)}}\right)\right], \tag{4.71f}$$

$$V_{td} = \left[\frac{(Y_u)_{13}^*}{(Y_u)_{33}^*} - \frac{(Y_u)_{23}^*}{(Y_u)_{33}^*} \frac{(M_d)_{21}^*}{(M_d)_{11}^*} + \frac{(M_d)_{31}^*}{(M_d)_{11}^*}\right] \frac{N_{Q_1}^{(0)}}{N_{Q_3}^{(0)}} \left[1 + \mathcal{O}\left(\frac{N_{d_1}^{(0)}}{N_{d_2}^{(0)}}, \frac{N_{u_2}^{(0)}}{N_{u_3}^{(0)}}\right)\right], \tag{4.71g}$$

$$V_{ts} = \left[\frac{(Y_u)_{23}^*}{(Y_u)_{33}^*} - \frac{(Y_d)_{23}^*}{(Y_d)_{33}^*}\right] \frac{N_{Q_2}^{(0)}}{N_{Q_3}^{(0)}} \left[1 + \mathcal{O}\left(\frac{N_{u_2,d_2}^{(0)}}{N_{u_3,d_3}^{(0)}}\right)\right], \tag{4.71h}$$

$$V_{tb} = 1 + \mathcal{O}\left(\frac{N^{(0)}_{Q_1}}{N^{(0)}_{Q_2}}\frac{N^{(0)}_{Q_1,u_1,d_1}}{N^{(0)}_{Q_2,u_2,d_2}}, \frac{N^{(0)}_{Q_2}}{N^{(0)}_{Q_3}}\frac{N^{(0)}_{Q_2,u_2,d_2}}{N^{(0)}_{Q_3,u_3,d_3}}\right), \tag{4.71i}$$

and

$$\lambda = \left|\frac{(M_d)_{21}}{(M_d)_{11}} - \frac{(M_u)_{21}}{(M_u)_{11}}\right| \frac{N^{(0)}_{Q_1}}{N^{(0)}_{Q_2}} \left[1 + \mathcal{O}\left(\frac{N^{(0)}_{u_1,d_1}}{N^{(0)}_{u_2,d_2}}\right)\right], \tag{4.72a}$$

$$A = \frac{\left|\frac{(Y_d)_{23}}{(Y_d)_{33}} - \frac{(Y_u)_{23}}{(Y_u)_{33}}\right|}{\left|\frac{(M_d)_{21}}{(M_d)_{11}} - \frac{(M_u)_{21}}{(M_u)_{11}}\right|^2} \frac{\left(N^{(0)}_{Q_2}\right)^3}{\left(N^{(0)}_{Q_1}\right)^2 N^{(0)}_{Q_3}} \left[1 + \mathcal{O}\left(\frac{N^{(0)}_{u_1,d_1}}{N^{(0)}_{u_2,d_2}}, \frac{N^{(0)}_{u_2,d_2}}{N^{(0)}_{u_3,d_3}}\right)\right], \tag{4.72b}$$

$$\bar{\rho} - i\bar{\eta} = -\frac{\frac{(Y_d)_{13}}{(Y_d)_{33}} - \frac{(M_u)_{21}}{(M_u)_{11}}\frac{(Y_d)_{23}}{(Y_d)_{33}} + \frac{(M_u)_{31}}{(M_u)_{11}}}{\left[\frac{(M_u)_{21}}{(M_u)_{11}} - \frac{(M_d)_{21}}{(M_d)_{11}}\right]\left[\frac{(Y_d)_{23}}{(Y_d)_{33}} - \frac{(Y_u)_{23}}{(Y_u)_{33}}\right]} \left[1 + \mathcal{O}\left(\frac{N^{(0)}_{u_1,d_1}}{N^{(0)}_{u_2,d_2}}, \frac{N^{(0)}_{u_2,d_2}}{N^{(0)}_{u_3,d_3}}\right)\right], \tag{4.72c}$$

recovering the expressions of Ref. [182]. These expressions are consistent with the CKM matrix at this level of approximation, calculated directly from (4.68). Note that $\bar{\rho}$ and $\bar{\eta}$ are at first order independent of the zero-mode localizations. The warped setup predicts that these parameters are thus not suppressed by any small parameters, while their precise order-one values remain unexplained. On the other hand, in order to explain λ and A, the localization parameters of the quark doublets must be correlated. Assuming that the magnitudes of the 5D Yukawa matrix elements are log-normally distributed as in Sec. 4.4.1, we show the correlations at 1σ (dark), 2σ (medium), and 3σ (light) confidence levels in Fig. 4.3. We see that the smallness of the CKM parameters leads to a definite preference that $c_{Q_1} < c_{Q_2} < c_{Q_3}$. Once the doublet localizations are chosen according to (4.72), the singlet localizations are determined by the expressions for the Yukawa couplings (4.64). We show the resulting correlations induced between the localization parameters of the singlets and the localization of any one doublet (we choose here to use c_{Q_3}) in Fig. 4.4. Comparing this to Fig. 4.1, we see the same general trend that heavier masses require greater UV-localization, although there is more freedom now that the Yukawa couplings are allowed to take an order-one spread. Note that in order to explain the top mass with $c_{u_3} > -10$ we require $c_{Q_3} \gtrsim 0.36$, which accordingly restricts the allowed range of localizations for the singlets. This bound is indicated in Fig. 4.4 as a dashed line; the allowed regions are above this line.

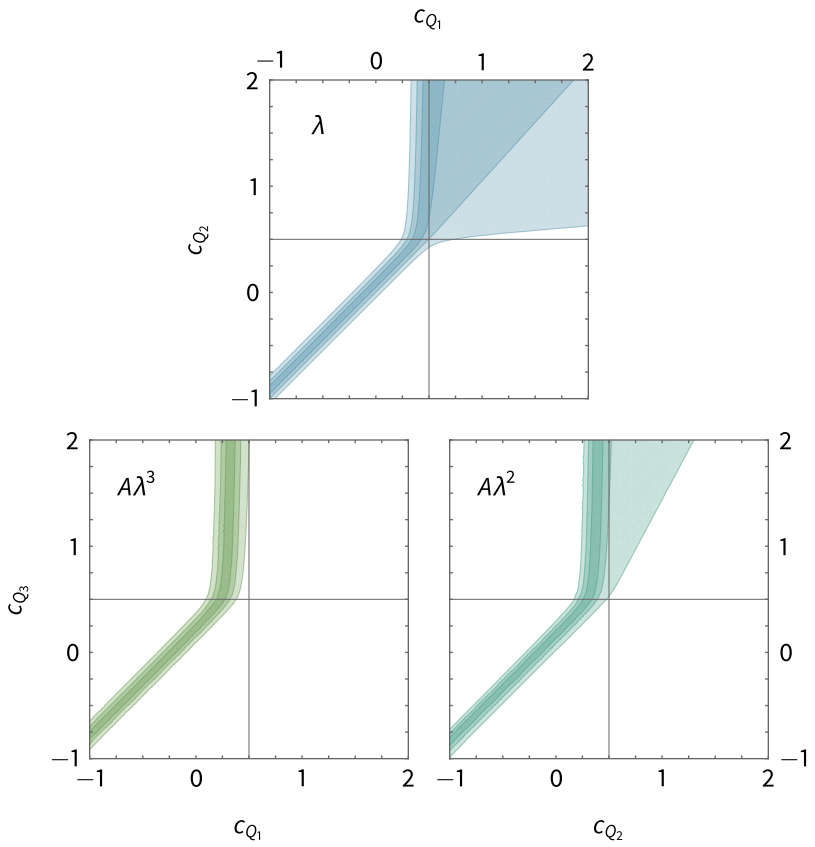

Figure 4.3: Plot of the estimated correlations among the localizations of the quark doublets required to explain the hierarchical CKM matrix parameters at the 1σ (dark), 2σ (medium), and 3σ (light) confidence levels according to (4.72). We take $\Lambda_{\text{IR}} = 10^7$ GeV and $\tan\beta = 5$.

4.3.4 Lepton sector

A similar analysis can be performed for the lepton sector. In this case we must specify the masses of the neutrinos. While the differences between the masses have been measured (see Table 4.2), neither the absolute mass scale nor the relative ordering of the hierarchy are currently known. In Fig. 4.5, we plot ratios of neutrino masses as functions of the lightest mass for both the normal and inverted hierarchy scenarios. Current direct kinematic measurements from beta decay (see Ref. [200], for example) probe the quasidegenerate regime $m_i > 0.2\,\text{eV}$, placing limits $m_i < \mathcal{O}(1)\,\text{eV}$ on each mass eigenvalue, while combined cosmological observations suggest $\sum_i m_i \lesssim 0.2\,\text{eV}$ [201]. In the case of normal ordering, the neutrino masses are moderately hierarchical when $m_1 < \mathcal{O}(1)\,\text{meV}$, such that we can safely

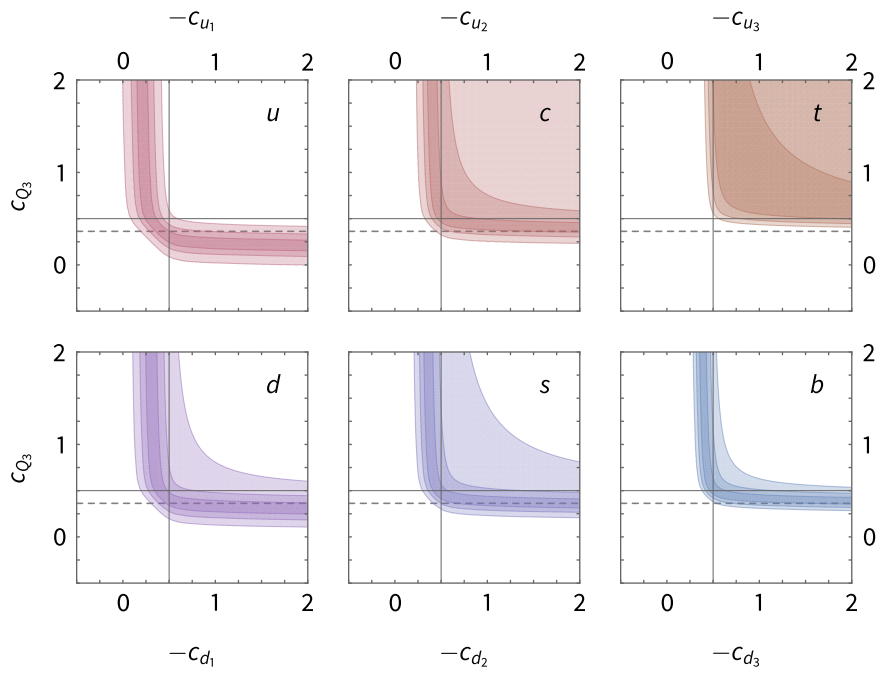

Figure 4.4: Plot of the estimated correlations between the localizations of the quark doublets and singlets required to explain the observed quark masses and CKM parameters at the 1σ (dark), 2σ (medium), and 3σ (light) confidence levels. We take $\Lambda_{\rm IR} = 10^7\,\text{GeV}$ and $\tan\beta = 5$.

employ the diagonalization approximation.

Dirac neutrinos

When the neutrinos are Dirac fermions with normally ordered masses, the lepton Yukawa couplings at the $n = 1$ level of approximation are:

$$y_{e,1}^2 = \frac{|\det \boldsymbol{y}_{e,\nu}|^2}{\operatorname{tr} \overline{\boldsymbol{y}}_{e,\nu}^\dagger\, \overline{\boldsymbol{y}}_{e,\nu}} + \mathcal{O}\left(\frac{y_{e,1}^4}{y_{\mu,2}^2}\right), \tag{4.73a}$$

$$y_{\mu,2}^2 = \frac{\operatorname{tr} \overline{\boldsymbol{y}}_{e,\nu}^\dagger\, \overline{\boldsymbol{y}}_{e,\nu}}{\operatorname{tr} \boldsymbol{y}_{e,\nu}^\dagger\, \boldsymbol{y}_{e,\nu}} + \mathcal{O}\left(\frac{y_{\mu,2}^4}{y_{\tau,3}^2}\right), \tag{4.73b}$$

$$y_{\tau,3}^2 = \operatorname{tr} \boldsymbol{y}_{e,\nu}^\dagger\, \boldsymbol{y}_{e,\nu} + \mathcal{O}(y_{\mu,2}^2)\,, \tag{4.73c}$$

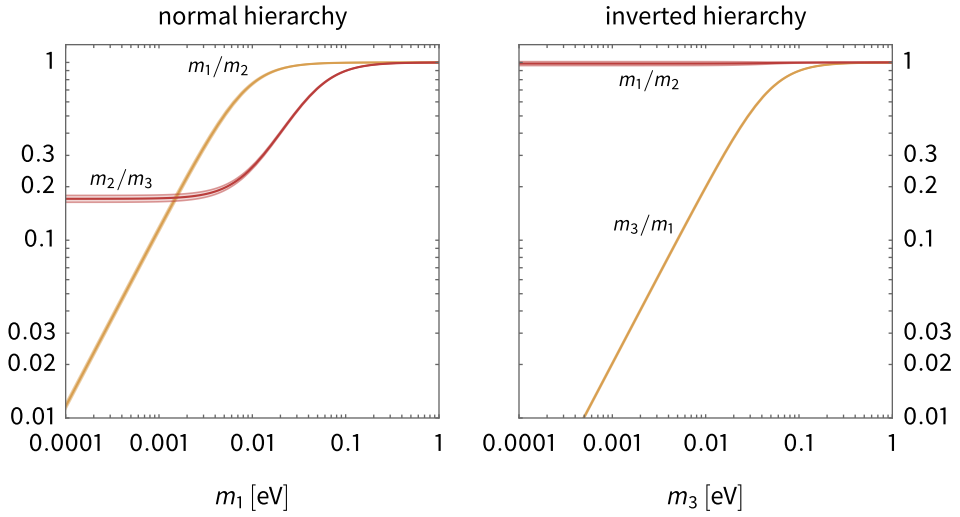

Figure 4.5: Plot of the neutrino mass hierarchies as a function of the lightest neutrino mass for the normal (left) and inverted (right) ordering scenarios, shown with 3σ uncertainty bands.

In terms of the five-dimensional Yukawa couplings and lepton profiles, we can express the traces in the same form as for the quark sector

$$\operatorname{tr} \boldsymbol{y}_{e,\nu}^{\dagger}\, \boldsymbol{y}_{e,\nu} = \sum_{ij} 4\, |(Y_{e,\nu})_{ij}|^2 \left(N^{(0)}_{e_i,\nu_i} N^{(0)}_{L_j}\right)^2 , \tag{4.74a}$$

$$\operatorname{tr} \overline{\boldsymbol{y}}_{e,\nu}^{\dagger}\, \overline{\boldsymbol{y}}_{e,\nu} = \sum_{ij} 4\, |(M_{e,\nu})_{ij}|^2 \prod_{m\neq i} \left(N^{(0)}_{e_m,\nu_m}\right)^2 \prod_{n\neq j} \left(N^{(0)}_{L_n}\right)^2 . \tag{4.74b}$$

Using this, we have

$$y_{e,1} = 2\, \frac{|\det \boldsymbol{Y}_{e,\nu}|}{|(M_{e,\nu})_{11}|}\, N^{(0)}_{L_1} N^{(0)}_{e_1,\nu_1} \left[1 + \mathcal{O}\left(\frac{N^{(0)}_{L_1}}{N^{(0)}_{L_2}}, \frac{N^{(0)}_{e_1,\nu_1}}{N^{(0)}_{e_2,\nu_2}}\right)\right] , \tag{4.75a}$$

$$y_{\mu,2} = 2\, \frac{|(M_{e,\nu})_{11}|}{|(Y_{e,\nu})_{33}|}\, N^{(0)}_{L_2} N^{(0)}_{e_2,\nu_2} \left[1 + \mathcal{O}\left(\frac{N^{(0)}_{L_1}}{N^{(0)}_{L_2}}, \frac{N^{(0)}_{e_1,\nu_1}}{N^{(0)}_{e_2,\nu_2}}, \frac{N^{(0)}_{L_2}}{N^{(0)}_{L_3}}, \frac{N^{(0)}_{e_2,\nu_2}}{N^{(0)}_{e_3,\nu_3}}\right)\right] , \tag{4.75b}$$

$$y_{\tau,3} = 2\, |(Y_{e,\nu})_{33}|\, N^{(0)}_{L_3} N^{(0)}_{e_3,\nu_3} \left[1 + \mathcal{O}\left(\frac{N^{(0)}_{L_2}}{N^{(0)}_{L_3}}, \frac{N^{(0)}_{e_2,\nu_2}}{N^{(0)}_{e_3,\nu_3}}\right)\right] , \tag{4.75c}$$

where we have assumed hierarchical profiles:

$$N^{(0)}_{L_1,e_1,\nu_1} \ll N^{(0)}_{L_2,e_2,\nu_2} \ll N^{(0)}_{L_3,e_3,\nu_3}\,. \tag{4.76}$$

Expressing the unitary matrices $\boldsymbol{V}_L^{e,\nu}$ in the *abc* parametrization (in the convention $\alpha = \beta = \gamma = 0$), we find in the $n = 1$ approximation:

$$a_{e,\nu} = -\frac{(\overline{\boldsymbol{y}}^\dagger_{e,\nu}\,\overline{\boldsymbol{y}}_{e,\nu})_{21}}{(\overline{\boldsymbol{y}}^\dagger_{e,\nu}\,\overline{\boldsymbol{y}}_{e,\nu})_{11}} + \mathcal{O}\!\left(\frac{y_{e,1}}{y_{\mu,2}}\right), \tag{4.77a}$$

$$b_{e,\nu} = \frac{(\boldsymbol{y}^\dagger_{e,\nu}\,\boldsymbol{y}_{e,\nu})_{13}}{(\boldsymbol{y}^\dagger_{e,\nu}\,\boldsymbol{y}_{e,\nu})_{33}} + \mathcal{O}\!\left(\frac{y_{e,1}}{y_{\tau,3}}\right), \tag{4.77b}$$

$$c_{e,\nu} = \frac{(\boldsymbol{y}^\dagger_{e,\nu}\,\boldsymbol{y}_{e,\nu})_{23}}{(\boldsymbol{y}^\dagger_{e,\nu}\,\boldsymbol{y}_{e,\nu})_{33}} + \mathcal{O}\!\left(\frac{y_{\mu,2}}{y_{\tau,3}}\right), \tag{4.77c}$$

$$\tilde{b}_{e,\nu} = -\frac{(\overline{\boldsymbol{y}}^\dagger_{e,\nu}\,\overline{\boldsymbol{y}}_{e,\nu})_{31}}{(\overline{\boldsymbol{y}}^\dagger_{e,\nu}\,\overline{\boldsymbol{y}}_{e,\nu})_{11}} + \mathcal{O}\!\left(\frac{y_{e,1}}{y_{\tau,3}}\right), \tag{4.77d}$$

which, in terms of the five-dimensional Yukawa couplings and lepton profiles, take the forms

$$a_{e,\nu} = \frac{(M_{e,\nu})_{21}}{(M_{e,\nu})_{11}}\frac{N^{(0)}_{L_1}}{N^{(0)}_{L_2}}\left[1 + \mathcal{O}\!\left(\frac{N^{(0)}_{e_1,\nu_1}}{N^{(0)}_{e_2,\nu_2}}\right)\right], \tag{4.78a}$$

$$b_{e,\nu} = \frac{(Y_{e,\nu})_{13}}{(Y_{e,\nu})_{33}}\frac{N^{(0)}_{L_1}}{N^{(0)}_{L_3}}\left[1 + \mathcal{O}\!\left(\frac{N^{(0)}_{e_2,\nu_2}}{N^{(0)}_{e_3,\nu_3}}\right)\right], \tag{4.78b}$$

$$c_{e,\nu} = \frac{(Y_{e,\nu})_{23}}{(Y_{e,\nu})_{33}}\frac{N^{(0)}_{L_2}}{N^{(0)}_{L_3}}\left[1 + \mathcal{O}\!\left(\frac{N^{(0)}_{e_2,\nu_2}}{N^{(0)}_{e_3,\nu_3}}\right)\right], \tag{4.78c}$$

$$\tilde{b}_{e,\nu} = -\frac{(M_{e,\nu})_{31}}{(M_{e,\nu})_{11}}\frac{N^{(0)}_{L_1}}{N^{(0)}_{L_3}}\left[1 + \mathcal{O}\!\left(\frac{N^{(0)}_{e_1,\nu_1}}{N^{(0)}_{e_2,\nu_2}}\right)\right], \tag{4.78d}$$

such that

$$\boldsymbol{V}_L^{e,\nu} \simeq \begin{pmatrix} 1 & \dfrac{(M_{e,\nu})_{21}}{(M_{e,\nu})_{11}}\dfrac{N_{L_1}^{(0)}}{N_{L_2}^{(0)}} & \dfrac{(Y_{e,\nu})_{13}}{(Y_{e,\nu})_{33}}\dfrac{N_{L_1}^{(0)}}{N_{L_3}^{(0)}} \\ -\dfrac{(M_{e,\nu})_{21}^*}{(M_{e,\nu})_{11}^*}\dfrac{N_{L_1}^{(0)}}{N_{L_2}^{(0)}} & 1 & \dfrac{(Y_{e,\nu})_{23}}{(Y_{e,\nu})_{33}}\dfrac{N_{L_2}^{(0)}}{N_{L_3}^{(0)}} \\ \dfrac{(M_{e,\nu})_{31}^*}{(M_{e,\nu})_{11}^*}\dfrac{N_{L_1}^{(0)}}{N_{L_3}^{(0)}} & -\dfrac{(Y_{e,\nu})_{23}^*}{(Y_{e,\nu})_{33}^*}\dfrac{N_{L_2}^{(0)}}{N_{L_3}^{(0)}} & 1 \end{pmatrix} . \tag{4.79}$$

The PMNS matrix elements are of the form (4.57), with $\boldsymbol{V}_{1,2} = \boldsymbol{V}_L^{e,\nu}$. In the $n = 1$ approximation, we find

$$U_{e1} = 1 + \mathcal{O}\Big(\frac{y_e}{y_\mu}, \frac{y_1}{y_2}\Big), \tag{4.80a}$$

$$U_{e2} = \frac{(\overline{\boldsymbol{y}}_\nu^\dagger\, \overline{\boldsymbol{y}}_\nu)_{21}}{(\overline{\boldsymbol{y}}_\nu^\dagger\, \overline{\boldsymbol{y}}_\nu)_{11}} - \frac{(\overline{\boldsymbol{y}}_e^\dagger\, \overline{\boldsymbol{y}}_e)_{21}}{(\overline{\boldsymbol{y}}_e^\dagger\, \overline{\boldsymbol{y}}_e)_{11}} + \mathcal{O}\Big(\frac{y_e}{y_\mu}, \frac{y_1}{y_2}\Big), \tag{4.80b}$$

$$U_{e3} = \frac{(\overline{\boldsymbol{y}}_e^\dagger\, \overline{\boldsymbol{y}}_e)_{31}}{(\overline{\boldsymbol{y}}_e^\dagger\, \overline{\boldsymbol{y}}_e)_{11}} + \frac{(\boldsymbol{y}_\nu^\dagger\, \boldsymbol{y}_\nu)_{13}}{(\boldsymbol{y}_\nu^\dagger\, \boldsymbol{y}_\nu)_{33}} + \mathcal{O}\Big(\frac{y_e}{y_\tau}, \frac{y_1}{y_3}\Big), \tag{4.80c}$$

$$U_{\mu 1} = \frac{(\overline{\boldsymbol{y}}_e^\dagger\, \overline{\boldsymbol{y}}_e)_{21}^*}{(\overline{\boldsymbol{y}}_e^\dagger\, \overline{\boldsymbol{y}}_e)_{11}^*} - \frac{(\overline{\boldsymbol{y}}_\nu^\dagger\, \overline{\boldsymbol{y}}_\nu)_{21}^*}{(\overline{\boldsymbol{y}}_\nu^\dagger\, \overline{\boldsymbol{y}}_\nu)_{11}^*} + \mathcal{O}\Big(\frac{y_e}{y_\mu}, \frac{y_1}{y_2}\Big), \tag{4.80d}$$

$$U_{\mu 2} = 1 + \mathcal{O}\Big(\frac{y_1}{y_2}\Big), \tag{4.80e}$$

$$U_{\mu 3} = \frac{(\boldsymbol{y}_\nu^\dagger\, \boldsymbol{y}_\nu)_{23}}{(\boldsymbol{y}_\nu^\dagger\, \boldsymbol{y}_\nu)_{33}} - \frac{(\boldsymbol{y}_e^\dagger\, \boldsymbol{y}_e)_{23}}{(\boldsymbol{y}_e^\dagger\, \boldsymbol{y}_e)_{33}} + \mathcal{O}\Big(\frac{y_2}{y_3}\Big), \tag{4.80f}$$

$$U_{\tau 1} = \frac{(\boldsymbol{y}_e^\dagger\, \boldsymbol{y}_e)_{13}^*}{(\boldsymbol{y}_e^\dagger\, \boldsymbol{y}_e)_{33}^*} + \frac{(\overline{\boldsymbol{y}}_\nu^\dagger\, \overline{\boldsymbol{y}}_\nu)_{31}^*}{(\overline{\boldsymbol{y}}_\nu^\dagger\, \overline{\boldsymbol{y}}_\nu)_{11}^*} + \mathcal{O}\Big(\frac{y_e}{y_\tau}, \frac{y_1}{y_3}\Big), \tag{4.80g}$$

$$U_{\tau 2} = \frac{(\boldsymbol{y}_e^\dagger\, \boldsymbol{y}_e)_{23}^*}{(\boldsymbol{y}_e^\dagger\, \boldsymbol{y}_e)_{33}^*} - \frac{(\boldsymbol{y}_\nu^\dagger\, \boldsymbol{y}_\nu)_{23}^*}{(\boldsymbol{y}_\nu^\dagger\, \boldsymbol{y}_\nu)_{33}^*} + \mathcal{O}\Big(\frac{y_2}{y_3}\Big), \tag{4.80h}$$

$$U_{\tau 3} = 1 + \mathcal{O}\Big(\frac{y_2}{y_3}\Big), \tag{4.80i}$$

such that the PMNS mixing angles are

$$\sin^2\theta_{12} = \frac{\left|\frac{(\overline{\boldsymbol{y}}_\nu^\dagger\,\overline{\boldsymbol{y}}_\nu)_{21}}{(\overline{\boldsymbol{y}}_\nu^\dagger\,\overline{\boldsymbol{y}}_\nu)_{11}} - \frac{(\overline{\boldsymbol{y}}_e^\dagger\,\overline{\boldsymbol{y}}_e)_{21}}{(\overline{\boldsymbol{y}}_e^\dagger\,\overline{\boldsymbol{y}}_e)_{11}}\right|^2}{1-\left|\frac{(\overline{\boldsymbol{y}}_e^\dagger\,\overline{\boldsymbol{y}}_e)_{31}}{(\overline{\boldsymbol{y}}_e^\dagger\,\overline{\boldsymbol{y}}_e)_{11}} + \frac{(\boldsymbol{y}_\nu^\dagger\,\boldsymbol{y}_\nu)_{13}}{(\boldsymbol{y}_\nu^\dagger\,\boldsymbol{y}_\nu)_{33}}\right|^2} + \mathcal{O}\left(\frac{y_e}{y_\mu},\frac{y_1}{y_2}\right), \tag{4.81a}$$

$$\sin^2\theta_{23} = \frac{\left|\frac{(\boldsymbol{y}_\nu^\dagger\,\boldsymbol{y}_\nu)_{23}}{(\boldsymbol{y}_\nu^\dagger\,\boldsymbol{y}_\nu)_{33}} - \frac{(\boldsymbol{y}_e^\dagger\,\boldsymbol{y}_e)_{23}}{(\boldsymbol{y}_e^\dagger\,\boldsymbol{y}_e)_{33}}\right|^2}{1-\left|\frac{(\overline{\boldsymbol{y}}_e^\dagger\,\overline{\boldsymbol{y}}_e)_{31}}{(\overline{\boldsymbol{y}}_e^\dagger\,\overline{\boldsymbol{y}}_e)_{11}} + \frac{(\boldsymbol{y}_\nu^\dagger\,\boldsymbol{y}_\nu)_{13}}{(\boldsymbol{y}_\nu^\dagger\,\boldsymbol{y}_\nu)_{33}}\right|^2} + \mathcal{O}\left(\frac{y_2}{y_3}\right), \tag{4.81b}$$

$$\sin^2\theta_{13} = \left|\frac{(\overline{\boldsymbol{y}}_e^\dagger\,\overline{\boldsymbol{y}}_e)_{31}}{(\overline{\boldsymbol{y}}_e^\dagger\,\overline{\boldsymbol{y}}_e)_{11}} + \frac{(\boldsymbol{y}_\nu^\dagger\,\boldsymbol{y}_\nu)_{13}}{(\boldsymbol{y}_\nu^\dagger\,\boldsymbol{y}_\nu)_{33}}\right|^2 + \mathcal{O}\left(\frac{y_e}{y_\tau},\frac{y_1}{y_3}\right). \tag{4.81c}$$

In terms of the profiles, we find

$$U_{e1} = 1 + \mathcal{O}\left(\frac{N_{L_1}^{(0)}}{N_{L_2}^{(0)}}\frac{N_{L_1,e_1,\nu_1}^{(0)}}{N_{L_2,e_2,\nu_2}^{(0)}}, \frac{N_{L_2}^{(0)}}{N_{L_3}^{(0)}}\frac{N_{L_2,e_2,\nu_2}^{(0)}}{N_{L_3,e_3,\nu_3}^{(0)}}\right), \tag{4.82a}$$

$$U_{e2} = \left[\frac{(M_\nu)_{21}}{(M_\nu)_{11}} - \frac{(M_e)_{21}}{(M_e)_{11}}\right]\frac{N_{L_1}^{(0)}}{N_{L_2}^{(0)}}\left[1+\mathcal{O}\left(\frac{N_{e_1,\nu_1}^{(0)}}{N_{e_2,\nu_2}^{(0)}}\right)\right], \tag{4.82b}$$

$$U_{e3} = \left[\frac{(Y_\nu)_{13}}{(Y_\nu)_{33}} - \frac{(M_e)_{21}}{(M_e)_{11}}\frac{(Y_\nu)_{23}}{(Y_\nu)_{33}} + \frac{(M_e)_{31}}{(M_e)_{11}}\right]\frac{N_{L_1}^{(0)}}{N_{L_3}^{(0)}}\left[1+\mathcal{O}\left(\frac{N_{e_1}^{(0)}}{N_{e_2}^{(0)}},\frac{N_{\nu_2}^{(0)}}{N_{\nu_3}^{(0)}}\right)\right], \tag{4.82c}$$

$$U_{\mu 1} = \left[\frac{(M_e)_{21}^*}{(M_e)_{11}^*} - \frac{(M_\nu)_{21}^*}{(M_\nu)_{11}^*}\right]\frac{N_{L_1}^{(0)}}{N_{L_2}^{(0)}}\left[1+\mathcal{O}\left(\frac{N_{e_1,\nu_1}^{(0)}}{N_{e_2,\nu_2}^{(0)}}\right)\right], \tag{4.82d}$$

$$U_{\mu 2} = 1 + \mathcal{O}\left(\frac{N_{L_1}^{(0)}}{N_{L_2}^{(0)}}\frac{N_{L_1,e_1,\nu_1}^{(0)}}{N_{L_2,e_2,\nu_2}^{(0)}}\right), \tag{4.82e}$$

$$U_{\mu 3} = \left[\frac{(Y_\nu)_{23}}{(Y_\nu)_{33}} - \frac{(Y_e)_{23}}{(Y_e)_{33}}\right]\frac{N_{L_2}^{(0)}}{N_{L_3}^{(0)}}\left[1+\mathcal{O}\left(\frac{N_{e_2,\nu_2}^{(0)}}{N_{e_3,\nu_3}^{(0)}}\right)\right], \tag{4.82f}$$

$$U_{\tau 1} = \left[\frac{(Y_e)_{13}^*}{(Y_e)_{33}^*} - \frac{(Y_e)_{23}^*}{(Y_e)_{33}^*}\frac{(M_\nu)_{21}^*}{(M_\nu)_{11}^*} + \frac{(M_\nu)_{31}^*}{(M_\nu)_{11}^*}\right]\frac{N_{L_1}^{(0)}}{N_{L_3}^{(0)}}\left[1+\mathcal{O}\left(\frac{N_{\nu_1}^{(0)}}{N_{\nu_2}^{(0)}},\frac{N_{e_2}^{(0)}}{N_{e_3}^{(0)}}\right)\right], \tag{4.82g}$$

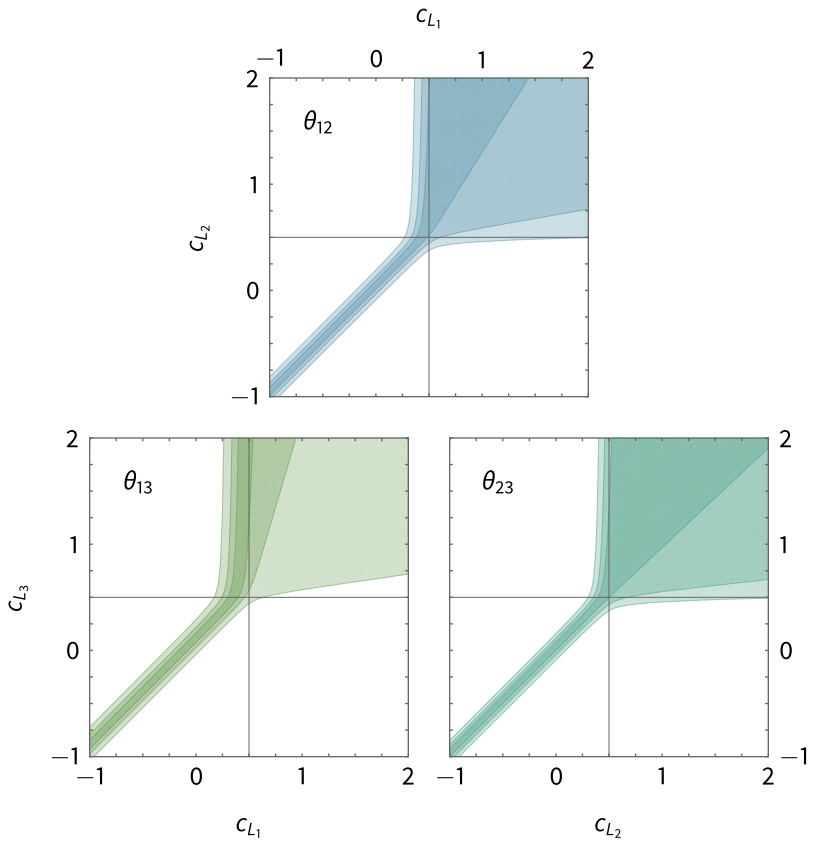

Figure 4.6: Plot of the estimated correlations among the localizations of the lepton doublets required to explain the PMNS mixing angles in the case of Dirac neutrinos at the 1σ (dark), 2σ (medium), and 3σ (light) confidence levels according to (4.83). We take $\Lambda_{\text{IR}} = 10^7\,\text{GeV}$ and $\tan\beta = 5$. The neutrino masses have the normal hierarchy, with the lightest set at $m_{\nu_1} = 1\,\text{meV}$.

$$U_{\tau 2} = \left[\frac{(Y_e)^*_{23}}{(Y_e)^*_{33}} - \frac{(Y_\nu)^*_{23}}{(Y_\nu)^*_{33}}\right] \frac{N^{(0)}_{L_2}}{N^{(0)}_{L_3}} \left[1 + \mathcal{O}\left(\frac{N^{(0)}_{e_2,\nu_2}}{N^{(0)}_{e_3,\nu_3}}\right)\right], \tag{4.82h}$$

$$U_{\tau 3} = 1 + \mathcal{O}\left(\frac{N^{(0)}_{L_1}}{N^{(0)}_{L_2}} \frac{N^{(0)}_{L_1,e_1,\nu_1}}{N^{(0)}_{L_2,e_2,\nu_2}}, \frac{N^{(0)}_{L_2}}{N^{(0)}_{L_3}} \frac{N^{(0)}_{L_2,e_2,\nu_2}}{N^{(0)}_{L_3,e_3,\nu_3}}\right), \tag{4.82i}$$

and

$$\sin^2\theta_{12} = \left|\frac{(M_\nu)_{21}}{(M_\nu)_{11}} - \frac{(M_e)_{21}}{(M_e)_{11}}\right|^2 \frac{\left(N^{(0)}_{L_1}\right)^2}{\left(N^{(0)}_{L_2}\right)^2} \left[1 + \mathcal{O}\left(\frac{N^{(0)}_{e_1,\nu_1}}{N^{(0)}_{e_2,\nu_2}}\right)\right], \tag{4.83a}$$

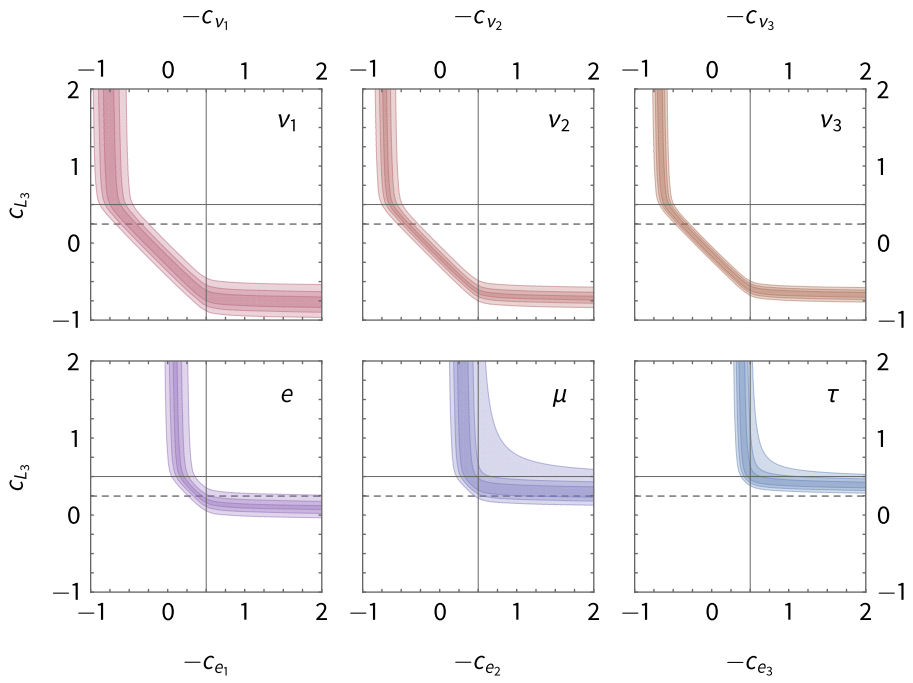

Figure 4.7: Plot of the estimated correlations between the localizations of the lepton doublets and singlets required to explain the observed lepton masses and PMNS mixing angles in the case of Dirac neutrinos at the 1σ (dark), 2σ (medium), and 3σ (light) confidence levels. We take $\Lambda_{\text{IR}} = 10^7\,\text{GeV}$ and $\tan\beta = 5$. The neutrino masses have the normal hierarchy, with the lightest set at $m_{\nu_1} = 1\,\text{meV}$.

$$\sin^2\theta_{23} = \left|\frac{(Y_\nu)_{23}}{(Y_\nu)_{33}} - \frac{(Y_e)_{23}}{(Y_e)_{33}}\right|^2 \frac{\left(N^{(0)}_{L_2}\right)^2}{\left(N^{(0)}_{L_3}\right)^2}\left[1 + \mathcal{O}\left(\frac{N^{(0)}_{e_2,\nu_2}}{N^{(0)}_{e_3,\nu_3}}\right)\right], \tag{4.83b}$$

$$\sin^2\theta_{13} = \left|\frac{(Y_\nu)_{13}}{(Y_\nu)_{33}} - \frac{(M_e)_{21}}{(M_e)_{11}}\frac{(Y_\nu)_{23}}{(Y_\nu)_{33}} + \frac{(M_e)_{31}}{(M_e)_{11}}\right|^2 \frac{\left(N^{(0)}_{L_1}\right)^2}{\left(N^{(0)}_{L_3}\right)^2}\left[1 + \mathcal{O}\left(\frac{N^{(0)}_{e_1}}{N^{(0)}_{e_2}}, \frac{N^{(0)}_{\nu_2}}{N^{(0)}_{\nu_3}}\right)\right]. \tag{4.83c}$$

Thus, in order to explain the PMNS mixing angles, the localization parameters of the lepton doublets must be correlated. Assuming that the order-one magnitudes of the 5D Yukawa matrix elements are log-normally distributed as described in Sec. 4.4.1, we show the correlations at 1σ (dark), 2σ (medium), and 3σ (light) confidence levels in Fig. 4.6. Generally, we see that the mild hierarchy of the PMNS mixing angles prefers a mild hierarchy in localization parameters, although this is somewhat relaxed when the doublets are UV-localized and the UV-brane profiles approximately order-one. Once the doublet localizations are chosen according to (4.83), the singlet localizations are determined by the expressions

for the Yukawa couplings (4.75). We show the resulting correlations induced between the localization parameters of the singlets and the localization of any one doublet (we choose here to use c_{L_3}) in Fig. 4.7 (compare to Fig. 4.1). As with the quark sector, we see the same general trend that heavier masses require greater UV-localization when comparing this to Fig. 4.1. Note that in order to explain the tau mass with $c_{e_3} > -10$ we require $c_{L_3} \gtrsim 0.25$, which accordingly restricts the allowed range of localizations for the singlets. This bound is indicated in Fig. 4.7 as a dashed line; the allowed regions are above this line.

4.4 Numeric Flavor Solutions

Although the approximation schemes discussed above in Sec. 4.3 can provide an analytical window into the flavor structure that emerges from the five-dimensional theory, the region of the model parameter space in which the standard model flavor observables are correctly reproduced can be directly characterized numerically. Due to the large size of the theory parameter space compared to the number of flavor observables available, the system is underspecified and cannot be solved exactly. Instead, we develop a method to determine a global fit the set of theory parameters to the renormalized quark and lepton low-energy observables, based on the numeric minimization of a χ^2 cost function in each sector.

4.4.1 Theory parameter space

The five-dimensional flavor parameters are listed in Table 4.4. A priori, there are few constraints on their allowed values, other than overall scale. Here, we give a precise construction of the theoretical parameter space we consider.

1. Yukawa couplings

For a (dimensionless) five-dimensional Yukawa coupling matrix $\boldsymbol{Y} = \boldsymbol{Y}_{e,u,d,\nu}$, we require the magnitude of each entry to be order-one. We therefore treat each entry as a random complex number, where the phase $\arg Y_{ij}$ is a random variable uniformly distributed over the interval $[-\pi, \pi]$ and the magnitude $|Y_{ij}|$ is a random variable whose logarithm $\log |Y_{ij}|$ is normally distributed around zero with standard deviation $\sigma = (\log 10)/3 \simeq 0.768$, corresponding to 3σ confidence (99.73 % probability) that $|Y_{ij}|$ will lie within an order of magnitude of one (i.e., in the interval $[0.1, 10]$). The magnitude $|Y_{ij}|$ is therefore distributed according to the log-normal distribution[14] with

[14] If the random variable y is normally distributed with mean μ and variance σ^2, then $x = \exp y$ has a

Table 4.4: Five-dimensional theory parameters defining the flavor structure of the MSSM in a slice of AdS_5 with the Higgs fields localized on the UV brane. In the case of Dirac (Majorana) neutrinos, there are 36 (33) complex parameters and 18 (15) real parameters that must be specified.

Dirac neutrinos		Majorana neutrinos	
parameters	degrees of freedom	parameters	degrees of freedom
$(Y_{u,d})_{ij}$	18 complex	$(Y_{u,d})_{ij}$	18 complex
c_{Q_i,u_i,d_i}	9 real	c_{Q_i,u_i,d_i}	9 real
$(Y_e)_{ij}$	9 complex	$(Y_e)_{ij}$	9 complex
$(Y_\nu)_{ij}$	9 complex	$(K_\nu)_{ij}$	6 complex
c_{L_i,e_i,ν_i}	9 real	c_{L_i,e_i}	6 real

shape parameters $\mu = 0$ and $\sigma = (\log 10)/3$.

2. Weinberg operator

In the case of Majorana neutrinos, each (dimensionless) operator coefficient $(K_\nu)_{ij}$ is also treated as a random complex number, where the phase $\arg(K_\nu)_{ij}$ is a random variable uniformly distributed over the interval $[-\pi, \pi]$ and the magnitude $|(K_\nu)_{ij}|$ is a random variable whose logarithm $\log|(K_\nu)_{ij}|$ is uniformly distributed over the interval $[\log K_\nu^{\min}, \log K_\nu^{\max}]$. As discussed in Sec. 4.1.2, the upper limit on the magnitude of the operator elements is $\mathcal{O}(1)$, so we take $K_\nu^{\max} = 3$. The lower limit, on the other hand, is not restricted, but in practice we take it to be the numeric tolerance of the renormalization procedure described in Sec. 4.2: $K_\nu^{\min} = 10^{-24}$. The magnitude $|(K_\nu)_{ij}|$ is therefore distributed according to a log-uniform distribution[15] over the

log-normal distribution with probability density function

$$f_{\text{log-normal}}(x) = \frac{1}{\sqrt{2\pi}\,\sigma}\,\frac{e^{-(\log x-\mu)^2/2\sigma^2}}{x}\,. \tag{4.84}$$

In the context of the probability density function, μ and σ, the mean and standard deviation of the variable $y = \log x$, are referred to as *shape parameters*.

[15] If the random variable y is uniformly distributed over the interval $[y_{\min}, y_{\max}]$, then $x = \exp y$ has a log-uniform distribution with probability density function

$$f_{\text{log-uniform}}(x) = \frac{1}{x\,(y_{\max} - y_{\min})} = \frac{1}{x\log(x_{\max}/x_{\min})}\,. \tag{4.85}$$

interval $[K_\nu^{\min}, K_\nu^{\max}]$.

3. Localization parameters

As order-one numbers, the quark and lepton localization parameters are nominally taken to be uniformly distributed in the range $[-10, 10]$. In practice, the matching conditions between the four-dimensional and five-dimensional Yukawa couplings enforces a more stringent lower (upper) bound for left-handed (right-handed) fields (this effect is visible in Fig. 4.1, where we see that the contour lines restrict the allowed range of $c_{L(R)}$ from below (above), and it is better to restrict the sampling range to forbid values corresponding to excessive IR localization (and exponentially small Yukawa couplings). As a heuristic for estimating this bound, we use the localization value where the fermion zero-mode profile on the UV brane is smaller than the numeric tolerance of our renormalization procedure, i.e., the root which satisfies

$$N^{(0)}_{\Psi_{L,R}} = \sqrt{\frac{1/2 \mp c_{L,R}}{e^{2(1/2 \mp c_{L,R})} - 1}} = 10^{-24}\,. \tag{4.86}$$

We plot the solution as a function of Λ_{IR} in Fig. 4.8. For $\Lambda_{\text{IR}} \lesssim 10^{16}\,\text{GeV}$ the bound calculated in this way is more restrictive than the order-one limit.

4.4.2 Application of experimental and theoretical constraints

Once a set of five-dimensional theory parameters have been specified, the zero-mode approximation matching approach discussed in Sec. 4.1 [characterized by the matching equations (4.2), (4.15), and (4.27)] is used to assemble the effective four-dimensional coupling matrices. These are then factorized to obtain predictions at the IR-brane scale for the running four-dimensional flavor parameters: the quark and charged lepton masses, the neutrino mass differences, and CKM and PMNS mixing parameters. The constraints on these predictions are provided by the quark and lepton low-energy observables. We use the renormalization procedure discussed in Sec. 4.2 to convert the experimental observables into MSSM running parameters and estimate their values and uncertainties at the IR-brane scale, where they can be directly compared with the theory predictions.

We evaluate the fit of the five-dimensional model to the experimental constraints separately

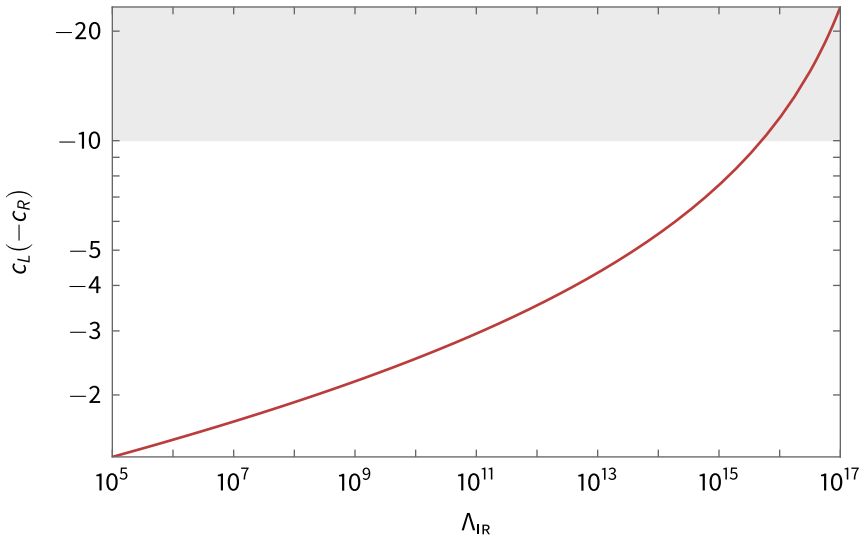

Figure 4.8: Plot of the approximate lower (upper) limit for the localization parameter for a left-handed (right-handed) fermion in the numeric flavor solution described in Sec. 4.4. The shaded region is forbidden by the requirement that the c parameter is order-one.

for the quark and lepton sectors by constructing χ^2 measures of the form

$$\chi^2_{\text{expr}} = \begin{cases} \chi^2_u + \chi^2_d + \chi^2_{\text{CKM}} & \text{for the quark sector}\,, \\ \chi^2_e + \chi^2_\nu + \chi^2_{\text{PMNS}} & \text{for the lepton sector}\,, \end{cases} \tag{4.87}$$

where the contributions from the quark and charged lepton Yukawa couplings are

$$\chi^2_u = \chi^2(\log y_u) + \chi^2(\log y_c) + \chi^2(\log y_t)\,, \tag{4.88a}$$

$$\chi^2_d = \chi^2(\log y_d) + \chi^2(\log y_s) + \chi^2(\log y_b)\,, \tag{4.88b}$$

$$\chi^2_e = \chi^2(\log y_e) + \chi^2(\log y_\mu) + \chi^2(\log y_\tau)\,, \tag{4.88c}$$

from the neutrino mass operator are

$$\chi^2_\nu = \begin{cases} \chi^2(\log \Delta m^2_{21}) + \chi^2(\log \Delta m^2_{31}) & \text{for a normal hierarchy}\,, \\ \chi^2(\log \Delta m^2_{21}) + \chi^2(\log \Delta m^2_{23}) & \text{for an inverted hierarchy}\,, \end{cases} \tag{4.89}$$

and from the CKM and PMNS matrix parameters are

$$\chi^2_{\text{CKM}} = \chi^2(\lambda) + \chi^2(A) + \chi^2(\bar{\rho}) + \chi^2(\bar{\eta})\,, \tag{4.90a}$$

$$\chi^2_{\text{PMNS}} = \chi^2(\theta_{12}) + \chi^2(\theta_{23}) + \chi^2(\theta_{13}) + \chi^2(\delta)\,. \tag{4.90b}$$

The χ^2 measure for a parameter x with predicted theory value x_{theory} and renormalized measured value with asymmetric uncertainties $x_{\text{expr}} \pm \sigma_x^{\pm}$ take the forms

$$\chi^2(x) = \begin{cases} \dfrac{(x_{\text{theory}} - x_{\text{expr}})^2}{(\sigma_x^+)^2} & \text{for } x_{\text{theory}} > x_{\text{expr}}\,, \\[2ex] \dfrac{(x_{\text{theory}} - x_{\text{expr}})^2}{(\sigma_x^-)^2} & \text{for } x_{\text{theory}} < x_{\text{expr}}\,, \end{cases} \tag{4.91a}$$

and

$$\chi^2(\log x) = \begin{cases} \dfrac{(\log x_{\text{theory}} - \log x_{\text{expr}})^2}{(\sigma_x^+/x_{\text{expr}})^2} & \text{for } x_{\text{theory}} > x_{\text{expr}}\,, \\[2ex] \dfrac{(\log x_{\text{theory}} - \log x_{\text{expr}})^2}{(\sigma_x^-/x_{\text{expr}})^2} & \text{for } x_{\text{theory}} < x_{\text{expr}}\,. \end{cases} \tag{4.91b}$$

From a theoretical perspective, we also want the magnitudes of the five-dimensional Yukawa parameters to be order-one numbers, so we include a measure of their separation from unity of the form

$$\chi^2_Y = \sum_{ij} \left(\frac{\log |Y_{ij}|}{(\log 10)/3} \right)^2 . \tag{4.92}$$

We include these contributions as a theory term in the measure of fit,

$$\chi^2_{\text{theory}} = \begin{cases} \chi^2_{Y_u} + \chi^2_{Y_d} & \text{for the quark sector}\,, \\ \chi^2_{Y_e} + \chi^2_{Y_\nu} & \text{for a lepton sector with Dirac neutrinos}\,, \\ \chi^2_{Y_e} & \text{for a lepton sector with Majorana neutrinos}\,, \end{cases} \tag{4.93}$$

such that the total χ^2 metric can be written as

$$\chi^2 = \chi^2_{\text{expr}} + \chi^2_{\text{theory}}\,. \tag{4.94}$$

4.4.3 Numeric minimization

In order to determine the theory parameter values which best fit the experimental and theoretical constraints, we use the MINUIT2 [202] minimization package via the IMINUIT module [203].[16] The package provides the MIGRAD algorithm, a robust variable-metric method with inexact line search, a stable metric updating scheme, and checks for positive-definiteness. Given a parametric objective (cost) function and a set of initial parameter values, MIGRAD looks for a local minimum by analyzing the function gradient. The parameter errors, the uncertainties in the estimated best parameter values, are obtained either with the HESSE algorithm, which estimates the covariance matrix by inverting the Hessian matrix at the minimum, or with the MINOS algorithm, which scans objective function around the minimum to construct a asymmetric confidence intervals for the parameters.

We perform the fit for the quark and lepton sectors separately. For a given set of random initial theory parameter values, we call MIGRAD to minimize the associated χ^2 objective function. A minimization is considered successful if it converges with $\chi^2 < 28$ for the quark sector, $\chi^2 < 27$ for the lepton sector with Dirac neutrinos, or $\chi^2 < 18$ with Majorana neutrinos. In the minimization, the values of the c parameters are directly constrained to the range discussed above in our construction of the flavor theory parameter space, as, in the case of Majorana neutrinos, are the logarithms of the magnitudes of Weinberg operator coefficients. The five-dimensional Yukawa couplings are unconstrained except by their contributions to the object function in the χ^2_{theory} term.

The quark and lepton minimizations are repeated by varying the initial parameter values, randomly sampling over the defined parameter space. It is not clear at this point if there are global minima for the χ^2 measures of fit in the flavor parameter space. Instead, due to the underspecification of the system, there may be degeneracies between sets of five-dimensional theory parameters, resulting in a more extended minimum structure (this is also a concern due to the use of the zero-mode approximation). For our purposes, we consider any successful minimization as a valid flavor solution, with uncertainty that is quantified by the HESSE or MINOS errors. In the next chapter, Chapter 5, we use the quark and lepton localization parameters and bulk-mass-basis Yukawa coupling matrices determined by this method to calculate the sfermion masses arising from supersymmetry breaking on the IR brane.

[16] We provide a Wolfram Language interface for IMINUIT [204]. The code is also available from the author upon request.

5 Supersymmetry Breaking on the Brane

In this chapter, we consider the breaking of supersymmetry on the IR brane of the five-dimensional theory. We review the tree-level results before discussing the important one-loop radiative corrections to the soft scalar masses, the Higgs sector soft terms, and the soft trilinear scalar couplings.

5.1 Tree-Level Analysis

Supersymmetry is assumed to be broken on the IR brane and is parameterized by the introduction of a spurion superfield $X = \theta\theta F_X$ that couples to the sfermions and the gauginos. The sfermions and gauginos acquire tree-level soft masses with a characteristic scale $F/\Lambda_{\rm IR}$, where $F = F_X e^{-2\pi kR}$, modulated by their overlap with the IR brane. A gravitino mass of order $F/M_{\rm P}$ is generated by the super-Higgs mechanism. The Higgs fields receive no tree-level soft masses, as they are confined to the UV brane and do not couple directly to the supersymmetry-breaking spurion. We do not include any mechanism to generate tree-level soft trilinear scalar couplings, although, like the Higgs-sector soft terms, they arise radiatively.

Contributions to the soft masses also generically arise from anomaly mediation. Because the gravitino mass is suppressed by the Planck scale (as opposed to the other soft masses, which are suppressed by the IR-brane scale), the anomaly-mediated contribution typically is subdominant to the effects (both at tree level and loop level) of the supersymmetry-breaking sector on the IR brane. An additional source of supersymmetry breaking arises due to the stabilization of the radion of the extra dimension, which generically requires a nonzero F-term for the radion superfield (equivalently, the introduction of a constant superpotential on the IR brane). The scale of the radion-mediated contribution to the soft masses depends on the details of the stabilization model. We are interested in the regime where such effects are subdominant to the effects of the supersymmetry-breaking sector on the IR brane. In the model of Ref. [116], this can be accomplished if the Goldberger-Wise hypermultiplet is sufficiently UV localized.

5.1.1 Gravitino

When supersymmetry is spontaneously broken on the IR boundary, the effective four-dimensional cosmological constant receives a positive contribution from the VEV of F_X. In the five-dimensional warped geometry, this contribution can be canceled by the addition of a constant superpotential W on the UV brane [116, 125, 205–209], which introduces a boundary mass term for the gravitino field:

$$S_5 \supset -\int d^5x\,\sqrt{-g}\,\frac{1}{2}\frac{W}{M_5^3}\left(\psi_\mu \frac{1}{2}\left[\sigma^\mu,\bar{\sigma}^\nu\right]\psi_\nu + \text{H.c.}\right) 2\delta(y)\,. \tag{5.1}$$

The cosmological constant vanishes when

$$|F|^2 \simeq 3\frac{|W|^2}{M_{\text{P}}^2}\,, \tag{5.2}$$

such that the lightest gravitino obtains a Majorana mass:

$$m_{3/2} \simeq \frac{F}{\sqrt{3}M_{\text{P}}}\,. \tag{5.3}$$

This is the super-Higgs mechanism.[1] This mass expression (5.3) assumes the zero-mode approximation for the gravitino profiles, where the backreaction of the boundary mass term is neglected, an approximation that is valid provided $\sqrt{F}/M_{\text{P}} \lesssim 1$. Using the results of Appendix C, we can find the higher order approximation

$$m_{3/2} \simeq \left[\frac{\sqrt{8\xi^2 + 4e^{-\pi kR}} - e^{-\pi kR}}{\xi\left(1 - e^{-2\pi kR}\right)}\right] k_{\text{IR}}\,. \tag{5.4}$$

Note that this expression is not useful for $\sqrt{F} \ll \Lambda_{\text{IR}}$, although it is valid for $\sqrt{F} \sim \Lambda_{\text{IR}}$ and approaches the twisted limit when $\sqrt{F} \gg \Lambda_{\text{IR}}$:

$$m_{3/2} \to \sqrt{8}\,k_{\text{IR}}\,. \tag{5.5}$$

In principle, the mass for arbitrary F can be determined by solving the full Kaluza-Klein mass quantization condition [this takes the form the Majorana fermion condition (B.90) for

[1] Note that a constant superpotential can also be introduced on the IR brane, as is generically expected in the context of radion stabilization. However, such a superpotential provides a positive contribution to the cosmological constant, and so it cannot be the sole source for the gravitino mass.

$c_L = \frac{3}{2}$],

$$\frac{J_1(x_0^{\mathrm{UV}}) + \xi\, J_2(x_0^{\mathrm{UV}})}{Y_1(x_0^{\mathrm{UV}}) + \xi\, Y_2(x_0^{\mathrm{UV}})} = \frac{J_1(x_0^{\mathrm{IR}})}{Y_1(x_0^{\mathrm{IR}})}\,, \tag{5.6}$$

where

$$\xi = \frac{F}{\sqrt{3} M_{\mathrm{P}} k}\,. \tag{5.7}$$

In practice this is not necessary, as the approximate formula (5.3) is valid throughout our parameter space. We discuss the numeric solution method for this condition in Sec. 3.2.4. As expected, due to the universality of gravity, this matches the usual four-dimensional result. Because the gravitational coupling is suppressed by the Planck scale, the gravitino mass is lower than the characteristic soft mass scale F/Λ_{IR} by a warp factor, and the gravitino is therefore always the lightest supersymmetric particle in the relevant regions of parameter space. This is consistent with the partial compositeness result in the four-dimensional dual theory, where the gravitino is mostly an elementary state [17].

5.1.2 Gauginos

For a bulk field strength superfield W_α^a of a vector supermultiplet V containing a standard model gauge field A_μ^a and its Weyl fermion gaugino superpartner λ_α^a (where a is the gauge index and α is the Weyl spinor index), we introduce the interaction

$$S_5 \supset \int d^5x\, \sqrt{-g} \int d^2\theta \left(\frac{1}{2} \frac{X}{\Lambda_{\mathrm{UV}} k}\, W^{a\alpha} W_\alpha^a + \mathrm{H.c.} \right) 2\delta(y - \pi R)\,. \tag{5.8}$$

This term gives rise to an IR-boundary Majorana mass for the even component of the bulk gaugino field of the vector supermultiplet containing the field strength superfield, breaking supersymmetry by shifting the masses of the Kaluza-Klein modes up such that there is no longer a massless gaugino zero-mode solution. At tree level, the lightest Kaluza-Klein mass is

$$M_\lambda \simeq g^2 \frac{F}{\Lambda_{\mathrm{IR}}}\,. \tag{5.9}$$

Note that the gaugino mass is suppressed relative to F/Λ_{IR} by g^2, the square of the four-dimensional gauge coupling,[2] and hence the gauginos in general obtain masses suppressed

[2] The gauge-coupling dependence arises because we assume a generic GUT symmetry that is broken by the Higgs mechanism on the UV brane, separated from the supersymmetry-breaking sector on the IR boundary (see sec. 3.2.2). The relation between the four-dimensional and five-dimensional coupling constants is given in (3.27). See Refs. [125] for an explicit derivation of the gaugino mass when the brane-localized kinetic terms (3.26) and (3.25b) included and Ref. [126] for the gaugino propagator matrix

below those of sfermions with flat profiles ($c_{L,R} = \pm\frac{1}{2}$). This suppression matches that found in the partial compositeness result, as expected from the AdS/CFT dictionary [17].

If the supersymmetry-breaking sector does not contain any singlets with large F-terms, the interaction (5.8) is forbidden. In this case, with a nonsinglet spurion X, the leading contribution to the gaugino mass is [210]

$$S_5 \supset \int d^5x\,\sqrt{-g}\int d^4\theta\left(\frac{1}{2}\frac{X^\dagger X}{\Lambda_{\rm UV}^3 k}\,W^{a\alpha}W^a_\alpha + \text{H.c.}\right)2\delta(y-\pi R)\,, \tag{5.10}$$

such that

$$M_\lambda \simeq g^2\frac{F^2}{\Lambda_{\rm IR}^3}\,. \tag{5.11}$$

Except in the regime $\sqrt{F}\sim\Lambda_{\rm IR}$, this mass is highly suppressed, and other supersymmetry-breaking contributions such as radion mediation may dominate.

The mass expressions (5.9) and (5.11) assume the zero-mode approximation for the profiles. Using the results of Appendix C, we can find the higher order approximation

$$M_\lambda \simeq \left[\frac{\sqrt{4+4g^4\xi^2\,(2\pi kR-1+e^{-2\pi kR})}-1}{g^2\xi\,(2\pi kR-1+e^{-2\pi kR})}\right]k_{\rm IR}\,. \tag{5.12}$$

As with the gravitino, this expression is not useful for $\sqrt{F}\ll\Lambda_{\rm IR}$, although it does smoothly meet the twisted limit when $\sqrt{F}\gg\Lambda_{\rm IR}$:

$$M_\lambda \to \sqrt{\frac{2}{\pi kR}}\,k_{\rm IR}\,. \tag{5.13}$$

The mass for arbitrary F can be determined by solving the full Kaluza-Klein mass quantization condition [this takes the form the Majorana fermion condition (B.90) for $c_L = \frac{1}{2}$],

$$\frac{J_0(x_0^{\rm UV})}{Y_0(x_0^{\rm UV})} = \frac{J_0(x_0^{\rm IR})+g^2\pi kR\,\xi\,J_1(x_0^{\rm IR})}{Y_0(x_0^{\rm IR})+g^2\pi kR\,\xi\,Y_1(x_0^{\rm IR})}\,, \tag{5.14}$$

where

$$\xi = \begin{cases} \dfrac{F}{\Lambda_{\rm IR}k_{\rm IR}} & \text{for a singlet spurion}\,, \\[2ex] \dfrac{F^2}{\Lambda_{\rm IR}^3 k_{\rm IR}} & \text{for a nonsinglet spurion}\,. \end{cases} \tag{5.15}$$

in this case.

We discuss the numeric solution method for this condition in Sec. 3.2.4.

5.1.3 Sfermions

For a family of bulk chiral supermultiplets Φ_i, each containing a Weyl fermion ψ_i and its complex scalar superpartner ϕ_i, we introduce the interactions

$$S_5 \supset \int d^5x \sqrt{-g} \int d^4\theta \, w_{ij} \frac{X^\dagger X}{\Lambda_{\rm UV}^2 k} \Phi_i^* \Phi_j \, 2\delta(y - \pi R) \,, \tag{5.16}$$

where $i, j = 1, 2, 3$ are indices in flavor space. We take the dimensionless coupling coefficients w_{ij} to be complex numbers and order-one in magnitude, where, because the mass term must be Hermitian, we require $w_{ji} = w_{ij}^*$. As with the gauginos, adding (5.16) as a boundary mass breaks supersymmetry. The interactions give rise to an IR-boundary mass matrix coupling the even bulk scalar fields of the hypermultiplets containing the chiral supermultiplets. Generically, in the basis in which the bulk mass matrix of the family of bulk scalars is diagonal (the bulk mass basis) we expect the boundary mass matrix to have offdiagonal terms. At tree level in this basis, the lightest Kaluza-Klein masses take the form

$$(m^2_{\phi_{L,R}})^{\rm tree}_{ij} \simeq w_{ij} \frac{F^2}{\Lambda_{\rm IR}^2} \sqrt{\frac{4\,(1/2 \mp c_i)\,(1/2 \mp c_j)}{\left(e^{2(1/2 \mp c_i)\pi kR} - 1\right)\left(e^{2(1/2 \mp c_j)\pi kR} - 1\right)}} \, e^{(1 \mp c_i \mp c_j)\pi kR} \tag{5.17}$$

where the upper (lower) signs apply for left-handed (right-handed) states. As with the gauginos, the scalar mass is valid in the limit $\sqrt{F}/\Lambda_{\rm IR} \lesssim 1$. Using the results of Appendix C, we can find a higher order approximation for the diagonal entries:

$$\begin{aligned}
&(m^2_{\phi_{L,R}})^{\rm tree}_{ii} \\
&\quad \simeq \frac{4\,(1/2 - c_i)\,(1/2 + c_i)\, w_{ii}\xi_{ii} k_{\rm IR}^2}{2 - 2e^{-2(1/2 \mp c_i)\pi kR} + w_{ii}\xi_{ii}\left[(1/2 \pm c_i) + (1/2 \mp c_i)\, e^{-2\pi kR} - e^{-2(1/2 \mp c_i)\pi kR}\right]} \,.
\end{aligned} \tag{5.18}$$

We note that this expression smoothly meets the twisted limit when $\sqrt{F} \gg \Lambda_{\rm IR}$:

$$(m^2_{\phi_{L,R}})^{\rm tree}_{ii} \to \left[\frac{4\,(1/2 - c_i)\,(1/2 + c_i)}{(1/2 \pm c_i) + (1/2 \mp c_i)\, e^{-2\pi kR} - e^{-2(1/2 \mp c_i)\pi kR}}\right] k_{\rm IR}^2 \,. \tag{5.19}$$

The entries of the mass matrix for arbitrary F can be determined by solving the full Kaluza-Klein mass quantization conditions, which are given by roots of the denominators of the

entries of the bulk propagator (6.35) with

$$\xi_{ij} = w_{ij} \frac{F^2}{\Lambda_{\text{IR}}^2 k_{\text{IR}}^2} \,. \tag{5.20}$$

The root for each entry can be found numerically using the method described in Sec. 3.2.4.

In terms of localization,

$$(m^2_{\phi_{L,R}})^{\text{tree}}_{ij} \sim \begin{cases} \sqrt{4\left(\frac{1}{2} \mp c_i\right)\left(\frac{1}{2} \mp c_j\right)}\, w_{ij}\, \dfrac{F^2}{\Lambda_{\text{IR}}^2}\, e^{(1 \mp c_i \mp c_j)\pi k R} & \pm c_{i,j} > \dfrac{1}{2}\,, \\ \dfrac{1}{\pi k R}\, w_{ij}\, \dfrac{F^2}{\Lambda_{\text{IR}}^2} & \pm c_{i,j} \sim \dfrac{1}{2}\,, \\ \sqrt{4\left(\frac{1}{2} \mp c_i\right)\left(\frac{1}{2} \mp c_j\right)}\, w_{ij}\, \dfrac{F^2}{\Lambda_{\text{IR}}^2} & \pm c_{i,j} < \dfrac{1}{2}\,. \end{cases} \tag{5.21}$$

Thus, the masses of UV-localized ($\pm c_{i,j} > \frac{1}{2}$) sfermions are suppressed by a warp factor relative to the masses of IR-localized ($\pm c_{i,j} < \frac{1}{2}$) sfermions because supersymmetry is broken on the IR brane. This behavior is illustrated in Figs. 5.1 and 5.2. Using the relations $\Lambda_{\text{IR}}/\Lambda_{\text{UV}} = e^{-\pi k R}$ and $\delta_i = \left|c_i \pm \frac{1}{2}\right|$, the expressions (5.17) are seen to be consistent with the masses obtained in the four-dimensional dual theory [17].

We also note that each offdiagonal element of (5.17) is the geometric mean of two of the masses on the diagonal, such that we can characterize the tree-level mass matrix as

$$(\boldsymbol{m}^{\mathbf{2}}_{\phi})^{\text{tree}} = \begin{pmatrix} m^2_{\phi_1} & \sqrt{m_{\phi_1} m_{\phi_2}} & \sqrt{m_{\phi_1} m_{\phi_3}} \\ \sqrt{m_{\phi_1} m_{\phi_2}} & m^2_{\phi_1} & \sqrt{m_{\phi_2} m_{\phi_3}} \\ \sqrt{m_{\phi_1} m_{\phi_3}} & \sqrt{m_{\phi_2} m_{\phi_3}} & m^2_{\phi_3} \end{pmatrix} . \tag{5.22}$$

Thus, if there is a hierarchy between any of the diagonal masses (arising due to differences in the localizations of the hypermultiplets in the family necessary to explain the standard model fermion mass hierarchy), that hierarchy will also be partially transmitted to the associated offdiagonal elements.

5.2 One-Loop Analysis

The soft masses generated at tree level by (5.16) can be exponentially small for UV-localized bulk scalar fields, in which case quantum corrections become significant. Further, since the

Higgs sector is localized on the UV brane, it is protected at tree level from the effects of supersymmetry breaking. In this section we construct the one-loop contributions to the soft scalar masses, to the soft Higgs masses and soft b term, and to the soft trilinear scalar couplings from the gauge sector and matter sector in the AdS_5 bulk.

5.2.1 Sfermions

At the one-loop level, supersymmetry breaking is transmitted to the bulk scalars via interactions with other bulk scalars and gauginos. In the next chapter, Chapter 7, we derive the resulting contributions to the bulk scalar mass-squared matrices in the five-dimensional theory. From the four-dimensional perspective, these appear as one-loop threshold corrections to the scalar soft masses squared at the IR-brane scale, arising when the Kaluza-Klein modes of the theory are integrated out.

Diagonal breaking

It is illustrative to first consider the simpler scenario in which the scalar supersymmetry breaking is diagonal in the bulk mass basis and CKM mixing and PMNS mixing are neglected (i.e., the Yukawa matrices are diagonal in the four-dimensional gauge-eigenstate basis). In this case, parametrized in terms of the gaugino and sfermion tree-level soft masses, the corrections take the forms

$$\begin{aligned}16\pi^2\,(\Delta m^2_{\tilde{Q}_i})^{\text{1-loop}} = {}& \frac{32}{3}g_3^2\,(X_{\tilde{Q}_i})_{\lambda_3}\,M_3^2 + 6g_2^2\,(X_{\tilde{Q}_i})_{\lambda_2}\,M_2^2 + \frac{2}{15}g_1^2\,(X_{\tilde{Q}_i})_{\lambda_1}\,M_1^2 \\ & - 2y_{u_i}^2\,(X_{\tilde{Q}_i})_{y_u}\,(m^2_{\tilde{u}_i})^{\text{tree}} - 2y_{d_i}^2\,(X_{\tilde{Q}_i})_{y_d}\,(m^2_{\tilde{d}_i})^{\text{tree}} \\ & + \frac{1}{5}g_1^2\Delta\mathcal{S}^{\text{1-loop}}\,, \end{aligned} \tag{5.23a}$$

$$\begin{aligned}16\pi^2\,(\Delta m^2_{\tilde{u}_i})^{\text{1-loop}} = {}& \frac{32}{3}g_3^2\,(X_{\tilde{u}_i})_{\lambda_3}\,M_3^2 + \frac{32}{15}g_1^2\,(X_{\tilde{u}_i})_{\lambda_1}\,M_1^2 \\ & - 4y_{u_i}^2\,(X_{\tilde{u}_i})_{y_u}\,(m^2_{\tilde{Q}_i})^{\text{tree}} - \frac{4}{5}g_1^2\Delta\mathcal{S}^{\text{1-loop}}\,, \end{aligned} \tag{5.23b}$$

$$\begin{aligned}16\pi^2\,(\Delta m^2_{\tilde{d}_i})^{\text{1-loop}} = {}& \frac{32}{3}g_3^2\,(X_{\tilde{d}_i})_{\lambda_3}\,M_3^2 + \frac{8}{15}g_1^2\,(X_{\tilde{d}_i})_{\lambda_1}\,M_1^2 \\ & - 4y_{d_i}^2\,(X_{\tilde{d}_i})_{y_d}\,(m^2_{\tilde{Q}_i})^{\text{tree}} + \frac{2}{5}g_1^2\Delta\mathcal{S}^{\text{1-loop}}\,, \end{aligned} \tag{5.23c}$$

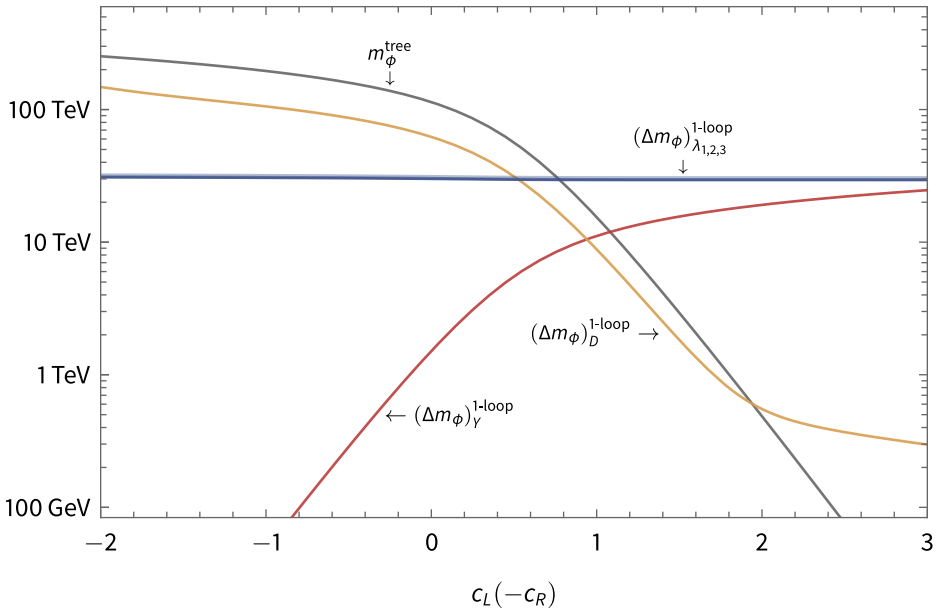

Figure 5.1: Plot of the magnitudes of the tree-level soft mass and the gauge-sector and Yukawa one-loop radiative corrections for a bulk scalar as a function of hypermultiplet localization when the supersymmetry-breaking spurion is a singlet, such that the gaugino masses are given by (5.9). We take $\Lambda_{\text{IR}} = 2 \times 10^{16}\,\text{GeV}$, $\sqrt{F} = 4.75 \times 10^{10}\,\text{GeV}$, and $\tan\beta = 3$.

$$16\pi^2\,(\Delta m^2_{\tilde{L}_i})^{\text{1-loop}} = 6g_2^2\,(X_{\tilde{L}_i})_{\lambda_2}\,M_2^2 + \frac{6}{5}g_1^2\,(X_{\tilde{L}_i})_{\lambda_1}\,M_1^2 - y_{e_i}^2\,(X_{\tilde{L}_i})_{y_e}\,(m^2_{\tilde{e}_i})^{\text{tree}} - \frac{3}{5}g_1^2\Delta\mathcal{S}^{\text{1-loop}}\,, \tag{5.23d}$$

$$16\pi^2\,(\Delta m^2_{\tilde{e}_i})^{\text{1-loop}} = \frac{24}{5}g_1^2\,(X_{\tilde{e}_i})_{\lambda_1}\,M_1^2 - 4y_{e_i}^2\,(X^{\tilde{e}_i})_{y_e}\,(m^2_{\tilde{L}_i})^{\text{tree}} + \frac{6}{5}g_1^2\Delta\mathcal{S}^{\text{1-loop}}\,, \tag{5.23e}$$

where the loop coefficients encoding the effect of the extra dimension are defined in Sec. 7.1.

The radiative corrections to the bulk scalar soft masses can be divided into three types of contributions: gauge corrections arising from loops involving vector supermultiplets, Yukawa corrections arising from loops of hypermultiplets and boundary Higgs fields, and corrections arising from the Fayet-Iliopoulos D-term for weak hypercharge. In Fig. 5.1 we plot the magnitudes of the various contributions as functions of the hypermultiplet localization when the spurion is a singlet such that the gaugino mass is given by (5.9) (singlet spurion), and in Fig. 5.2 the magnitudes when the supersymmetry-breaking sector does not

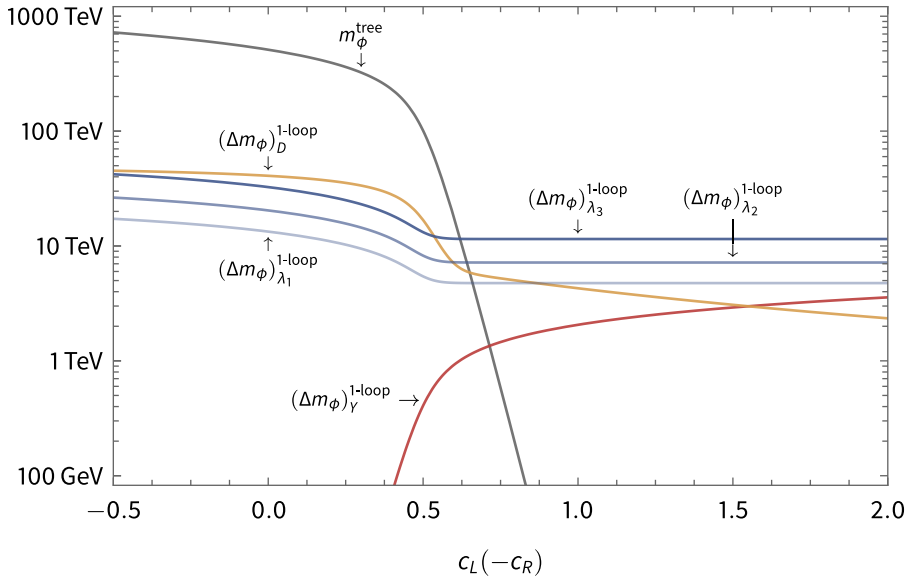

Figure 5.2: Plot of the magnitudes of the tree-level soft mass and the gauge-sector and Yukawa one-loop radiative corrections for a bulk scalar as a function of hypermultiplet localization when the supersymmetry-breaking spurion is a not a singlet, such that the gaugino masses are given by (5.11). We take $\Lambda_{\text{IR}} = 6.5 \times 10^6\,\text{GeV}$, $\sqrt{F} = 2 \times 10^6\,\text{GeV}$, and $\tan\beta = 5$.

contain any singlets with large F-terms and the gaugino mass takes the form (5.11). In each case, we plot the tree-level sfermion mass; the one-loop $\text{U}(1)_Y$, $\text{SU}(2)_L$, and $\text{SU}(3)_c$ gaugino contributions; and the magnitude of the maximal contribution from a single Yukawa coupling (this corresponds to $c_L = \frac{1}{2}$ or $c_R = -\frac{1}{2}$ for the corresponding doublet and singlet hypermultiplet running in the loop). Also shown is the magnitude of the one-loop D-term radiative contribution due to a single scalar mode.[3] Note that the Yukawa contribution is negative, while the D-term contribution may be either positive or negative, depending on the relative sign between the hypercharges of the internal and external scalars.

Due to the conformal flatness of the vector supermultiplet, the gauge corrections take a universal value for UV-localized sfermions that is of order of the gaugino masses. These contributions are positive and set the characteristic scale of the radiative corrections. Because the tree-level contribution is dominant for IR-localized sfermions, which accordingly receive a mass of order of the characteristic soft mass scale $\sqrt{F}/\Lambda_{\text{IR}}$, the sfermion sector thus

[3] As seen in Sec. 7.1.1, unlike the other radiative contributions, one-loop D-term corrections are independent of the localization of the *external* scalar, and so here we plot the contribution as a function of the localization of the *internal* scalar running in the loop.

accommodates a hierarchy $m_\phi^{\rm UV}/m_\phi^{\rm IR} \sim M_a\Lambda_{\rm IR}/F$. When the gaugino mass is given by (5.9), as in Fig. 5.1, the sfermion hierarchy is $m_\phi^{\rm UV}/m_\phi^{\rm IR} \sim g_a^2 \sim \mathcal{O}(0.4\text{–}1)$, which may be increased modestly in individual families with the inclusion of D-term and Yukawa radiative contributions. The moderate size of this hierarchy is an important result of the inclusion of radiative corrections, which wash out the exponential localization dependence of the sfermion soft masses that is a tree-level feature of the extra dimension.

A larger hierarchy can be achieved if the supersymmetry-breaking sector does not contain any singlets with large F terms, as in Fig. 5.2. In this case, the gaugino masses take the form (5.11), and the characteristic sfermion hierarchy is $m_\phi^{\rm UV}/m_\phi^{\rm IR} \sim g_a^2 F/\Lambda_{\rm IR}$. The maximum splitting that can be accommodated between the two sfermion mass scales is limited by the requirement that no sfermions receive negative soft masses at the IR-brane scale or in the subsequent renormalization group evolution of the theory to lower scales. The constraints this condition imposes on the pattern of sfermion mass spectrum at the IR-brane scale are discussed in Sec. 8.1.6.

In the sfermion sector, localization in the extra dimension thus distinguishes between two scales: a tree-level mass scale associated with IR-localized sfermions and a lower mass scale arising from radiative corrections for UV-localized sfermions. When the localizations of the matter hypermultiplets are chosen to explain the SM fermion mass hierarchy (i.e., the third-generation fermions must be predominantly UV-localized, while the lighter generations are mostly IR-localized), the result is a split sfermion spectrum, with the third-generation sfermions hierarchically lighter than the first two generations. We note that the sfermion spectrum inverts the ordering of the fermion spectrum, a consequence of the separation of the supersymmetry-breaking sector and the Higgs sector on opposite orbifold fixed points. Additionally, although both are explained by the same localization mechanism, the sfermion hierarchy is necessarily less split than the fermion hierarchy. This is because the Yukawa couplings only receive wave function renormalization, while the scalar masses are soft parameters and can receive large radiative corrections from the extra dimension and MSSM running.

General flavor mixing

More generally, we consider IR-brane boundary mass terms for the sfermions that are not diagonal and include CKM and PMNS mixing. The one-loop radiative corrections in this

case take the forms

$$(\Delta m^2_{\tilde{Q}})^{\text{1-loop}}_{ij} = \frac{16}{3} g_3^2 \, (\Delta m^2_{\tilde{Q}_i})^{\text{1-loop}}_{\lambda_3} \, \delta_{ij} + 3 g_2^2 \, (\Delta m^2_{\tilde{Q}_i})^{\text{1-loop}}_{\lambda_2} \, \delta_{ij} + \frac{1}{15} g_1^2 \, (\Delta m^2_{\tilde{Q}_i})^{\text{1-loop}}_{\lambda_1} \, \delta_{ij} + (y_u^\dagger)_{ik} \left[(\Delta m^2_{\tilde{Q}_i})^{\text{1-loop}}_{y_u} \right]_{iklj} \, (y_u)_{lj} + (y_d^\dagger)_{ik} \left[(\Delta m^2_{\tilde{Q}_i})^{\text{1-loop}}_{y_d} \right]_{iklj} \, (y_d)_{lj} + \frac{1}{10} g_1^2 \, \Delta\mathcal{S}^{\text{1-loop}} \, \delta_{ij} \,, \tag{5.24a}$$

$$(\Delta m^2_{\tilde{u}})^{\text{1-loop}}_{ij} = \frac{16}{3} g_3^2 \, (\Delta m^2_{\tilde{u}_i})^{\text{1-loop}}_{\lambda_3} \, \delta_{ij} + \frac{16}{15} g_1^2 \, (\Delta m^2_{\tilde{u}_i})^{\text{1-loop}}_{\lambda_1} \, \delta_{ij} + 2 \, (y_u)_{ik} \left[(\Delta m^2_{\tilde{u}_i})^{\text{1-loop}}_{y_u} \right]_{iklj} \, (y_u^\dagger)_{lj} - \frac{2}{5} g_1^2 \, \Delta\mathcal{S}^{\text{1-loop}} \, \delta_{ij} \,, \tag{5.24b}$$

$$(\Delta m^2_{\tilde{d}})^{\text{1-loop}}_{ij} = \frac{16}{3} g_3^2 \, (\Delta m^2_{\tilde{d}_i})^{\text{1-loop}}_{\lambda_3} \, \delta_{ij} + \frac{4}{15} g_1^2 \, (\Delta m^2_{\tilde{d}_i})^{\text{1-loop}}_{\lambda_1} \, \delta_{ij} + 2 \, (y_d)_{ik} \left[(\Delta m^2_{\tilde{d}_i})^{\text{1-loop}}_{y_d} \right]_{iklj} \, (y_d^\dagger)_{lj} + \frac{1}{5} g_1^2 \, \Delta\mathcal{S}^{\text{1-loop}} \, \delta_{ij} \,, \tag{5.24c}$$

$$(\Delta m^2_{\tilde{L}})^{\text{1-loop}}_{ij} = 3 g_3^2 \, (\Delta m^2_{\tilde{L}_i})^{\text{1-loop}}_{\lambda_2} \, \delta_{ij} + \frac{3}{5} g_1^2 \, (\Delta m^2_{\tilde{L}_i})^{\text{1-loop}}_{\lambda_1} \, \delta_{ij} + (y_e^\dagger)_{ik} \left[(\Delta m^2_{\tilde{L}_i})^{\text{1-loop}}_{y_e} \right]_{iklj} \, (y_e)_{lj} - \frac{3}{10} g_1^2 \, \Delta\mathcal{S}^{\text{1-loop}} \, \delta_{ij} \,, \tag{5.24d}$$

$$(\Delta m^2_{\tilde{e}})^{\text{1-loop}}_{ij} = \frac{12}{5} g_1^2 \, (\Delta m^2_{\tilde{e}_i})^{\text{1-loop}}_{\lambda_1} \, \delta_{ij} + 2 \, (y_e)_{ik} \left[(\Delta m^2_{\tilde{e}_i})^{\text{1-loop}}_{y_e} \right]_{iklj} \, (y_e^\dagger)_{lj} + \frac{3}{5} g_1^2 \, \Delta\mathcal{S}^{\text{1-loop}} \, \delta_{ij} \,, \tag{5.24e}$$

where the mass corrections are defined in Sec. 7.1. These corrections exhibit the same behavior as in the diagonal case, and we can therefore draw the same conclusions about the generic shape of the sfermion spectrum. Note, however, that the offdiagonal terms in the mass matrices only receive negative Yukawa contributions, which may be subdominant to the tree-level values [see, for example, (5.22)].

5.2.2 Higgs sector

The Higgs sector, confined to the UV brane, does not couple directly to the supersymmetry-breaking sector, and thus the Higgs soft terms at the IR-brane scale are zero at tree level.

Nevertheless, as with the sfermions, the breaking is transmitted to the Higgs fields at the quantum level. We derive the one-loop corrections to $m_{H_u}^2$, $m_{H_d}^2$, and b from the bulk theory in Chapter 7.

Diagonal breaking

We first consider the scenario in which the scalar supersymmetry breaking is diagonal in the bulk mass basis and CKM mixing and PMNS mixing are neglected. In this case, parametrized in terms of the gaugino and sfermion tree-level soft masses, the Higgs soft terms at one loop take the forms

$$\begin{aligned} 16\pi^2 m_{H_u}^2 = {} & 6g_2^2\,(X_H)_{\lambda_2}\,M_2^2 + \frac{6}{5}g_1^2\,(X_H)_{\lambda_1}\,M_1^2 \\ & - 6y_{u_i}^2\left[(X_H)_{\tilde{Q}_i}^{y_u}\,(m_{\tilde{Q}_i}^2)^{\text{tree}} + (X_H)_{\tilde{u}_i}^{y_u}\,(m_{\tilde{u}_i}^2)^{\text{tree}}\right] + \frac{3}{5}g_1^2\Delta\mathcal{S}^{\text{1-loop}}\,, \end{aligned} \tag{5.25a}$$

$$\begin{aligned} 16\pi^2 m_{H_d}^2 = {} & 6g_2^2\,(X_H)_{\lambda_2}\,M_2^2 + \frac{6}{5}g_1^2\,(X_H)_{\lambda_1}\,M_1^2 \\ & - 6y_{d_i}^2\left[(X_H)_{\tilde{Q}_i}^{y_d}\,(m_{\tilde{Q}_i}^2)^{\text{tree}} + (X_H)_{\tilde{d}_i}^{y_d}\,(m_{\tilde{d}_i}^2)^{\text{tree}}\right] \\ & - 2y_{e_i}^2\left[(X_H)_{\tilde{L}_i}^{y_e}\,(m_{\tilde{L}_i}^2)^{\text{tree}} + (X_H)_{\tilde{e}_i}^{y_e}\,(m_{\tilde{e}_i}^2)^{\text{tree}}\right] - \frac{3}{5}g_1^2\Delta\mathcal{S}^{\text{1-loop}}\,, \end{aligned} \tag{5.25b}$$

$$16\pi^2 b = -\mu\left(6g_2^2\,(X_b)_{\lambda_1}\,M_2 + \frac{6}{5}g_1^2\,(X_b)_{\lambda_2}\,M_1\right)\,, \tag{5.25c}$$

where the loop coefficients encoding the effect of the extra dimension are defined in Sec. 7.2. The origin of the μ term on the UV brane is assumed to arise from the Kim-Nilles mechanism, as discussed in Sec. 3.2.3; its magnitude is determined as necessary to ensure that electroweak symmetry is broken, along with the value of $\tan\beta$, as described in Sec. 5.3.

In Figs. 5.3 and 5.4 we plot the magnitudes of the various one-loop contributions to the Higgs soft masses as functions of hypermultiplet localization in the singlet spurion and nonsinglet spurion cases, respectively. The $\mathrm{U}(1)_Y$ and $\mathrm{SU}(2)_L$ gauge-sector contributions are independent of localization. We also give the maximal contribution from a single Yukawa coupling (this corresponds to $c_L = \frac{1}{2}$ or $c_R = -\frac{1}{2}$ for the other doublet or singlet hypermultiplet running in the loop) as well as the D-term contribution from a single bulk scalar. The Yukawa contribution is negative, while the D-term contribution may be either positive or negative, depending on the relative sign between the hypercharge of the Higgs

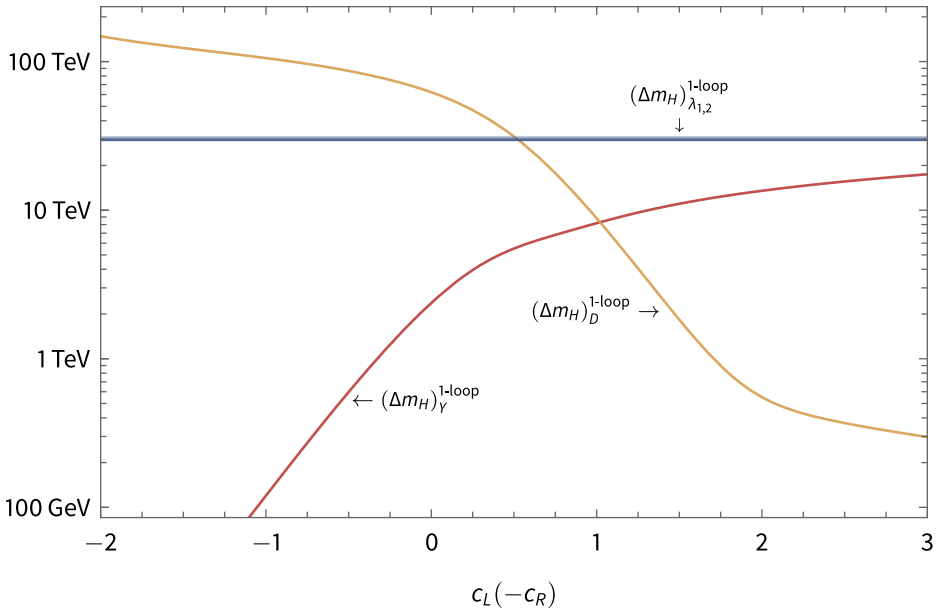

Figure 5.3: Plot of the magnitudes of the gauge-sector and Yukawa one-loop radiative corrections for the soft Higgs masses as a function of hypermultiplet localization when the supersymmetry-breaking spurion is a singlet, such that the gaugino masses are given by (5.9). We take $\Lambda_{\text{IR}} = 2 \times 10^{16}\,\text{GeV}$, $\sqrt{F} = 4.75 \times 10^{10}\,\text{GeV}$, and $\tan\beta = 3$.

field and the hypercharge of the scalar.

General flavor mixing

In the more general case that the IR-brane boundary mass terms that break supersymmetry for the sfermions are not diagonal in the bulk mass basis and CKM mixing and PMNS mixing are included, the one-loop soft Higgs masses are

$$\begin{aligned} m^2_{H_u} = {} & 3g_2^2\,(\Delta m^2_{H_u})^{1\text{-loop}}_{\lambda_2} + \frac{3}{5}g_1^2\,(\Delta m^2_{H_u})^{1\text{-loop}}_{\lambda_1} \\ & + 3\,(y_u)_{ij}\left[(\Delta m^2_{H_u})^{1\text{-loop}}_{\tilde{Q}}\right]_{ijk}(y_u^\dagger)_{ki} + 3\,(y_u^\dagger)_{ij}\left[(\Delta m^2_{H_u})^{1\text{-loop}}_{\tilde{u}}\right]_{ijk}(y_u)_{ki} \\ & + \frac{3}{10}g_1^2\Delta\mathcal{S}^{1\text{-loop}}\,, \end{aligned} \tag{5.26a}$$

$$m^2_{H_d} = 3g_2^2\,(\Delta m^2_{H_u})^{1\text{-loop}}_{\lambda_2} + \frac{3}{5}g_1^2\,(\Delta m^2_{H_u})^{1\text{-loop}}_{\lambda_1}$$

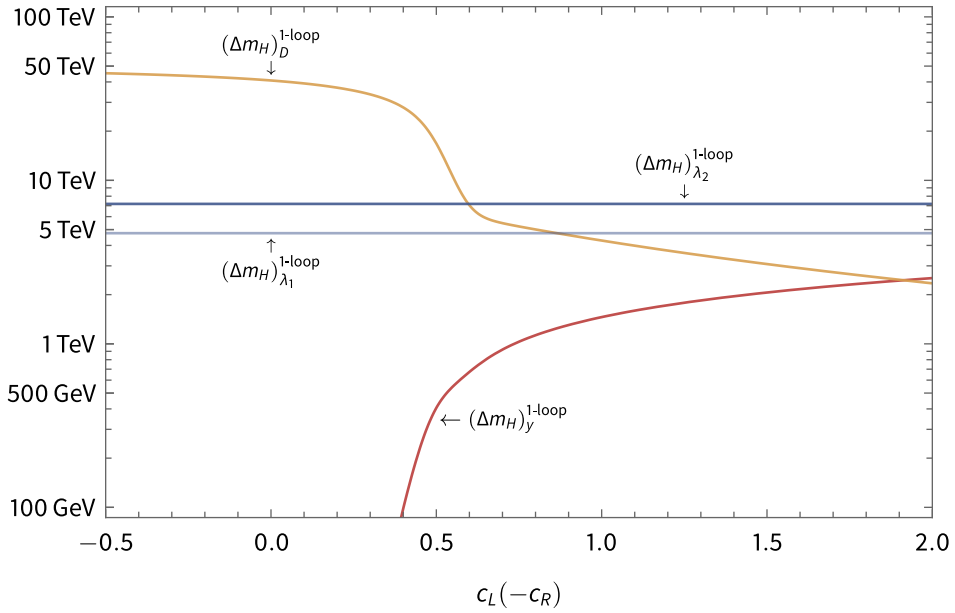

Figure 5.4: Plot of the magnitudes of the gauge-sector and Yukawa one-loop radiative corrections for the soft Higgs masses as a function of hypermultiplet localization when the supersymmetry-breaking spurion is not a singlet, such that the gaugino masses are given by (5.11). We take $\Lambda_{\text{IR}} = 6.5 \times 10^6$ GeV, $\sqrt{F} = 2 \times 10^6$ GeV, and $\tan\beta = 5$.

$$
\begin{aligned}
&+ 3\,(y_d)_{ij} \left[(\Delta m^2_{H_d})^{1\text{-loop}}_{\tilde{Q}}\right]_{ijk} (y_d^\dagger)_{ki} + 3\,(y_d^\dagger)_{ij} \left[(\Delta m^2_{H_d})^{1\text{-loop}}_{\tilde{d}}\right]_{ijk} (y_d)_{ki} \\
&+ (y_e)_{ij} \left[(\Delta m^2_{H_d})^{1\text{-loop}}_{\tilde{L}}\right]_{ijk} (y_e^\dagger)_{ki} + (y_e^\dagger)_{ij} \left[(\Delta m^2_{H_d})^{1\text{-loop}}_{\tilde{e}}\right]_{ijk} (y_e)_{ki} \\
&- \frac{3}{5} g_1^2 \Delta\mathcal{S}^{1\text{-loop}}\,,
\end{aligned}
\tag{5.26b}
$$

where the corrections are defined in Sec. 7.2. The corrections to the b term take the same form (5.25c) as in the diagonal-breaking case. For consistency, we also give the nonparametric form:

$$
b = 3g_2^2\,\Delta b^{1\text{-loop}}_{\lambda_2} + \frac{3}{5} g_1^2\,\Delta b^{1\text{-loop}}_{\lambda_1}\,. \tag{5.27}
$$

5.2.3 Trilinear soft scalar couplings

Soft a terms are also generated radiatively. We derive the one-loop corrections in Chapter 7. Parametrized in terms of the tree-level gaugino masses, the$a$ terms at one loop take the

form:

$$16\pi^2 \frac{(a_u)_{ij}}{(y_u)_{ij}} = -\frac{32}{3} g_3^2 \left[(X_a)^{\lambda_3}_{\tilde{Q}\tilde{u}}\right]_{ij} M_3 - 6 g_2^2 \left[(X_a)^{\lambda_2}_{\tilde{Q}}\right]_{ij} M_2 - g_1^2 \left(-\frac{2}{5}\left[(X_a)^{\lambda_1}_{\tilde{Q}}\right]_{ij} + \frac{8}{5}\left[(X_a)^{\lambda_1}_{\tilde{u}}\right]_{ij} + \frac{8}{15}\left[(X_a)^{\lambda_1}_{\tilde{Q}\tilde{u}}\right]_{ij}\right) M_1 \,, \tag{5.28a}$$

$$16\pi^2 \frac{(a_d)_{ij}}{(y_d)_{ij}} = -\frac{32}{3} g_3^2 \left[(X_a)^{\lambda_3}_{\tilde{Q}\tilde{d}}\right]_{ij} M_3 - 3 g_2^2 \left[(X_a)^{\lambda_2}_{\tilde{Q}}\right]_{ij} M_2 - g_1^2 \left(\frac{2}{5}\left[(X_a)^{\lambda_1}_{\tilde{Q}}\right]_{ij} + \frac{4}{5}\left[(X_a)^{\lambda_1}_{\tilde{d}}\right]_{ij} - \frac{4}{15}\left[(X_a)^{\lambda_1}_{\tilde{Q}\tilde{d}}\right]_{ij}\right) M_1 \,, \tag{5.28b}$$

$$16\pi^2 \frac{(a_e)_{ij}}{(y_e)_{ij}} = -6 g_2^2 \left[(X_a)^{\lambda_2}_{\tilde{L}}\right]_{ij} M_2 - g_1^2 \left(-\frac{6}{5}\left[(X_a)^{\lambda_1}_{\tilde{L}}\right]_{ij} + \frac{12}{5}\left[(X_a)^{\lambda_1}_{\tilde{e}}\right]_{ij} + \frac{12}{5}\left[(X_a)^{\lambda_1}_{\tilde{L}\tilde{e}}\right]_{ij}\right) M_1 \,, \tag{5.28c}$$

where the loop coefficients encoding the effect of the extra dimension are defined in Sec. 7.4. In terms of soft mass corrections defined in Sec. 7.4, these are

$$\frac{(a_u)_{ij}}{(y_u)_{ij}} = \frac{16}{3} g_3^2 \left[(\Delta a_{\lambda_3})^{\text{1-loop}}_{\tilde{Q}\tilde{u}}\right]_{ij} + 3 g_2^2 \left[(\Delta a_{\lambda_2})^{\text{1-loop}}_{\tilde{Q}}\right]_{ij} - \frac{1}{5} g_1^2 \left[(\Delta a_{\lambda_1})^{\text{1-loop}}_{\tilde{Q}}\right]_{ij} + \frac{4}{5} g_1^2 \left[(\Delta a_{\lambda_1})^{\text{1-loop}}_{\tilde{u}}\right]_{ij} + \frac{4}{15} g_1^2 \left[(\Delta a_{\lambda_1})^{\text{1-loop}}_{\tilde{Q}\tilde{u}}\right]_{ij} \,, \tag{5.29a}$$

$$\frac{(a_d)_{ij}}{(y_d)_{ij}} = \frac{16}{3} g_3^2 \left[(\Delta a_{\lambda_3})^{\text{1-loop}}_{\tilde{Q}\tilde{d}}\right]_{ij} + \frac{3}{2} g_2^2 \left[(\Delta a_{\lambda_2})^{\text{1-loop}}_{\tilde{Q}}\right]_{ij} + \frac{1}{5} g_1^2 \left[(\Delta a_{\lambda_1})^{\text{1-loop}}_{\tilde{Q}}\right]_{ij} + \frac{2}{5} g_1^2 \left[(\Delta a_{\lambda_1})^{\text{1-loop}}_{\tilde{d}}\right]_{ij} - \frac{2}{15} g_1^2 \left[(\Delta a_{\lambda_1})^{\text{1-loop}}_{\tilde{Q}\tilde{d}}\right]_{ij} \,, \tag{5.29b}$$

$$\frac{(a_e)_{ij}}{(y_e)_{ij}} = 3 g_2^2 \left[(\Delta a_{\lambda_2})^{\text{1-loop}}_{\tilde{L}}\right]_{ij} - \frac{3}{5} g_1^2 \left[(\Delta a_{\lambda_1})^{\text{1-loop}}_{\tilde{L}}\right]_{ij} + \frac{6}{5} g_1^2 \left[(\Delta a_{\lambda_1})^{\text{1-loop}}_{\tilde{e}}\right]_{ij}$$

$$+ \frac{6}{5} g_1^2 \left[(\Delta a_{\lambda_1})^{\text{1-loop}}_{\tilde{L}\tilde{e}} \right]_{ij} . \tag{5.29c}$$

The magnitude of these corrections is small enough compared to the other soft masses that they can be safely neglected.[4]

5.3 Electroweak Symmetry Breaking

In the MSSM, the tree-level scalar potential has a minimum breaking electroweak symmetry if the following two equations are satisfied:

$$m_{H_u}^2 + |\mu|^2 - b \cot\beta - \frac{1}{8}\left(g_1^2 + g_2^2\right) v^2 \cos 2\beta = 0 \,, \tag{5.30a}$$

$$m_{H_d}^2 + |\mu|^2 - b \tan\beta + \frac{1}{8}\left(g_1^2 + g_2^2\right) v^2 \cos 2\beta = 0 \,. \tag{5.30b}$$

In our model, $m_{H_u}^2$, $m_{H_d}^2$, and b, given by (5.26), are radiatively generated at the IR-brane scale when the extra dimension is integrated out. Solving (5.30) determines two parameters: the magnitude of the higgsino mass parameter $|\mu|$ and the ratio of Higgs VEVs $\tan\beta$. In the limit that the scale of supersymmetry breaking is much larger than the scale of electroweak symmetry breaking ($F/\Lambda_{\text{IR}} \gg v$) the physical solutions are

$$\tan\beta \simeq \frac{\left(m_{H_d}^2 - m_{H_u}^2\right)}{2b} + \frac{\sqrt{\left(m_{H_d}^2 - m_{H_u}^2\right)^2 + 4b^2}}{2b} + \mathcal{O}\left(\frac{v^2}{b}\right), \tag{5.31a}$$

$$|\mu|^2 \simeq \frac{m_{H_d}^2 - m_{H_u}^2 \tan^2\beta}{\tan^2\beta - 1} + \mathcal{O}(v^2) \,. \tag{5.31b}$$

We note that because b is constrained to have the opposite sign from μ at the IR-brane scale according to (5.25c) (and this typically remains true under renormalization group evolution), these equations only have a solution when $\operatorname{sgn}\mu = -1$. Additionally, in order for these conditions to be consistent, it is necessary that $m_{H_d}^2 > m_{H_u}^2 \tan^2\beta$.

The conditions (5.31) for EWSB strongly favor $m_{H_u}^2 < 0$. Although these equations are modified when (four-dimensional) loop corrections to the Higgs scalar potential are included, they remain practical constraints because the iterative method employed to determine electroweak symmetry breaking in the numeric renormalization procedure (see Sec. 9.1)

[4] This is reminiscent of the similar result in gauge-mediated supersymmetry breaking scenarios in four-dimensions.

requires an initial tree-level solution. It is not guaranteed that the Higgs soft terms (5.26) permit a tree-level solution at the IR-brane scale, in which case electroweak symmetry must be broken radiatively (such that the combined radiative corrections to $m_{H_u}^2$ from both the bulk effects calculated at the IR-brane scale and the MSSM running to lower scales is overall negative). We discuss the constraints this pattern of electroweak symmetry breaking imposes on the parameter space of our theory in Sec. 8.1.7.

6 Bulk Propagators in a Slice of AdS_5

In this chapter we consider the propagation of bulk fields in a slice of AdS_5. For bulk fields in the two-brane scenario, the expressions for the five-dimensional propagators in the mixed momentum-position representation are derived in many placed in the literature: for a nonexhaustive selection, see Refs. [95, 125, 126, 211–214]. Here, we catalog the Euclidean[1] forms of the various propagators we employ in Chapter 7 to calculate radiative corrections to the soft supersymmetry-breaking masses. As a new result, we present the construction (6.35) for the propagator matrix for a family of scalar fields in the presence of a boundary mass term on the IR brane that mixes flavors.

6.1 Auxiliary Bessel Functions

First, we establish some notation: the auxiliary functions

$$S^{\alpha_1}_{\alpha_2}(x_1, x_2) = I_{\alpha_1}(x_1)\, K_{\alpha_2}(x_2) + K_{\alpha_1}(x_1)\, I_{\alpha_2}(x_2)\,, \tag{6.2a}$$

$$T^{\alpha_1}_{\alpha_2}(x_1, x_2) = I_{\alpha_1}(x_1)\, K_{\alpha_2}(x_2) - K_{\alpha_1}(x_1)\, I_{\alpha_2}(x_2)\,, \tag{6.2b}$$

are combinations of the modified Bessel functions I, K. For propagators in the bulk carrying four-dimensional momentum p, the natural argument of these Bessel functions is the dimensionless variable

$$x = p_{\mathrm{E}} z\,, \tag{6.3}$$

where $p^2_{\mathrm{E}} = p^2$ is the magnitude of the Euclidean momentum. In the following, we suppress repeated indices: i.e., $T_\alpha(x_1, x_2) \equiv T^\alpha_\alpha(x_1, x_2)$. We note that the auxiliary function S is symmetric with respect to interchange of indices, while T is antisymmetric:

$$S^{\alpha_2}_{\alpha_1}(x_1, x_2) = S^{\alpha_1}_{\alpha_2}(x_2, x_1)\,, \tag{6.4a}$$

[1] With our mostly positive metric signature, a Wick rotation is equivalent to a transformation acting on four-vectors as

$$a^\mu \to a^\mu_{\mathrm{E}} = \left(-ia^0, a^i\right)\,. \tag{6.1}$$

$$-T^{\alpha_2}_{\alpha_1}(x_1,x_2) = T^{\alpha_1}_{\alpha_2}(x_2,x_1)\,. \tag{6.4b}$$

We also note the special case in which the symmetric function reduces to the Wronskian:

$$S^{\alpha}_{\alpha\pm1}(x,x) = \frac{1}{x}\,, \tag{6.5}$$

an identity which is useful when comparing the bulk propagators in various limits.

6.2 Matter Hypermultiplet

We consider a family of three on-shell hypermultiplets in five-dimensional $\mathcal{N}=1$ supergravity, consisting of three Dirac fermion fields Ψ_i and three pairs of complex scalar fields Φ_L and Φ_R. Here, as in Sec. D.2, we identify the scalar fields by the chirality of the fermion component with the same parity assignment.

6.2.1 Unbroken supersymmetry

When supersymmetry is unbroken (and the IR-brane scale sufficiently above the electroweak scale that flavor mixing through the Yukawa couplings can be neglected), the four-dimensional mass basis for a family of hypermultiplet fields coincides with the bulk mass basis. In this case, the propagator matrix of the Dirac fermions of the hypermultiplets is also diagonal in the bulk mass basis:

$$\boldsymbol{G}_{\Psi} = \mathrm{diag}\Big(G_{\Psi_3}, G_{\Psi_2}, G_{\Psi_3}\Big)\,, \tag{6.6}$$

where, in the mixed five-dimensional position and four-dimensional Euclidean[2] momentum space formalism, the two-point functions satisfy

$$e^{-4A}\left(ie^{A}p_{\mathrm{E}\mu}\gamma^{\mu}_{\mathrm{E}} + \gamma_5\partial_5 - 2A'\gamma_5 + c_i A' I_4\right) G_{\Psi_i}(p_{\mathrm{E}},y,y') = \delta(y-y')\,. \tag{6.7}$$

in the bulk. The solution takes the form (cf. Refs. [125, 214])

$$G_{\Psi_i}(p_{\mathrm{E}},y,y') = \begin{pmatrix} G^{LR}_{\Psi_i}(p_{\mathrm{E}},y,y') & G^{LL}_{\Psi_i}(p_{\mathrm{E}},y,y') \\ G^{RR}_{\Psi_i}(p_{\mathrm{E}},y,y') & G^{RL}_{\Psi_i}(p_{\mathrm{E}},y,y') \end{pmatrix}$$

[2]Note that Euclidean vectors are contracted with the Euclidean metric $\delta_{\mu\nu}$.

$$= \begin{pmatrix} \delta_a{}^c\, \mathcal{D}_R\, G_{\psi_{i,R}}(p_{\rm E}, y, y') & p_{{\rm E}\mu}\, \sigma^{\mu}_{{\rm E}a\dot{c}}\, G_{\psi_{i,L}}(p_{\rm E}, y, y') \\ p_{{\rm E}\mu}\, \overline{\sigma}^{\mu\dot{a}c}_{\rm E}\, G_{\psi_{i,R}}(p_{\rm E}, y, y') & -\delta^{\dot{a}}{}_{\dot{c}}\, \mathcal{D}_L\, G_{\psi_{i,L}}(p_{\rm E}, y, y') \end{pmatrix}, \tag{6.8}$$

with

$$\mathcal{D}_{L,R} = e^{-A}\left[\partial_5 - (2 \mp c)A'\right] \tag{6.9}$$

and

$$G_{\psi_{i\,L,R}}(p_{\rm E}, y, y') = \frac{1}{2}\,(zz')^{5/2}\,k^4 \times \begin{cases} \dfrac{S^{\alpha_{i\,R,L}}_{\alpha_{i\,L,R}}(x_{\rm UV}, x_<)\, S^{\alpha_{i\,L,R}}_{\alpha_{i\,R,L}}(x_>, x_{\rm IR})}{T_{\alpha_{i\,R,L}}(x_{\rm UV}, x_{\rm IR})} & \text{for } \Psi^{(+,+)}_{i\,L,R}\,, \\ \dfrac{S^{\alpha_{i\,R,L}}_{\alpha_{i\,L,R}}(x_{\rm UV}, x_<)\, T_{\alpha_{i\,L,R}}(x_>, x_{\rm IR})}{T^{\alpha_{i\,R,L}}_{\alpha_{i\,L,R}}(x_{\rm UV}, x_{\rm IR})} & \text{for } \Psi^{(+,-)}_{i\,L,R}\,, \\ \dfrac{T_{\alpha_{i\,L,R}}(x_{\rm UV}, x_<)\, S^{\alpha_{i\,L,R}}_{\alpha_{i\,R,L}}(x_>, x_{\rm IR})}{T^{\alpha_{i\,L,R}}_{\alpha_{i\,R,L}}(x_{\rm UV}, x_{\rm IR})} & \text{for } \Psi^{(-,+)}_{i\,L,R}\,, \\ \dfrac{T_{\alpha_{i\,L,R}}(x_{\rm UV}, x_<)\, T_{\alpha_{i\,L,R}}(x_>, x_{\rm IR})}{T_{\alpha_{i\,L,R}}(x_{\rm UV}, x_{\rm IR})} & \text{for } \Psi^{(-,-)}_{i\,L,R}\,. \end{cases} \tag{6.10}$$

Here, $x_{<(>)}$ refers to the less (greater) of x and x' and the indices of the Bessel functions are[3]

$$\alpha_{i\,L,R} = c_i \pm \tfrac{1}{2}\,, \tag{6.12}$$

where c_i are the hypermultiplet localization parameters (also the bulk mass parameters of the fermions). The propagator functions obey the equations

$$e^{-5A'}\left[-e^{2A}p_{\rm E}^2 + \partial_5^2 - 5A'\partial_5 - \left(c_i^2 \pm c_i - 6\right)k^2\right] G_{\Psi_{i\,L,R}}(p_{\rm E}, y, y') = \delta(y - y')\,, \tag{6.13}$$

along with either Neumann (N)

$$\left[\partial_5 - (2 - c_i)\,A'\right] G_{\Psi_{i,L}}(p_{\rm E}, y, y')\,\big|_{y=0^+,\pi R^-} = 0\,, \tag{6.14a}$$

[3]In some areas of the parameter space, greater numeric stability may be achieved with the alternative formulation

$$\alpha_{i\,L,R} \to \left|c_i \pm \tfrac{1}{2}\right|\,, \tag{6.11a}$$

$$\alpha_{i\,R,L} \to \mathrm{sgn}(c_i \pm \tfrac{1}{2})\left(c_i \mp \tfrac{1}{2}\right) = \begin{cases} c_i \mp \frac{1}{2} & \text{for } \pm c_i \geq -\frac{1}{2}\,, \\ -c_i \pm \frac{1}{2} & \text{for } \pm c_i < -\frac{1}{2}\,. \end{cases} \tag{6.11b}$$

$$\left[\partial_5 - (2 + c_i)\, A'\right] G_{\Psi_{i,R}}(p_{\rm E}, y, y')\,\big|_{y=0^+,\pi R^-} = 0\,, \tag{6.14b}$$

or Dirichlet (D),

$$G_{\Psi_{i\,L,R}}(p_{\rm E}, y, y')\,\big|_{y=0,\pi R} = 0\,. \tag{6.15}$$

The boundary conditions required on each brane are determined by the fermion component boundary parities according to Table B.2.

The propagator matrix of each of the scalars takes a similar form:

$$\boldsymbol{G}_{\Phi_{L,R}} = \mathrm{diag}\Big(G_{\Phi_{1\,L,R}}, G_{\Phi_{2\,L,R}}, G_{\Phi_{3\,L,R}}\Big)\,, \tag{6.16}$$

where,

$$G_{\Phi_{i\,L,R}}(p_{\rm E}, y, y') = -\frac{1}{2}\,(zz')^2\,k^3 \times \begin{cases} \dfrac{S^{\alpha_{i\,R,L}}_{\alpha_{i\,L,R}}(x_{\rm UV}, x_<)\, S^{\alpha_{i\,L,R}}_{\alpha_{i\,R,L}}(x_>, x_{\rm IR})}{T_{\alpha_{i\,R,L}}(x_{\rm UV}, x_{\rm IR})} & \text{for } \Phi^{(+,+)}_{i\,L,R}\,, \\[2ex] \dfrac{S^{\alpha_{i\,R,L}}_{\alpha_{i\,L,R}}(x_{\rm UV}, x_<)\, T_{\alpha_{i\,L,R}}(x_>, x_{\rm IR})}{T^{\alpha_{i\,R,L}}_{\alpha_{i\,L,R}}(x_{\rm UV}, x_{\rm IR})} & \text{for } \Phi^{(+,-)}_{i\,L,R}\,, \\[2ex] \dfrac{T_{\alpha_{i\,L,R}}(x_{\rm UV}, x_<)\, S^{\alpha_{i\,L,R}}_{\alpha_{i\,R,L}}(x_>, x_{\rm IR})}{T^{\alpha_{i\,L,R}}_{\alpha_{i\,R,L}}(x_{\rm UV}, x_{\rm IR})} & \text{for } \Phi^{(-,+)}_{i\,L,R}\,, \\[2ex] \dfrac{T_{\alpha_{i\,L,R}}(x_{\rm UV}, x_<)\, T_{\alpha_{i\,L,R}}(x_>, x_{\rm IR})}{T_{\alpha_{i\,L,R}}(x_{\rm UV}, x_{\rm IR})} & \text{for } \Phi^{(-,-)}_{i\,L,R}\,, \end{cases} \tag{6.17}$$

is a solution to

$$e^{-4A'}\left[e^{2A}p_{\rm E}^2 - \partial_5^2 + 4A'\partial_5 + \left(c_i^2 \pm c_i - \tfrac{15}{4}\right)k^2\right] G_{\Phi_{i\,L,R}}(p_{\rm E}, y, y') = \delta(y - y')\,, \tag{6.18}$$

along with either Neumann (N)

$$\left[\partial_5 - \left(\tfrac{3}{2} \pm c_i\right) A'\right] G_{\Phi_{i\,L,R}}(p_{\rm E}, y, y')\,\big|_{y=0^+,\pi R^-} = 0\,, \tag{6.19}$$

or Dirichlet (D),

$$G_{\Phi_{i\,L,R}}(p_{\rm E}, y, y')\,\big|_{y=0,\pi R} = 0\,. \tag{6.20}$$

The boundary conditions required on each brane are determined by the scalar boundary parities according to Table 3.2. As in the fermion case, if $\Phi_{i\,L,R}$ is even, then $\Phi_{i\,R,L}$ is odd and vice versa.

Limiting forms

On the UV brane, the propagators for $\Psi^{(+,+)}_{i\,L,R}$ and $\Phi^{(+,+)}_{i\,L,R}$ take the forms

$$G_{\psi_{i\,L,R}}(p_{\rm E},0,0) = -G_{\Phi_{i\,L,R}}(p_{\rm E},0,0) = \frac{1}{2}\frac{1}{p_{\rm E}}\frac{S^{\alpha_{i\,L,R}}_{\alpha_{i\,R,L}}(x_{\rm UV},x_{\rm IR})}{T_{\alpha_{i\,R,L}}(x_{\rm UV},x_{\rm IR})}\,, \tag{6.21}$$

and, on the IR brane,

$$G_{\psi_{i\,L,R}}(p_{\rm E},\pi R,\pi R) = \frac{1}{2}\frac{1}{p_{\rm E}}\,(z_{\rm IR}k)^4\,\frac{S^{\alpha_{i\,R,L}}_{\alpha_{i\,L,R}}(x_{\rm UV},x_{\rm IR})}{T_{\alpha_{i\,R,L}}(x_{\rm UV},x_{\rm IR})}\,. \tag{6.22a}$$

$$G_{\Phi_{i\,L,R}}(p_{\rm E},\pi R,\pi R) = -\frac{1}{2}\frac{1}{p_{\rm E}}\,(z_{\rm IR}k)^3\,\frac{S^{\alpha_{i\,R,L}}_{\alpha_{i\,L,R}}(x_{\rm UV},x_{\rm IR})}{T_{\alpha_{i\,R,L}}(x_{\rm UV},x_{\rm IR})}\,, \tag{6.22b}$$

The brane-to-brane propagators are

$$G_{\psi_{i\,L,R}}(p_{\rm E},0,\pi R) = \frac{1}{2}\frac{1}{p_{\rm E}}\frac{(z_{\rm IR}k)^{5/2}}{x_{\rm IR}}\frac{1}{T_{\alpha_{i\,R,L}}(x_{\rm UV},x_{\rm IR})}\,. \tag{6.23a}$$

$$G_{\Phi_{i\,L,R}}(p_{\rm E},0,\pi R) = -\frac{1}{2}\frac{1}{p_{\rm E}}\frac{(z_{\rm IR}k)^{2}}{x_{\rm IR}}\frac{1}{T_{\alpha_{i\,R,L}}(x_{\rm UV},x_{\rm IR})}\,, \tag{6.23b}$$

Kaluza-Klein description

Using the Kaluza-Klein decompositions of the hypermultiplet fields, the 5D propagators can be decomposed into sums of four-dimensional propagators. For the fermions,

$$G^{LR}_{\Psi_i}(p_{\rm E},y,y') = \sum_n \frac{m_n \delta_a{}^c}{p_{\rm E}^2+m_n^2}\,f^{(n)}_{\Psi_{i,L}}(y)\,f^{(n)}_{\Psi_{i,R}}(y')\,, \tag{6.24a}$$

$$G^{LL}_{\Psi_i}(p_{\rm E},y,y') = -\sum_n \frac{p_{{\rm E}\mu}\,\sigma^{\mu}_{{\rm E}a\dot{c}}}{p_{\rm E}^2+m_n^2}\,f^{(n)}_{\Psi_{i,L}}(y)\,f^{(n)}_{\Psi_{i,L}}(y')\,, \tag{6.24b}$$

$$G^{RR}_{\Psi_i}(p_{\rm E},y,y') = -\sum_n \frac{p_{{\rm E}\mu}\,\overline{\sigma}^{\mu\dot{a}c}_{\rm E}}{p_{\rm E}^2+m_n^2}\,f^{(n)}_{\Psi_{i,R}}(y)\,f^{(n)}_{\Psi_{i,R}}(y')\,, \tag{6.24c}$$

$$G^{RL}_{\Psi_i}(p_{\rm E},y,y') = \sum_n \frac{m_n \delta^{\dot{a}}_{\dot{c}}}{p_{\rm E}^2+m_n^2}\,f^{(n)}_{\Psi_{i,R}}(y)\,f^{(n)}_{\Psi_{i,L}}(y')\,, \tag{6.24d}$$

where the four-dimensional propagator

$$G^{(n)}_{\Psi_i}(p_{\mathrm{E}}, y, y') = \frac{-ip_{\mathrm{E}\mu}\gamma^\mu_{\mathrm{E}} + m_n I_4}{p^2_{\mathrm{E}} + m^2_n} \tag{6.25}$$

satisfies the four-dimensional Euclidean Dirac equation:

$$\left(ip_{\mathrm{E}\mu}\gamma^\mu_{\mathrm{E}} + m_n I_4\right) G^{(n)}_{\Psi_i}(p_{\mathrm{E}}, y, y') = I_4\,. \tag{6.26}$$

For the scalars,

$$G_{\Phi_{i\,L,R}}(p_{\mathrm{E}}, y, y') = \sum_n \frac{1}{p^2_{\mathrm{E}} + m^2_n}\, f^{(n)}_{\Phi_{i\,L,R}}(y)\, f^{(n)}_{\Phi_{i\,L,R}}(y')\,, \tag{6.27}$$

where the four-dimensional propagator

$$G^{(n)}_{\Phi_{i\,L,R}}(p_{\mathrm{E}}, y, y') = \frac{1}{p^2_{\mathrm{E}} + m^2_n} \tag{6.28}$$

satisfies the four-dimensional Euclidean Klein-Gordon equation:

$$\left(p^2_{\mathrm{E}} + m_n\right) G^{(n)}_{\Phi_{i\,L,R}}(p_{\mathrm{E}}, y, y') = 1\,. \tag{6.29}$$

6.2.2 Broken supersymmetry

Here, we consider the effect of a supersymmetry-breaking sector localized on the IR brane.

Diagonal breaking

When supersymmetry is broken on the IR brane, the bulk scalar fields $\Phi^{(+,+)}_{i\,L,R}$ receive localized mass terms that can be parametrized as [cf. (5.16)]

$$S_5 \supset -\int d^5x\,\sqrt{-g}\int d^4\theta\,\xi_{ij}\Phi^\dagger_i\Phi_j\,2k\,\delta(y-\pi R)\,. \tag{6.30}$$

If the coupling matrix is diagonal in the bulk mass basis,

$$\boldsymbol{\xi} = \mathrm{diag}(\xi_1, \xi_2, \xi_3)\,, \tag{6.31}$$

then the scalar field propagator matrix remains diagonal in the bulk mass basis, with entries

$$G_{\Phi_{i\,L,R}}(p_{\rm E},y,y') = -\frac{1}{2}\,(zz')^2k^3\,S^{\alpha_{i\,R,L}}_{\alpha_{i\,L,R}}(x_{\rm UV},x_<) \times \frac{x_{\rm IR}S^{\alpha_{i\,R,L}}_{\alpha_{i\,L,R}}(x_>,x_{\rm IR}) - \xi_i\,T_{\alpha_{i\,L,R}}(x_>,x_{\rm IR})}{x_{\rm IR}T_{\alpha_{i\,R,L}}(x_{\rm UV},x_{\rm IR}) - \xi_i\,S^{\alpha_{i\,R,L}}_{\alpha_{i\,L,R}}(x_{\rm UV},x_{\rm IR})}\,. \tag{6.32}$$

We note that these can each be decomposed into a supersymmetric piece of the form (6.17) and a supersymmetry-breaking term:

$$G_{\Phi_{i\,L,R}} = G^{\rm SUSY}_{\Phi_{i\,L,R}} + \delta G_{\Phi_{i\,L,R}}\,, \tag{6.33}$$

where

$$\delta G_{\Phi_{i\,L,R}}(p_{\rm E},y,y') = -\frac{1}{2}\,\frac{(zz')^2k^3}{x_{\rm IR}}\,\frac{1}{T_{\alpha_{i\,R,L}}(x_{\rm UV},x_{\rm IR})} \times \frac{\xi_i\,S^{\alpha_{i\,R,L}}_{\alpha_{i\,L,R}}(x_{\rm UV},x)\,S^{\alpha_{i\,R,L}}_{\alpha_{i\,L,R}}(x_{\rm UV},x')}{x_{\rm IR}T_{\alpha_{i\,R,L}}(x_{\rm UV},x_{\rm IR}) - \xi_i\,S^{\alpha_{i\,R,L}}_{\alpha_{i\,L,R}}(x_{\rm UV},x_{\rm IR})}\,. \tag{6.34}$$

IR-brane flavor mixing

If, however, the supersymmetry-breaking coupling matrix $\boldsymbol{\xi}$ on the IR brane has offdiagonal terms in the bulk mass basis, it will mix the even scalar fields of the family of hypermultiplets. In this case, the scalar propagator matrix can be decomposed into a flavor-diagonal supersymmetric piece of the form (6.16) and a flavor-mixing term containing the effects of supersymmetry breaking,

$$\boldsymbol{G}_{\Phi_{L,R}} = \boldsymbol{G}^{\rm SUSY}_{\Phi_{L,R}} + \boldsymbol{\delta G}_{\Phi_{L,R}}\,, \tag{6.35}$$

the latter of which can itself be constructed in the bulk mass basis as a dressed propagator matrix resulting from the sum of a series of supersymmetric propagators and mass insertions, schematically,

$$\begin{aligned}(\delta G_{\Phi_{L,R}})_{ij} &= \; i \text{ ---------- } j \\ &= \; i \text{ -----}\underset{m_{ij}}{\times}\text{----- } j \;+\; i \text{ -----}\underset{m_{ik}}{\times}\text{----}\underset{m_{kj}}{\times}\text{----- } j \;+\; \cdots\,,\end{aligned} \tag{6.36}$$

where

$$\boldsymbol{m} \equiv 2ke^{-4\pi kR}\boldsymbol{\xi} = \frac{2}{z_{\rm IR}^4k^3}\,\boldsymbol{\xi} \tag{6.37}$$

is the effective mass coupling between the five-dimensional fields on the IR brane. For the Euclidean propagator matrix, the supersymmetry-breaking part of the propagator can be written

$$\begin{aligned}
&\boldsymbol{\delta G}_{\Phi_{L,R}}(p_{\mathrm{E}}, y, y') \\
&\quad = \boldsymbol{G}^{\mathrm{SUSY}}_{\Phi_{L,R}}(p_{\mathrm{E}}, y, \pi R)\, \boldsymbol{m} \left(\sum_{n=0}^{\infty} \Big[\boldsymbol{G}^{\mathrm{SUSY}}_{\Phi_{L,R}}(p_{\mathrm{E}}, \pi R, \pi R)\, \boldsymbol{m} \Big]^n \right) \boldsymbol{G}^{\mathrm{SUSY}}_{\Phi_{L,R}}(p_{\mathrm{E}}, \pi R, y')\,, \\
&\quad = \boldsymbol{G}^{\mathrm{SUSY}}_{\Phi_{L,R}}(p_{\mathrm{E}}, y, \pi R)\, \boldsymbol{m} \Big[\boldsymbol{I}_3 - \boldsymbol{G}^{\mathrm{SUSY}}_{\Phi_{L,R}}(p_{\mathrm{E}}, \pi R, \pi R)\, \boldsymbol{m} \Big]^{-1} \boldsymbol{G}^{\mathrm{SUSY}}_{\Phi_{L,R}}(p_{\mathrm{E}}, \pi R, y')\,. \qquad (6.38)
\end{aligned}$$

We note the Kaluza-Klein masses of the scalars in the bulk mass basis are given by the poles of this expression (the roots of the denominators of each element).

In the limit that $\boldsymbol{\xi}$ is diagonal as in (6.31), (6.38) reduces to the form

$$\boldsymbol{\delta G}_{\Phi_{L,R}} \to \mathrm{diag}\Big(\delta G_{\Phi_{1\,L,R}}, \delta G_{\Phi_{2\,L,R}}, \delta G_{\Phi_{3\,L,R}} \Big)\,, \qquad (6.39)$$

where the diagonal entries take the form of (6.34). This limit provides a check on the derivation of the nondiagonal relation (6.38).

Limiting forms

On the UV brane, the diagonal components of the propagator for $\Phi^{(+,+)}_{i\,L,R}$ in the presence of diagonal supersymmetry breaking take the forms

$$G_{\Phi_{i\,L,R}}(p_{\mathrm{E}}, 0, 0) = -\frac{1}{2}\frac{1}{p_{\mathrm{E}}} \frac{x_{\mathrm{IR}} S^{\alpha_{i\,L,R}}_{\alpha_{i\,R,L}}(x_{\mathrm{UV}}, x_{\mathrm{IR}}) - \xi_i\, T_{\alpha_{i\,L,R}}(x_{\mathrm{UV}}, x_{\mathrm{IR}})}{x_{\mathrm{IR}} T_{\alpha_{i\,R,L}}(x_{\mathrm{UV}}, x_{\mathrm{IR}}) - \xi_i\, S^{\alpha_{i\,R,L}}_{\alpha_{i\,L,R}}(x_{\mathrm{UV}}, x_{\mathrm{IR}})}\,, \qquad (6.40)$$

and, on the IR brane,

$$G_{\Phi_{i\,L,R}}(p_{\mathrm{E}}, \pi R, \pi R) = -\frac{1}{2}\frac{1}{p_{\mathrm{E}}} (z_{\mathrm{IR}} k)^3 \frac{x_{\mathrm{IR}} S^{\alpha_{i\,R,L}}_{\alpha_{i\,L,R}}(x_{\mathrm{UV}}, x_{\mathrm{IR}})}{x_{\mathrm{IR}} T_{\alpha_{i\,R,L}}(x_{\mathrm{UV}}, x_{\mathrm{IR}}) - \xi_i\, S^{\alpha_{i\,R,L}}_{\alpha_{i\,L,R}}(x_{\mathrm{UV}}, x_{\mathrm{IR}})}\,. \qquad (6.41)$$

The brane-to-brane propagator components are

$$G_{\Phi_{i\,L,R}}(p_{\mathrm{E}}, 0, \pi R) = -\frac{1}{2}\frac{1}{p_{\mathrm{E}}} (z_{\mathrm{IR}} k)^2 \frac{1}{x_{\mathrm{IR}} T_{\alpha_{i\,R,L}}(x_{\mathrm{UV}}, x_{\mathrm{IR}}) - \xi_i\, S^{\alpha_{i\,R,L}}_{\alpha_{i\,L,R}}(x_{\mathrm{UV}}, x_{\mathrm{IR}})}\,. \qquad (6.42)$$

Restricting now to the supersymmetry-breaking part of the propagator, we find

$$\delta G_{\Phi_i\, L,R}(p_{\rm E},0,0) = -\frac{1}{2}\frac{1}{p_{\rm E}}\frac{1}{x_{\rm UV}x_{\rm IR}}\frac{1}{T_{\alpha_i\, R,L}(x_{\rm UV},x_{\rm IR})} \times \frac{\xi_i}{x_{\rm IR}T_{\alpha_i\, R,L}(x_{\rm UV},x_{\rm IR}) - \xi_i\, S^{\alpha_i\, R,L}_{\alpha_i\, L,R}(x_{\rm UV},x_{\rm IR})}\,. \tag{6.43}$$

on the UV brane and

$$\delta G_{\Phi_i\, L,R}(p_{\rm E},\pi R,\pi R) = -\frac{1}{2}\frac{1}{p_{\rm E}}\,(z_{\rm IR}k)^3\,\frac{S^{\alpha_i\, R,L}_{\alpha_i\, L,R}(x_{\rm UV},x_{\rm IR})}{T_{\alpha_i\, R,L}(x_{\rm UV},x_{\rm IR})} \times \frac{\xi_i\, S^{\alpha_i\, R,L}_{\alpha_i\, L,R}(x_{\rm UV},x_{\rm IR})}{x_{\rm IR}T_{\alpha_i\, R,L}(x_{\rm UV},x_{\rm IR}) - \xi_i\, S^{\alpha_i\, R,L}_{\alpha_i\, L,R}(x_{\rm UV},x_{\rm IR})}\,. \tag{6.44}$$

on the IR brane. The brane-to-brane forms are

$$\delta G_{\Phi_i\, L,R}(p_{\rm E},0,\pi R) = -\frac{1}{2}\frac{1}{p_{\rm E}}\frac{(z_{\rm IR}k)^2}{x_{\rm IR}}\frac{1}{T_{\alpha_i\, R,L}(x_{\rm UV},x_{\rm IR})} \times \frac{\xi_i}{x_{\rm IR}T_{\alpha_i\, R,L}(x_{\rm UV},x_{\rm IR}) - \xi_i\, S^{\alpha_i\, R,L}_{\alpha_i\, L,R}(x_{\rm UV},x_{\rm IR})}\,. \tag{6.45}$$

6.3 Vector Supermultiplet

An on-shell vector multiplet in five-dimensional $\mathcal{N}=1$ supergravity consists of a gauge field A_M, an $n=1$ symplectic Majorana spinor Λ_i, and a real scalar Σ which transforms in the adjoint representation. Here, we consider the gauge group U(1) for simplicity; the generalization to nonabelian groups is straightforward. As in Sec. D.3, we take the parity assignments to be those given in (D.26), a configuration that preserves four-dimensional gauge invariance.

6.3.1 Unbroken supersymmetry

For the gauginos, we construct the propagator of the Dirac spinor

$$\Lambda \equiv \Lambda_+ + \Lambda_- = \begin{pmatrix} (\lambda_+)_a \\ (\lambda_-^\dagger)^{\dot a} \end{pmatrix}\,. \tag{6.46}$$

In the mixed momentum-position formalism, the two-point functions satisfy

$$e^{-4A}\left(ie^{A}p_{\mathrm{E}\mu}\gamma_{\mathrm{E}}^{\mu}+\gamma_5\partial_5-2A'\gamma_5+\frac{1}{2}A'I_4\right)G_\Lambda(p_{\mathrm{E}},y,y')=\delta(y-y')\,. \tag{6.47}$$

in the bulk. The solution takes the same form as that of the Dirac fermions in the hypermultiplet:

$$\begin{aligned}G_\Lambda(p_{\mathrm{E}},y,y')&=\begin{pmatrix}G_{\lambda_+\lambda_-}(p_{\mathrm{E}},y,y') & G_{\lambda_+\lambda_+^\dagger}(p_{\mathrm{E}},y,y')\\ G_{\lambda_-^\dagger\lambda_-}(p_{\mathrm{E}},y,y') & G_{\lambda_-^\dagger\lambda_+^\dagger}(p_{\mathrm{E}},y,y')\end{pmatrix}\\ &=\begin{pmatrix}\delta_a{}^c\,\mathcal{D}_R\,G_{\lambda_-}(p_{\mathrm{E}},y,y') & p_{\mathrm{E}\mu}\,\sigma^{\mu}_{\mathrm{E}a\dot{c}}\,G_{\lambda_+}(p_{\mathrm{E}},y,y')\\ p_{\mathrm{E}\mu}\,\overline{\sigma}^{\mu\dot{a}c}_{\mathrm{E}}\,G_{\lambda_-}(p_{\mathrm{E}},y,y') & -\delta^{\dot{a}}{}_{\dot{c}}\,\mathcal{D}_L\,G_{\lambda_+}(p_{\mathrm{E}},y,y')\end{pmatrix},\end{aligned} \tag{6.48}$$

with

$$G_{\lambda_+}(p_{\mathrm{E}},y,y')=\frac{1}{2}\,(zz')^{5/2}k^4\,\frac{S_1^0(x_{\mathrm{UV}},x_<)\,S_0^1(x_>,x_{\mathrm{IR}})}{T_0(x_{\mathrm{UV}},x_{\mathrm{IR}})}\,, \tag{6.49a}$$

$$G_{\lambda_-}(p_{\mathrm{E}},y,y')=\frac{1}{2}\,(zz')^{5/2}k^4\,\frac{T_0(x_{\mathrm{UV}},x_<)\,T_0(x_>,x_{\mathrm{IR}})}{T_0(x_{\mathrm{UV}},x_{\mathrm{IR}})}\,. \tag{6.49b}$$

The propagator functions obey the equations

$$e^{-5A'}\left[-e^{2A}p_{\mathrm{E}}^2+\partial_5^2-5A'\partial_5+\left(2\mp\frac{1}{2}\right)\left(3\pm\frac{1}{2}\right)k^2\right]G_{\lambda_\pm}(p_{\mathrm{E}},y,y')=\delta(y-y')\,, \tag{6.50}$$

along with the boundary conditions

$$\left(\partial_5-\frac{3}{2}A'\right)G_{\lambda_+}(p_{\mathrm{E}},y,y')\Big|_{y=0^+,\pi R^-}=0\,, \tag{6.51a}$$

$$G_{\lambda_-}(p_{\mathrm{E}},y,y')\,|_{y=0,\pi R}=0\,. \tag{6.51b}$$

In the R_ξ gauge, the components of the gauge boson propagators satisfy the equations

$$\begin{aligned}e^{-2A'}\Big[&\left(e^{2A}p_{\mathrm{E}}^2-\partial_5^2+2A'\partial_5\right)\delta^{\rho\mu}\\ &-e^{2A}\left(1-\frac{1}{\xi}\right)p_{\mathrm{E}}^{\rho}\,p_{\mathrm{E}}^{\mu}\Big]\,G^A_{\mu\nu}(p_{\mathrm{E}},y,y')=\delta^{\rho}{}_{\nu}\delta(y-y')\,,\end{aligned} \tag{6.52a}$$

$$e^{-4A'}\left[\frac{1}{\xi}e^{2A}p_{\rm E}^2-\partial_5^2+4A'\partial_5-4k^2\right]G^A_{55}(p_{\rm E},y,y')=\delta(y-y')\,. \tag{6.52b}$$

with boundary conditions

$$\partial_5 G^A_{\mu\nu}(p_{\rm E},y,y')\,\big|_{0^+,\pi R^-}=0\,, \tag{6.53a}$$

$$G^A_{55}(p_{\rm E},y,y')\,\big|_{0,\pi R}=0\,. \tag{6.53b}$$

The solutions take the forms [128]

$$G^A_{\mu\nu}(p_{\rm E},y,y')=\left(\delta_{\mu\nu}-\frac{p_{{\rm E}\mu}\,p_{{\rm E}\nu}}{p_{\rm E}^2}\right)G_{A_\mu}(p_{\rm E},y,y')+\frac{p_{{\rm E}\mu}\,p_{{\rm E}\nu}}{p_{\rm E}^2}\,G^\xi_{A_\mu}(p_{\rm E},y,y')\,, \tag{6.54a}$$

$$G^A_{55}(p_{\rm E},y,y')=\frac{1}{\xi}\,G^\xi_{A_5}(p_{\rm E},y,y')\,, \tag{6.54b}$$

where we introduce the scalar propagator functions

$$G_{A_\mu}(p_{\rm E},y,y')=-\frac{1}{2}\,zz'k\,\frac{S^0_1(x_{\rm UV},x_<)\,S^1_0(x_>,x_{\rm IR})}{T_0(x_{\rm UV},x_{\rm IR})}\,, \tag{6.55a}$$

$$G_{A_5}(p_{\rm E},y,y')=-\frac{1}{2}\,(zz')^2k^3\,\frac{T_0(x_{\rm UV},x_<)\,T_0(x_>,x_{\rm IR})}{T_0(x_{\rm UV},x_{\rm IR})}\,, \tag{6.55b}$$

$$G^\xi_{A_{\mu,5}}(p_{\rm E},y,y')=G_{A_{\mu,5}}(p_{\rm E}/\sqrt{\xi},y,y')\,, \tag{6.55c}$$

which obey the equations

$$e^{-2A'}\left[e^{2A}p_{\rm E}^2-\partial_5^2+2A'\partial_5\right]G_{A_\mu}(p_{\rm E},y,y')=\delta(y-y')\,, \tag{6.56a}$$

$$e^{-4A'}\left[e^{2A}p_{\rm E}^2-\partial_5^2+4A'\partial_5-4k^2\right]G_{A_5}(p_{\rm E},y,y')=\delta(y-y')\,, \tag{6.56b}$$

and boundary conditions

$$\partial_5 G_{A_\mu}(p_{\rm E},y,y')\,\big|_{0^+,\pi R^-}=0\,, \tag{6.57a}$$

$$G_{A_5}(p_{\rm E},y,y')\,\big|_{0,\pi R}=0\,. \tag{6.57b}$$

Limiting forms

On the UV brane, the propagators for λ_+ and A_μ take the forms

$$G_{\lambda_+}(p_{\mathrm{E}},0,0) = -G_{A_\mu}(p_{\mathrm{E}},0,0) = \frac{1}{2}\frac{1}{p_{\mathrm{E}}}\frac{S_0^1(x_{\mathrm{UV}},x_{\mathrm{IR}})}{T_0(x_{\mathrm{UV}},x_{\mathrm{IR}})}\,, \tag{6.58}$$

and, on the IR brane,

$$G_{\lambda_+}(p_{\mathrm{E}},\pi R,\pi R) = \frac{1}{2}\frac{1}{p_{\mathrm{E}}}\,(z_{\mathrm{IR}}k)^4\,\frac{S_1^0(x_{\mathrm{UV}},x_{\mathrm{IR}})}{T_0(x_{\mathrm{UV}},x_{\mathrm{IR}})}\,. \tag{6.59a}$$

$$G_{A_\mu}(p_{\mathrm{E}},\pi R,\pi R) = -\frac{1}{2}\frac{1}{p_{\mathrm{E}}}\,z_{\mathrm{IR}}k\,\frac{S_1^0(x_{\mathrm{UV}},x_{\mathrm{IR}})}{T_0(x_{\mathrm{UV}},x_{\mathrm{IR}})}\,, \tag{6.59b}$$

The brane-to-brane propagators are

$$G_{\lambda_+}(p_{\mathrm{E}},0,\pi R) = \frac{1}{2}\frac{1}{p_{\mathrm{E}}}\frac{(z_{\mathrm{IR}}k)^{5/2}}{x_{\mathrm{IR}}}\frac{1}{T_0(x_{\mathrm{UV}},x_{\mathrm{IR}})}\,. \tag{6.60a}$$

$$G_{A_\mu}(p_{\mathrm{E}},0,\pi R) = -\frac{1}{2}\frac{1}{p_{\mathrm{E}}}\frac{z_{\mathrm{IR}}k}{x_{\mathrm{IR}}}\frac{1}{T_0(x_{\mathrm{UV}},x_{\mathrm{IR}})}\,, \tag{6.60b}$$

Kaluza-Klein description

Using the Kaluza-Klein decompositions of the vector multiplet fields, the five-dimensional propagators can be decomposed into sums of four-dimensional propagators. For the gauginos,

$$G_{\lambda_+\lambda_-}(p_{\mathrm{E}},y,y') = \sum_n \frac{m_n \delta_a{}^c}{p_{\mathrm{E}}^2+m_n^2}\,f_{\lambda_-}^{(n)}(y)\,f_{\lambda_+}^{(n)}(y')\,, \tag{6.61a}$$

$$G_{\lambda_+\lambda_+^\dagger}(p_{\mathrm{E}},y,y') = -\sum_n \frac{p_{\mathrm{E}\mu}\,\sigma^\mu_{\mathrm{E}a\dot{c}}}{p_{\mathrm{E}}^2+m_n^2}\,f_{\lambda_+}^{(n)}(y)\,f_{\lambda_+}^{(n)}(y')\,, \tag{6.61b}$$

$$G_{\lambda_-^\dagger\lambda_-}(p_{\mathrm{E}},y,y') = -\sum_n \frac{p_{\mathrm{E}\mu}\,\overline{\sigma}_{\mathrm{E}}^{\mu\dot{a}c}}{p_{\mathrm{E}}^2+m_n^2}\,f_{\lambda_-}^{(n)}(y)\,f_{\lambda_-}^{(n)}(y')\,, \tag{6.61c}$$

$$G_{\lambda_-^\dagger\lambda_+^\dagger}(p_{\mathrm{E}},y,y') = \sum_n \frac{m_n \delta^{\dot{a}}{}_{\dot{c}}}{p_{\mathrm{E}}^2+m_n^2}\,f_{\lambda_+}^{(n)}(y)\,f_{\lambda_-}^{(n)}(y')\,, \tag{6.61d}$$

where the four-dimensional propagator

$$G_{\Lambda}^{(n)}(p_{\mathrm{E}}, y, y') = \frac{-ip_{\mathrm{E}\mu}\gamma_{\mathrm{E}}^{\mu} + m_n I_4}{p_{\mathrm{E}}^2 + m_n^2} \tag{6.62}$$

satisfies the four-dimensional Euclidean Dirac equation:

$$\left(ip_{\mathrm{E}\mu}\gamma_{\mathrm{E}}^{\mu} + m_n I_4\right) G_{\Lambda}^{(n)}(p_{\mathrm{E}}, y, y') = I_4\,. \tag{6.63}$$

For the gauge boson,

$$G_{A_{\mu,5}}(p_{\mathrm{E}}, y, y') = \sum_n \frac{1}{p_{\mathrm{E}}^2 + m_n^2}\, f_{A_{\mu,5}}^{(n)}(y)\, f_{A_{\mu,5}}^{(n)}(y')\,, \tag{6.64}$$

where the four-dimensional propagator

$$G_{A_{\mu,5}}^{(n)}(p_{\mathrm{E}}, y, y') = \frac{1}{p_{\mathrm{E}}^2 + m_n^2} \tag{6.65}$$

satisfies the four-dimensional Euclidean Klein-Gordon equation:

$$\left(p_{\mathrm{E}}^2 + m_n\right) G_{A_{\mu,5}}^{(n)}(p_{\mathrm{E}}, y, y') = 1\,. \tag{6.66}$$

6.3.2 Broken supersymmetry

Here, we consider the effect of a supersymmetry-breaking sector localized on the IR brane. The gauginos receive a localized mass term that can be parametrized as [cf. (5.8)]

$$S_5 \supset -\int d^5x\,\sqrt{-g}\int d^2\theta\left(\frac{1}{2}\,\xi\,(\lambda_+)^a\,(\lambda_+)_a\,+\mathrm{H.c.}\right)2\delta(y-\pi R)\,. \tag{6.67}$$

This boundary term modifies the Dirac propagator functions for the even gaugino and additionally introduces a Majorana mass mixing. Constructing the Majorana spinor

$$\Lambda_+^{\mathrm{M}} \equiv \Lambda_+ + \Lambda_+^{\mathrm{c}} = \begin{pmatrix} (\lambda_+)_a \\ (\lambda_+^{\dagger})^{\dot{a}} \end{pmatrix}\,, \tag{6.68}$$

the associated propagator takes the form (cf. Ref. [126])

$$G_{\Lambda_+^{\rm M}}(p_{\rm E},y,y') = \begin{pmatrix} G_{\lambda_+\lambda_+}(p_{\rm E},y,y') & G_{\lambda_+\lambda_+^\dagger}(p_{\rm E},y,y') \\ G_{\lambda_+^\dagger\lambda_+}(p_{\rm E},y,y') & G_{\lambda_+^\dagger\lambda_+^\dagger}(p_{\rm E},y,y') \end{pmatrix}$$
$$= \begin{pmatrix} \delta_a{}^c\,\delta G^\times_{\lambda_+}(p_{\rm E},y,y') & p_{{\rm E}\mu}\,\sigma^\mu_{{\rm E}a\dot c}\,G_{\lambda_+}(p_{\rm E},y,y') \\ p_{{\rm E}\mu}\,\overline\sigma^{\mu\dot a c}_{\rm E}\,G_{\lambda_+}(p_{\rm E},y,y') & \delta^{\dot a}{}_{\dot c}\,\delta G^\times_{\lambda_+}(p_{\rm E},y,y') \end{pmatrix}. \tag{6.69}$$

Here,[4]

$$G_{\lambda_+}(p_{\rm E},y,y') = \frac{1}{2}\,(zz')^{5/2}k^4\,S_1^0(x_{\rm UV},x_<) \times \frac{S_1^0(x_>,x_{\rm IR}) + ig_5^2k\,\xi\,T_1(x_>,x_{\rm IR})}{T_0(x_{\rm UV},x_{\rm IR}) + ig_5^2k\,\xi\,S_1^0(x_{\rm UV},x_{\rm IR})}\,, \tag{6.70}$$

which can be decomposed into a supersymmetric piece of the form (6.49) and a supersymmetry-breaking term:

$$G_{\lambda_+} = G^{\rm SUSY}_{\lambda_+} + \delta G_{\lambda_+}\,, \tag{6.71}$$

where

$$\delta G_{\lambda_+}(p_{\rm E},y,y') = -\frac{1}{2}\frac{(zz')^{5/2}k^4}{x_{\rm IR}}\frac{1}{T_0(x_{\rm UV},x_{\rm IR})} \times \frac{ig_5^2k\,\xi\,S_1^0(x_{\rm UV},x)\,S_1^0(x_{\rm UV},x')}{T_0(x_{\rm UV},x_{\rm IR}) + ig_5^2k\,\xi\,S_1^0(x_{\rm UV},x_{\rm IR})}\,. \tag{6.72}$$

The Majorana-mass mixing component function is a purely supersymmetry-breaking effect. It takes the form

$$\delta G^\times_{\lambda_+}(p_{\rm E},y,y') = -\frac{1}{2}\frac{(zz')^{5/2}k^4}{z_{\rm IR}}\frac{i}{S_1^0(x_{\rm UV},x_{\rm IR})} \times \frac{S_1^0(x_{\rm UV},x)\,S_1^0(x_{\rm UV},x')}{T_0(x_{\rm UV},x_{\rm IR}) + ig_5^2k\,\xi\,S_1^0(x_{\rm UV},x_{\rm IR})}\,. \tag{6.73}$$

[4] The propagator corresponds to the *real* part of this expression. We write it in this form for notational simplicity and for ease of comparison with the scalar susy-breaking in the hypermultiplet. Note that below the scale of GUT symmetry breaking, the five-dimensional gauge coupling can be replaced with the four-dimensional coupling as $g_5^2 \to g^2\pi R$.

Note that this propagator function is dimensionless, unlike all the others, which have inverse mass dimension.

Limiting forms

On the UV brane, the diagonal components of the propagator for λ_+ in the presence of supersymmetry breaking take the form

$$G_{\lambda_+}(p_{\rm E},0,0) = \frac{1}{2}\frac{1}{p_{\rm E}}\frac{S_1^0(x_{\rm UV},x_{\rm IR}) + ig_5^2 k\,\xi\, T_1(x_{\rm UV},x_{\rm IR})}{T_0(x_{\rm UV},x_{\rm IR}) + ig_5^2 k\,\xi\, S_1^0(x_{\rm UV},x_{\rm IR})}\,, \tag{6.74}$$

and, on the IR brane,

$$G_{\lambda_+}(p_{\rm E},\pi R,\pi R) = \frac{1}{2}\frac{1}{p_{\rm E}}\,(z_{\rm IR}k)^4\,\frac{S_1^0(x_{\rm UV},x_{\rm IR})}{T_0(x_{\rm UV},x_{\rm IR}) + ig_5^2 k\,\xi\, S_1^0(x_{\rm UV},x_{\rm IR})}\,. \tag{6.75}$$

The brane-to-brane propagator components are

$$G_{\lambda_+}(p_{\rm E},0,\pi R) = \frac{1}{2}\frac{1}{p_{\rm E}}\,\frac{(z_{\rm IR}k)^{5/2}}{x_{\rm IR}}\,\frac{1}{T_0(x_{\rm UV},x_{\rm IR}) + ig_5^2 k\,\xi\, S_1^0(x_{\rm UV},x_{\rm IR})}\,. \tag{6.76}$$

Restricting now to the supersymmetry-breaking parts of the propagator, we find

$$\begin{aligned}\delta G_{\lambda_+}(p_{\rm E},0,0) = -\frac{1}{2}\frac{1}{p_{\rm E}}\frac{1}{x_{\rm UV}x_{\rm IR}}\frac{1}{T_0(x_{\rm UV},x_{\rm IR})} \\ \times \frac{ig_5^2 k\,\xi}{T_0(x_{\rm UV},x_{\rm IR}) + ig_5^2 k\,\xi\, S_1^0(x_{\rm UV},x_{\rm IR})}\,,\end{aligned} \tag{6.77}$$

and

$$\begin{aligned}\delta G^{\times}_{\lambda_+}(p_{\rm E},0,0) = -\frac{1}{2}\frac{1}{x_{\rm UV}x_{\rm IR}}\frac{1}{S_1^0(x_{\rm UV},x_{\rm IR})} \\ \times \frac{i}{T_0(x_{\rm UV},x_{\rm IR}) + ig_5^2 k\,\xi\, S_1^0(x_{\rm UV},x_{\rm IR})}\,,\end{aligned} \tag{6.78}$$

on the UV brane. On the IR brane,

$$\begin{aligned}\delta G_{\lambda_+}(p_{\rm E},\pi R,\pi R) = -\frac{1}{2}\frac{1}{p_{\rm E}}\,(z_{\rm IR}k)^4\,\frac{S_1^0(x_{\rm UV},x_{\rm IR})}{T_0(x_{\rm UV},x_{\rm IR})} \\ \times \frac{ig_5^2 k\,\xi\, S_1^0(x_{\rm UV},x_{\rm IR})}{T_0(x_{\rm UV},x_{\rm IR}) + ig_5^2 k\,\xi\, S_1^0(x_{\rm UV},x_{\rm IR})}\,,\end{aligned} \tag{6.79}$$

and

$$\delta G^{\times}_{\lambda_+}(p_{\rm E}, \pi R, \pi R) = -\frac{1}{2}(z_{\rm IR}k)^4 \, \frac{i\, S^0_1(x_{\rm UV}, x_{\rm IR})}{T_0(x_{\rm UV}, x_{\rm IR}) + i g_5^2 k\, \xi\, S^0_1(x_{\rm UV}, x_{\rm IR})} \,. \tag{6.80}$$

The brane-to-brane forms are

$$\delta G_{\lambda_+}(p_{\rm E}, 0, \pi R) = -\frac{1}{2}\frac{1}{p_{\rm E}}\frac{(z_{\rm IR}k)^{5/2}}{x_{\rm IR}}\frac{1}{T_0(x_{\rm UV}, x_{\rm IR})} \times \frac{i g_5^2 k\, \xi\, S^0_1(x_{\rm UV}, x_{\rm IR})}{T_0(x_{\rm UV}, x_{\rm IR}) + i g_5^2 k\, \xi\, S^0_1(x_{\rm UV}, x_{\rm IR})} \,, \tag{6.81}$$

and

$$\delta G^{\times}_{\lambda_+}(p_{\rm E}, 0, \pi R) = -\frac{1}{2}\frac{(z_{\rm IR}k)^{5/2}}{x_{\rm IR}}\frac{i}{T_0(x_{\rm UV}, x_{\rm IR}) + i g_5^2 k\, \xi\, S^0_1(x_{\rm UV}, x_{\rm IR})} \,. \tag{6.82}$$

7 Radiative Corrections in the Bulk

In this chapter we calculate the radiative corrections to the scalar masses as well as the soft mass parameters in the Higgs sector arising from the five-dimensional bulk in our model when supersymmetry is broken on the IR brane as discussed in Chapter 5. The results for diagonal supersymmetry breaking in the absence of flavor mixing are presented in our earlier work [17].

7.1 Soft Bulk Scalar Masses

Although the sfermions receive soft masses at tree level from their couplings to the supersymmetry-breaking sector on the IR brane, as discussed in Sec. 5.1.3, quantum corrections from the bulk can become significant for UV-localized fields. At one loop in a supersymmetric theory, these corrections arise from the gauginos and through Yukawa and D-term couplings to the other sfermions. Here, we consider the corrections to the soft mass-squared matrices of bulk scalar zero-modes. Corrections for brane-localized scalars in AdS_5 are derived in detail for exact supersymmetry in Ref. [215] and for the case of flat space in Refs. [216–218]. The results are easily extended to the zero modes of bulk scalars.

7.1.1 Gauge-sector corrections

We consider a hypermultiplet containing a Dirac fermion field Ψ, an even complex scalar field Φ, and an odd complex scalar field Φ^c. The gauge interactions between the hypermultiplet and a bulk vector multiplet composed of a gauge field A_M, an $n = 1$ symplectic Majorana spinor Λ_i, and a real scalar Σ generate corrections to the soft mass squared of the zero mode $\Phi^{(0)}$ of the even scalar Φ at one loop. The contributing diagrams are shown in Fig. 7.1 for two cases of left-handed and of right-handed zero modes. Supersymmetry enforces a rather complicated cancellation between these fermionic and bosonic contributions (see Refs. [215, 216] for a discussion). When supersymmetry is broken the cancellation becomes inexact and two resulting corrections to the soft mass squared of the scalar zero-mode can be isolated.

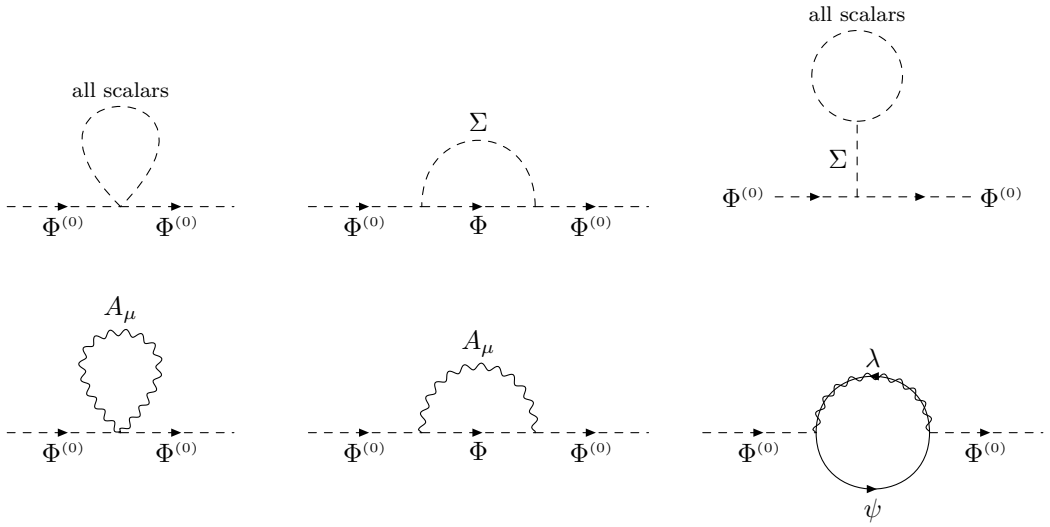

Figure 7.1: One-loop diagrams contributing to the soft mass of a bulk scalar zero-mode through gauge couplings.

Gaugino contributions

The first contribution arises when the even gaugino λ_+ acquires a soft mass, taking the form

$$(\Delta m_0^2)^{\text{1-loop}} \supset 4g^2 C(R_\Phi)\,(\Delta m_0^2)_\lambda^{\text{1-loop}}\,, \tag{7.1}$$

where g is the four-dimensional gauge coupling at the IR-brane scale and $C(R)$ is the quadratic Casimir [in the SU(5) normalization] of the representation R. The gaugino contribution to the scalar zero-mode soft mass squared is a purely supersymmetry-breaking effect and accordingly can be written in terms of a loop integral over the supersymmetry-breaking term of the bulk gaugino propagator (6.72), which is precisely the uncanceled difference between the gauge boson and gaugino loop contributions in the bulk:

$$(\Delta m_0^2)_\lambda^{\text{1-loop}} = \Pi\,, \tag{7.2}$$

where

$$\Pi = -2\,\frac{\pi kR}{k}\int \frac{d^4p}{(2\pi)^4}\int_{-\pi R}^{\pi R} dy\,\left(\tilde{f}_\Phi^{(0)}(y)\right)^2\,\delta\widetilde{G}_{\lambda_+}(p,y,y)\,, \tag{7.3}$$

in the limit in which we neglect the external momentum. Here, $\delta\widetilde{G}_{\lambda_+} = e^{-3A}\delta G_{\lambda_+}$ is the rescaled (conformally flat) propagator. After a Wick rotation, we can transform (7.3) into

an integral over dimensionless variables:

$$8\pi^2 i\Pi = -4\,(\pi kR)^2\,\frac{k_{\rm IR}^4}{k^2}\int dx\int_0^1 du\,x^3\left(\tilde{f}_\Phi^{(0)}(u)\right)^2\delta\widetilde{G}_{\lambda_+}(x,u,u)\,, \tag{7.4}$$

where $x = p_{\rm E} z_{\rm IR}$, $u = y/\pi R$.

The momentum integral in (7.3) is quadratically divergent. This divergence arises because the addition of boundary masses as in Sec. 5 deforms the gaugino Kaluza-Klein wave function profiles, which results in a difference between the effective couplings of the gauge boson and of the gauginos, leading to a parametrically hard breaking of supersymmetry on the IR brane. The extra dimension protects the UV brane and the bulk from the hard breaking, but on the IR brane, where there is no finite distance separating the scalar mode from the source of supersymmetry breaking, quantum corrections to the scalar masses squared are not finite and thus sensitive to the cutoff scale. We note that this divergent behavior is a peculiar feature of warped spaces and does not occur in the flat case, where this type of supersymmetry breaking is globally realized (and hence does not lead to a local distortion of field profiles). Thus, the flat-space breaking is soft, and quantum corrections are finite and independent of the cutoff scale [95, 217, 219, 220].

In the four-dimensional dual theory, this divergence is a result of the breakdown of the perturbativity of the loop expansion as the gauge coupling becomes strong. Because we lose control over the corrections near the compactification scale, we wish to extract a well-defined, finite portion of the correction associated with the long-range physics, which includes the breaking of supersymmetry. The correspondence between the renormalization scale in the four-dimensional dual theory and position in the fifth dimension suggests an appropriate regularization procedure in which we scale the effective IR brane seen by the propagators in the loop with position in the extra dimension [128]: i.e.,

$$\begin{aligned} 8\pi^2 i\Pi \to -4\,(\pi kR)^2\,\frac{k_{\rm IR}^4}{k^2} \\ \times\int_1^{\exp\pi kR} dx\int_0^{1-(\log x)/\pi kR} du\,x^3\left(\tilde{f}_\Phi^{(0)}(u)\right)^2\left[\delta\widetilde{G}_{\lambda_+}(x,u,u)\right]_{z_{\rm IR}\to z}\,. \end{aligned} \tag{7.5}$$

The equivalent procedure in the five-dimensional perspective is to isolate the portion of the loop correction due to the compactification of the theory, absorbing the remaining infinite part into a counterterm [123, 221–223]. Because the presence of the IR brane in AdS_5 explicitly breaks five-dimensional Lorentz symmetry, this finite correction is nonlocal,

associated with a winding around the compact dimension. This purely curvature-dependent contribution to (7.4) can be extracted by employing a cutoff $\Lambda = k_{\text{IR}}$ on the four-dimensional momentum integral:

$$8\pi^2 i\Pi \to -4\,(\pi kR)^2\,\frac{k_{\text{IR}}^4}{k^2}\int_0^1 dx \int_0^1 du\, x^3 \left(\tilde{f}_\Phi^{(0)}(u)\right)^2 \delta\widetilde{G}_{\lambda_+}(x,u,u)\,. \tag{7.6}$$

We have checked that both of these renormalization methods are numerically equivalent, and therefore may be used interchangeably. For calculational convenience, we employ the simple cutoff scheme.

After regularization, the resulting finite part of the correction is positive and can be parametrized in terms of the tree-level gaugino mass as

$$8\pi^2\,(\Delta m_0^2)_\lambda^{\text{1-loop}} = (X_\Phi^{(0)})_\lambda\, M_\lambda^2\,, \tag{7.7}$$

where

$$(X_\Phi^{(0)})_\lambda = \frac{8\pi^2}{M_\lambda^2}\,\text{Re}\, i\Pi \tag{7.8}$$

is a positive parameter that depends on the amount of supersymmetry breaking as well as the localization of the hypermultiplet containing the scalar field (and on the IR-brane scale). We plot $(X_\Phi^{(0)})_\lambda$ in Fig. 7.2 as a function of ξ, the supersymmetry-breaking parameter defined in Sec. 6.3, for three cases of the hypermultiplet localization: the two limits in which the scalar is confined to the UV and IR branes ($c_{L,R} \to \pm\infty$ and $c_{L,R} \to \mp\infty$, respectively) as well as the case $c_{L,R} = \pm\frac{1}{2}$ (flat) in between. For each localization, we give the $\text{U}(1)_Y$ (light), $\text{SU}(2)_L$ (medium), and $\text{SU}(3)_c$ (dark) contributions. The effect of the supersymmetry breaking saturates for $\xi \gg 1$ and the gaugino contribution coefficient approaches a constant value that is independent of the gauge group.

D-term contributions

In models such as ours, where the pattern of supersymmetry breaking is nonuniversal in flavor-space, Fayet-Iliopoulos $\text{U}(1)_Y$ D-term corrections to scalar soft masses squared due to supersymmetry breaking arise. At one loop, these take the form

$$(\Delta m_0^2)^{\text{1-loop}} \supset \frac{3}{5} g_1^2\, Y(\Phi)\, \Delta\mathcal{S}^{\text{1-loop}}\,, \tag{7.9}$$

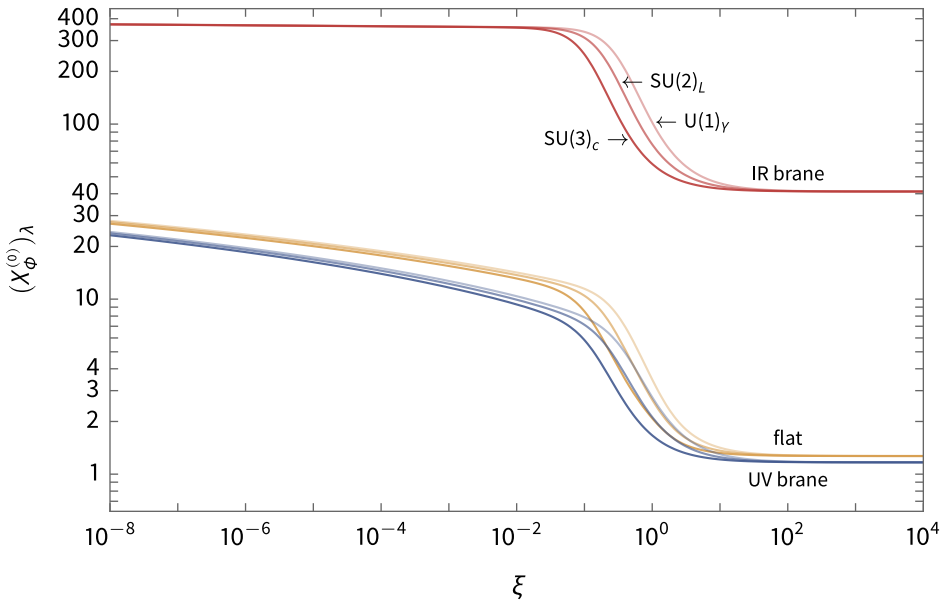

Figure 7.2: Plot of the coefficient $(X_\Phi^{(0)})_\lambda$, which parametrizes the one-loop gaugino corrections to the soft mass squared of a bulk scalar zero mode, for the $\mathrm{U}(1)_Y$, $\mathrm{SU}(2)_L$, and $\mathrm{SU}(3)_c$ gauge groups as a function of the relative amount supersymmetry breaking ξ on the IR brane with $\Lambda_{\mathrm{IR}} = 10^7$ GeV.

where Y is the hypercharge. The contribution to the scalar zero-mode self-energy $\Delta\mathcal{S}^{\text{1-loop}}$ is universal for all scalars that are charged under $\mathrm{U}(1)_Y$. It is also a purely supersymmetry-breaking effect[1] and accordingly can be written in terms of loop integrals over the supersymmetry-breaking terms of the bulk scalar propagators (6.38), which are precisely the uncanceled difference between the various even and odd scalar D-term loop contributions in the bulk:

$$\Delta\mathcal{S}^{\text{1-loop}} = \sum_{\Phi} Y(\Phi)\,(\Delta m_\Phi^2)_D^{\text{1-loop}}$$

[1]Note that the in a five-dimensional theory, D-term contributions can give rise to divergent quantum corrections even when supersymmetry is unbroken. In particular, linear divergences arise both the bulk and on the branes. These can be absorbed in a renormalization of the hypermultiplet bulk masses when regularized with a position-dependent cutoff [224]. Another interesting difference from four-dimensional supersymmetry are the quadratic divergences that arise on the branes unless the $\mathrm{U}(1)_Y$ gauge symmetry is anomaly-free, as required by supersymmetry [215, 224]. (The quadratic divergences depend on the hypercharge and hence vanish when all scalar contributions are included, provided that the sum of the scalar hypercharges is zero, as is true in supersymmetric models.) Neither of these effects are parametrically dependent on supersymmetry breaking, and do not contribute to the D-term contribution we consider here.

$$= \mathrm{tr}\Big[(\boldsymbol{\Delta m}^{\mathbf{2}}_{\tilde{Q}})^{\text{1-loop}}_{D} - 2\,(\boldsymbol{\Delta m}^{\mathbf{2}}_{\tilde{u}})^{\text{1-loop}}_{D} + (\boldsymbol{\Delta m}^{\mathbf{2}}_{\tilde{d}})^{\text{1-loop}}_{D} - (\boldsymbol{\Delta m}^{\mathbf{2}}_{\tilde{L}})^{\text{1-loop}}_{D} + (\boldsymbol{\Delta m}^{\mathbf{2}}_{\tilde{e}})^{\text{1-loop}}_{D}\Big]\,, \tag{7.10}$$

where the sum is over all even bulk scalars. For a family of bulk scalars Φ_i $(i = 1, 2, 3)$,

$$(\boldsymbol{\Delta m}^{\mathbf{2}}_{\Phi})^{\text{1-loop}}_{D} = \boldsymbol{\Pi}_{\Phi} \tag{7.11}$$

where the loop integral is

$$(\Pi_\Phi)_{ij} = -\int \frac{d^4p}{(2\pi)^4} \int_{-\pi R}^{\pi R} dy \left[\delta \widetilde{G}_\Phi(p, y, y)\right]_{ij}. \tag{7.12}$$

Here, $\left[\delta \widetilde{G}_\Phi(p, y, y)\right]_{ij} = e^{-2A}\left[\delta G_\Phi(p, y, y)\right]_{ij}$ are the elements of the rescaled (conformally flat) propagator matrix. After a Wick rotation, we can transform (7.12) into an integral over dimensionless variables:

$$8\pi^2 i\,(\Pi_\Phi)_{ij} = 2\pi kR\,\frac{k_{\text{IR}}^4}{k} \int dx \int_0^1 du\, x^3 \left[\delta \widetilde{G}_\Phi(x, u, u)\right]_{ij}. \tag{7.13}$$

The momentum integral in (7.12) is linearly divergent. After regularizing with the method discussed for the gaugino corrections above, the resulting finite part of the correction is negative and can be parametrized in terms of the scalar mass:

$$\Delta\mathcal{S}^{\text{1-loop}} = -(X^D_{\tilde{Q}})_{ii}\,(m^2_{\tilde{Q}})^{\text{tree}}_{ii} + 2\,(X^D_{\tilde{u}})_{ii}\,(m^2_{\tilde{u}})^{\text{tree}}_{ii} - (X^D_{\tilde{d}})_{ii}\,(m^2_{\tilde{d}})^{\text{tree}}_{ii} + (X^D_{\tilde{L}})_{ii}\,(m^2_{\tilde{L}})^{\text{tree}}_{ii} - (X^D_{\tilde{e}})_{ii}\,(m^2_{\tilde{e}})^{\text{tree}}_{ii}\,, \tag{7.14}$$

where

$$(X^D_\Phi)_{ij} = -\frac{8\pi^2}{(m^2_0)^{\text{tree}}_{ij}}\,\mathrm{Re}\, i\,(\Pi_\Phi)_{ij} \tag{7.15}$$

is positive and depends on the amount of supersymmetry breaking as well as the localizations of the hypermultiplets containing the bulk scalars.

In the limit that the supersymmetry breaking is diagonal in flavor space, the structure of the D-term corrections is also diagonal. That is

$$\boldsymbol{\Pi}_\Phi = \mathrm{diag}\Big(\Pi_{\Phi_1}, \Pi_{\Phi_2}, \Pi_{\Phi_3}\Big) \implies \boldsymbol{X}^D_\Phi = \mathrm{diag}\Big(X^D_{\Phi_1}, X^D_{\Phi_2}, X^D_{\Phi_3}\Big)\,, \tag{7.16}$$

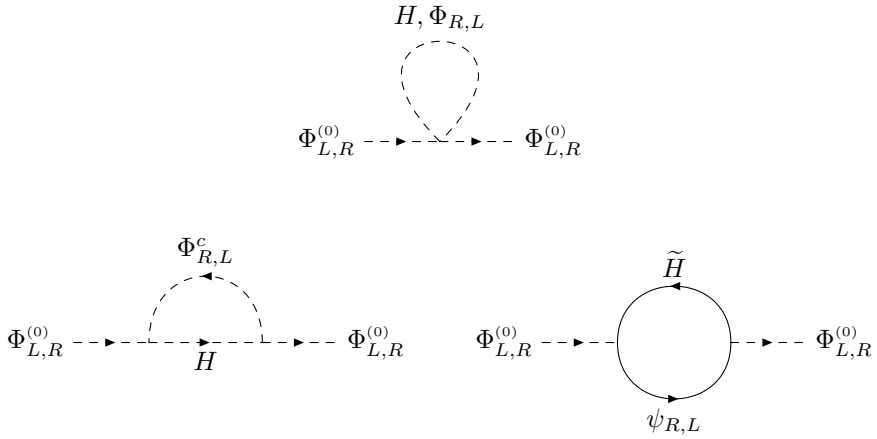

Figure 7.3: One-loop diagrams contributing to the soft mass of a bulk scalar zero-mode through Yukawa couplings.

such that

$$\Delta\mathcal{S}^{\text{1-loop}} = -X^D_{\tilde{Q}_i}\,(m^2_{\tilde{Q}_i})^{\text{tree}} + 2\,X^D_{\tilde{u}_i}\,(m^2_{\tilde{u}_i})^{\text{tree}} - X^D_{\tilde{d}_i}\,(m^2_{\tilde{d}_i})^{\text{tree}} + X^D_{\tilde{L}_i}\,(m^2_{\tilde{L}_i})^{\text{tree}} - X^D_{\tilde{e}_i}\,(m^2_{\tilde{e}_i})^{\text{tree}}\,, \tag{7.17}$$

7.1.2 Yukawa corrections

Here we consider two families of hypermultiplets, one of $\mathrm{SU}(2)_L$ doublets in which the even scalar is left-handed and the other of $\mathrm{SU}(2)_L$ singlets in which it is right-handed. The Yukawa interactions between these families of hypermultiplets and a UV-brane-localized Higgs chiral multiplet composed of a complex scalar Higgs field H and a Weyl fermion higgsino $\widetilde{H}$ generate corrections to the soft mass squared matrices of the zero modes $\Phi^{(0)}_{i\,L,R}$ of the even scalars $\Phi_{i\,L,R}$ at one loop. The contributing diagrams are shown in Fig. 7.3. Supersymmetry enforces a rather complicated cancellation between these fermionic and bosonic contributions (see Refs. [215, 218] for a discussion). When supersymmetry is broken the cancellation becomes inexact and finite contributions to the soft mass squared matrices of the scalar zero modes can be isolated.

At one loop, these corrections take the form:

$$(\Delta m^2_{0,L})^{\text{1-loop}}_{ij} \supset Y^\dagger_{ik}\left[(\Delta m^2_{0,L})^{\text{1-loop}}_{Y}\right]_{iklj} Y_{lj}\,, \tag{7.18a}$$

$$(\Delta m^2_{0,R})^{\text{1-loop}}_{ij} \supset Y_{ik} \left[(\Delta m^2_{0,R})^{\text{1-loop}}_{Y}\right]_{iklj} Y^\dagger_{lj} \,, \tag{7.18b}$$

where $\boldsymbol{Y}$ is the (dimensionless) 5D Yukawa coupling. Using the zero-mode-approximation matching condition (4.36) we can write this in terms of the effective 4D matrix $\boldsymbol{y}$ by absorbing the profile factors into the mass corrections:

$$(\Delta m^2_{0,L})^{\text{1-loop}}_{ij} \supset y^\dagger_{ik} \left[(\Delta m^2_{0,L})^{\text{1-loop}}_{y}\right]_{iklj} y_{lj} \,, \tag{7.19a}$$

$$(\Delta m^2_{0,R})^{\text{1-loop}}_{ij} \supset y_{ik} \left[(\Delta m^2_{0,R})^{\text{1-loop}}_{y}\right]_{iklj} y^\dagger_{lj} \,. \tag{7.19b}$$

The Yukawa contributions to the scalar zero-mode soft mass squared are purely supersymmetry-breaking effects and accordingly can be written in terms of loop integrals over the supersymmetry-breaking term of the bulk scalar propagators (6.38), which are precisely the uncanceled differences between the scalar and fermion loop contributions in the bulk:

$$\left[(\Delta m^2_{0\,L,R})^{\text{1-loop}}_{y}\right]_{ijkl} = (\Pi_{\Phi_{R,L}})_{ijkl} \,, \tag{7.20}$$

where

$$(\Pi_{\Phi_{L,R}})_{ijkl} = \frac{N^{(0)}_{\Phi_{i\,R,L}} N^{(0)}_{\Phi_{l\,R,L}}}{(\mathcal{N}^{(0)}_{L,R})_{ijkl}} \frac{1}{k} \int \frac{d^4p}{(2\pi)^4} \left[\delta G_{\Phi_{L,R}}(p,0,0)\right]_{jk} . \tag{7.21}$$

Here,

$$(\mathcal{N}^{(0)}_{L,R})_{ijkl} \equiv N^{(0)}_{\Psi_{i\,R,L}} N^{(0)}_{\Psi_{j\,L,R}} N^{(0)}_{\Psi_{k\,L,R}} N^{(0)}_{\Psi_{l\,R,L}} \tag{7.22}$$

is a combined normalization factor from the zero-mode-approximation Yukawa matching procedure. Note that when we neglect the backreaction of the supersymmetry-breaking boundary mass terms on the scalar zero-mode profiles,[2]

$$\frac{N^{(0)}_{\Phi_{i\,R,L}} N^{(0)}_{\Phi_{l\,R,L}}}{(\mathcal{N}^{(0)}_{L,R})_{ijkl}} = \frac{1}{N^{(0)}_{\Psi_{j\,L,R}} N^{(0)}_{\Psi_{k\,L,R}}} \equiv \frac{1}{(\mathcal{N}^{(0)}_{L,R})_{jk}} \,, \tag{7.23}$$

and the loop integral takes a simpler form:

$$(\Pi_{\Phi_{L,R}})_{ijkl} \to (\Pi_{\Phi_{L,R}})_{jk} = \frac{1}{(\mathcal{N}^{(0)}_{L,R})_{jk}} \frac{1}{k} \int \frac{d^4p}{(2\pi)^4} \left[\delta G_{\Phi_{L,R}}(p,0,0)\right]_{jk} . \tag{7.24}$$

[2] This is a good approximation, as the deformation of the zero-mode profile only becomes significant when the scalar is highly IR-localized, in which case its Yukawa coupling is necessarily small and its contribution to the radiative corrections subdominant.

After a Wick rotation, we can transform (7.21) into an integral over a dimensionless variable:

$$8\pi^2 i\,(\Pi_{\Phi_{L,R}})_{ijkl} = \frac{N^{(0)}_{\Phi_{i\,R,L}} N^{(0)}_{\Phi_{l\,R,L}}}{(\mathcal{N}^{(0)}_{L,R})_{ijkl}} \frac{k_{\rm IR}^4}{k} \int dx\, x^3 \left[\delta G_{\Phi_{L,R}}(x,0,0)\right]_{jk}. \tag{7.25}$$

Unlike the gauge sector corrections, the momentum integral (7.21) is finite, even when supersymmetry is broken. The resulting correction is negative and can be parametrized in terms of the soft scalar masses as

$$8\pi^2 \left[(\Delta m^2_{0\,L,R})^{\text{1-loop}}_y\right]_{ijkl} = -(X^{(0)}_{\Phi_{L,R}})^y_{ijkl}\,(m^2_{0\,R,L})^{\rm tree}_{jk}, \tag{7.26}$$

where

$$(X^{(0)}_{\Phi_{L,R}})^y_{ijkl} = -\frac{8\pi^2}{(m^2_{0\,R,L})^{\rm tree}_{jk}}\ \mathrm{Re}\, i(\Pi_{\Phi_{R,L}})_{ijkl} \tag{7.27}$$

is positive and depends on the amount of supersymmetry breaking and the localizations of the hypermultiplets.

In the limit that the supersymmetry breaking is diagonal in flavor space and the Yukawa matrices are diagonal in the bulk mass basis, the structure of the Yukawa corrections is also diagonal. In this case, for a single generation,

$$8\pi^2\,(\Delta m^2_{0\,L,R})^{\text{1-loop}}_y = -(X^{(0)}_{\Phi_{L,R}})_y\,(m^2_{0\,R,L})^{\rm tree}, \tag{7.28}$$

with

$$(X^{(0)}_{\Phi_{L,R}})_y = -\frac{8\pi^2}{(m^2_{0\,R,L})^{\rm tree}}\ \mathrm{Re}\, i\Pi_{\Phi_{R,L}}. \tag{7.29}$$

7.2 Soft Higgs Masses

When the Higgs fields are confined to the UV brane, they have no direct couplings to the supersymmetry-breaking sector on the IR brane. The Higgs-sector soft mass terms are therefore zero at tree level and are generated instead at higher loop order by radiative corrections involving bulk fields that transmit the supersymmetry breaking from the IR brane. Here, we consider the one-loop corrections to the soft mass squared for a generic Higgs field completely localized on the UV brane. As for the bulk scalars, these corrections arise from the gauginos and through Yukawa and D-term couplings to the bulk sfermions. Similar one-loop analyses are presented in the four-dimensional Kaluza-Klein formalism for the Higgs sector in unbroken supersymmetry for the case of AdS_5 in Ref. [215] and for flat

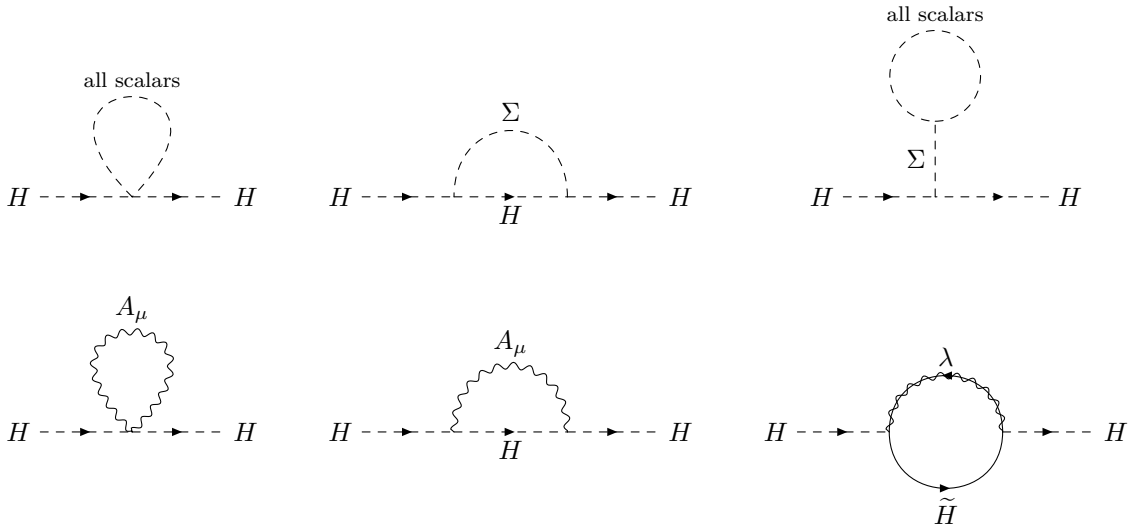

Figure 7.4: One-loop diagrams contributing to the Higgs scalar soft mass through gauge couplings.

space in Refs. [216–218].

7.2.1 Gauge-sector corrections

We consider a chiral multiplet containing a complex scalar Higgs field H and a Weyl fermion higgsino field $\widetilde{H}$ localized on the UV brane. The gauge interactions between the Higgs chiral multiplet and a bulk vector multiplet composed of a gauge field A_M, an $n = 1$ symplectic Majorana spinor Λ_i, and a real scalar Σ generate corrections to the soft mass squared of the Higgs field H at one loop. The contributing diagrams are shown in Fig. 7.4. Supersymmetry enforces a rather complicated cancellation between these fermionic and bosonic contributions (see Refs. [215, 216] for a discussion). When supersymmetry is broken the cancellation becomes inexact and two resulting corrections to the soft mass squared of the scalar zero-mode can be isolated.

Gaugino contribution

The first contribution arises when the even gaugino λ_+ acquires a soft mass, taking the form [216, 217, 220, 225, 226]

$$(\Delta m_H^2)^{\text{1-loop}} \supset 4g^2 C(R_H)\,(\Delta m_H^2)_\lambda^{\text{1-loop}}\,, \tag{7.30}$$

The gaugino contribution to the Higgs soft mass squared is a purely supersymmetry-breaking effect and accordingly can be written in terms of a loop integral over the supersymmetry-breaking term of the bulk gaugino propagator (6.77), which is precisely the uncanceled difference between the gauge boson and gaugino loop contributions in the bulk:

$$(\Delta m_H^2)_\lambda^{\text{1-loop}} = \Pi\,, \tag{7.31}$$

where

$$\Pi = -2\,\frac{\pi k R}{k}\int \frac{d^4p}{(2\pi)^4}\,\delta G_{\lambda_+}(p,0,0)\,, \tag{7.32}$$

in the limit in which we neglect the external momentum. After a Wick rotation, we can transform this into an integral over a dimensionless variable

$$8\pi^2 i\Pi = -2\pi k R\,\frac{k_{\text{IR}}^4}{k}\int dx\, x^3 \delta G_{\lambda_+}(x,0,0)\,. \tag{7.33}$$

We note that this correction (7.30) is a special case of the general bulk scalar soft mass squared correction (7.1), corresponding to the limit in which the scalar is confined to the UV brane.

The momentum integral in (7.32) is finite, unlike the bulk scalar case (7.3), due to the finite separation between the Higgs fields on UV brane and the supersymmetry-breaking sector on the IR brane. The resulting contribution to the Higgs soft masses squared can be parametrized in terms of the gaugino mass as:

$$8\pi^2\,(\Delta m_H^2)_\lambda = (X_H)_\lambda\, M_\lambda^2\,, \tag{7.34}$$

where

$$(X_H)_\lambda = \frac{8\pi^2}{M_\lambda^2}\,\text{Re}\, i\Pi \tag{7.35}$$

depends on the amount of supersymmetry breaking. We plot $(X_H)_\lambda$ in Fig. 7.5 for the $\text{U}(1)_Y$ and $\text{SU}(2)_L$ gauge groups as a function of the relative amount of supersymmetry breaking ξ. This behavior matches the UV-brane limit of the bulk scalar corrections in Fig. 7.2 and reproduces the result in Ref. [226] up to an order-one shift due to a difference in the definition of the supersymmetry-breaking gaugino IR-brane operator and the UV cutoff of the four-dimensional momentum integration.

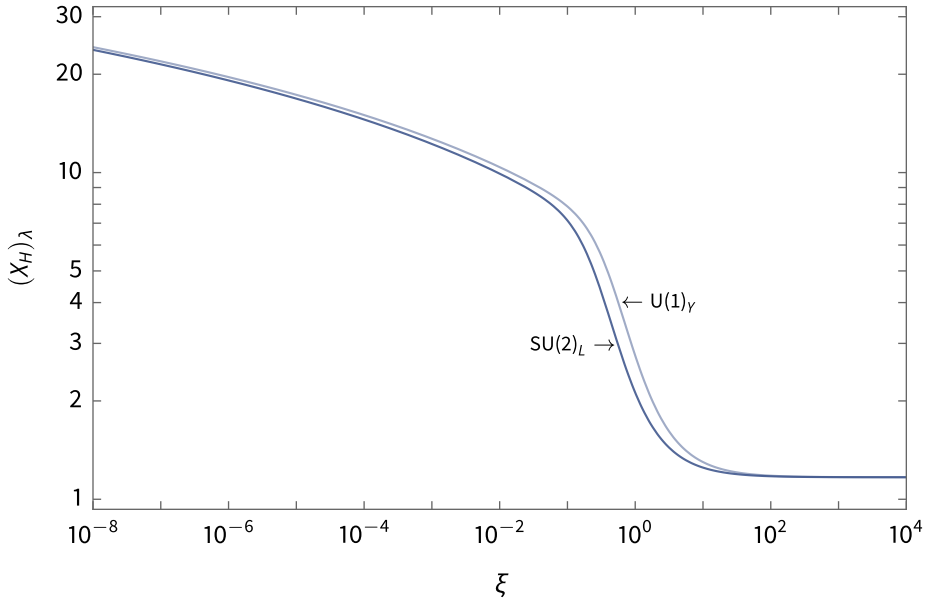

Figure 7.5: Plot of the coefficient $(X_H)_\lambda$, which parametrizes the one-loop gaugino corrections to the soft mass squared of a Higgs field localized on the UV brane, for the $\mathrm{U}(1)_Y$ and $\mathrm{SU}(2)_L$ gauge groups as a function of the relative amount supersymmetry breaking ξ on the IR brane with $\Lambda_{\mathrm{IR}} = 10^7\,\mathrm{GeV}$.

D-term corrections

Because, as discussed above, the D-term corrections to the scalar soft masses squared are independent of the localization of the scalar, the corrections for the Higgs fields on the boundary take the same form as the corrections in the bulk:

$$(\Delta m_H^2)^{\text{1-loop}} \supset -\frac{3}{5} g_1^2\, Y(H)\, \Delta\mathcal{S}^{\text{1-loop}}\,, \tag{7.36}$$

where $\Delta\mathcal{S}^{\text{1-loop}}$ is defined in (7.10).

7.2.2 Yukawa corrections

We again consider a Higgs chiral multiplet composed of a complex scalar Higgs field H and a Weyl fermion higgsino $\widetilde{H}$ localized on the UV brane. The Yukawa interactions between this chiral multiplet and two families of hypermultiplets, one of $\mathrm{SU}(2)_L$ doublets in which the even scalar is left-handed and the other of $\mathrm{SU}(2)_L$ singlets in which it is right-handed, generate corrections to the soft mass squared of the Higgs field H at one loop. The contributing

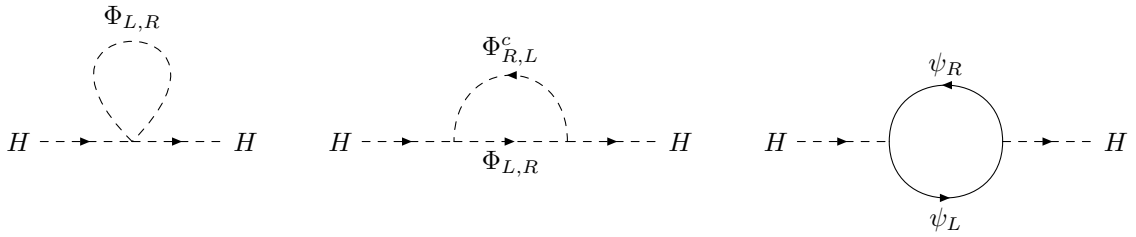

Figure 7.6: One-loop diagrams contributing to the Higgs scalar soft mass through Yukawa couplings.

diagrams are shown in Fig. 7.6. Supersymmetry enforces a rather complicated cancellation between these fermionic and bosonic contributions (see Refs. [215, 218] for a discussion). When supersymmetry is broken the cancellation becomes inexact and finite contributions to the soft mass squared matrices of the Higgs field soft mass can be isolated.

The corrections take the form

$$(\Delta m_H^2)^{\text{1-loop}} \supset \text{tr}\Big[\boldsymbol{Y}(\boldsymbol{\Delta m_H^2})^{\text{1-loop}}_{\Phi_L}\boldsymbol{Y}^\dagger + \boldsymbol{Y}^\dagger(\boldsymbol{\Delta m_H^2})^{\text{1-loop}}_{\Phi_R}\boldsymbol{Y}\Big]\,, \tag{7.37}$$

where $\boldsymbol{Y}$ is the dimensionless 5D Yukawa coupling matrix. Using the zero-mode-approximation matching condition (4.36) we can write this in terms of the 4D matrix $\boldsymbol{y}$ by absorbing the profile factors into the mass corrections:

$$(\Delta m_H^2)^{\text{1-loop}} \supset y_{ij}\left[(\Delta m_H^2)^{\text{1-loop}}_{\Phi_L}\right]_{ijk} y^\dagger_{ki} + y^\dagger_{ij}\left[(\Delta m_H^2)^{\text{1-loop}}_{\Phi_R}\right]_{ijk} y_{ki}\,, \tag{7.38}$$

The Yukawa contributions to the Higgs soft mass squared are purely supersymmetry-breaking effects and accordingly can be written in terms of loop integrals over the supersymmetry-breaking term of the bulk scalar propagators (6.38), which are precisely the uncanceled differences between the scalar and fermion loop contributions in the bulk:

$$\left[(\Delta m_H^2)^{\text{1-loop}}_{\Phi_L}\right]_{ijk} = (\Pi_{\Phi_{L,R}})_{ijk}\,, \tag{7.39}$$

where

$$(\Pi_{\Phi_{L,R}})_{ijk} = \frac{1}{(\mathcal{N}^{(0)}_{L,R})_{ijki}}\frac{1}{k^2}\int\frac{d^4p}{(2\pi)^4}\,p^2\,G_{\psi_{i\,R,L}}(p,0,0)\left[\delta G_{\Phi_{L,R}}(p,0,0)\right]_{jk}\,, \tag{7.40}$$

in the limit in which we neglect the external momentum. Here, $G_{\psi_{i\,R,L}}$ is the fermion propagator function defined in (6.21) and $(\mathcal{N}^{(0)}_{L,R})_{ijkl}$ is defined in (7.22). After a Wick

rotation, we can transform (7.40) into an integral over a dimensionless variable

$$8\pi^2 i\,(\Pi_{\Phi_{L,R}})_{ijk} = \frac{1}{(\mathcal{N}^{(0)}_{L,R})_{ijki}}\frac{k_{\rm IR}^6}{k^2} \times \int dx\, x^5\, G_{\psi_{i\,R,L}}(x,0,0)\left[\delta G_{\Phi_{L,R}}(p,0,0)\right]_{jk}. \tag{7.41}$$

As in the bulk scalar case, the momentum integral (7.40) is finite. The resulting contribution to the Higgs soft masses squared is negative and can be parametrized in terms of the soft masses of the scalar zero modes as

$$8\pi^2\left[(\Delta m_H^2)^{\text{1-loop}}_{\Phi_{L,R}}\right]_{ijkl} = -\left[(X_H)^y_{\Phi_{L,R}}\right]_{ijkl}(m^2_{0\,L,R})^{\rm tree}_{jk}\,, \tag{7.42}$$

where

$$\left[(X_H)^y_{\Phi_{L,R}}\right]_{ijkl} = -\frac{8\pi^2}{(m^2_{0\,L,R})^{\rm tree}_{jk}}\,{\rm Re}\, i\,(\Pi_{\Phi_{L,R}})_{ijkl} \tag{7.43}$$

is positive and depends on the amount of supersymmetry breaking as well as the localizations of the bulk fields.

In the limit that the supersymmetry breaking is diagonal in flavor space and the Yukawa matrices are diagonal in the bulk mass basis, the structure of the Yukawa corrections is also diagonal. In this case, for a single generation,

$$8\pi^2\,(\Delta m_H^2)^{\text{1-loop}}_{\Phi_{L,R}} = -(X_H)^y_{\Phi_{L,R}}(m^2_{0\,L,R})^{\rm tree}\,, \tag{7.44}$$

with

$$(X_H)^y_{\Phi_{L,R}} = -\frac{8\pi^2}{(m^2_{0\,L,R})^{\rm tree}}\,{\rm Re}\, i\Pi_{\Phi_{L,R}}\,. \tag{7.45}$$

7.3 Soft Higgs *b* term

The Higgs soft b term, like the Higgs soft masses squared, is zero at tree level, and so is generated at loop order once supersymmetry is broken. Here we consider the two MSSM Higgs chiral multiplets containing the Higgs scalars H_u and H_d and the higgsino Weyl fermions $\widetilde{H}_u$ and $\widetilde{H}_d$ localized on the UV brane. When supersymmetry is broken, the gauge interactions between the Higgs chiral multiplets and a bulk vector multiplet composed of a gauge field A^a_M, an $n=1$ symplectic Majorana spinor Λ^a_i, and a real scalar Σ^a generate corrections to the Higgs soft b term at one loop. The contributing diagram is shown in

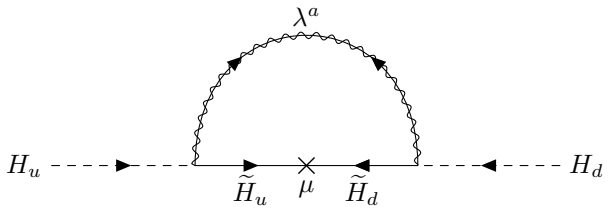

Figure 7.7: One-loop diagram contributing to the Higgs soft b term.

Fig. 7.7. Unlike the previous loop corrections, the one-loop quantum correction to the b term depends explicitly on supersymmetry breaking through the Majorana gaugino mass, and no complementary loop of superpartners is present.

The correction takes the form

$$\Delta b^{\text{1-loop}} = 4g^2\, T^a(R_{H_u})\, T^a(R_{H_d})\, \Delta b_\lambda^{\text{1-loop}}\,, \tag{7.46}$$

where $T^a(R)$ is the generator of the gauge group in representation R. The gaugino correction to the b term is a purely supersymmetry-breaking effect and can be written in terms of a loop integral over the Majorana-mass mixing component of the gaugino propagator (6.78):

$$\Delta b_\lambda^{\text{1-loop}} = \mu\, \Pi\,, \tag{7.47}$$

where

$$\Pi = 2\, \frac{\pi k R}{k} \int \frac{d^4p}{(2\pi)^4} \frac{1}{p^2}\, \delta G^{\times}_{\lambda_+}(p,0,0)\,. \tag{7.48}$$

After a Wick rotation, we can transform this into an integral over a dimensionless variable

$$8\pi^2 i\Pi = 2\pi k R\, \frac{k_{\text{IR}}^2}{k} \int dx\, x\, \delta G^{\times}_{\lambda_+}(x,0,0)\,, \tag{7.49}$$

The resulting contribution is finite and negative, and we parametrize it in terms of the higgsino mass μ and the tree-level gaugino mass as:

$$8\pi^2 \Delta b_\lambda^{\text{1-loop}} = -\mu\, (X_b)_\lambda M_\lambda\,, \tag{7.50}$$

where

$$(X_b)_\lambda = -\frac{8\pi^2}{M_\lambda}\, \text{Re}\, i\Pi \tag{7.51}$$

is positive and depends on the amount of supersymmetry breaking. We plot $(X_b)_\lambda$ in Fig. 7.8

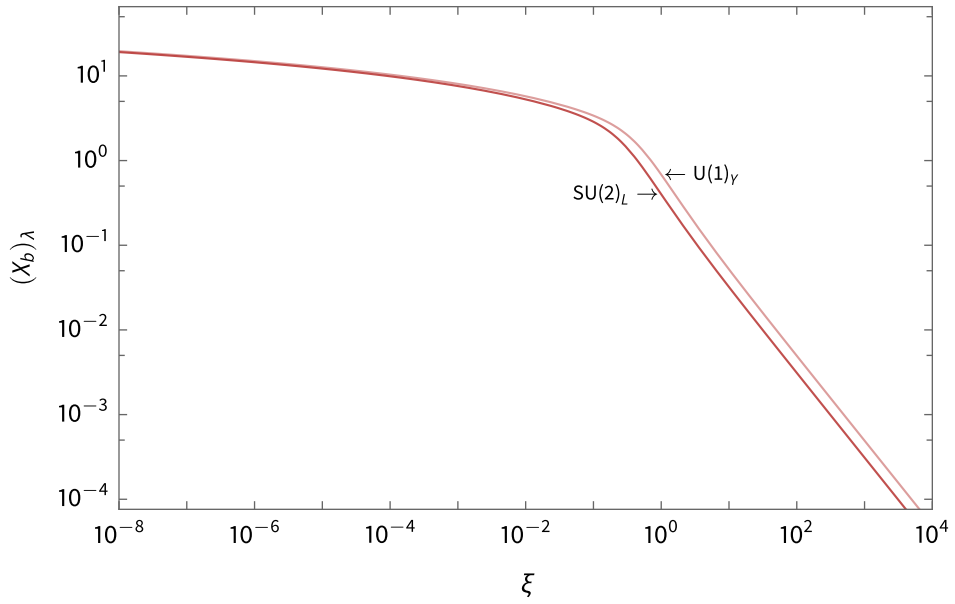

Figure 7.8: Plot of the coefficient $(X_b)_\lambda$, which parametrizes the one-loop gaugino correction to the soft b term for Higgs fields localized on the UV brane, as a function of the relative amount supersymmetry breaking ξ on the IR brane with $\Lambda_{\text{IR}} = 10^7$ GeV.

as a function of ξ for the $\text{U}(1)_Y$ (lighter) and $\text{SU}(2)_L$ (darker) gauge groups. In the limit $\xi \gg 1$, $(X_b)_\lambda$ tends to zero as ξ^{-1}. This is a result of the fact that in the twisted limit the gaugino mass is pure Dirac and the Majorana mixing that generates the soft coupling disappears. When $\xi \ll 1$, the effect of the supersymmetry breaking saturates, and $(X_b)_\lambda$ approaches a constant value.

7.4 Soft Trilinear Scalar Couplings

The trilinear soft scalar a-term interactions, like the Higgs-sector soft terms, vanish at tree level but are generated at loop order once supersymmetry is broken. Here we consider a Higgs chiral multiplet composed of a complex scalar Higgs field H and a Weyl fermion higgsino $\widetilde{H}$ localized on the UV brane and two families of hypermultiplets, one of $\text{SU}(2)_L$ doublets in which the even scalar is left-handed and the other of $\text{SU}(2)_L$ singlets in which it is right-handed. The Yukawa interactions between the Higgs chiral multiplet and the hypermultiplets and the gauge interactions between the matter fields and a bulk vector multiplet composed of a gauge field A_M^a, an $n = 1$ symplectic Majorana spinor Λ_i^a, and a real

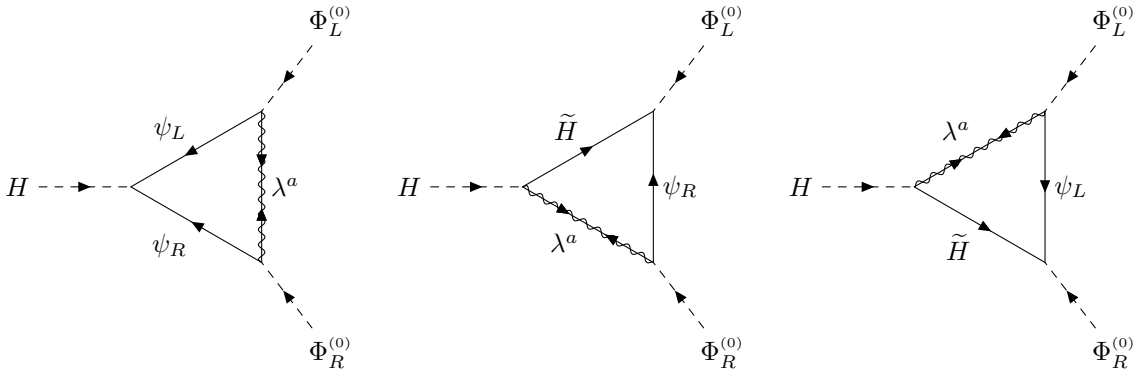

Figure 7.9: One-loop diagrams contributing to the soft a terms.

scalar Σ^a, generate corrections to the soft a terms at one loop. The contributing diagrams are shown in Fig. 7.9. Like the b-term loop corrections, the one-loop quantum corrections to the a terms depend explicitly on supersymmetry breaking through the Majorana gaugino mass, and no complementary loops of superpartners are present. One loop corrections to the a for a brane-localized matter sector coupled to a bulk gauge theory are considered for the case of AdS_5 in Ref. [126] and for flat space in Ref. [217, 220].

The corrections take the form

$$\begin{aligned}(\Delta a)_{ij}^{\text{1-loop}} \supset 4g^2 y_{ij} \Big(& T^a(R_H)\, T^a(R_{\Phi_L}) \left[(\Delta a_\lambda)_{\Phi_L}^{\text{1-loop}}\right]_{ij} \\ & + T^a(R_H)\, T^a(R_{\Phi_R}) \left[(\Delta a_\lambda)_{\Phi_R}^{\text{1-loop}}\right]_{ij} \\ & + T^a(R_{\Phi_L})\, T^a(R_{\Phi_R}) \left[(\Delta a_\lambda)_{\Phi_L\Phi_R}^{\text{1-loop}}\right]_{ij} \Big) . \end{aligned} \tag{7.52}$$

The gaugino corrections to the a terms are purely supersymmetry-breaking effects and can be written in terms of loop integrals over the Majorana-mass mixing component of the gaugino propagator (6.73):

$$(\boldsymbol{\Delta a}_\lambda)_{\Phi_{L,R}}^{\text{1-loop}} = \boldsymbol{\Pi}_{\Phi_{L,R}} , \tag{7.53a}$$

$$(\boldsymbol{\Delta a}_\lambda)_{\Phi_L\Phi_R}^{\text{1-loop}} = \boldsymbol{\Pi}_{\Phi_L\Phi_R} , \tag{7.53b}$$

where

$$(\Pi_{\Phi_L})_{ij} = 2\,\frac{N^{(0)}_{\Phi_{i,R}}}{\mathcal{N}^{(0)}_{ij}}\,\frac{\pi kR}{k^{3/2}}\int\frac{d^4p}{(2\pi)^4}\int_{-\pi R}^{\pi R}dy\,\tilde{f}^{(0)}_{\Phi_{j,L}}(y)\,\widetilde{G}_{\psi_{j,L}}(p,0,y)\,\delta\widetilde{G}^{\times}_{\lambda_+}(p,y,0)\,, \tag{7.54a}$$

$$(\Pi_{\Phi_R})_{ij} = 2\,\frac{N^{(0)}_{\Phi_{j,L}}}{\mathcal{N}^{(0)}_{ij}}\,\frac{\pi kR}{k^{3/2}}\int\frac{d^4p}{(2\pi)^4}\int_{-\pi R}^{\pi R}dy\,\tilde{f}^{(0)}_{\Phi_{i,R}}(y)\,\widetilde{G}_{\psi_{i,R}}(p,0,y)\,\delta\widetilde{G}^{\times}_{\lambda_+}(p,y,0)\,, \tag{7.54b}$$

$$\begin{aligned}(\Pi_{\Phi_L\Phi_R})_{ij} = \frac{2}{\mathcal{N}^{(0)}_{ij}}\,\frac{\pi kR}{k^2}\int\frac{d^4p}{(2\pi)^4}\int_{-\pi R}^{\pi R}dy\int_{-\pi R}^{\pi R}dy'\,p^2\,\tilde{f}^{(0)}_{\Phi_{i,R}}(y)\,\tilde{f}^{(0)}_{\Phi_{j,L}}(y')\\ \times\,\widetilde{G}_{\psi_{i,R}}(p,0,y)\,\delta\widetilde{G}^{\times}_{\lambda_+}(p,y,y')\,\widetilde{G}_{\psi_{j,L}}(p,y',0)\,,\end{aligned} \tag{7.54c}$$

Here,

$$\mathcal{N}^{(0)}_{ij} \equiv N^{(0)}_{\Psi_{i,R}} N^{(0)}_{\Psi_{j,L}} \tag{7.55}$$

is a combined normalization factor and

$$\widetilde{G}_{\psi_{L,R}}(p,y,y') = e^{-(3/2)\,A(y)}e^{-(3/2)\,A(y')}G_{\psi_{L,R}}(p,y,y')\,, \tag{7.56a}$$

$$\delta\widetilde{G}^{\times}_{\lambda_+}(p,y,y') = e^{-(3/2)\,A(y)}e^{-(3/2)\,A(y')}\delta G^{\times}_{\lambda_+}(p,y,y')\,, \tag{7.56b}$$

are rescaled (conformally flat) propagators. After a Wick rotation, we can write (7.54) as integrals over dimensionless variables:

$$\begin{aligned}8\pi^2 i\,(\Pi_{\Phi_L})_{ij} = 4\,\frac{N^{(0)}_{\Phi_{i,R}}}{\mathcal{N}^{(0)}_{ij}}\,(\pi kR)^2\,\frac{k^4_{\rm IR}}{k^{5/2}}\\ \times\int dx\int_0^1 du\,x^3\,\tilde{f}^{(0)}_{\Phi_{j,L}}(u)\,\widetilde{G}_{\psi_{j,L}}(x,0,u)\,\delta\widetilde{G}^{\times}_{\lambda_+}(x,u,0)\,,\end{aligned} \tag{7.57a}$$

$$\begin{aligned}8\pi^2 i\,(\Pi_{\Phi_R})_{ij} = 4\,\frac{N^{(0)}_{\Phi_{j,L}}}{\mathcal{N}^{(0)}_{ij}}\,(\pi kR)^2\,\frac{k^4_{\rm IR}}{k^{5/2}}\\ \times\int dx\int_0^1 du\,x^3\,\tilde{f}^{(0)}_{\Phi_{i,R}}(u)\,\widetilde{G}_{\psi_{i,R}}(x,0,u)\,\delta\widetilde{G}^{\times}_{\lambda_+}(x,u,0)\,,\end{aligned} \tag{7.57b}$$

$$8\pi^2 i\,(\Pi_{\Phi_L\Phi_R})_{ij} = 8\,\frac{1}{\mathcal{N}^{(0)}_{ij}}\,(\pi kR)^3\,\frac{k_{\text{IR}}^6}{k^4} \tag{7.57c}$$
$$\times \int dx \int_0^1 du \int_0^1 du'\, x^5\, \tilde{f}^{(0)}_{\Phi_{i,R}}(u)\, \tilde{f}^{(0)}_{\Phi_{j,L}}(u')$$
$$\times\, \widetilde{G}_{\psi_{i,R}}(x,0,x)\, \delta\widetilde{G}^{\times}_{\lambda_+}(x,u,u')\, \widetilde{G}_{\psi_{j,L}}(x,u',0)\,,$$

The loop integrals (7.54) are finite, despite their extension into the bulk. The resulting correction is negative and can be parametrized in terms of the gaugino mass as

$$(\boldsymbol{\Delta a}_\lambda)^{\text{1-loop}}_{\Phi_{L,R}} = -(\boldsymbol{X}_a)^\lambda_{\Phi_{L,R}}\, M_\lambda\,, \tag{7.58a}$$

$$(\boldsymbol{\Delta a}_\lambda)^{\text{1-loop}}_{\Phi_L\Phi_R} = -(\boldsymbol{X}_a)^\lambda_{\Phi_L\Phi_R}\, M_\lambda\,, \tag{7.58b}$$

where

$$(\boldsymbol{X}_a)^\lambda_{\Phi_{L,R}} = -\frac{8\pi^2}{M_\lambda}\,\text{Re}\, i\,\boldsymbol{\Pi}_{\Phi_{L,R}}\,, \tag{7.59a}$$

$$(\boldsymbol{X}_a)^\lambda_{\Phi_L\Phi_R} = -\frac{8\pi^2}{M_\lambda}\,\text{Re}\, i\,\boldsymbol{\Pi}_{\Phi_L\Phi_R}\,, \tag{7.59b}$$

are positive and depend on the amount of supersymmetry breaking and the localizations of the hypermultiplets.

In the limit that the Yukawa matrices are diagonal in the bulk mass basis, the structure of the a-term corrections is also diagonal. That is,

$$\boldsymbol{\Pi}_{\Phi_{L,R}} = \text{diag}\Big(\Pi_{\Phi_{L,R}1}, \Pi_{\Phi_{L,R}2}, \Pi_{\Phi_{L,R}3}\Big)\,, \tag{7.60a}$$

$$\boldsymbol{\Pi}_{\Phi_L\Phi_R} = \text{diag}\Big(\Pi_{\Phi_{L,1}\Phi_{R,1}}, \Pi_{\Phi_{L,2}\Phi_{R,2}}, \Pi_{\Phi_{L,3}\Phi_{R,3}}\Big) \tag{7.60b}$$

such that

$$(\boldsymbol{X}_a)^\lambda_{\Phi_{L,R}} = \text{diag}\Big[(X_a)^\lambda_{\Phi_{L,R}1}, (X_a)^\lambda_{\Phi_{L,R}2}, (X_a)^\lambda_{\Phi_{L,R}3}\Big]\,, \tag{7.61a}$$

$$(\boldsymbol{X}_a)^\lambda_{\Phi_L\Phi_R} = \text{diag}\Big[(X_a)^\lambda_{\Phi_{L,1}\Phi_{R,1}}, (X_a)^\lambda_{\Phi_{L,2}\Phi_{R,2}}, (X_a)^\lambda_{\Phi_{L,3}\Phi_{R,3}}\Big] \tag{7.61b}$$

8 Phenomenology and Parameter Space

As we have seen in our discussions of flavor physics in Chapter 4 and of supersymmetry breaking in Chapter 5, the parameter space available for our partially composite supersymmetric model is in general quite large. The overall mass scale of our sparticle spectrum is jointly determined by Λ_{IR}, the scale of the IR brane, and $\sqrt{F}$, the scale of supersymmetry breaking. As we discuss in Sec. 5.3, we do not have the usual freedom in $\tan\beta$ and the sign of μ, which are in this case determined by electroweak symmetry breaking. In addition to these universal parameters, our model features nonuniversal IR-scale boundary conditions for the sfermion soft masses, which we specify in a flavor-dependent way by choosing field localizations to explain the standard model fermion mass spectrum, as described in Chapter 4. The flavor solution also determines the full set of Yukawa matrices at the IR-brane scale. In this chapter we discuss various phenomenological and theoretical constraints that impose limits on the set of model parameters and give a characterization of the resulting parameter space.

8.1 Phenomenological and Theoretical Considerations

Here, we consider several phenomenological and theoretical desiderata that constrain our model.

8.1.1 Gravitino dark matter

Because the gravitino mass is Planck-scale-suppressed, it is the lightest supersymmetric particle throughout our parameter space. In the absence of R-parity violation, the LSP is absolutely stable, and as such, the gravitino makes an attractive dark matter candidate. However, the stability of a gravitino LSP can lead to cosmological problems, as the thermal gravitino mass density arising from freeze-out is sufficient to overclose the universe unless the gravitino is very light [$\mathcal{O}(100)\,\text{GeV}$] [227, 228]. In this case, observations of the matter power spectrum at small cosmological scales limit the free-streaming length of the gravitino, further requiring $m_{3/2} < 4.7\,\text{eV}$ in order for the gravitino to be adequately cold [229], and gravitinos in this scenario cannot therefore account for all of the observed dark matter density.

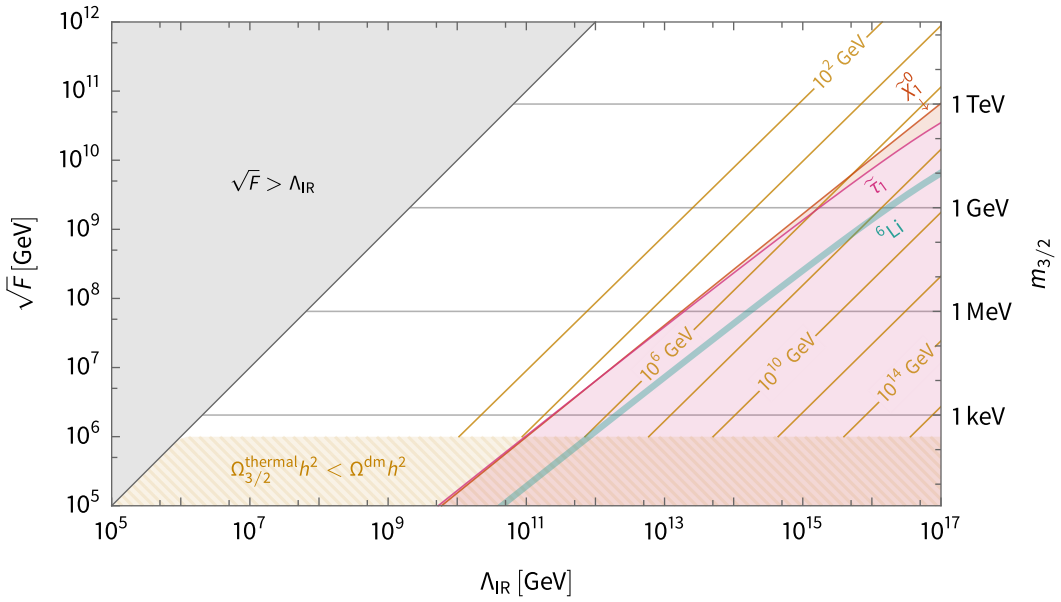

Figure 8.1: Plot of the estimated gravitino dark matter constraints on the parameter space of our model when the supersymmetry-breaking spurion is a singlet, such that the gaugino mass is given by (5.9).

Throughout the relevant parameter space of our model, the gravitino is sufficiently heavy that we require inflation to dilute the initial thermal population [230] and must restrict the reheating temperature so that the gravitino does not subsequently come back into thermal equilibrium. In this case, structure-formation constraints are weaker, requiring $m_{3/2} \gtrsim \mathcal{O}(1)\,\mathrm{keV}$ for generic warm dark matter candidates [231–233], in which case the gravitino may be the dominant component of dark matter. In this scenario, gravitinos may still be produced from the scattering of particles in thermal equilibrium with the plasma. The largest contribution arises from gluinos, such that the thermal gravitino density takes the form

$$\Omega_{3/2}^{\mathrm{thermal}} h^2 \sim 0.3 \left(\frac{100\,\mathrm{GeV}}{m_{3/2}}\right) \left(\frac{m_{\tilde{g}}}{1\,\mathrm{TeV}}\right)^2 \left(\frac{T_{\mathrm{R}}}{10^{10}\,\mathrm{GeV}}\right) . \tag{8.1}$$

For $m_{3/2} \lesssim 1\,\mathrm{keV}$, thermal scattering production of gravitinos cannot supply all of the observed dark matter density unless T_{R} is high enough to bring the gravitino into thermal equilibrium.

Gravitinos are also produced nonthermally, via decays of the next-to-lightest supersymmetric particle, which in our model is typically either a (binolike or higgsinolike) neutralino or a (mainly right-handed) stau. In both cases, the NLSP is sufficiently long-lived throughout

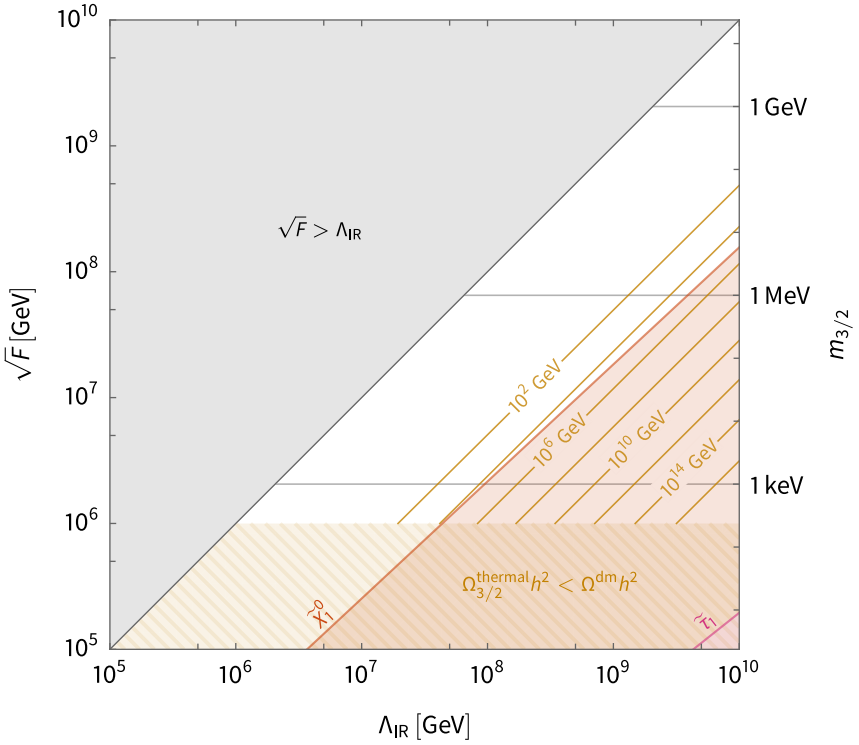

Figure 8.2: Plot of the estimated gravitino dark matter constraints on the parameter space of our model when the supersymmetry-breaking spurion is not a singlet, such that the gaugino mass is given by (5.11).

our parameter space to decay after freeze-out, such that the resulting nonthermal gravitino population takes the form (this is the superWIMP scenario [234]):

$$\Omega_{3/2}^{\text{nonthermal}} h^2 = \frac{m_{3/2}}{m_{\text{NLSP}}} \Omega_{\text{NLSP}} h^2 \,. \tag{8.2}$$

The initial NLSP population that contributes to $\Omega_{\text{NLSP}} h^2$ is moderated by T_{R}. In particular, if the reheating temperature is low enough that the NLSP never comes into thermal equilibrium after inflation ($T_{\text{R}} \lesssim m_{\text{NLSP}}/20$), the initial NLSP population is Boltzmann-suppressed.

The observed dark matter abundance ($\Omega_{\text{dm}} h^2 = 0.1186 \pm 0.0020$ [20]) thus places an upper limit on the reheating temperature. We show an estimate of these limits in the space of $(\Lambda_{\text{IR}}, \sqrt{F})$ in Figs. 8.1 and 8.2. In each case, the contours give the reheating temperature necessary for the thermal gravitino relic density (8.1) to provide the dominant component of dark matter. If nonthermal production is significant, the reheating temperature must

be lowered to suppress the contribution from thermal production. In the hatched regions, the thermal relic density is insufficient to provide all of the dark matter, and some level of nonthermal production is required to obtain the observed dark matter density.

Further parameter space constraints arise from big bang nucleosynthesis (BBN), which strongly limits the energy density of the NLSP if it is long-lived enough to decay to the gravitino during or after the formation of the light elements. To avoid altering the successful predictions of the standard BBN scenario, decays to the gravitino must be prompt, limiting the lifetime of the NLSP to $\tau_{\mathrm{NLSP}} < \mathcal{O}(0.1\text{–}100)\,\mathrm{s}$, or, for $m_{3/2} \ll m_{\mathrm{NLSP}}$,

$$m_{\mathrm{NLSP}} > \mathcal{O}(1\text{–}4)\,\mathrm{TeV}\left(\frac{m_{3/2}}{10\,\mathrm{GeV}}\right)^{2/5}, \tag{8.3}$$

as a conservative estimate. This condition places constraints in the space of Λ_{IR} and $\sqrt{F}$. We show the regions where $\tau_{\mathrm{NLSP}} < 0.1\,\mathrm{s}$ in the neutralino and stau cases in Figs. 8.1 and 8.2. Evading these limits restricts the reheating temperature for our model to the range $T_{\mathrm{R}} \sim \mathcal{O}(10^2\text{–}10^6)\,\mathrm{GeV}$, necessitating an alternative to thermal leptogenesis to generate the baryon asymmetry.

If the NLSP is the stau and is sufficiently stable to survive into BBN, the formation of bound states with nuclei can catalyze the production of light elements [235]. In particular, if $10^3\,\mathrm{s} \lesssim \tau_{\tilde{\tau}_1} \lesssim 5 \times 10^3\,\mathrm{s}$, the catalytic enhancement for ^{6}Li can solve the lithium problem in the standard BBN scenario [236]. We show an estimate of the region in which the stau lifetime falls within these limits in Fig. 8.1, although we note that this solution to the lithium problem is ruled out for our model as the entirety of the catalytic region is excluded by current LHC limits (see Fig. 8.6). In the nonsinglet spurion case, the stau is not sufficiently long-lived to survive into BBN anywhere in the relevant parameter space.

8.1.2 The supersymmetric flavor problem

The additional couplings and degrees of freedom introduced in supersymmetry can generate flavor-changing neutral currents and CP violation at levels above current experimental limits. This problem can be alleviated if the sfermions of the first and second generations are heavy, $\mathcal{O}(100)\,\mathrm{TeV}$, or even heavier, a solution that has gained popularity in the absence of any low-energy experimental signatures of supersymmetry.[1] Such a solution is a natural and elegant choice in our model, as the inverted hierarchy in the sfermion soft mass spectrum naturally separates the scale of the first two generations from that of the third, which can

[1] In the language of Sec. 2.2, this is the *irrelevancy* solution.

remain light enough to explain the Higgs mass and offer the possibility of experimental detection.

Thus, to ameliorate the flavor problem, we restrict the masses of the first- and second-generation sfermions to be at least 100 TeV. As a constraint, this condition places an upper limit on the degree of UV-localization of the first- and second-generation hypermultiplet fields (this corresponds directly to a limit on the associated localization parameter). This is a further limit on the hypermultiplet localizations beyond the structure necessary to explain the standard model fermion mass spectrum. In Figs. 8.6 and 8.7, we show an estimate of the region in the space of $(\Lambda_{\text{IR}}, \sqrt{F})$ where this limit is incompatible with the a mass solution for at least one standard model fermion field (the strictest constraint typically comes from the muon, the heaviest of the first- and second-generation fermions).

It is important to note that this constraint condition is conservative, because, as noted in Sec. 5.1.3, the localization structure imposed on the matter hypermultiplets in order to explain the standard model fermion mass hierarchy can lead to some suppression of the offdiagonal elements of the sfermion soft mass matrices.[2] (Essentially, the sfermion soft mass matrices in our model have some flavor structure that may help to ameliorate the supersymmetric flavor problem, which bears some similarity with alignment-type solutions.) In addition, the soft a terms which can also source FCNCs and CP violation, are naturally suppressed in our model, as they are generated only at loop level.

8.1.3 Direct detection limits

In the MSSM, the tree-level mass of the neutral scalar Higgs boson is bounded from above by $m_h^{\text{tree}} < m_Z$. Radiative corrections, the largest arising from top and stop loops, can raise m_h considerably, and accordingly, the observed value of $(125.18 \pm 0.16)\,\text{GeV}$ [20–22] offers an important constraint on the sparticle spectrum, particularly on the masses of the stops. In the MSSM, the observed Higgs mass constrains the general stop mass scale $\sqrt{m_{\tilde{t}_1} m_{\tilde{t}_2}}$ and is broadly compatible with stop masses ranging from $\mathcal{O}(1)$ TeV for $\tan\beta \sim 50$ to $\mathcal{O}(100)$ TeV for $\tan\beta \sim 3$ [85]. In our model, the stop masses depend critically (at least $\mathcal{O}(1)$) on the localizations of the sfermion hypermultiplets, and hence the Higgs mass principally induces constraints on the localization parameters of the theory. The precise calculation of the Higgs mass requires a complete numerical analysis (see Sec. 9.1.2). To obtain a conservative evaluation of the constraint induced by the Higgs mass on our model we can exclude the region where the stop masses are always greater than 100 TeV. We show an estimate of this

[2] This is true at tree level, and is only improved at one loop by the addition of negative Yukawa contributions.

region in the space of $(\Lambda_{\rm IR}, \sqrt{F})$ in Figs. 8.6 and 8.7.

Further limits on sparticle masses are set by experiments searching for direct sparticle production at colliders. In the context of our model, the strictest of these constraints arise from the exclusion limits on the masses of the gluino and the squarks, which must be heavier than $\mathcal{O}(1)$ TeV when the LSP is the gravitino [237–240].[3] Qualitatively, these limits place an effective lower bound on the soft mass scale of our model, restricting the ratio $\sqrt{F}/\Lambda_{\rm IR}$. We show an estimate of the excluded region in Figs. 8.6 and 8.7.

8.1.4 Gauge coupling unification

Gauge coupling unification is a generic feature of the minimal supersymmetric standard model. The renormalization of gauge couplings depends on the number of degrees of freedom present in the theory at a given energy scale; in the MSSM, unification is most sensitive to the higgsino mass μ as well as the ratio of the wino mass to the gluino mass [241], and it can be spoiled if the magnitude of μ is larger than a few hundred TeV [86]. As discussed in Sec. 5.3, μ is determined as necessary to achieve electroweak symmetry breaking. Generically, this implies that the scale of μ is of the same order of magnitude as the soft masses in the Higgs sector, i.e., $|\mu|^2 \sim |b| \sim |m_{H_u}^2| \sim |m_{H_d}^2|$. Because the Higgs soft masses are generated radiatively (and therefore characteristically of the scale of the gaugino masses) a first-order estimate of this constraint is $|\mu| \sim M_2 \lesssim 100\,\text{TeV}$. A more precise constraint can be obtained by solving the tree-level EWSB equations (5.30). We show an estimate of the excluded region in the space of $(\Lambda_{\rm IR}, \sqrt{F})$ where $|\mu| \gtrsim 100\,\text{TeV}$ in Figs. 8.6 and 8.7.

Note that when $\Lambda_{\rm IR} \ll m_{\rm GUT} \sim 10^{16}\,\text{GeV}$, we are implicitly assuming that the gauge boson Kaluza-Klein states form complete SU(5) multiplets so that there is a universal shift in the running of the gauge couplings (see Sec. 3.2.2). In the warped extra dimension this can be modeled by considering the full SU(5) gauge symmetry in the bulk, although there are no Kaluza-Klein states for the UV-localized higgsino. For simplicity, we do not consider the full SU(5) extension here, because it does not affect the details of our low-energy spectrum.[4]

[3] These limits are weakly model-dependent: see the review [20].

[4] We note that in a theory with IR-localized hypermultiplets, higher-dimension operators may only be suppressed by the IR-brane scale, which, in the context of grand unification, can lead to proton decay constraints [94]. These may be addressed by the introduction of an additional global symmetry in the bulk, such as a $\text{U}(1)_B$ baryon number symmetry as in Refs. [242, 243], or by an orbifold GUT scenario [124].

8.1.5 Minimal supersymmetric particle content

In the construction of our model, we are motivated to explain the observed Higgs mass using only the minimal supersymmetric particle content at low energy. While the orbifold compactification allows us to recover this particle content as the zero modes of the five-dimensional)$\mathcal{N} = 1$ supersymmetric theory, the essentially Dirac nature of fermions in five dimensions is a nontrivial feature of the model and can have phenomenological implications when the scale of four-dimensional $\mathcal{N} = 1$ supersymmetry breaking on the IR brane, $\sqrt{F}$, approaches the local compactification scale, Λ_{IR}. In this case, the backreaction of the supersymmetry-breaking boundary masses on the wave function profiles of the gaugino and sfermion fields cannot be neglected. In particular for the gauginos, the effect of larger $\sqrt{F}/\Lambda_{\text{IR}}$ is to increase the zero-mode mass, but at the same time to decrease the magnitude of the mass of the next-to-lightest KK mode, $m_\lambda^{(1)}$. This behavior smoothly approaches the twisted limit ($\sqrt{F}/\Lambda_{\text{IR}} \gg 1$), where the magnitudes of the masses of the lowest two gaugino KK modes meet at a common value and the two states form a Dirac spinor. To illustrate this, we plot in Fig. 8.3 the masses of the first two Kaluza-Klein states for λ_1 as a function of the generic boundary mass ξ [as in (5.15)], which parametrizes the amount of supersymmetry breaking. For $\sqrt{F}/\Lambda_{\text{IR}} \lesssim 1$, the gaugino mass is only approximately Dirac, but the first KK mode is light enough that it must be included in the spectrum. While the presence of such modes in the theory at low energy can be helpful to achieve a more natural model, we leave the exploration of this region of parameter space for the future. Under this criterion, we exclude the region in which $m_{\lambda_1}^{(1)} < ke^{-\pi kR}$, shown in Figs. 8.6 and 8.7.

8.1.6 Charge- and color-breaking minima

One of the primary features of our model is the presence of significant hierarchies in the soft mass parameters—both within the sfermion sector and between the heavier sfermions and the gauginos—resulting from the localizations imposed on the hypermultiplets in order to explain the standard model fermion mass spectrum. Although such hierarchies have desirable phenomenological features, they can also be the source of considerable constraints in the renormalization of the spectrum, as radiative corrections from heavier scalars may be large enough compared to the lighter scalar mass scale to destabilize the running masses. While, this may be favorable in the Higgs sector for electroweak symmetry breaking, for the sfermions it results in phenomenologically unacceptable charge- and color-breaking minima. We discuss three possible sources of large negative contributions to the scalar soft masses.

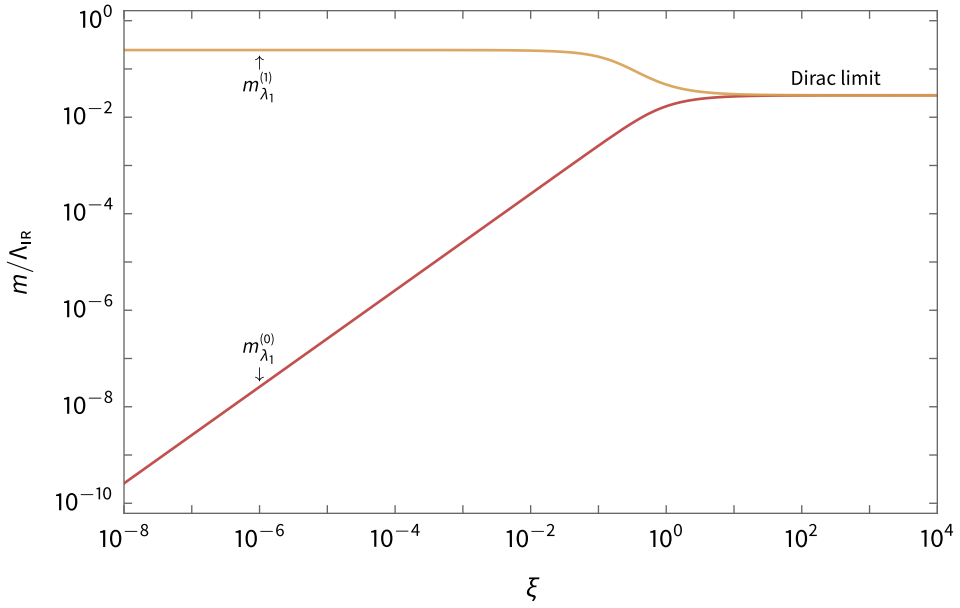

Figure 8.3: Plot of the masses of the first two Kaluza-Klein states for λ_1 as a function of the generic boundary mass ξ.

1. Bulk *D*-term corrections

In our model, large negative radiative corrections to the scalars can arise both in the five-dimensional bulk theory and in the effective four-dimensional MSSM below the scale of compactification. As discussed in Secs. 5.2.1 and 5.2.2, we calculate the bulk contributions as threshold corrections to the scalar soft masses squared at the IR-brane scale. Due to the flavor-dependent localization structure that explains the Yukawa coupling mass hierarchy, the one-loop D-term trace $\Delta\mathcal{S}^{\text{1-loop}}$ defined in (7.10) is generically nonzero.[5] If the spectrum also contains sufficiently IR-localized scalars, the bulk D-term corrections (7.9) may provide the dominant radiative contributions to the scalar masses. The sign of the contribution may be positive or negative, depending both on the sign of $\Delta\mathcal{S}^{\text{1-loop}}$, which depends on the hypercharges of the most IR-localized scalars in the theory, and on the hypercharge of the scalar receiving the correction. In order to avoid negative sfermion soft masses squared at the IR-brane scale in this case, the localizations of the matter hypermultiplets must be correlated. The corresponding restrictions on the allowed ranges for the localization parameters

[5] The trace $\Delta\mathcal{S}^{\text{1-loop}}$ can, of course, be tuned to zero, but this requires some additional intergenerational or interfamilial correlation.

have a distinctive structure that depends on hypercharge. In particular, an upper limit arises on the degree of UV-localization for sfermions with hypercharge of the opposite sign as the sign of $\Delta\mathcal{S}^{\text{1-loop}}$, which corresponds directly to limits on the hypermultiplet localization parameters.

2. Bulk Yukawa corrections

Scalars in our theory also receive negative Yukawa corrections of the form (7.19) from the bulk. As a result of the hypermultiplet localization structure necessary to explain the Yukawa coupling hierarchies, the magnitude of the Yukawa contribution to a left-handed (right-handed) field grows as that field becomes more UV-localized (see Figs. 5.1 and 5.2). These corrections can become large, particularly for the third-generation fields, such that upper limits on the degree of UV localization must be imposed in order to avoid any tachyonic masses. In some cases, the combined D-term and Yukawa limits (note that these are additive) for one or more of the third-generation fields may exclude all solutions compatible with the standard model fermion mass spectrum.

3. MSSM running

Further contributions from heavy scalars arise in the MSSM running below the IR-brane scale. At the one-loop level, the β function of each scalar soft mass matrix $\boldsymbol{m}_\phi^2$ includes a contribution from the tree-level Fayet-Iliopoulos (FI) D-term for weak hypercharge [77, 79]

$$16\pi^2\,(\beta_{m_\phi^2})_{ij}^{\text{1-loop}} \supset \frac{6}{5} g_1^2\, Y(\phi)\, \mathcal{S}\, \delta_{ij}\,, \tag{8.4}$$

where $\mathcal{S}$ is the trace

$$\mathcal{S} \equiv \sum_\phi Y(\phi)\, m_\phi^2 = m_{H_u}^2 - m_{H_d}^2 + \mathrm{Tr}\Big(\boldsymbol{m}_{\tilde{Q}}^{\boldsymbol{2}} - 2\,\boldsymbol{m}_{\tilde{u}}^{\boldsymbol{2}} + \boldsymbol{m}_{\tilde{d}}^{\boldsymbol{2}} - \boldsymbol{m}_{\tilde{L}}^{\boldsymbol{2}} + \boldsymbol{m}_{\tilde{e}}^{\boldsymbol{2}}\Big)\,. \tag{8.5}$$

and Y is the hypercharge.

The scalar soft mass matrices also receive negative contributions from scalars at the two-loop level. In the MSSM, the dominant contributions take the form

$$(16\pi^2)^2\,(\beta_{m_\phi^2})_{ij}^{\text{2-loop}} \supset 4\sum_a g_a^4\, C_a(R_\phi)\, \sigma_a\, \delta_{ij}\,, \tag{8.6}$$

where

$$\sigma_1 = \frac{1}{5}\left[3m_{H_u}^2 + 3m_{H_d}^2 + \mathrm{Tr}\Big(\boldsymbol{m}_{\tilde{Q}}^{\boldsymbol{2}} + 8\,\boldsymbol{m}_{\tilde{u}}^{\boldsymbol{2}} + 2\,\boldsymbol{m}_{\tilde{d}}^{\boldsymbol{2}} + 3\,\boldsymbol{m}_{\tilde{L}}^{\boldsymbol{2}} + 6\,\boldsymbol{m}_{\tilde{e}}^{\boldsymbol{2}}\Big)\right], \tag{8.7a}$$

$$\sigma_2 = m_{H_u}^2 + m_{H_d}^2 + \mathrm{Tr}\Big(3\,\boldsymbol{m}_{\tilde{Q}}^{\boldsymbol{2}} + \boldsymbol{m}_{\tilde{L}}^{\boldsymbol{2}}\Big), \tag{8.7b}$$

$$\sigma_3 = \mathrm{Tr}\Big(2\,\boldsymbol{m}_{\tilde{Q}}^{\boldsymbol{2}} + \boldsymbol{m}_{\tilde{u}}^{\boldsymbol{2}} + \boldsymbol{m}_{\tilde{d}}^{\boldsymbol{2}}\Big), \tag{8.7c}$$

and $C^a(R)$ is the quadratic Casimir [in the SU(5) normalization] of the representation R. These terms are loop-suppressed compared to (8.4) but cannot be reduced by tuning the scalar masses to obtain cancellations between the various masses as can be done for the one-loop contribution.[6]

In the context of the supersymmetric flavor problem and high-scale supersymmetry breaking it was noted in Ref. [81] that the two-loop contributions from heavy scalars provide considerable tachyonic constraints on the allowable hierarchy among the scalar soft mass parameters unless the effect can be balanced by positive contributions from the gauginos. This analysis assumed a common mass for the heavy scalars. When this assumption is lifted, the presence of nonuniversality among the soft scalar masses generically induces a nonzero value for the trace $\mathcal{S}$. Like the bulk D-term contributions, the sign of the MSSM D-term contributions depend on the hypercharge of the scalar receiving the correction. The contributions to scalars with hypercharge of sign opposite to that of the trace $\mathcal{S}$ are positive, and consequently may ameliorate the effect of the negative two-loop contributions. This comes, however, at the cost of additional negative contributions for scalars with hypercharge of the same sign as that of $\mathcal{S}$.

To illustrate this behavior we give a simple analytical estimate of the limits on the degree of hierarchy that is phenomenologically viable in the sfermion mass spectrum of the MSSM by extending the analysis of Ref. [81] to include the one-loop D-term correction (8.4). Following Ref. [81], we write the RGE for the soft mass squared of a third-generation scalar ϕ_3 as

$$\begin{aligned}\frac{d}{dt}m_{\phi_3}^2 \simeq &-\frac{1}{16\pi^2}\,8\sum_a g_a^2\,C^a(R_{\phi_3})\,M_a^2 \\ &+\frac{1}{16\pi^2}\frac{6}{5}g_1^2\,Y(\phi_3)\,\mathcal{S} + \frac{1}{(16\pi^2)^2}\,4\sum_a g_a^2\,C^a(R_{\phi_3})\,m_{\phi_{1,2}}^2\,,\end{aligned} \tag{8.8}$$

[6] Note that if some symmetry or universality in the soft mass boundary conditions are assumed such that (8.4) is zero, it remains zero at all scales.

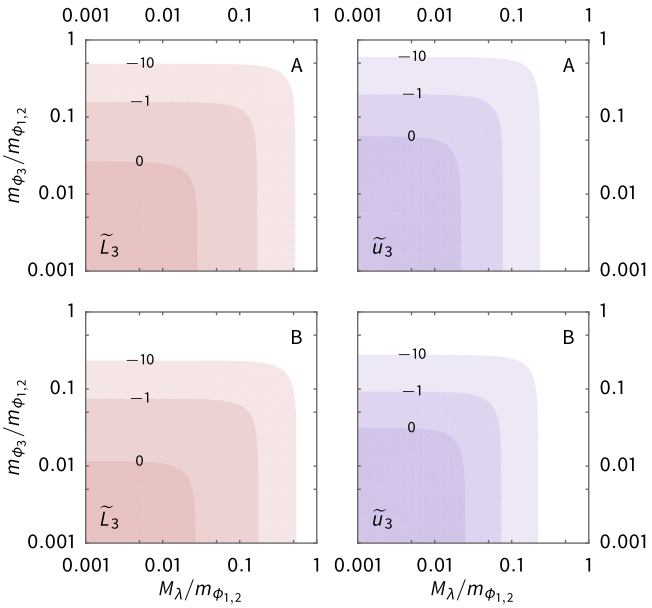

Figure 8.4: Plot of the estimated tachyonic constraint on the sfermion masses in the MSSM for negative $\mathcal{S}$, where $\Lambda_{\rm IR} = 2 \times 10^{16}\,\text{GeV}$ (upper row) and $\Lambda_{\rm IR} = 6.5 \times 10^{6}\,\text{GeV}$ (lower row), corresponding to the scenarios A and B given in Table 9.1. The shaded regions are excluded in each case. We take $m_{\phi_{1,2}} = 100\,\text{TeV}$ and $m_{\rm SUSY} = 10\,\text{TeV}$.

where t is the logarithmic scale parameter. The parameters M_a are the gaugino masses and $m_{\phi_{1,2}}$ is the characteristic soft mass scale for the first- and second-generation scalars. The D-term contribution, parametrized by $\mathcal{S}$, can be positive or negative and typically is of order the scale of $m^2_{\phi_{1,2}}$. Starting the running from a high scale (such as $\Lambda_{\rm IR}$), we decouple the D-term and the two-loop contribution at the mass scale of the heavy scalars $m_{\phi_{1,2}}$ (which we take to be constant) and the gaugino contribution at the lower scale $m_{\rm SUSY}$.

The scalar RGE (8.8) can be solved analytically. We take the running gaugino masses to unify with a value $M_a(m_{\rm GUT}) \equiv M_\lambda$ at the scale $m_{\rm GUT} = 2 \times 10^{16}\,\text{GeV}$. Enforcing $m_{\phi_3}(m_{\rm SUSY}) > 0$ as a tachyon condition,[7] we obtain lower limits on the ratios $m_{\phi_3}(\Lambda_{\rm IR})/m_{\phi_{1,2}}$, $M_\lambda/m_{\phi_{1,2}}$, and $\mathcal{S}/m^2_{\phi_{1,2}}$. These limits are shown in Figs. 8.4 and 8.5 for each third-generation sfermion. On the qualitative level, the limits are

[7] This is aggressive, as the $\overline{\rm DR}$ soft masses may take negative values, while the corresponding pole masses remain positive. See Ref. [244] for further details.

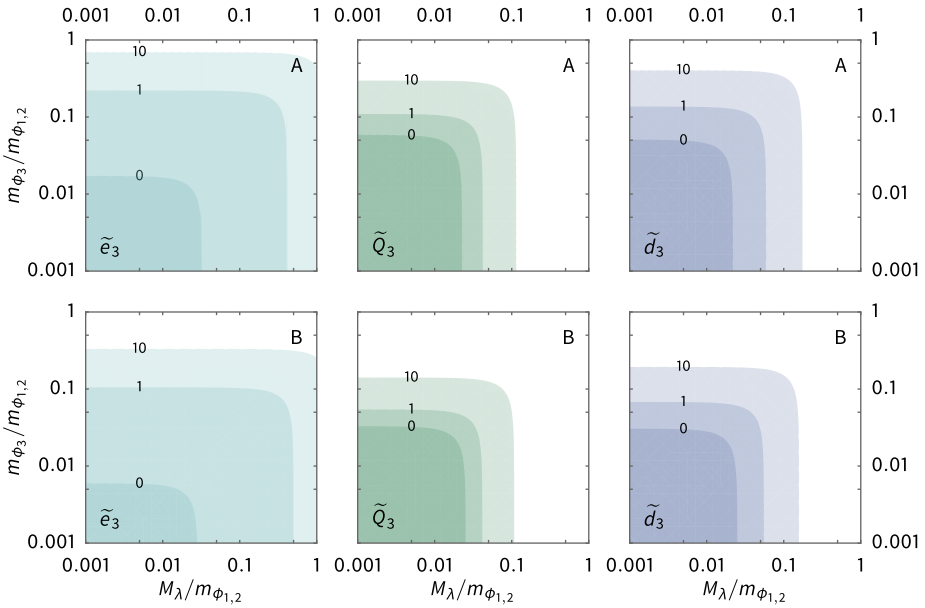

Figure 8.5: Contours of the estimated tachyonic constraint on the sfermion masses in the MSSM for positive of the ratio $\mathcal{S}$, where $\Lambda_{\rm IR} = 2 \times 10^{16}\,\text{GeV}$ (upper row) and $\Lambda_{\rm IR} = 6.5 \times 10^{6}\,\text{GeV}$ (lower row), corresponding to the scenarios A and B given in Table 9.1. The shaded regions are excluded in each case. We take $m_{\phi_{1,2}} = 100\,\text{TeV}$ and $m_{\rm SUSY} = 10\,\text{TeV}$.

collectively weakest when $\mathcal{S} = 0$. The presence of a positive D-term contribution ameliorates the limits for the sfermions with negative hypercharge ($\widetilde{L}_3$ and $\widetilde{u}_3$), but worsens those of the positive hypercharge fields ($\widetilde{e}_3$, $\widetilde{Q}_3$, and $\widetilde{d}_3$), and vice versa when the D-term contribution is negative. Quantitatively, we expect these tachyon bounds to be accurate up to about an order of magnitude.

For our model, the MSSM corrections further restrict the accessible ranges for the localization of the matter hypermultiplets. The MSSM limits generally reinforce the bulk limits, further restricting the viable IR-brane hierarchies for sfermions (particularly squarks) with hypercharge of the same sign as $\mathcal{S}$, which receive large negative corrections. Large hierarchies in the high-scale spectrum are only allowed for sfermions with hypercharge sign opposite to the sign of $\mathcal{S}$. For example, if $\mathcal{S} > 0$, then members of the families $\widetilde{u}$ and $\widetilde{L}$ (hypercharge $Y = -\frac{2}{3}, -\frac{1}{2}$, respectively) may receive large negative corrections, and therefore cannot have masses significantly lower than the scale of the other sfermions. Conversely, members of the families $\widetilde{Q}$, $\widetilde{d}$, and $\widetilde{e}$ (hypercharge

$Y = \frac{1}{6}, \frac{1}{3}, 1$, respectively) can accommodate masses hierarchically smaller than the heavy sfermion mass scale. Such high-scale sfermion structure is a generic signature of a nonuniversal split sfermion spectrum.

8.1.7 Electroweak symmetry breaking

A similar analysis can be performed in the Higgs sector, where, conversely, large negative corrections are typically favorable for electroweak symmetry breaking. Negative corrections to the Higgs soft masses squared $m_{H_u}^2$ and $m_{H_d}^2$ may arise from both the bulk, in the form of Yukawa contributions (7.38) and D-term contributions (7.36) at one loop, or from the MSSM, in the form of Yukawa corrections

$$16\pi^2 \, (\beta_{m_{H_u}^2})^{\text{1-loop}} \supset \operatorname{tr}\Big[6\, \boldsymbol{y}_u \left(m_{H_u}^2 \boldsymbol{I}_3 + \boldsymbol{m}_{\tilde{Q}}^{\boldsymbol{2}}\right) \boldsymbol{y}_u^\dagger + 6\, \boldsymbol{y}_u^\dagger \boldsymbol{m}_{\tilde{u}}^{\boldsymbol{2}} \boldsymbol{y}_u\Big] \,, \tag{8.9a}$$

$$\begin{aligned} 16\pi^2 \, (\beta_{m_{H_d}^2})^{\text{1-loop}} \supset \operatorname{tr}\Big[&6\, \boldsymbol{y}_d \left(m_{H_d}^2 \boldsymbol{I}_3 + \boldsymbol{m}_{\tilde{Q}}^{\boldsymbol{2}}\right) \boldsymbol{y}_d^\dagger + 6\, \boldsymbol{y}_d^\dagger \boldsymbol{m}_{\tilde{d}}^{\boldsymbol{2}} \boldsymbol{y}_d \\ &+ 2\, \boldsymbol{y}_e \left(m_{H_d}^2 \boldsymbol{I}_3 + \boldsymbol{m}_{\tilde{L}}^{\boldsymbol{2}}\right) \boldsymbol{y}_e^\dagger + 2\, \boldsymbol{y}_e^\dagger \boldsymbol{m}_{\tilde{e}}^{\boldsymbol{2}} \boldsymbol{y}_e\Big] \end{aligned} \tag{8.9b}$$

and D-term corrections

$$16\pi^2 \, (\beta_{m_{H_{u,d}}^2})^{\text{1-loop}} \supset \frac{6}{5} g_1^2 \, Y(H_{u,d}) \, \mathcal{S} \,, \tag{8.10}$$

at one loop and the corrections

$$(16\pi^2)^2 \, (\beta_{m_{H_{u,d}}^2})^{\text{2-loop}} \supset 4 \sum_a g_a^4 \, C_a(R_{H_{u,d}}) \, \sigma_a \,, \tag{8.11}$$

at two loops.

As discussed in Sec. 5.3, EWSB in our model requires $m_{H_u}^2 < m_{H_d}^2 / \tan^2\beta$). If the sfermion hierarchy is relatively modest, such that at least one of the third-generation squarks is relatively heavy, this may be achieved in the familiar way in the MSSM through Yukawa radiative corrections. If, however, the sfermion splitting is large, the MSSM Yukawa contributions may be suppressed, and successful EWSB may rely on the presence of D-term contributions to destabilize the Higgs VEV (or, at least, the D-term contributions may be of the same order as the Yukawa corrections). In this case, we require that $\Delta\mathcal{S}^{\text{1-loop}} < 0$ and $S > 0$ so that the D-term contributions to $m_{H_u}^2$ are negative and also that they are large enough to be the dominant mass contribution (in particular, they must overcome

the positive contribution from the gauginos). The predicted Higgs boson mass in this case is also correlated with the D-term corrections, and consistency with the observation may require additional limits on $\Delta\mathcal{S}^{\text{1-loop}}$ and $\mathcal{S}$. Together, these requirements imply a lower limit on the masses of the heavy sfermions(typically, first- and second-generation) sfermions which give the dominant contributions to $\Delta\mathcal{S}^{\text{1-loop}}$ and $\mathcal{S}$ that is correlated with a global constraint on their localizations. Because sfermions from the $\widetilde{Q}$, $\widetilde{d}$, or $\widetilde{e}$ families will also receive large negative D-term contributions in this case, additional tachyonic limits on the matter hypermultiplet may be introduced.

In some regions of the parameter space of our model, the union of all limits imposed on the hypermultiplet localizations by these effects excludes all solutions compatible with the standard model fermion mass spectrum. When the gaugino mass is given by (5.9) (singlet spurion), the splitting between the masses of the third-generation sfermions and the heavier mass scale of the first and second generations is small enough throughout the parameter space that tachyonic constraints are not significant, but when the gaugino mass is given by (5.11) (nonsinglet spurion), larger hierarchies arise, excluding some areas of the parameter space. We show an estimate of the excluded region in the space of $(\Lambda_{\text{IR}}, \sqrt{F})$ in Fig. 8.7.

8.2 Physical Parameter Space

Together, the constraints discussed in the previous section lead to restrictions on the $(\Lambda_{\text{IR}}, \sqrt{F})$ parameter space, which are shown in Figs. 8.6 and 8.7 for the singlet spurion and nonsinglet spurion cases, respectively. The region of each plot in which $\sqrt{F} > \Lambda_{\text{IR}}$ is excluded as the dynamics of the spurion are restricted by Λ_{IR} as a cutoff scale. The constraints leading to the other excluded regions are discussed in Sec. 8.1. We summarize them here.

- Along the edges of the $\sqrt{F} > \Lambda_{\text{IR}}$ regions, we show the area in which the next-to-lightest gaugino KK mode must be included in the low-energy spectrum. These regions are not excluded on theoretical or phenomenological grounds, but simply as a matter of practicality.

- The regions labeled "LHC" give an estimate of the exclusions due to collider direct-detection limits.

- The regions of Fig. 8.6 labeled "$\widetilde{\chi}_1^0$" and "$\widetilde{\tau}_1$" show our estimate of the BBN exclusions when the NLSP is the lightest neutralino or the lightest stau (also see Fig. 8.1). The

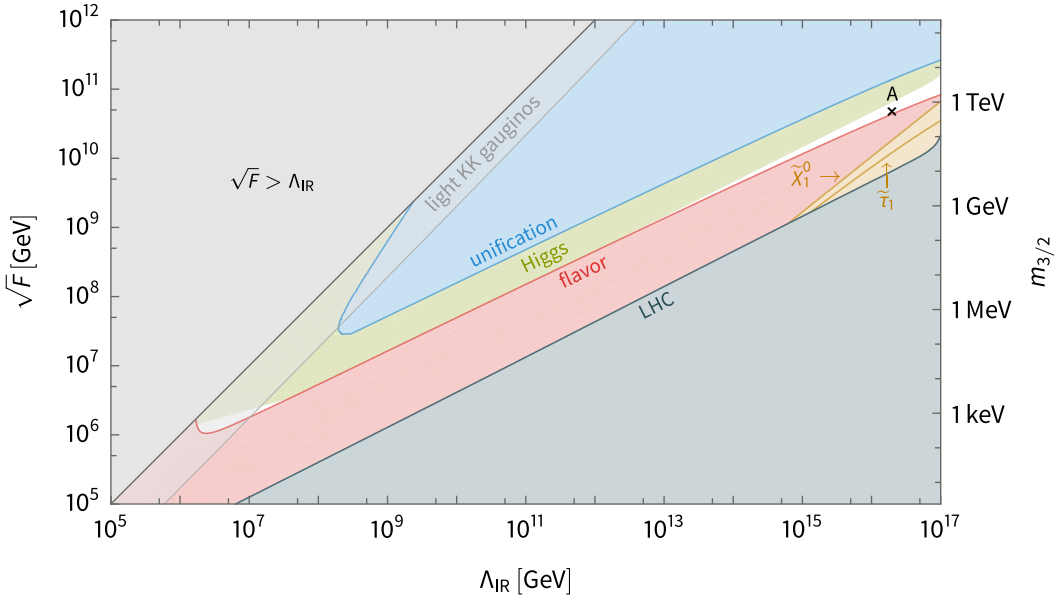

Figure 8.6: Plot of the constraints on the parameter space of our model in the $(\Lambda_{\text{IR}}, \sqrt{F})$ when the supersymmetry-breaking spurion is a singlet, such that the gaugino mass is given by (5.9).

corresponding limits in the nonsinglet spurion case (see Fig. 8.2) are less strict than the collider constraint, and therefore not visible in Fig. 8.7.

- The regions in which $|\mu| > 100\,\text{TeV}$ are labeled "unification" and are excluded in order to preserve gauge coupling unification.
- In the regions labeled "flavor", the matter hypermultiplet localizations cannot be chosen such that all of the first- and second-generation sfermions have masses that are at least 100 TeV as is necessary to suppress supersymmetric flavor-changing neutral currents and CP violation.
- In the regions labeled "Higgs", we estimate that the stop masses are heavier than 100 TeV, and hence we expect the resulting Higgs boson mass to be too heavy to match the observed value.
- In region of Fig. 8.7 labeled "tachyons", one or more of the sfermions receives a tachyonic mass, either on the IR brane or in the subsequent MSSM running.

The remaining white areas are the regions of interest, simultaneously satisfying all

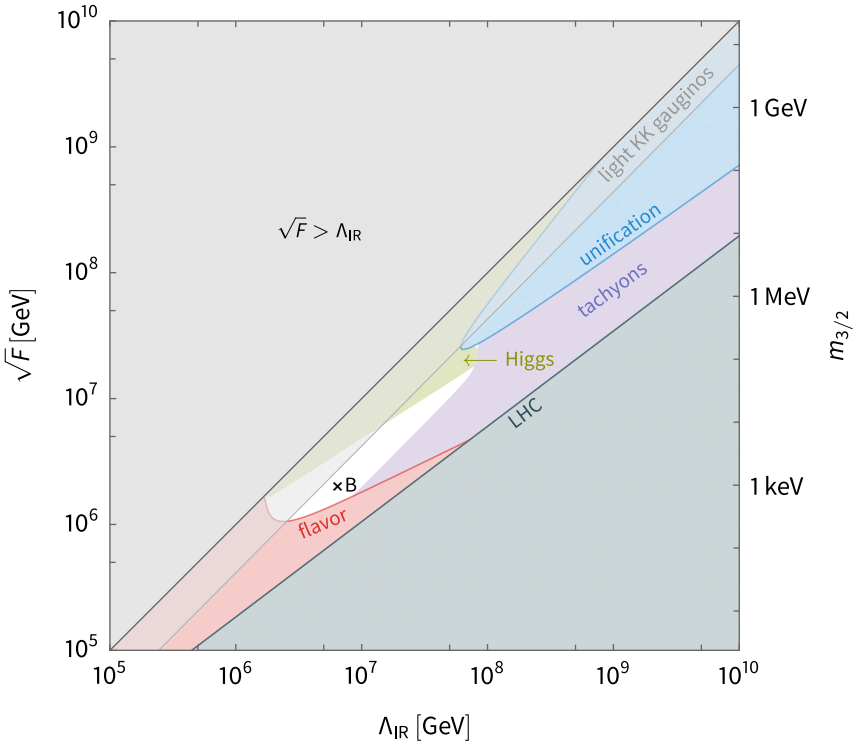

Figure 8.7: Plot of the constraints on the parameter space of our model in the $(\Lambda_{\text{IR}}, \sqrt{F})$ when the supersymmetry-breaking spurion is not a singlet, such that the gaugino mass is given by (5.11).

constraints. Within these regions, flavor constraints, the observed Higgs boson mass, and radiative corrections impose additional restrictions on the possible localizations of the matter hypermultiplets. The constraints favor two regions: either $\Lambda_{\text{IR}} \sim 10^7$ GeV, with a keV-scale gravitino and a singlet spurion, or a GUT-scale value for Λ_{IR}, with an approximately 500 GeV gravitino and a nonsinglet spurion. In Sec. 9.2, we calculate detailed sparticle spectra for two benchmark scenarios (marked as A and B in Figs. 8.6 and 8.7, respectively).

9 Numeric Analysis

In this chapter we discuss the details of the numeric procedure we use to obtain predictions for the spectrum of our partially composite mode before giving the results of this calculation for two benchmark scenarios identified from the parameter space survey in Chapter 8.

9.1 Renormalization Procedure

We first describe the numeric renormalization procedure we use to obtain predictions for the sparticle spectrum and Higgs pole mass from a particular point in the parameter space of the five-dimensional theory. Connecting this with the numeric flavor solution discussed in Chapter 4 and the radiative corrections derived in Chapter 5, we are able to construct an overview of the complete numeric methodology.

9.1.1 MSSM spectrum calculation

The matching between the five-dimensional bulk theory and the four-dimensional MSSM in which the five-dimensional Yukawa couplings and hypermultiplet localization parameters are determined according to the method described in Chapter 4 (specifically Sec. 4.4 for the numeric procedure) and the loop-corrected MSSM soft parameters calculated as discussed in Chapter 5 occurs at the IR-brane scale. In order to obtain pole mass predictions for the superpartners and the neutral scalar Higgs boson mass, we run selected points down from the input scale to lower energy within the MSSM. To solve the renormalization boundary value problem, we use the public spectrum calculator FlexibleSUSY [245, 246], which incorporates elements of SARAH [247–250] and SOFTSUSY [251, 252], which employs a nested iterative algorithm, using the three-loop MSSM β functions (the renormalization procedure includes components and corrections from [253–259]) between boundary conditions imposed at the high scale, Λ_{IR}, and the SM at the electroweak scale. Electroweak symmetry breaking is determined by numeric minimization of the loop-corrected Higgs potential, with the value of $\tan\beta$ and the magnitude of the higgsino mass parameter μ determined iteratively. Loop-corrected pole masses are calculated from the full self-energies for each particle.

The renormalization procedure is made more complicated by the fact that the soft mass spectrum at the IR-brane scale depends on the values of the supersymmetric parameters (the gauge and Yukawa couplings and the higgsino mass parameter) at that scale. As discussed in Chapter 4, the value of the four-dimensional Yukawa couplings at the IR-brane scale must be known in order to choose the localizations of the matter hypermultiplets to explain the fermion mass hierarchy; additionally, the radiative corrections included for the soft masses at the IR-brane scale explicitly incorporate gauge and Yukawa couplings as well as the higgsino mass parameter. The IR-brane values of these parameters in turn depend (weakly) on the resulting sparticle pole masses. In order to consistently determine the sparticle mass spectrum, we must therefore apply the renormalization procedure iteratively.

To do this, we first obtain an initial estimate of the high-scale theory using the renormalization procedure described in Sec. 4.2 to extract the standard model fermion masses and mixing parameters and the gauge couplings from low-energy experimental data and run them up in the SM and MSSM to Λ_{IR}. As we noted in Sec. 4.2, the IR-scale couplings calculated using this procedure are insensitive to the details of the sparticle spectrum, because the tree-level matching between the SM and the MSSM neglects threshold corrections at the scale m_{SUSY}. This is a generic problem that arises in the renormalization of all theories with boundary conditions at different scales and is typically solved iteratively by updating the initial guess with corrections from the subsequently calculated spectrum and repeating the renormalization until the spectrum converges. For our theory, an associated complication obtains due to the fact the conversion between the $\overline{\text{MS}}$ and $\overline{\text{DR}}$ renormalization schemes that occurs in this process requires the specification of the value of $\tan\beta$ (the Yukawa couplings in particular are multiplicatively sensitive to the value of $\tan\beta$). As discussed in Sec. 5.3, the correlation between the IR-brane-scale values for the higgsino mass parameter μ and the soft b term implies that $\tan\beta$ is not a free parameter but instead determined by electroweak symmetry breaking. Therefore, an initial guess of its value must be used to obtain the estimated high-scale couplings.

To obtain a better estimate of the coupling values, a particular spectrum must be specified by performing the numeric flavor minimization described in Sec. 4.4 to determine a full set of five-dimensional Yukawa couplings and matter hypermultiplet localization parameters. Together, these parameters define the four-dimensional Yukawa couplings at the IR-brane scale in the gauge-eigenstate basis, and the localization parameters along with the Yukawa and gauge couplings allow the loop-corrected soft supersymmetry-breaking terms of the MSSM to be calculated. Given these, the IR-brane couplings calculated as above can be

combined with an initial guess for $|\mu|$ to obtain a preliminary estimate of the IR-brane scale soft mass spectrum. This spectrum is then renormalized and EWSB computed using the full FlexibleSUSY MSSM routine. Unlike our spectrum-agnostic procedure above, this renormalization and matching procedure includes threshold effects from the soft masses, and the running values of the resulting supersymmetric parameters are spectrum-dependent. The values of the parameters extracted at the IR-brane scale are then used to construct an updated input spectrum and the procedure is repeated until the values of the input parameters converge.

As a word of caution, we note that the hierarchies present in the sfermion mass spectrum of our model complicate the numeric renormalization procedure, because they necessitate a careful account of particle decoupling if precision in mass spectrum calculations is to be obtained. In mass-independent renormalization schemes such as $\overline{\text{DR}}$, the effects of heavy particles do not decouple, and hence, at renormalization scales small compared to the particle masses, finite quantum corrections may involve terms with large logarithms of the masses of these particles.[1] In order for mass calculations to be precise when large hierarchies in the soft mass parameters are present, such large logarithmic corrections need to be resummed, a process which is most naturally accomplished by the use of an effective theory, or of a tower of effective theories [260]. Precision in the case of scalar hierarchies is especially critical, because the light scalar masses depend crucially on the heavy scalar masses through the factors such as (8.4) and (8.6). It is important to note as well that the scale of supersymmetry breaking in our model, the IR brane, which can be significantly lower than the Planck scale or the GUT scale due to the warped five-dimensional geometry, is the natural cutoff for the IR-localized (or composite) part of the four-dimensional MSSM. Thus, the effects of the heavy scalars, which may receive masses very near (or even above, depending on the choice of $\sqrt{F}$ and k) the IR-brane scale, may decouple after a little running, minimizing the effect of the heavy scalar contributions. In an effective field theory approach, these heavy scalars are integrated out, introducing threshold corrections to the lighter scalar masses. At the one- and two-loop level, such corrections can be large and negative as a result of the effects mentioned above, but overall, the decoupling procedure may substantially relax the tachyonic bounds indicated in purely MSSM $\overline{\text{DR}}$ renormalization [261, 262].

The numeric MSSM renormalization procedure discussed here does not implement decoupling. Instead, it matches the MSSM to the SM at the electroweak scale, and we expect the resulting threshold corrections to the light scalar masses to be large enough that some

[1] For the MSSM, these are given by Ref. [244] and are accordingly sometimes referred to as *DBMZ* corrections.

regions of our parameter space may be unnecessarily excluded on tachyonic grounds, solely as an artifact of the numeric renormalization method.

9.1.2 Higgs mass calculation

In supersymmetric theories, the neutral scalar Higgs mass is sensitive to the scale and structure of the sparticle spectrum (particularly to the stop masses) and therefore offers a valuable constraint on the underlying physics. In order to be useful in this capacity, however, the predicted pole mass must be known with precision. The arguments for the necessity of appropriate decoupling for the precise calculation of light scalar masses when the scale of supersymmetry is high are also applicable to the neutral scalar Higgs boson and the other particles of the standard model. For the Higgs mass, this is implemented by the public spectrum calculators HSSUSY [245–252, 263–274] and FlexibleEFTHiggs [245–257, 264–275]. Both of these are based on an effective field theory approach in which all supersymmetric particles are integrated out at a common threshold (namely, $m_{\text{SUSY}} = \sqrt{m_{\tilde{t}_1} m_{\tilde{t}_2}}$), at which point the theory is run down in the SM to the electroweak scale, where the standard model couplings are matched to experimental data and the Higgs pole mass is extracted. To characterize this procedure, we discuss the sources of theoretical uncertainty.

1. **SM uncertainty**

   The first source of uncertainty we identify is due to neglected higher-order corrections at the electroweak scale. Missing corrections in the extraction of the standard model running parameters from experimental data at the electroweak scale induce uncertainty that can be estimated as the effect of higher loop corrections on the calculated value of the Higgs pole mass. (Specifically, we estimate this uncertainty as the shift in the calculated Higgs pole mass when three-loop QCD corrections to the top Yukawa coupling are included compared to the two-loop result.) Missing corrections in the calculation of the Higgs pole mass itself lead to residual renormalization-scale dependence in the calculated value. We estimate this uncertainty by varying the scale at which the pole mass is calculated over the range $[m_t/2, 2m_t]$ and taking the difference between the maximum and minimum. The total SM uncertainty is the linear sum of these two contributions.

2. **MSSM uncertainty**

   The second source of uncertainty is due to neglected threshold corrections in the matching of the SM to the MSSM. In the EFT approach, the Higgs pole mass is

primarily sensitive to new physics via threshold corrections from supersymmetric particles to the Higgs quartic coupling, calculated at the matching scale m_{SUSY}. The matching in HSSUSY and FlexibleEFTHiggs is complete up through the two-loop level and includes some three-loop corrections. The uncertainty due to the missing higher-order corrections to the Higgs quartic coupling can be estimated by the residual matching-scale dependence in the Higgs pole mass. To estimate this, we vary the scale at which the SM is matched to the MSSM over the interval $[m_{\text{SUSY}}/2, 2m_{\text{SUSY}}]$ and take the difference between the maximum and minimum value of the calculated Higgs pole mass.

3. EFT uncertainty

The third source of uncertainty is due to neglected higher-dimensional operators in the SM EFT below the matching scale. Both HSSUSY and FlexibleEFTHiggs only include terms up to order $\mathcal{O}(v/m_{\text{SUSY}})$ in the SM EFT. In a pure EFT approach, the uncertainty due to the missing terms of order $\mathcal{O}(v^2/m_{\text{SUSY}}^2)$ and higher can be estimated as a shift in the supersymmetric threshold corrections to the Higgs quartic coupling. Accordingly, with HSSUSY, we calculate this uncertainty as the shift in the Higgs pole mass induced by multiplying all one-loop threshold corrections to the Higgs quartic coupling at the scale m_{SUSY} by a factor $1 + v^2/m_{\text{SUSY}}^2$. In FlexibleEFTHiggs, conversely, this uncertainty is not present, as the calculation departs from the pure EFT approach at low energy by switching to a diagrammatic calculation that correctly resums leading and subleading logarithms to all orders.

The total uncertainty in the Higgs mass calculation is taken to be the linear sum of the SM, MSSM, and EFT uncertainties. As our Higgs mass estimate, we take the average of the HSSUSY and FlexibleEFTHiggs results, with uncertainty given by the union of the two calculated ranges.

9.1.3 Overview

In Fig. 9.1 we give a schematic overview of the complete numeric procedure we use to obtain predictions for the sparticle spectrum in this model of partially composite supersymmetry. Details of the methodology used to match the five-dimensional theory to four-dimensional flavor and electroweak observables are discussed in Chapter 4. The calculation of the loop-corrected soft masses at the IR brane scale is given in Chapter 5. In this chapter we

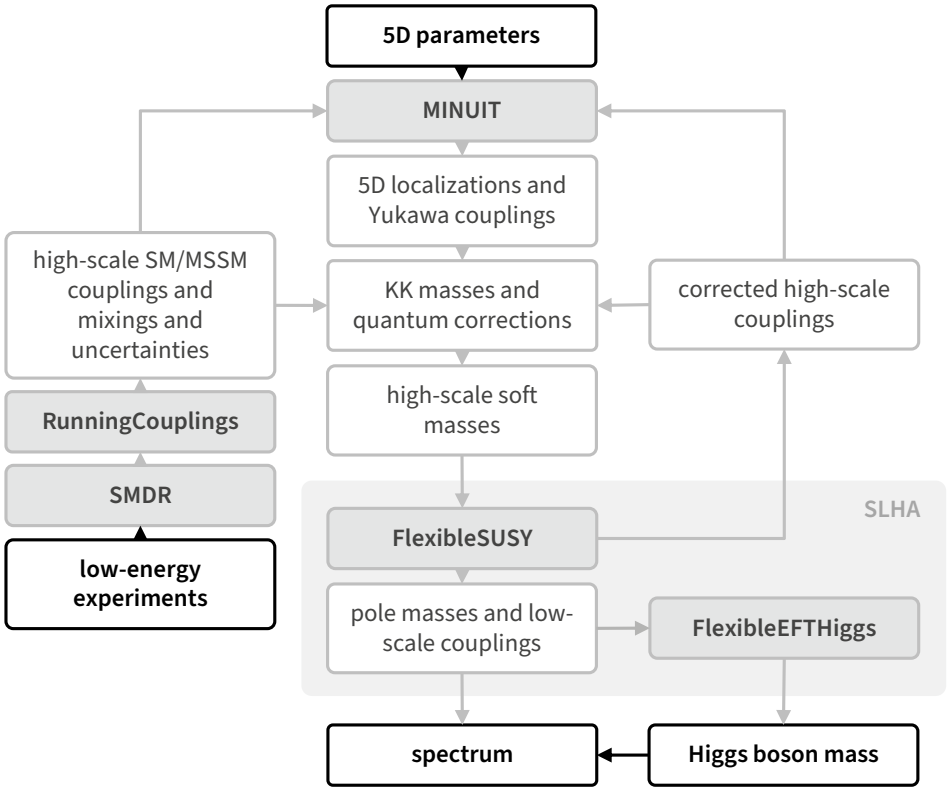

Figure 9.1: Schematic of the complete numeric procedure used to match the five-dimensional theory to four-dimensional flavor and electroweak observables, calculate the soft masses at the IR brane scale, and renormalize the theory to obtain predictions for the sparticle spectrum.

present a procedure to consistently renormalize the theory and assemble a sparticle pole mass spectrum and Higgs mass prediction.

We note that the public spectrum generators FlexibleSUSY, FlexibleEFTHiggs, and HSSUSY used in this procedure comply with a common convention in their file structure interface defined by the Supersymmetric Les Houches Accord (SLHA) [276, 277]. this is indicated in the region labeled "SLHA" in Fig. 9.1. As part of our numeric procedure we have implemented import rules and conversion for the SLHA interface into the Wolfram Language, available as the package LesHouches [278].[2]

Besides the weakness of the supersymmetric spectrum generation with respect to sfermion hierarchies (discussed above in Sec. 9.1.1), the main limitation in our numeric procedure is its

[2]The code is also available from the author upon request.

lack of global optimization. The five-dimensional flavor structure and the sparticle spectrum are both calculated separately, and solutions that satisfy the constraints are determined by the inefficient (but eventually effective) method of randomly sampling the parameter space. It may be possible to address these concerns by implementing a global adaptive method such as a Monte Carlo Markov chain (MCMC) algorithm or other machine learning technique to search for solutions.

9.2 Benchmark Spectra

Based on the constraints considered in Chapter 8, we select the regions of parameter space given in Table 9.1 as our benchmark scenarios. With these parameters we determine the sparticle mass spectrum and Higgs boson mass predicted by the partially composite supersymmetric model. The IR brane scale, Λ_{IR}, and the scale of supersymmetry breaking, $\sqrt{F}$, set the overall soft mass scale, and are chosen to comply with all phenomenological constraints in Sec. 8.1. $\tan\beta$ is determined by the measured Higgs boson mass and the sign of μ is set in order to achieve the correct pattern of EWSB. To simplify the calculation and discussion, we do not incorporate flavor mixing in the Yukawa couplings or sfermion soft mass matrices. A universal value $Y = 1$ is taken for all 5D Yukawa couplings (as in Fig. 4.1) and $w = 1$ for all sfermion spurion couplings. These results were first presented Refs. [17, 18].

In Fig. 9.2 we present the resulting superpartner pole mass spectra obeying all phenomenological constraints and consistent with the measured value of the Higgs boson mass. The corresponding ranges for the sfermion, gaugino, and higgsino masses in the gauge-eigenstate basis are shown in Fig. 9.3. In general, the spread in the masses is a result of the freedom in the hypermultiplet localizations remaining after the application of all constraints, combined with the uncertainty in the numerical calculations.

In both cases A and B, the allowed mass ranges for the third-generation sfermions are relatively unconstrained on phenomenological grounds, and their limits are principally determined by the restriction of the hypermultiplet localization parameters to order-one numbers. In particular, we note that for the stops (below 100 TeV, these can be identified unequivocally with the two lightest up-squark mass eigenstates $\widetilde{u}_{1,2}$), the general mass scale $m_{\tilde{t}} \sim \sqrt{m_{\tilde{t}_1} m_{\tilde{t}_2}}$ is broadly consistent with the observed Higgs mass throughout allowed localization ranges.

The observed Higgs boson mass provides stronger constraints indirectly, due to the

Table 9.1: Selected parameter space sampling regions.

	A	B
Λ_{IR}	$2 \times 10^{16}\,\text{GeV}$	$6.5 \times 10^{6}\,\text{GeV}$
$\sqrt{F}$	$4.75 \times 10^{10}\,\text{GeV}$	$2 \times 10^{6}\,\text{GeV}$
$\tan\beta$[a]	~ 3	~ 5
$\operatorname{sgn}\mu$	-1	-1
spurion	singlet	nonsinglet
M_1[a]	52.9 TeV	14.60 TeV
M_2[a]	50.7 TeV	22.9 TeV
M_3[a]	49.85 TeV	38.94 TeV
$m_{3/2}$	535 GeV	1 keV

[a] At scale Λ_{IR}.

particular structure of EWSB in our model that makes it sensitive to the D-term corrections arising either from the extra dimension or in the MSSM running (see Sec. 8.1.6). We show the Higgs boson mass estimates in Fig. 9.4 as smoothed functions of $\tan\beta$. For both benchmark scenarios, consistency with the observed Higgs boson mass only occurs within a restricted range of $\tan\beta$, which in turn put constraints on the D-term contributions that can have a significant impact on EWSB, introducing correlations among the heavy sfermion masses that contribute most to the corrections. The primary constraint arises on the localizations the heavies sfermions (typically, these are from the first generation), which must be correlated such that $\Delta\mathcal{S}^{\text{1-loop}}$ and $\mathcal{S}$ are of the correct scale.

As an example, we show this correlation for scenario A in Fig. 9.5. In this case, the pattern of electroweak symmetry breaking necessary to achieve the observed Higgs mass prefers $\Delta\mathcal{S}^{\text{1-loop}} < 0$ and $\mathcal{S} > 0$, while the explanation of the standard model fermion mass hierarchy typically requires that either $\widetilde{u}_L$ or $\widetilde{u}_R$ is the heaviest sfermion. If $m_{\tilde{u}_R} > m_{\tilde{u}_L}$, $\tilde{e}_R$ must also be heavy (and, further, $m_{\tilde{e}_R} > m_{\tilde{e}_L}$) in order to compensate for the contribution of $\tilde{u}_R$ and ensure that $\Delta\mathcal{S}^{\text{1-loop}}$ and $\mathcal{S}$ have the correct sign and magnitude. (When $m_{\tilde{u}_L} > m_{\tilde{u}_R}$, then we can have $m_{\tilde{e}_L} > m_{\tilde{e}_R}$.) Note that the Higgs mass measurement constrains the allowed spread of the first-generation sfermion masses more than the condition imposed to suppress

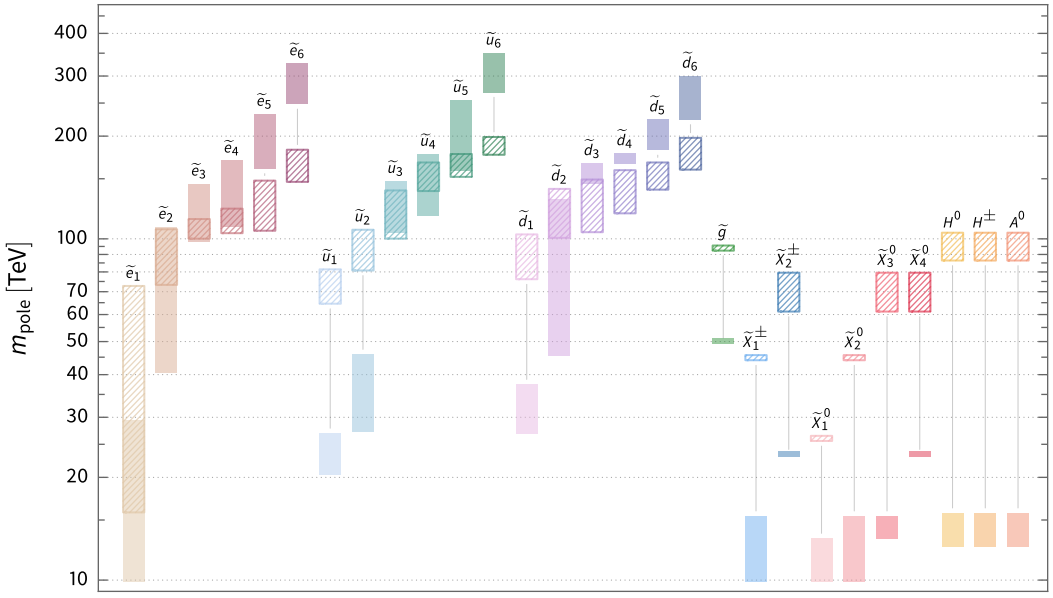

Figure 9.2: Predicted superpartner pole mass spectra for benchmark scenarios A (hatched) and B (solid) given in Table 9.1.

FCNCs, which merely restricts the masses to be above 100 TeV.

For the third-generation sfermions, the D-term corrections necessary to obtain the observed Higgs boson mass may necessitate additional constraints in order to avoid tachyonic masses. For both scenarios, this effect imposes the lower limit on $m_{\tilde{\tau}_R}$, and for scenario B it also imposes the lower limit on $m_{\tilde{\tau}_L}$. These are the only constraints on the third-generation sfermion masses that are stronger than those set by the requirement that the c parameters are order-one. For both scenarios, the right-handed stau may thus be the lightest sfermion, and $\tilde{\tau}_1$ may accordingly be the NLSP. On the other hand, when $\tilde{\tau}_1$ is heavy, the NLSP for both scenarios is $\tilde{\chi}_1^0$. For scenario A, $\tilde{\chi}_1^0$ is binolike and $\tilde{\chi}_2^{\pm}$ and $\tilde{\chi}_2^0$ are winolike, while the heavy charginos, $\tilde{\chi}_2^{\pm}$, and the heavy neutralinos, $\tilde{\chi}_{3,4}^0$, are higgsinolike. This is reversed for scenario B, where $\tilde{\chi}_{1,2,3}^0$ and $\tilde{\chi}_1^{\pm}$ are binolike or higgsinolike and $\tilde{\chi}_2^{\pm}$ and $\tilde{\chi}_4^0$ are winolike.

The spread in the masses of the higgsinolike states is due to the spread of the higgsino mass parameter μ, which is fixed by EWSB. In both cases, μ correlates with the soft mass parameter $m_{H_u}^2$, which is predominantly determined by Yukawa radiative corrections from $m_{\tilde{Q}_3}^2$ and $m_{\tilde{u}_3}^2$. Thus, the spread of μ is ultimately tied to freedom in the localizations of the Q and $\bar{u}$ hypermultiplets (which, as we discussed above, are limited only by the constraint that they are order-one numbers). The masses of the heavy Higgs, H^0, $H^{\pm}$, and A^0 also

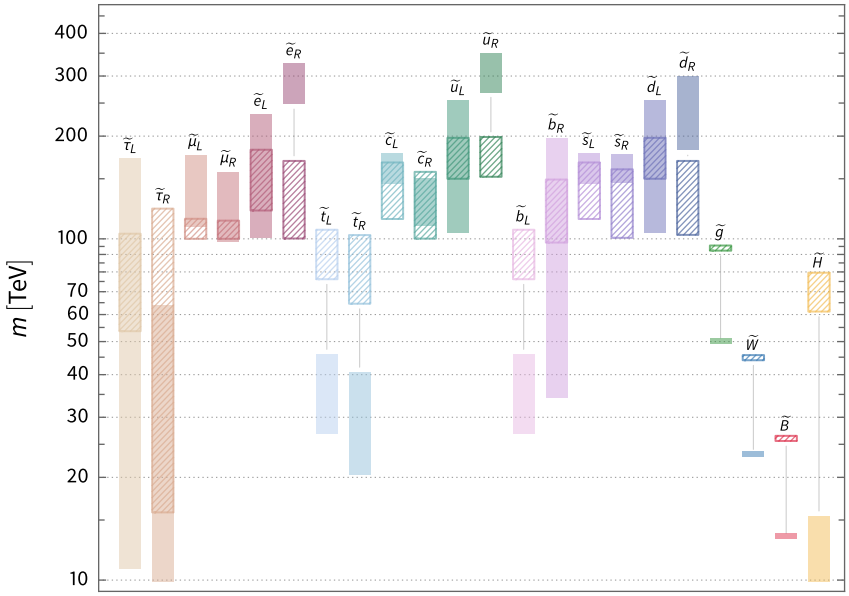

Figure 9.3: Predicted sfermion mass spectra in the gauge-eigenstate basis for benchmark scenarios A (hatched) and B (solid) given in Table 9.1.

scale with μ, but about 10 % of their spread is due to the running of the soft masses $m^2_{H_u}$ and $m^2_{H_d}$. The spread in the gluino and the binolike and winolike states is due primarily to the uncertainty in the gauge and Yukawa couplings. In Figs. 9.2 and 9.3 that spread is exaggerated for clarity.

In both scenarios, the hierarchical structure of the mass spectrum is clear. The largest hierarchy occurs for $\tilde{\tau}_1$, where we find ratios up to $m_{\tilde{u}_6,\tilde{d}_6}/m_{\tilde{\tau}_1} \sim 13$ in the singlet spurion case and up to $m_{\tilde{u}_6}/m_{\tilde{\tau}_1} \sim 35$ in the nonsinglet spurion case. The hierarchy for the stops is relatively more modest: we find ratios up to $m_{\tilde{u}_6,\tilde{d}_6}/m_{\tilde{t}_1} \sim 3$ in the singlet spurion case and up to $m_{\tilde{u}_6}/m_{\tilde{t}_1} \sim 18$ in the nonsinglet spurion case. The size of these mass splittings, which cannot be generated by MSSM running alone, is a direct consequence of the hierarchy in the sfermion IR-brane soft mass boundary conditions, and hence is ultimately a signature of the standard model fermion mass spectrum, mediated by the radiative corrections of the extra dimension and the MSSM.

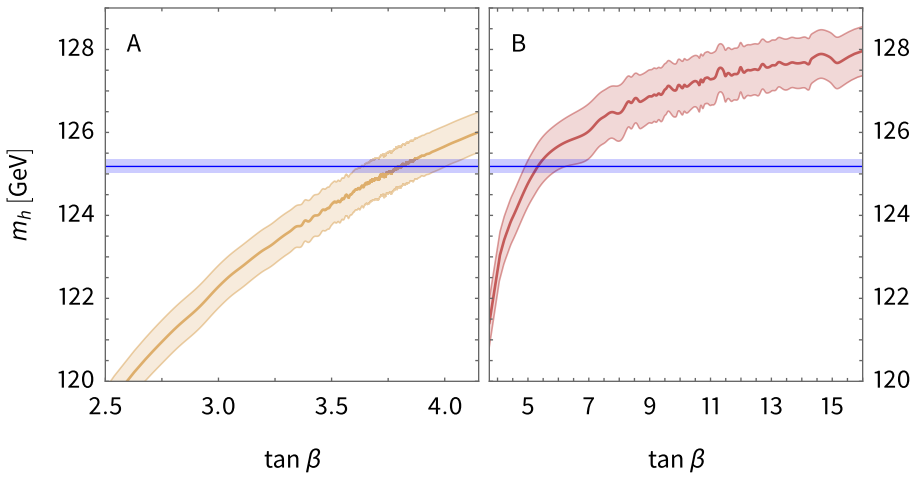

Figure 9.4: Plot of the predicted Higgs boson mass and uncertainty for benchmark scenarios A (left) and B (right) as functions of $\tan\beta$ at the scale $m_{\text{SUSY}} = \sqrt{m_{\tilde{t}_1} m_{\tilde{t}_2}}$. The horizontal line and surrounding region show the observed Higgs mass value and its uncertainty.

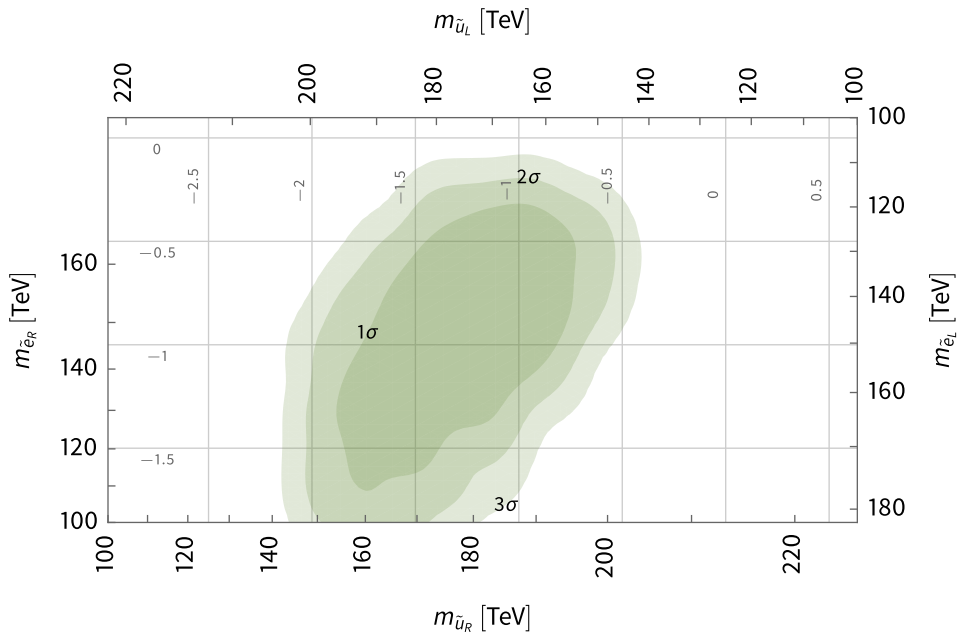

Figure 9.5: Plot of the correlation between first-generation gauge-eigenstate slepton and up-squark masses for points in benchmark scenario A (given in Table 9.1) that correctly predict the Higgs mass. The shaded regions give smoothed estimates of the area preferred by the experimentally measured Higgs boson mass at 1σ, 2σ, and 3σ confidence levels. The horizontal (vertical) lines give the range of c_{L_1} (c_{Q_1}).

10 Conclusion

We have presented a minimal supersymmetric model that uses a warped extra dimension to relate the standard model fermion mass hierarchy to the sfermion mass hierarchy. This occurs by assuming that the Higgs sector is confined to the UV brane of a slice of AdS_5, while the remaining MSSM superfields are located in the bulk. Supersymmetry breaking occurs on the IR brane. The MSSM fields are identified with the zero modes of the corresponding 5D fields. The zero-mode profile depends on a bulk mass (dimensionless) parameter c that can be arbitrarily varied to localize the zero-mode superfield anywhere in the bulk. The fermion and sfermion mass hierarchy is now dictated by the 5D fermion geography. Since the Higgs fields are confined to the UV brane, the third-generation SM fermions are UV-localized, while the first- and second-generation SM fermions are IR-localized. This naturally leads to an *inverted* sfermion mass hierarchy, where the first- and second-generation sfermions are heavy, while those of the third generation are light. The masses of the gauginos are also somewhat suppressed below the heavy scalar mass scale. The gravitino is strongly UV-localized, and accordingly is much lighter than the gauginos. It therefore becomes the LSP that can play the role of dark matter.

Using the AdS/CFT correspondence, we can provide an equivalent description in terms of the 4D strongly coupled large-N gauge theory that is dual to our 5D model. In this case, we assume that the standard model gauge fields, the Higgs sector, and the third-generation matter are (mostly) elementary, while the first two generations of matter are composite due to some unknown strong dynamics that confines at a scale $\Lambda_{\rm IR}$. Hierarchies are then generated when elementary superfields linearly mix with supersymmetric operators that have large anomalous dimensions. Since the Higgs fields are elementary, the more composite the fermion, the lighter the corresponding fermion mass. The strong dynamics is also assumed to dynamically break supersymmetry, such that the composite sparticle states directly feel the supersymmetry breaking. The predominantly elementary states, such as the third-generation sfermions, higgsinos, and gauginos, are therefore split from the much heavier first- and second-generation composite sfermions. Thus, the partially composite supersymmetric model generically predicts that light (heavy) SM fermions, have heavy (light)

sfermion superpartners. Moreover, since the gravity multiplet mixes with the stress-energy tensor (via an irrelevant term), the gravitino is much lighter than the gauginos.

At tree level in the five-dimensional model, the sfermion hierarchy may be exponentially large due to the suppressed coupling between the UV-localized fields and the supersymmetry-breaking sector. The mass scale of the third-generation sfermions is therefore set by radiative corrections from the heavy states, which transmit the breaking of supersymmetry at loop order and become the dominant soft mass contribution. At one loop in five dimensions, these corrections arise from bulk gauginos and scalars. Since the Higgs fields are localized on the UV brane, both the Higgs-sector soft masses and the soft trilinear scalar couplings are zero at tree level, but they, too, receive radiative corrections from the bulk.

The overall scales in the five-dimensional model can be fixed by imposing a number of phenomenological constraints: (i) the LSP gravitino is assumed to be the dark matter with a mass greater than $\mathcal{O}(1)$ keV; (ii) electroweak symmetry is broken, consistent with a 125 GeV Higgs boson; (iii) the first- and second-generation sfermions are at least as heavy as 100 TeV to ameliorate the supersymmetric flavor problem; (iv) the gaugino and higgsino masses are constrained, so as to preserve gauge coupling unification as in the usual MSSM [assuming any underlying dynamics preserves SU(5)]; and (v) only the MSSM fields are present in the theory below the scale of compactification. The standard model fermion mass spectrum and mixings are used to constrain the matter hypermultiplet localizations and the entries of the five-dimensional Yukawa coupling matrices. The 5D model then predicts the soft masses masses at the IR-brane scale, which are run down to lower energies using renormalization group equations. Since the boundary conditions for the sfermion masses are nonuniversal and flavor-dependent, tachyonic constraints that avoid charge- and color-breaking minima must be imposed to further restrict the parameter space.

The numerical results of the benchmark scenarios given in Table 9.1 predict a hierarchical sfermion mass spectrum. The third-generation sfermions have masses in the approximate range 10–100 TeV (20–100 TeV for the stops), while the first- and second-generation sfermions have masses in the range 100–350 TeV. We do not obtain a unique prediction because we assume that there is no relation between the $c_{L,R}$ parameters of the left- and right-handed fermions. Nevertheless, the numerical results reveal some interesting features. Most obvious is the hierarchical nature of the spectrum. Typical MSSM running cannot produce a mass spectrum with widely separated sparticle masses, and thus, with minimal particle content, the origin of the mass hierarchy must necessarily reside in the high-scale boundary conditions. Such conditions are a generic feature of our model and result in a distinctive split spectrum.

The nonuniversality of the sfermion boundary conditions is also visible at a finer level, as it is responsible for the presence of sizable D-term radiative corrections to the scalar masses. Although the sign and magnitude of these corrections are highly constrained on tachyonic grounds, they can be favorable for EWSB and can offset negative contributions to the scalars that arise at two loops. Due to the structure of EWSB in our model (imposed by radiative corrections from the bulk), the predicted Higgs boson mass is also sensitive to D-term corrections, and the experimentally measured mass value can therefore indirectly constrain the heaviest mass scales in the theory. In fact, since the measured Higgs mass is broadly consistent with stop masses in the 10–100 TeV range (as predicted in both benchmark scenarios) it is primarily through this effect that it constrains our benchmark spectra.

Our model is not too different from the usual MSSM, where a hidden sector with strong dynamics is typically invoked to dynamically break supersymmetry (e.g., via gaugino condensation). The supersymmetry breaking is then mediated via gravity (or alternatively, gauge interactions) to the visible sector with universal boundary conditions for the sfermion masses. The difference in our model is that the matter fields couple directly to the supersymmetry breaking sector, but that coupling is effectively mediated by their propagation in the AdS_5 bulk, thereby giving rise to strongly flavor-dependent sfermion mass boundary conditions. Furthermore, assuming that the AdS_5 bulk is SU(5) invariant (similar to what is imposed on the messenger sector in gauge-mediated models), gauge coupling unification is still preserved with the GUT scale at approximately 10^{16} GeV.

In light of the Higgs boson discovery and its implications for the supersymmetric spectrum, our model thus provides a more predictive, splitlike supersymmetry scenario by explicitly relating the standard model fermion mass hierarchy to the sfermion mass spectrum. It would be interesting to construct models of the nontrivial dynamics (perhaps going beyond large-N theories) that may constrain the anomalous dimensions even further, and therefore lead to exact predictions for the sparticle spectrum. Nonetheless, the partially composite supersymmetric model provides the raison d'être for the inverted sfermion hierarchy with a gravitino LSP. The NLSP is typically a bino, higgsino, or right-handed stau, which decays to the gravitino and could eventually come under scrutiny at a future 100 TeV collider. Alternatively, the heavy first- and second-generation sfermions could be indirectly probed via rare-decay experiments, such as the flavor-violating Mu2e experiment [279], or experiments attempting to measure the electric dipole moment of the electron [280]. Of course, with heavy superpartners, our model is tuned, and the question of why the overall scale of the sparticle spectrum is much heavier than the TeV scale remains a mystery. Perhaps

this is just evidence of the multiverse, as speculated in split-supersymmetric models, or a supersymmetric relaxion mechanism is at play (or, from the 4D dual perspective, the tuning could be related to the strong dynamics of the supersymmetry-breaking sector). In any case, we have attempted to provide further rationale for why low-energy supersymmetry may be concealed at a scale of 10–1000 TeV.

Bibliography

[1] S. Glashow, "Partial Symmetries of Weak Interactions", Nucl. Phys. **22**, 579 (1961) (cit. on pp. 1, 15).

[2] S. Weinberg, "A Model of Leptons", Phys. Rev. Lett. **19**, 1264 (1967) (cit. on pp. 1, 15).

[3] A. Salam, "Weak and Electromagnetic Interactions", Conf. Proc. C **680519**, 367 (1968) (cit. on pp. 1, 15).

[4] D. J. Gross and F. Wilczek, "Ultraviolet Behavior of Nonabelian Gauge Theories", Phys. Rev. Lett. **30**, edited by J. Taylor, 1343 (1973) (cit. on p. 1).

[5] D. Gross and F. Wilczek, "Asymptotically Free Gauge Theories - I", Phys. Rev. D **8**, 3633 (1973) (cit. on p. 1).

[6] D. Gross and F. Wilczek, "ASYMPTOTICALLY FREE GAUGE THEORIES. 2.", Phys. Rev. D **9**, 980 (1974) (cit. on p. 1).

[7] H. Politzer, "Asymptotic Freedom: An Approach to Strong Interactions", Phys. Rept. **14**, 129 (1974) (cit. on p. 1).

[8] S. Herb et al., "Observation of a Dimuon Resonance at 9.5-GeV in 400-GeV Proton-Nucleus Collisions", Phys. Rev. Lett. **39**, 252 (1977) (cit. on p. 1).

[9] F. Abe et al. (CDF), "Observation of top quark production in $\bar{p}p$ collisions", Phys. Rev. Lett. **74**, 2626 (1995), arXiv:hep-ex/9503002 (cit. on p. 1).

[10] S. Abachi et al. (D0), "Search for high mass top quark production in $p\bar{p}$ collisions at $\sqrt{s} = 1.8$ TeV", Phys. Rev. Lett. **74**, 2422 (1995), arXiv:hep-ex/9411001 (cit. on p. 1).

[11] K. Kodama et al. (DONUT), "Observation of tau neutrino interactions", Phys. Lett. B **504**, 218 (2001), arXiv:hep-ex/0012035 (cit. on p. 1).

[12] S. Chatrchyan et al. (CMS), "Observation of a new boson at a mass of 125 GeV with the CMS experiment at the LHC", Phys. Lett. **B716**, 30 (2012), arXiv:1207.7235 [hep-ex] (cit. on pp. 1, 23).

[13] G. Aad et al. (ATLAS), "Observation of a new particle in the search for the Standard Model Higgs boson with the ATLAS detector at the LHC", Phys. Lett. **B716**, 1 (2012), arXiv:1207.7214 [hep-ex] (cit. on pp. 1, 23).

[14] N. Arkani-Hamed, S. Dimopoulos, and G. R. Dvali, "The Hierarchy problem and new dimensions at a millimeter", Phys. Lett. **B429**, 263 (1998), arXiv:hep-ph/9803315 [hep-ph] (cit. on pp. 2, 17, 30).

[15] N. Arkani-Hamed, S. Dimopoulos, and G. Dvali, "Phenomenology, astrophysics and cosmology of theories with submillimeter dimensions and TeV scale quantum gravity", Phys. Rev. D **59**, 086004 (1999), arXiv:hep-ph/9807344 (cit. on pp. 2, 17).

[16] L. Randall and R. Sundrum, "A Large mass hierarchy from a small extra dimension", Phys. Rev. Lett. **83**, 3370 (1999), arXiv:hep-ph/9905221 [hep-ph] (cit. on pp. 2, 17, 25, 30, 36).

[17] Y. Buyukdag, T. Gherghetta, and A. S. Miller, "Partially composite supersymmetry", Phys. Rev. **D99**, 035046 (2019), arXiv:1811.12388 [hep-ph] (cit. on pp. 2, 28, 46–48, 50, 97, 98, 100, 128, 169).

[18] Y. Buyukdag, T. Gherghetta, and A. S. Miller, "Predicting the superpartner spectrum from partially composite supersymmetry", Phys. Rev. **D99**, 055018 (2019), arXiv:1811.08034 [hep-ph] (cit. on pp. 2, 28, 46, 47, 169).

[19] M. Srednicki, *Quantum field theory* (Cambridge University Press, Jan. 2007) (cit. on p. 5).

[20] M. Tanabashi et al. (Particle Data Group), "Review of Particle Physics", Phys. Rev. **D98**, 030001 (2018) (cit. on pp. 10, 13–15, 30, 42, 62, 66, 68, 149, 151, 152).

[21] A. M. Sirunyan et al. (CMS), "Measurements of properties of the Higgs boson decaying into the four-lepton final state in pp collisions at $\sqrt{s} = 13$ TeV", JHEP **11**, 047 (2017), arXiv:1706.09936 [hep-ex] (cit. on pp. 10, 151).

[22] G. Aad et al. (ATLAS, CMS), "Combined Measurement of the Higgs Boson Mass in *pp* Collisions at $\sqrt{s} = 7$ and 8 TeV with the ATLAS and CMS Experiments", Phys. Rev. Lett. **114**, 191803 (2015), arXiv:1503.07589 [hep-ex] (cit. on pp. 10, 23, 151).

[23] S. Glashow, J. Iliopoulos, and L. Maiani, "Weak Interactions with Lepton-Hadron Symmetry", Phys. Rev. D **2**, 1285 (1970) (cit. on p. 11).

[24] A. G. Riess et al. (Supernova Search Team), "Observational evidence from supernovae for an accelerating universe and a cosmological constant", Astron. J. **116**, 1009 (1998), arXiv:astro-ph/9805201 (cit. on p. 13).

[25] S. Perlmutter et al. (Supernova Cosmology Project), "Measurements of Ω and Λ from 42 high redshift supernovae", Astrophys. J. **517**, 565 (1999), arXiv:astro-ph/9812133 (cit. on p. 13).

[26] S. Weinberg, "The Cosmological Constant Problem", Rev. Mod. Phys. **61**, edited by J.-P. Hsu and D. Fine, 1 (1989) (cit. on p. 13).

[27] M. Li, X.-D. Li, S. Wang, and Y. Wang, "Dark Energy", Commun. Theor. Phys. **56**, 525 (2011), arXiv:1103.5870 [astro-ph.CO] (cit. on p. 13).

[28] H. Georgi and S. Glashow, "Unity of All Elementary Particle Forces", Phys. Rev. Lett. **32**, 438 (1974) (cit. on p. 15).

[29] P. A. Dirac, "The Cosmological constants", Nature **139**, 323 (1937) (cit. on p. 17).

[30] P. A. Dirac, "New basis for cosmology", Proc. Roy. Soc. Lond. A **A165**, 199 (1938) (cit. on p. 17).

[31] G. 't Hooft, "Naturalness, chiral symmetry, and spontaneous chiral symmetry breaking", NATO Sci. Ser. B **59**, edited by G. 't Hooft, C. Itzykson, A. Jaffe, H. Lehmann, P. Mitter, I. Singer, and R. Stora, 135 (1980) (cit. on p. 17).

[32] M. A. Luty and T. Okui, "Conformal technicolor", JHEP **09**, 070 (2006), arXiv:hep-ph/0409274 (cit. on p. 17).

[33] R. Rattazzi, V. S. Rychkov, E. Tonni, and A. Vichi, "Bounding scalar operator dimensions in 4D CFT", JHEP **12**, 031 (2008), arXiv:0807.0004 [hep-th] (cit. on p. 17).

[34] I. Antoniadis, N. Arkani-Hamed, S. Dimopoulos, and G. R. Dvali, "New dimensions at a millimeter to a Fermi and superstrings at a TeV", Phys. Lett. **B436**, 257 (1998), arXiv:hep-ph/9804398 [hep-ph] (cit. on pp. 17, 30).

[35] N. Arkani-Hamed and S. Dimopoulos, "Supersymmetric unification without low energy supersymmetry and signatures for fine-tuning at the LHC", JHEP **06**, 073 (2005), arXiv:hep-th/0405159 [hep-th] (cit. on pp. 18, 24).

[36] S. R. Coleman and J. Mandula, "All Possible Symmetries of the S Matrix", Phys. Rev. **159**, edited by A. Zichichi, 1251 (1967) (cit. on p. 19).

[37] R. Haag, J. T. Lopuszanski, and M. Sohnius, "All Possible Generators of Supersymmetries of the s Matrix", Nucl. Phys. B **88**, 257 (1975) (cit. on p. 19).

[38] M. T. Grisaru, W. Siegel, and M. Rocek, "Improved Methods for Supergraphs", Nucl. Phys. B **159**, 429 (1979) (cit. on p. 19).

[39] N. Seiberg, "Naturalness versus supersymmetric nonrenormalization theorems", Phys. Lett. B **318**, 469 (1993), arXiv:hep-ph/9309335 (cit. on p. 19).

[40] S. P. Martin, "A Supersymmetry primer", in *Perspectives on supersymmetry. Vol.2*, Vol. 21, edited by G. L. Kane (2010), pp. 1–153, arXiv:hep-ph/9709356 (cit. on p. 19).

[41] S. P. Martin, "Some simple criteria for gauged R-parity", Phys. Rev. D **46**, 2769 (1992), arXiv:hep-ph/9207218 (cit. on p. 22).

[42] R. Kuchimanchi and R. Mohapatra, "No parity violation without R-parity violation", Phys. Rev. D **48**, 4352 (1993), arXiv:hep-ph/9306290 (cit. on p. 22).

[43] R. Kuchimanchi and R. Mohapatra, "Upper bound on the W(R) mass in automatically R conserving SUSY models", Phys. Rev. Lett. **75**, 3989 (1995), arXiv:hep-ph/9509256 (cit. on p. 22).

[44] S. P. Martin, "Implications of supersymmetric models with natural R-parity conservation", Phys. Rev. D **54**, 2340 (1996), arXiv:hep-ph/9602349 (cit. on p. 22).

[45] C. S. Aulakh, K. Benakli, and G. Senjanovic, "Reconciling supersymmetry and left-right symmetry", Phys. Rev. Lett. **79**, 2188 (1997), arXiv:hep-ph/9703434 (cit. on p. 22).

[46] C. S. Aulakh, A. Melfo, and G. Senjanovic, "Minimal supersymmetric left-right model", Phys. Rev. D **57**, 4174 (1998), arXiv:hep-ph/9707256 (cit. on p. 22).

[47] H. Goldberg, "Constraint on the Photino Mass from Cosmology", Phys. Rev. Lett. **50**, edited by M. Srednicki, [Erratum: Phys.Rev.Lett. 103, 099905 (2009)], 1419 (1983) (cit. on p. 22).

[48] J. R. Ellis, J. Hagelin, D. V. Nanopoulos, K. A. Olive, and M. Srednicki, "Supersymmetric Relics from the Big Bang", Nucl. Phys. B **238**, edited by M. Srednicki, 453 (1984) (cit. on p. 22).

[49] A. H. Chamseddine, R. L. Arnowitt, and P. Nath, "Locally Supersymmetric Grand Unification", Phys. Rev. Lett. **49**, 970 (1982) (cit. on p. 23).

[50] R. Barbieri, S. Ferrara, and C. A. Savoy, "Gauge Models with Spontaneously Broken Local Supersymmetry", Phys. Lett. B **119**, 343 (1982) (cit. on p. 23).

[51] H. P. Nilles, M. Srednicki, and D. Wyler, "Weak Interaction Breakdown Induced by Supergravity", Phys. Lett. B **120**, 346 (1983) (cit. on p. 23).

[52] E. Cremmer, P. Fayet, and L. Girardello, "Gravity Induced Supersymmetry Breaking and Low-Energy Mass Spectrum", Phys. Lett. B **122**, 41 (1983) (cit. on p. 23).

[53] L. E. Ibanez, "Locally Supersymmetric SU(5) Grand Unification", Phys. Lett. B **118**, 73 (1982) (cit. on p. 23).

[54] N. Ohta, "GRAND UNIFIED THEORIES BASED ON LOCAL SUPERSYMMETRY", Prog. Theor. Phys. **70**, 542 (1983) (cit. on p. 23).

[55] J. R. Ellis, D. V. Nanopoulos, and K. Tamvakis, "Grand Unification in Simple Supergravity", Phys. Lett. B **121**, 123 (1983) (cit. on p. 23).

[56] L. J. Hall, J. D. Lykken, and S. Weinberg, "Supergravity as the Messenger of Supersymmetry Breaking", Phys. Rev. D **27**, 2359 (1983) (cit. on p. 23).

[57] S. K. Soni and H. Weldon, "Analysis of the Supersymmetry Breaking Induced by N=1 Supergravity Theories", Phys. Lett. B **126**, 215 (1983) (cit. on p. 23).

[58] L. Alvarez-Gaume, J. Polchinski, and M. B. Wise, "Minimal Low-Energy Supergravity", Nucl. Phys. B **221**, 495 (1983) (cit. on p. 23).

[59] M. Dine, W. Fischler, and M. Srednicki, "Supersymmetric Technicolor", Nucl. Phys. B **189**, edited by J. Leveille, L. Sulak, and D. Unger, 575 (1981) (cit. on p. 23).

[60] S. Dimopoulos and S. Raby, "Supercolor", Nucl. Phys. B **192**, 353 (1981) (cit. on p. 23).

[61] M. Dine and W. Fischler, "A Phenomenological Model of Particle Physics Based on Supersymmetry", Phys. Lett. B **110**, 227 (1982) (cit. on p. 23).

[62] C. R. Nappi and B. A. Ovrut, "Supersymmetric Extension of the SU(3) x SU(2) x U(1) Model", Phys. Lett. B **113**, 175 (1982) (cit. on p. 23).

[63] L. Alvarez-Gaume, M. Claudson, and M. B. Wise, "Low-Energy Supersymmetry", Nucl. Phys. B **207**, 96 (1982) (cit. on p. 23).

[64] M. Dine and A. E. Nelson, "Dynamical supersymmetry breaking at low-energies", Phys. Rev. D **48**, 1277 (1993), arXiv:hep-ph/9303230 (cit. on p. 23).

[65] M. Dine, A. E. Nelson, Y. Nir, and Y. Shirman, "New tools for low-energy dynamical supersymmetry breaking", Phys. Rev. D **53**, 2658 (1996), arXiv:hep-ph/9507378 (cit. on p. 23).

[66] G. Giudice and R. Rattazzi, "Theories with gauge mediated supersymmetry breaking", Phys. Rept. **322**, 419 (1999), arXiv:hep-ph/9801271 (cit. on p. 23).

[67] A. M. Sirunyan et al. (CMS), "Search for top squark pair production in pp collisions at $\sqrt{s} = 13$ TeV using single lepton events", JHEP **10**, 019 (2017), arXiv:1706.04402 [hep-ex] (cit. on p. 23).

[68] A. M. Sirunyan et al. (CMS), "Search for natural and split supersymmetry in proton-proton collisions at $\sqrt{s} = 13$ TeV in final states with jets and missing transverse momentum", JHEP **05**, 025 (2018), arXiv:1802.02110 [hep-ex] (cit. on p. 23).

[69] M. Aaboud et al. (ATLAS), "Search for top squarks decaying to tau sleptons in *pp* collisions at $\sqrt{s} = 13$ TeV with the ATLAS detector", Phys. Rev. D **98**, 032008 (2018), arXiv:1803.10178 [hep-ex] (cit. on p. 23).

[70] G. Aad et al. (ATLAS), "Search for squarks and gluinos in final states with same-sign leptons and jets using 139 fb^{-1} of data collected with the ATLAS detector", JHEP **06**, 046 (2020), arXiv:1909.08457 [hep-ex] (cit. on p. 23).

[71] A. M. Sirunyan et al. (CMS), "Search for supersymmetry in proton-proton collisions at 13 TeV in final states with jets and missing transverse momentum", JHEP **10**, 244 (2019), arXiv:1908.04722 [hep-ex] (cit. on p. 23).

[72] A. M. Sirunyan et al. (CMS), "Search for supersymmetry in pp collisions at $\sqrt{s} =$ 13 TeV with 137 fb^{-1} in final states with a single lepton using the sum of masses of large-radius jets", Phys. Rev. D **101**, 052010 (2020), arXiv:1911.07558 [hep-ex] (cit. on p. 23).

[73] M. Aaboud et al. (ATLAS), "Search for supersymmetry in final states with missing transverse momentum and multiple *b*-jets in proton-proton collisions at $\sqrt{s} = 13$ TeV with the ATLAS detector", JHEP **06**, 107 (2018), arXiv:1711.01901 [hep-ex] (cit. on p. 23).

[74] L. Hall and L. Randall, "Weak scale effective supersymmetry", Phys. Rev. Lett. **65**, 2939 (1990) (cit. on p. 24).

[75] Y. Nir and N. Seiberg, "Should squarks be degenerate?", Phys. Lett. B **309**, 337 (1993), arXiv:hep-ph/9304307 (cit. on p. 24).

[76] M. Dine, A. Kagan, and S. Samuel, "Naturalness in Supersymmetry, or Raising the Supersymmetry Breaking Scale", Phys. Lett. **B243**, 250 (1990) (cit. on p. 24).

[77] S. Dimopoulos and G. F. Giudice, "Naturalness constraints in supersymmetric theories with nonuniversal soft terms", Phys. Lett. **B357**, 573 (1995), arXiv:hep-ph/9507282 [hep-ph] (cit. on pp. 24, 155).

[78] A. Pomarol and D. Tommasini, "Horizontal symmetries for the supersymmetric flavor problem", Nucl. Phys. **B466**, 3 (1996), arXiv:hep-ph/9507462 [hep-ph] (cit. on p. 24).

[79] A. G. Cohen, D. B. Kaplan, and A. E. Nelson, "The More minimal supersymmetric standard model", Phys. Lett. **B388**, 588 (1996), arXiv:hep-ph/9607394 [hep-ph] (cit. on pp. 24, 155).

[80] F. Gabbiani, E. Gabrielli, A. Masiero, and L. Silvestrini, "A Complete analysis of FCNC and CP constraints in general SUSY extensions of the standard model", Nucl. Phys. **B477**, 321 (1996), arXiv:hep-ph/9604387 [hep-ph] (cit. on p. 24).

[81] N. Arkani-Hamed and H. Murayama, "Can the supersymmetric flavor problem decouple?", Phys. Rev. **D56**, R6733 (1997), arXiv:hep-ph/9703259 [hep-ph] (cit. on pp. 24, 156).

[82] T. Moroi and M. Nagai, "Probing Supersymmetric Model with Heavy Sfermions Using Leptonic Flavor and CP Violations", Phys. Lett. **B723**, 107 (2013), arXiv:1303.0668 [hep-ph] (cit. on p. 24).

[83] J. D. Wells, "PeV-scale supersymmetry", Phys. Rev. **D71**, 015013 (2005), arXiv:hep-ph/0411041 [hep-ph] (cit. on pp. 24, 25).

[84] L. J. Hall and Y. Nomura, "A Finely-Predicted Higgs Boson Mass from A Finely-Tuned Weak Scale", JHEP **03**, 076 (2010), arXiv:0910.2235 [hep-ph] (cit. on p. 25).

[85] G. F. Giudice and A. Strumia, "Probing High-Scale and Split Supersymmetry with Higgs Mass Measurements", Nucl. Phys. **B858**, 63 (2012), arXiv:1108.6077 [hep-ph] (cit. on pp. 25, 151).

[86] A. Arvanitaki, N. Craig, S. Dimopoulos, and G. Villadoro, "Mini-Split", JHEP **02**, 126 (2013), arXiv:1210.0555 [hep-ph] (cit. on pp. 25, 152).

[87] N. Arkani-Hamed, A. Gupta, D. E. Kaplan, N. Weiner, and T. Zorawski, "Simply Unnatural Supersymmetry", (2012), arXiv:1212.6971 [hep-ph] (cit. on p. 25).

[88] B. Batell, G. F. Giudice, and M. McCullough, "Natural Heavy Supersymmetry", JHEP **12**, 162 (2015), arXiv:1509.00834 [hep-ph] (cit. on p. 25).

[89] J. L. Evans, T. Gherghetta, N. Nagata, and Z. Thomas, "Naturalizing Supersymmetry with a Two-Field Relaxion Mechanism", JHEP **09**, 150 (2016), arXiv:1602.04812 [hep-ph] (cit. on p. 25).

[90] C. Froggatt and H. B. Nielsen, "Hierarchy of Quark Masses, Cabibbo Angles and CP Violation", Nucl. Phys. B **147**, 277 (1979) (cit. on p. 26).

[91] K. Babu, "TASI Lectures on Flavor Physics", in Theoretical Advanced Study Institute in Elementary Particle Physics: The Dawn of the LHC Era (2010), pp. 49–123, arXiv:0910.2948 [hep-ph] (cit. on p. 26).

[92] W. Altmannshofer, C. Frugiuele, and R. Harnik, "Fermion Hierarchy from Sfermion Anarchy", JHEP **12**, 180 (2014), arXiv:1409.2522 [hep-ph] (cit. on p. 26).

[93] Y. Grossman and M. Neubert, "Neutrino masses and mixings in nonfactorizable geometry", Phys. Lett. **B474**, 361 (2000), arXiv:hep-ph/9912408 [hep-ph] (cit. on pp. 26, 53).

[94] T. Gherghetta and A. Pomarol, "Bulk fields and supersymmetry in a slice of AdS", Nucl. Phys. **B586**, 141 (2000), arXiv:hep-ph/0003129 [hep-ph] (cit. on pp. 26, 30, 38, 53, 152, 202, 236, 257, 260, 264).

[95] T. Gherghetta and A. Pomarol, "A Warped supersymmetric standard model", Nucl. Phys. **B602**, 3 (2001), arXiv:hep-ph/0012378 [hep-ph] (cit. on pp. 28, 30, 38, 50, 112, 130, 236).

[96] M. Gabella, T. Gherghetta, and J. Giedt, "A Gravity dual and LHC study of single-sector supersymmetry breaking", Phys. Rev. **D76**, 055001 (2007), arXiv:0704.3571 [hep-ph] (cit. on pp. 28, 50, 53).

[97] G. Nordstrom, "On the possibility of unifying the electromagnetic and the gravitational fields", Phys. Z. **15**, 504 (1914), arXiv:physics/0702221 [physics.gen-ph] (cit. on p. 29).

[98] O. Klein, "Quantum Theory and Five-Dimensional Theory of Relativity. (In German and English)", Z. Phys. **37**, [,76(1926)], 895 (1926) (cit. on p. 29).

[99] T. Appelquist, A. Chodos, and P. G. O. Freund, eds., *MODERN KALUZA-KLEIN THEORIES* (1987) (cit. on p. 29).

[100] J. M. Maldacena, "The Large N limit of superconformal field theories and supergravity", Int. J. Theor. Phys. **38**, 1113 (1999), arXiv:hep-th/9711200 (cit. on pp. 30, 45).

[101] H. Davoudiasl, J. L. Hewett, and T. G. Rizzo, "Bulk gauge fields in the Randall-Sundrum model", Phys. Lett. **B473**, 43 (2000), arXiv:hep-ph/9911262 [hep-ph] (cit. on p. 30).

[102] S. Chang, J. Hisano, H. Nakano, N. Okada, and M. Yamaguchi, "Bulk standard model in the Randall-Sundrum background", Phys. Rev. **D62**, 084025 (2000), arXiv:hep-ph/9912498 [hep-ph] (cit. on p. 30).

[103] L. Randall and R. Sundrum, "An Alternative to compactification", Phys. Rev. Lett. **83**, 4690 (1999), arXiv:hep-th/9906064 [hep-th] (cit. on p. 30).

[104] G. R. Dvali, G. Gabadadze, and M. Porrati, "4-D gravity on a brane in 5-D Minkowski space", Phys. Lett. **B485**, 208 (2000), arXiv:hep-th/0005016 [hep-th] (cit. on p. 30).

[105] E. Witten, "Search for a Realistic Kaluza-Klein Theory", Nucl. Phys. **B186**, [,29(1981)], 412 (1981) (cit. on p. 30).

[106] E. G. Adelberger, J. H. Gundlach, B. R. Heckel, S. Hoedl, and S. Schlamminger, "Torsion balance experiments: A low-energy frontier of particle physics", Prog. Part. Nucl. Phys. **62**, 102 (2009) (cit. on p. 31).

[107] J. Murata and S. Tanaka, "A review of short-range gravity experiments in the LHC era", Class. Quant. Grav. **32**, 033001 (2015), arXiv:1408.3588 [hep-ex] (cit. on p. 31).

[108] C. Csaki, "TASI lectures on extra dimensions and branes", in Theoretical Advanced Study Institute in Elementary Particle Physics (TASI 2002): Particle Physics and Cosmology: The Quest for Physics Beyond the Standard Model(s) (Apr. 2004), pp. 605–698, arXiv:hep-ph/0404096 (cit. on p. 31).

[109] R. Sundrum, "Tasi 2004 lectures: To the fifth dimension and back", in Theoretical Advanced Study Institute in Elementary Particle Physics: Physics in D $\geqq$ 4 (Aug. 2005), pp. 585–630, arXiv:hep-th/0508134 (cit. on p. 31).

[110] G. D. Kribs, "TASI 2004 lectures on the phenomenology of extra dimensions", in Theoretical Advanced Study Institute in Elementary Particle Physics: Physics in D $\geqq$ 4 (May 2006), pp. 633–699, arXiv:hep-ph/0605325 (cit. on p. 31).

[111] T. Gherghetta and A. Pomarol, "A Distorted MSSM Higgs Sector from Low-Scale Strong Dynamics", JHEP **12**, 069 (2011), arXiv:1107.4697 [hep-ph] (cit. on p. 31).

[112] E. Ponton, "TASI 2011: Four Lectures on TeV Scale Extra Dimensions", in The Dark Secrets of the Terascale: Proceedings, TASI 2011, Boulder, Colorado, USA, Jun 6 - Jul 11, 2011 (2013), pp. 283–374, arXiv:1207.3827 [hep-ph] (cit. on pp. 31, 206, 227).

[113] J. Bagger and D. V. Belyaev, "Supersymmetric branes with (almost) arbitrary tensions", Phys. Rev. **D67**, 025004 (2003), arXiv:hep-th/0206024 [hep-th] (cit. on p. 36).

[114] W. D. Goldberger and M. B. Wise, "Modulus stabilization with bulk fields", Phys. Rev. Lett. **83**, 4922 (1999), arXiv:hep-ph/9907447 [hep-ph] (cit. on p. 36).

[115] H.-S. Goh, M. A. Luty, and S.-P. Ng, "Supersymmetry without supersymmetry", JHEP **01**, 040 (2005), arXiv:hep-th/0309103 [hep-th] (cit. on p. 36).

[116] T. Gherghetta, B. von Harling, and N. Setzer, "A natural little hierarchy for RS from accidental SUSY", JHEP **07**, 011 (2011), arXiv:1104.3171 [hep-ph] (cit. on pp. 36, 95, 96).

[117] K. Agashe, H. Davoudiasl, G. Perez, and A. Soni, "Warped Gravitons at the LHC and Beyond", Phys. Rev. **D76**, 036006 (2007), arXiv:hep-ph/0701186 [hep-ph] (cit. on p. 37).

[118] A. Lukas, B. A. Ovrut, K. S. Stelle, and D. Waldram, "The Universe as a domain wall", Phys. Rev. **D59**, 086001 (1999), arXiv:hep-th/9803235 [hep-th] (cit. on p. 37).

[119] S. S. Gubser, I. R. Klebanov, and A. M. Polyakov, "Gauge theory correlators from noncritical string theory", Phys. Lett. **B428**, 105 (1998), arXiv:hep-th/9802109 [hep-th] (cit. on pp. 37, 45).

[120] H. L. Verlinde, "Holography and compactification", Nucl. Phys. **B580**, 264 (2000), arXiv:hep-th/9906182 [hep-th] (cit. on p. 37).

[121] I. R. Klebanov and M. J. Strassler, "Supergravity and a confining gauge theory: Duality cascades and chi SB resolution of naked singularities", JHEP **08**, 052 (2000), arXiv:hep-th/0007191 [hep-th] (cit. on p. 37).

[122] S. B. Giddings, S. Kachru, and J. Polchinski, "Hierarchies from fluxes in string compactifications", Phys. Rev. **D66**, 106006 (2002), arXiv:hep-th/0105097 [hep-th] (cit. on p. 37).

[123] H. Georgi, A. K. Grant, and G. Hailu, "Brane couplings from bulk loops", Phys. Lett. **B506**, 207 (2001), arXiv:hep-ph/0012379 [hep-ph] (cit. on pp. 41, 130).

[124] W. D. Goldberger, Y. Nomura, and D. Tucker-Smith, "Warped supersymmetric grand unification", Phys. Rev. **D67**, 075021 (2003), arXiv:hep-ph/0209158 [hep-ph] (cit. on pp. 41, 42, 152).

[125] Z. Chacko and E. Ponton, "Bulk gauge fields in warped space and localized supersymmetry breaking", JHEP **11**, 024 (2003), arXiv:hep-ph/0301171 [hep-ph] (cit. on pp. 41, 42, 96, 97, 112, 113).

[126] Y. Nomura and D. Tucker-Smith, "Spectrum of TeV particles in warped supersymmetric grand unification", Phys. Rev. **D68**, 075003 (2003), arXiv:hep-ph/0305214 [hep-ph] (cit. on pp. 41, 42, 97, 112, 125, 144).

[127] A. Pomarol, "Grand unified theories without the desert", Phys. Rev. Lett. **85**, 4004 (2000), arXiv:hep-ph/0005293 (cit. on p. 41).

[128] L. Randall and M. D. Schwartz, "Quantum field theory and unification in AdS5", JHEP **11**, 003 (2001), arXiv:hep-th/0108114 [hep-th] (cit. on pp. 41, 122, 130, 227).

[129] L. Randall and M. D. Schwartz, "Unification and the hierarchy from AdS5", Phys. Rev. Lett. **88**, 081801 (2002), arXiv:hep-th/0108115 (cit. on p. 41).

[130] R. Contino, P. Creminelli, and E. Trincherini, "Holographic evolution of gauge couplings", JHEP **10**, 029 (2002), arXiv:hep-th/0208002 (cit. on p. 41).

[131] K.-w. Choi, H. D. Kim, and I.-W. Kim, "Radius dependent gauge unification in AdS(5)", JHEP **03**, 034 (2003), arXiv:hep-ph/0207013 (cit. on p. 41).

[132] W. D. Goldberger and I. Z. Rothstein, "High-energy field theory in truncated AdS backgrounds", Phys. Rev. Lett. **89**, 131601 (2002), arXiv:hep-th/0204160 (cit. on p. 41).

[133] W. D. Goldberger and I. Z. Rothstein, "Effective field theory and unification in AdS backgrounds", Phys. Rev. D **68**, 125011 (2003), arXiv:hep-th/0208060 (cit. on p. 41).

[134] K. Agashe, A. Delgado, and R. Sundrum, "Gauge coupling renormalization in RS1", Nucl. Phys. B **643**, 172 (2002), arXiv:hep-ph/0206099 (cit. on p. 41).

[135] A. Falkowski and H. D. Kim, "Running of gauge couplings in AdS(5) via deconstruction", JHEP **08**, 052 (2002), arXiv:hep-ph/0208058 (cit. on p. 41).

[136] L. Randall, Y. Shadmi, and N. Weiner, "Deconstruction and gauge theories in AdS(5)", JHEP **01**, 055 (2003), arXiv:hep-th/0208120 (cit. on p. 41).

[137] K.-w. Choi and I.-W. Kim, "One loop gauge couplings in AdS(5)", Phys. Rev. D **67**, 045005 (2003), arXiv:hep-th/0208071 (cit. on p. 41).

[138] K. Agashe and A. Delgado, "A Note on CFT dual of RS model with gauge fields in bulk", Phys. Rev. **D67**, 046003 (2003), arXiv:hep-th/0209212 [hep-th] (cit. on p. 41).

[139] K. Agashe, A. Delgado, and R. Sundrum, "Grand unification in RS1", Annals Phys. **304**, 145 (2003), arXiv:hep-ph/0212028 (cit. on p. 41).

[140] G. F. Giudice and A. Masiero, "A Natural Solution to the mu Problem in Supergravity Theories", Phys. Lett. **B206**, 480 (1988) (cit. on p. 42).

[141] J. E. Kim and H. P. Nilles, "The mu Problem and the Strong CP Problem", Phys. Lett. **138B**, 150 (1984) (cit. on p. 42).

[142] M. Dine, W. Fischler, and M. Srednicki, "A Simple Solution to the Strong CP Problem with a Harmless Axion", Phys. Lett. B **104**, 199 (1981) (cit. on p. 42).

[143] A. Zhitnitsky, "On Possible Suppression of the Axion Hadron Interactions. (In Russian)", Sov. J. Nucl. Phys. **31**, 260 (1980) (cit. on p. 42).

[144] A. S. Miller, *NDRoot*, (2019) https://github.com/statius/NDRoot (cit. on p. 44).

[145] E. Witten, "Anti-de Sitter space and holography", Adv. Theor. Math. Phys. **2**, 253 (1998), arXiv:hep-th/9802150 (cit. on p. 45).

[146] O. Aharony, S. S. Gubser, J. M. Maldacena, H. Ooguri, and Y. Oz, "Large N field theories, string theory and gravity", Phys. Rept. **323**, 183 (2000), arXiv:hep-th/9905111 (cit. on p. 46).

[147] D. B. Kaplan, "Flavor at SSC energies: A New mechanism for dynamically generated fermion masses", Nucl. Phys. **B365**, 259 (1991) (cit. on p. 46).

[148] S. Weinberg, "Implications of Dynamical Symmetry Breaking", Phys. Rev. D **13**, [Addendum: Phys.Rev.D 19, 1277–1280 (1979)], 974 (1976) (cit. on p. 46).

[149] L. Susskind, "Dynamics of Spontaneous Symmetry Breaking in the Weinberg-Salam Theory", Phys. Rev. **D20**, 2619 (1979) (cit. on p. 46).

[150] J. D. Bjorken, "Neutral Current Results Without Gauge Theories", Phys. Rev. **D19**, 335 (1979) (cit. on p. 46).

[151] S. Dimopoulos and L. Susskind, "Mass Without Scalars", **2**, edited by A. Zichichi, 930 (1979) (cit. on p. 46).

[152] E. Eichten and K. D. Lane, "Dynamical Breaking of Weak Interaction Symmetries", Phys. Lett. B **90**, 125 (1980) (cit. on p. 46).

[153] E. Farhi and L. Susskind, "Technicolor", Phys. Rept. **74**, 277 (1981) (cit. on p. 46).

[154] B. Holdom, "Raising the Sideways Scale", Phys. Rev. D **24**, 1441 (1981) (cit. on p. 46).

[155] B. Holdom, "Techniodor", Phys. Lett. B **150**, 301 (1985) (cit. on p. 46).

[156] K. Yamawaki, M. Bando, and K.-i. Matumoto, "Scale Invariant Technicolor Model and a Technidilaton", Phys. Rev. Lett. **56**, 1335 (1986) (cit. on p. 46).

[157] T. W. Appelquist, D. Karabali, and L. Wijewardhana, "Chiral Hierarchies and the Flavor Changing Neutral Current Problem in Technicolor", Phys. Rev. Lett. **57**, 957 (1986) (cit. on p. 46).

[158] T. Appelquist and L. Wijewardhana, "Chiral Hierarchies and Chiral Perturbations in Technicolor", Phys. Rev. D **35**, 774 (1987) (cit. on p. 46).

[159] T. Appelquist and L. Wijewardhana, "Chiral Hierarchies from Slowly Running Couplings in Technicolor Theories", Phys. Rev. D **36**, 568 (1987) (cit. on p. 46).

[160] D. B. Kaplan and H. Georgi, "SU(2) x U(1) Breaking by Vacuum Misalignment", Phys. Lett. B **136**, 183 (1984) (cit. on p. 46).

[161] D. B. Kaplan, H. Georgi, and S. Dimopoulos, "Composite Higgs Scalars", Phys. Lett. B **136**, 187 (1984) (cit. on p. 46).

[162] K. Agashe, R. Contino, and A. Pomarol, "The Minimal composite Higgs model", Nucl. Phys. B **719**, 165 (2005), arXiv:hep-ph/0412089 (cit. on p. 46).

[163] R. Contino, L. Da Rold, and A. Pomarol, "Light custodians in natural composite Higgs models", Phys. Rev. D **75**, 055014 (2007), arXiv:hep-ph/0612048 (cit. on p. 46).

[164] N. Arkani-Hamed, A. G. Cohen, T. Gregoire, and J. G. Wacker, "Phenomenology of electroweak symmetry breaking from theory space", JHEP **08**, 020 (2002), arXiv:hep-ph/0202089 (cit. on p. 46).

[165] M. Schmaltz, "The Simplest little Higgs", JHEP **08**, 056 (2004), arXiv:hep-ph/0407143 (cit. on p. 46).

[166] G. Cacciapaglia, G. Marandella, and J. Terning, "Dimensions of Supersymmetric Operators from AdS/CFT", JHEP **06**, 027 (2009), arXiv:0802.2946 [hep-th] (cit. on p. 48).

[167] G. 't Hooft, "A Planar Diagram Theory for Strong Interactions", Nucl. Phys. B **72**, edited by J. Taylor, 461 (1974) (cit. on p. 48).

[168] G. 't Hooft, "A Two-Dimensional Model for Mesons", Nucl. Phys. B **75**, 461 (1974) (cit. on p. 48).

[169] E. Witten, "Baryons in the 1/n Expansion", Nucl. Phys. **B160**, 57 (1979) (cit. on pp. 48, 49).

[170] R. Contino and A. Pomarol, "Holography for fermions", JHEP **11**, 058 (2004), arXiv:hep-th/0406257 [hep-th] (cit. on p. 48).

[171] B. Batell and T. Gherghetta, "Holographic mixing quantified", Phys. Rev. **D76**, 045017 (2007), arXiv:0706.0890 [hep-th] (cit. on p. 50).

[172] N. Arkani-Hamed, M. A. Luty, and J. Terning, "Composite quarks and leptons from dynamical supersymmetry breaking without messengers", Phys. Rev. **D58**, 015004 (1998), arXiv:hep-ph/9712389 [hep-ph] (cit. on p. 50).

[173] M. A. Luty and J. Terning, "Improved single sector supersymmetry breaking", Phys. Rev. **D62**, 075006 (2000), arXiv:hep-ph/9812290 [hep-ph] (cit. on p. 50).

[174] S. Franco and S. Kachru, "Single-Sector Supersymmetry Breaking in Supersymmetric QCD", Phys. Rev. **D81**, 095020 (2010), arXiv:0907.2689 [hep-th] (cit. on p. 50).

[175] N. Craig, R. Essig, S. Franco, S. Kachru, and G. Torroba, "Dynamical Supersymmetry Breaking, with Flavor", Phys. Rev. **D81**, 075015 (2010), arXiv:0911.2467 [hep-ph] (cit. on p. 50).

[176] O. Aharony, L. Berdichevsky, M. Berkooz, Y. Hochberg, and D. Robles-Llana, "Inverted Sparticle Hierarchies from Natural Particle Hierarchies", Phys. Rev. **D81**, 085006 (2010), arXiv:1001.0637 [hep-ph] (cit. on p. 50).

[177] S. J. Huber and Q. Shafi, "Fermion masses, mixings and proton decay in a Randall-Sundrum model", Phys. Lett. **B498**, 256 (2001), arXiv:hep-ph/0010195 [hep-ph] (cit. on p. 53).

[178] S. J. Huber and Q. Shafi, "Majorana neutrinos in a warped 5-D standard model", Phys. Lett. **B544**, 295 (2002), arXiv:hep-ph/0205327 [hep-ph] (cit. on p. 53).

[179] S. J. Huber and Q. Shafi, "Seesaw mechanism in warped geometry", Phys. Lett. **B583**, 293 (2004), arXiv:hep-ph/0309252 [hep-ph] (cit. on pp. 53, 57, 215).

[180] S. J. Huber, "Flavor violation and warped geometry", Nucl. Phys. **B666**, 269 (2003), arXiv:hep-ph/0303183 [hep-ph] (cit. on p. 53).

[181] S. Chang, C. S. Kim, and M. Yamaguchi, "Hierarchical mass structure of fermions in warped extra dimension", Phys. Rev. **D73**, 033002 (2006), arXiv:hep-ph/0511099 [hep-ph] (cit. on p. 53).

[182] S. Casagrande, F. Goertz, U. Haisch, M. Neubert, and T. Pfoh, "Flavor Physics in the Randall-Sundrum Model: I. Theoretical Setup and Electroweak Precision Tests", JHEP **10**, 094 (2008), arXiv:0807.4937 [hep-ph] (cit. on pp. 53–55, 70, 71, 77, 78, 80).

[183] M. Bauer, S. Casagrande, U. Haisch, and M. Neubert, "Flavor Physics in the Randall-Sundrum Model: II. Tree-Level Weak-Interaction Processes", JHEP **09**, 017 (2010), arXiv:0912.1625 [hep-ph] (cit. on p. 53).

[184] A. M. Iyer and S. K. Vempati, "Lepton Masses and Flavor Violation in Randall Sundrum Model", Phys. Rev. **D86**, 056005 (2012), arXiv:1206.4383 [hep-ph] (cit. on pp. 53, 57, 215).

[185] A. M. Iyer and S. K. Vempati, "Bulk Majorana mass terms and Dirac neutrinos in the Randall-Sundrum model", Phys. Rev. **D88**, 073005 (2013), arXiv:1307.5773 [hep-ph] (cit. on p. 53).

[186] A. M. Iyer and S. K. Vempati, "Warped Alternatives to Froggatt-Nielsen Models", Phys. Rev. **D88**, 016005 (2013), arXiv:1304.3558 [hep-ph] (cit. on p. 53).

[187] L. Wolfenstein, "Parametrization of the Kobayashi-Maskawa Matrix", Phys. Rev. Lett. **51**, 1945 (1983) (cit. on p. 55).

[188] S. Descotes-Genon and P. Koppenburg, "The CKM Parameters", Ann. Rev. Nucl. Part. Sci. **67**, 97 (2017), arXiv:1702.08834 [hep-ex] (cit. on p. 55).

[189] A. J. Buras, M. E. Lautenbacher, and G. Ostermaier, "Waiting for the top quark mass, K+ —> pi+ neutrino anti-neutrino, B(s)0 - anti-B(s)0 mixing and CP asymmetries in B decays", Phys. Rev. **D50**, 3433 (1994), arXiv:hep-ph/9403384 [hep-ph] (cit. on p. 55).

[190] J. Charles, A. Hocker, H. Lacker, S. Laplace, F. R. Le Diberder, J. Malcles, J. Ocariz, M. Pivk, and L. Roos (CKMfitter Group), "CP violation and the CKM matrix: Assessing the impact of the asymmetric B factories", Eur. Phys. J. **C41**, 1 (2005), arXiv:hep-ph/0406184 [hep-ph] (cit. on pp. 56, 57).

[191] CKMfitter Group, *Updated results on the CKM matrix including results presented up to Summer 18 (Preliminary)*, (2018) http://ckmfitter.in2p3.fr (cit. on pp. 56, 57).

[192] C. Jarlskog, "Commutator of the Quark Mass Matrices in the Standard Electroweak Model and a Measure of Maximal CP Violation", Phys. Rev. Lett. **55**, 1039 (1985) (cit. on p. 56).

[193] I. Esteban, M. C. Gonzalez-Garcia, A. Hernandez-Cabezudo, M. Maltoni, and T. Schwetz, "Global analysis of three-flavour neutrino oscillations: synergies and tensions in the determination of $\theta_{23}, \delta_C P$, and the mass ordering", JHEP **01**, 106 (2019), arXiv:1811.05487 [hep-ph] (cit. on p. 60).

[194] NuFIT, *NuFIT v4.1: Three-neutrino fit based on data available in July 2019*, (2019) http://www.nu-fit.org (cit. on p. 60).

[195] F. Capozzi, E. Di Valentino, E. Lisi, A. Marrone, A. Melchiorri, and A. Palazzo, "Global constraints on absolute neutrino masses and their ordering", Phys. Rev. **D95**, 096014 (2017), arXiv:1703.04471 [hep-ph] (cit. on p. 60).

[196] S. P. Martin and D. G. Robertson, "Standard model parameters in the tadpole-free pure $\overline{\rm MS}$ scheme", Phys. Rev. D **100**, 073004 (2019), arXiv:1907.02500 [hep-ph] (cit. on p. 66).

[197] S. P. Martin and M. T. Vaughn, "Regularization dependence of running couplings in softly broken supersymmetry", Phys. Lett. B **318**, 331 (1993), arXiv:hep-ph/9308222 (cit. on p. 67).

[198] A. S. Miller, *RunningCouplings*, (2019) https://github.com/statius/RunningCouplings (cit. on p. 67).

[199] G. von Gersdorff, "Universal approximations for flavor models", JHEP **07**, 131 (2019), arXiv:1903.11077 [hep-ph] (cit. on pp. 70–74).

[200] M. Aker et al. (KATRIN), "An improved upper limit on the neutrino mass from a direct kinematic method by KATRIN", (2019), arXiv:1909.06048 [hep-ex] (cit. on p. 81).

[201] A. Loureiro et al., "On The Upper Bound of Neutrino Masses from Combined Cosmological Observations and Particle Physics Experiments", Phys. Rev. Lett. **123**, 081301 (2019), arXiv:1811.02578 [astro-ph.CO] (cit. on p. 81).

[202] F. James and M. Roos, "Minuit: A System for Function Minimization and Analysis of the Parameter Errors and Correlations", Comput. Phys. Commun. **10**, 343 (1975) (cit. on p. 94).

[203] iminuit team, *Iminuit – a python interface to minuit*, https://github.com/scikit-hep/iminuit (cit. on p. 94).

[204] A. S. Miller, *Minuit*, (2019) https://github.com/statius/Minuit (cit. on p. 94).

[205] L. Randall and R. Sundrum, "Out of this world supersymmetry breaking", Nucl. Phys. **B557**, 79 (1999), arXiv:hep-th/9810155 [hep-th] (cit. on p. 96).

[206] M. A. Luty and R. Sundrum, "Hierarchy stabilization in warped supersymmetry", Phys. Rev. **D64**, 065012 (2001), arXiv:hep-th/0012158 [hep-th] (cit. on p. 96).

[207] M. A. Luty, "Weak scale supersymmetry without weak scale supergravity", Phys. Rev. Lett. **89**, 141801 (2002), arXiv:hep-th/0205077 [hep-th] (cit. on p. 96).

[208] T. Gherghetta and A. Pomarol, "A Stuckelberg formalism for the gravitino from warped extra dimensions", Phys. Lett. **B536**, 277 (2002), arXiv:hep-th/0203120 [hep-th] (cit. on pp. 96, 236).

[209] H. Itoh, N. Okada, and T. Yamashita, "Low scale gravity mediation with warped extra dimension and collider phenomenology on the hidden sector", Phys. Rev. **D74**, 055005 (2006), arXiv:hep-ph/0606156 [hep-ph] (cit. on p. 96).

[210] B. Heidenreich and Y. Nakai, "Natural Supersymmetry in Warped Space", JHEP **10**, 182 (2014), arXiv:1407.5095 [hep-ph] (cit. on p. 98).

[211] J. Garriga and T. Tanaka, "Gravity in the brane world", Phys. Rev. Lett. **84**, 2778 (2000), arXiv:hep-th/9911055 [hep-th] (cit. on p. 112).

[212] S. B. Giddings, E. Katz, and L. Randall, "Linearized gravity in brane backgrounds", JHEP **03**, 023 (2000), arXiv:hep-th/0002091 [hep-th] (cit. on p. 112).

[213] B. Grinstein, D. R. Nolte, and W. Skiba, "On a Covariant determination of mass scales in warped backgrounds", Phys. Rev. **D63**, 105005 (2001), arXiv:hep-th/0012074 [hep-th] (cit. on p. 112).

[214] C. Csaki, Y. Grossman, P. Tanedo, and Y. Tsai, "Warped penguin diagrams", Phys. Rev. **D83**, 073002 (2011), arXiv:1004.2037 [hep-ph] (cit. on pp. 112, 113).

[215] C. Bouchart, A. Knochel, and G. Moreau, "Discriminating 4D supersymmetry from its 5D warped version", Phys. Rev. **D84**, 015016 (2011), arXiv:1101.0634 [hep-ph] (cit. on pp. 128, 132, 134, 136, 137, 140).

[216] E. A. Mirabelli and M. E. Peskin, "Transmission of supersymmetry breaking from a four-dimensional boundary", Phys. Rev. **D58**, 065002 (1998), arXiv:hep-th/9712214 [hep-th] (cit. on pp. 128, 137).

[217] A. Delgado, A. Pomarol, and M. Quiros, "Supersymmetry and electroweak breaking from extra dimensions at the TeV scale", Phys. Rev. **D60**, 095008 (1999), arXiv:hep-ph/9812489 [hep-ph] (cit. on pp. 128, 130, 137, 144).

[218] N. Arkani-Hamed, L. J. Hall, Y. Nomura, D. Tucker-Smith, and N. Weiner, "Finite radiative electroweak symmetry breaking from the bulk", Nucl. Phys. **B605**, 81 (2001), arXiv:hep-ph/0102090 [hep-ph] (cit. on pp. 128, 134, 137, 140).

[219] I. Antoniadis, S. Dimopoulos, and G. R. Dvali, "Millimeter range forces in superstring theories with weak scale compactification", Nucl. Phys. **B516**, 70 (1998), arXiv:hep-ph/9710204 [hep-ph] (cit. on p. 130).

[220] I. Antoniadis, S. Dimopoulos, A. Pomarol, and M. Quiros, "Soft masses in theories with supersymmetry breaking by TeV compactification", Nucl. Phys. **B544**, 503 (1999), arXiv:hep-ph/9810410 [hep-ph] (cit. on pp. 130, 137, 144).

[221] H.-C. Cheng, K. T. Matchev, and M. Schmaltz, "Radiative corrections to Kaluza-Klein masses", Phys. Rev. **D66**, 036005 (2002), arXiv:hep-ph/0204342 [hep-ph] (cit. on p. 130).

[222] M. Puchwein and Z. Kunszt, "Radiative corrections with 5-D mixed position / momentum space propagators", Annals Phys. **311**, 288 (2004), arXiv:hep-th/0309069 [hep-th] (cit. on p. 130).

[223] A. Freitas, K. Kong, and D. Wiegand, "Radiative corrections to masses and couplings in Universal Extra Dimensions", JHEP **03**, 093 (2018), arXiv:1711.07526 [hep-ph] (cit. on p. 130).

[224] T. Hirayama and K. Yoshioka, "Anomalies and Fayet-Iliopoulos terms on warped orbifolds and large hierarchies", JHEP **01**, 032 (2004), arXiv:hep-th/0311233 [hep-th] (cit. on p. 132).

[225] T. Gherghetta and A. Pomarol, "The Standard model partly supersymmetric", Phys. Rev. **D67**, 085018 (2003), arXiv:hep-ph/0302001 [hep-ph] (cit. on p. 137).

[226] S. Abel and T. Gherghetta, "A slice of AdS_5 as the large N limit of Seiberg duality", JHEP **12**, 091 (2010), arXiv:1010.5655 [hep-th] (cit. on pp. 137, 138).

[227] H. Pagels and J. R. Primack, "Supersymmetry, Cosmology and New TeV Physics", Phys. Rev. Lett. **48**, 223 (1982) (cit. on p. 147).

[228] J. L. Feng, M. Kamionkowski, and S. K. Lee, "Light Gravitinos at Colliders and Implications for Cosmology", Phys. Rev. **D82**, 015012 (2010), arXiv:1004.4213 [hep-ph] (cit. on p. 147).

[229] K. Osato, T. Sekiguchi, M. Shirasaki, A. Kamada, and N. Yoshida, "Cosmological Constraint on the Light Gravitino Mass from CMB Lensing and Cosmic Shear", JCAP **1606**, 004 (2016), arXiv:1601.07386 [astro-ph.CO] (cit. on p. 147).

[230] J. R. Ellis, A. D. Linde, and D. V. Nanopoulos, "Inflation Can Save the Gravitino", Phys. Lett. **118B**, 59 (1982) (cit. on p. 148).

[231] M. Viel, J. Lesgourgues, M. G. Haehnelt, S. Matarrese, and A. Riotto, "Constraining warm dark matter candidates including sterile neutrinos and light gravitinos with WMAP and the Lyman-alpha forest", Phys. Rev. **D71**, 063534 (2005), arXiv:astro-ph/0501562 [astro-ph] (cit. on p. 148).

[232] V. Iršič et al., "New Constraints on the free-streaming of warm dark matter from intermediate and small scale Lyman-α forest data", Phys. Rev. **D96**, 023522 (2017), arXiv:1702.01764 [astro-ph.CO] (cit. on p. 148).

[233] C. Yèche, N. Palanque-Delabrouille, J. Baur, and H. du Mas des Bourboux, "Constraints on neutrino masses from Lyman-alpha forest power spectrum with BOSS and XQ-100", JCAP **1706**, 047 (2017), arXiv:1702.03314 [astro-ph.CO] (cit. on p. 148).

[234] J. L. Feng, A. Rajaraman, and F. Takayama, "Superweakly interacting massive particles", Phys. Rev. Lett. **91**, 011302 (2003), arXiv:hep-ph/0302215 [hep-ph] (cit. on p. 149).

[235] M. Pospelov, "Particle physics catalysis of thermal Big Bang Nucleosynthesis", Phys. Rev. Lett. **98**, 231301 (2007), arXiv:hep-ph/0605215 [hep-ph] (cit. on p. 150).

[236] J. Pradler and F. D. Steffen, "Constraints on the Reheating Temperature in Gravitino Dark Matter Scenarios", Phys. Lett. **B648**, 224 (2007), arXiv:hep-ph/0612291 [hep-ph] (cit. on p. 150).

[237] V. Khachatryan et al. (CMS), "Search for new physics in final states with two opposite-sign, same-flavor leptons, jets, and missing transverse momentum in pp collisions at sqrt(s) = 13 TeV", JHEP **12**, 013 (2016), arXiv:1607.00915 [hep-ex] (cit. on p. 152).

[238] V. Khachatryan et al. (CMS), "Search for supersymmetry in events with photons and missing transverse energy in pp collisions at 13 TeV", Phys. Lett. **B769**, 391 (2017), arXiv:1611.06604 [hep-ex] (cit. on p. 152).

[239] A. M. Sirunyan et al. (CMS), "Search for supersymmetry in events with at least one photon, missing transverse momentum, and large transverse event activity in proton-proton collisions at $\sqrt{s} = 13$ TeV", JHEP **12**, 142 (2017), arXiv:1707.06193 [hep-ex] (cit. on p. 152).

[240] G. Aad et al. (ATLAS), "Search for direct top squark pair production in final states with two tau leptons in pp collisions at $\sqrt{s} = 8$ TeV with the ATLAS detector", Eur. Phys. J. **C76**, 81 (2016), arXiv:1509.04976 [hep-ex] (cit. on p. 152).

[241] M. Carena, S. Pokorski, and C. E. M. Wagner, "On the unification of couplings in the minimal supersymmetric Standard Model", Nucl. Phys. **B406**, 59 (1993), arXiv:hep-ph/9303202 [hep-ph] (cit. on p. 152).

[242] K. Agashe and G. Servant, "Baryon number in warped GUTs: Model building and (dark matter related) phenomenology", JCAP **0502**, 002 (2005), arXiv:hep-ph/0411254 [hep-ph] (cit. on p. 152).

[243] M. Frigerio, J. Serra, and A. Varagnolo, "Composite GUTs: models and expectations at the LHC", JHEP **06**, 029 (2011), arXiv:1103.2997 [hep-ph] (cit. on p. 152).

[244] D. M. Pierce, J. A. Bagger, K. T. Matchev, and R.-j. Zhang, "Precision corrections in the minimal supersymmetric standard model", Nucl. Phys. **B491**, 3 (1997), arXiv:hep-ph/9606211 [hep-ph] (cit. on pp. 157, 165).

[245] P. Athron, J.-h. Park, D. Stöckinger, and A. Voigt, "FlexibleSUSY—A spectrum generator generator for supersymmetric models", Comput. Phys. Commun. **190**, 139 (2015), arXiv:1406.2319 [hep-ph] (cit. on pp. 163, 166).

[246] P. Athron, M. Bach, D. Harries, T. Kwasnitza, J.-h. Park, D. Stöckinger, A. Voigt, and J. Ziebell, "FlexibleSUSY 2.0: Extensions to investigate the phenomenology of SUSY and non-SUSY models", (2017), arXiv:1710.03760 [hep-ph] (cit. on pp. 163, 166).

[247] F. Staub, "From Superpotential to Model Files for FeynArts and CalcHep/CompHep", Comput. Phys. Commun. **181**, 1077 (2010), arXiv:0909.2863 [hep-ph] (cit. on pp. 163, 166).

[248] F. Staub, "Automatic Calculation of supersymmetric Renormalization Group Equations and Self Energies", Comput. Phys. Commun. **182**, 808 (2011), arXiv:1002.0840 [hep-ph] (cit. on pp. 163, 166).

[249] F. Staub, "SARAH 3.2: Dirac Gauginos, UFO output, and more", Comput. Phys. Commun. **184**, 1792 (2013), arXiv:1207.0906 [hep-ph] (cit. on pp. 163, 166).

[250] F. Staub, "SARAH 4 : A tool for (not only SUSY) model builders", Comput. Phys. Commun. **185**, 1773 (2014), arXiv:1309.7223 [hep-ph] (cit. on pp. 163, 166).

[251] B. C. Allanach, "SOFTSUSY: a program for calculating supersymmetric spectra", Comput. Phys. Commun. **143**, 305 (2002), arXiv:hep-ph/0104145 [hep-ph] (cit. on pp. 163, 166).

[252] B. C. Allanach, P. Athron, L. C. Tunstall, A. Voigt, and A. G. Williams, "Next-to-Minimal SOFTSUSY", Comput. Phys. Commun. **185**, 2322 (2014), arXiv:1311.7659 [hep-ph] (cit. on pp. 163, 166).

[253] G. Degrassi, P. Slavich, and F. Zwirner, "On the neutral Higgs boson masses in the MSSM for arbitrary stop mixing", Nucl. Phys. **B611**, 403 (2001), arXiv:hep-ph/0105096 [hep-ph] (cit. on pp. 163, 166).

[254] A. Brignole, G. Degrassi, P. Slavich, and F. Zwirner, "On the O(alpha(t)**2) two loop corrections to the neutral Higgs boson masses in the MSSM", Nucl. Phys. **B631**, 195 (2002), arXiv:hep-ph/0112177 [hep-ph] (cit. on pp. 163, 166).

[255] A. Dedes and P. Slavich, "Two loop corrections to radiative electroweak symmetry breaking in the MSSM", Nucl. Phys. **B657**, 333 (2003), arXiv:hep-ph/0212132 [hep-ph] (cit. on pp. 163, 166).

[256] A. Brignole, G. Degrassi, P. Slavich, and F. Zwirner, "On the two loop sbottom corrections to the neutral Higgs boson masses in the MSSM", Nucl. Phys. **B643**, 79 (2002), arXiv:hep-ph/0206101 [hep-ph] (cit. on pp. 163, 166).

[257] A. Dedes, G. Degrassi, and P. Slavich, "On the two loop Yukawa corrections to the MSSM Higgs boson masses at large tan beta", Nucl. Phys. **B672**, 144 (2003), arXiv:hep-ph/0305127 [hep-ph] (cit. on pp. 163, 166).

[258] I. Jack, D. R. T. Jones, and A. F. Kord, "Three loop soft running, benchmark points and semiperturbative unification", Phys. Lett. **B579**, 180 (2004), arXiv:hep-ph/0308231 [hep-ph] (cit. on p. 163).

[259] I. Jack, D. R. T. Jones, and A. F. Kord, "Snowmass benchmark points and three-loop running", Annals Phys. **316**, 213 (2005), arXiv:hep-ph/0408128 [hep-ph] (cit. on p. 163).

[260] C. Tamarit, "Decoupling heavy sparticles in Effective SUSY scenarios: Unification, Higgs masses and tachyon bounds", JHEP **06**, 080 (2012), arXiv:1204.2645 [hep-ph] (cit. on p. 165).

[261] C. Tamarit, "Decoupling heavy sparticles in hierarchical SUSY scenarios: Two-loop Renormalization Group equations", (2012), arXiv:1204.2292 [hep-ph] (cit. on p. 165).

[262] C. Tamarit, "Large, negative threshold contributions to light soft masses in models with Effective Supersymmetry", Phys. Rev. **D86**, 115003 (2012), arXiv:1206.6140 [hep-ph] (cit. on p. 165).

[263] E. Bagnaschi, J. Pardo Vega, and P. Slavich, "Improved determination of the Higgs mass in the MSSM with heavy superpartners", Eur. Phys. J. **C77**, 334 (2017), arXiv:1703.08166 [hep-ph] (cit. on p. 166).

[264] K. G. Chetyrkin and M. Steinhauser, "The Relation between the MS-bar and the on-shell quark mass at order alpha(s)**3", Nucl. Phys. **B573**, 617 (2000), arXiv:hep-ph/9911434 [hep-ph] (cit. on p. 166).

[265] K. Melnikov and T. v. Ritbergen, "The Three loop relation between the MS-bar and the pole quark masses", Phys. Lett. **B482**, 99 (2000), arXiv:hep-ph/9912391 [hep-ph] (cit. on p. 166).

[266] K. G. Chetyrkin, J. H. Kuhn, and M. Steinhauser, "RunDec: A Mathematica package for running and decoupling of the strong coupling and quark masses", Comput. Phys. Commun. **133**, 43 (2000), arXiv:hep-ph/0004189 [hep-ph] (cit. on p. 166).

[267] G. Degrassi, S. Di Vita, J. Elias-Miro, J. R. Espinosa, G. F. Giudice, G. Isidori, and A. Strumia, "Higgs mass and vacuum stability in the Standard Model at NNLO", JHEP **08**, 098 (2012), arXiv:1205.6497 [hep-ph] (cit. on p. 166).

[268] S. P. Martin and D. G. Robertson, "Higgs boson mass in the Standard Model at two-loop order and beyond", Phys. Rev. **D90**, 073010 (2014), arXiv:1407.4336 [hep-ph] (cit. on p. 166).

[269] S. P. Martin, "Four-Loop Standard Model Effective Potential at Leading Order in QCD", Phys. Rev. **D92**, 054029 (2015), arXiv:1508.00912 [hep-ph] (cit. on p. 166).

[270] A. V. Bednyakov, A. F. Pikelner, and V. N. Velizhanin, "Higgs self-coupling beta-function in the Standard Model at three loops", Nucl. Phys. **B875**, 552 (2013), arXiv:1303.4364 [hep-ph] (cit. on p. 166).

[271] D. Buttazzo, G. Degrassi, P. P. Giardino, G. F. Giudice, F. Sala, A. Salvio, and A. Strumia, "Investigating the near-criticality of the Higgs boson", JHEP **12**, 089 (2013), arXiv:1307.3536 [hep-ph] (cit. on p. 166).

[272] J. Pardo Vega and G. Villadoro, "SusyHD: Higgs mass Determination in Supersymmetry", JHEP **07**, 159 (2015), arXiv:1504.05200 [hep-ph] (cit. on p. 166).

[273] K. G. Chetyrkin and M. F. Zoller, "Leading QCD-induced four-loop contributions to the β-function of the Higgs self-coupling in the SM and vacuum stability", JHEP **06**, 175 (2016), arXiv:1604.00853 [hep-ph] (cit. on p. 166).

[274] A. V. Bednyakov and A. F. Pikelner, "Four-loop strong coupling beta-function in the Standard Model", Phys. Lett. **B762**, 151 (2016), arXiv:1508.02680 [hep-ph] (cit. on p. 166).

[275] P. Athron, J.-h. Park, T. Steudtner, D. Stöckinger, and A. Voigt, "Precise Higgs mass calculations in (non-)minimal supersymmetry at both high and low scales", JHEP **01**, 079 (2017), arXiv:1609.00371 [hep-ph] (cit. on p. 166).

[276] P. Z. Skands et al., "SUSY Les Houches accord: Interfacing SUSY spectrum calculators, decay packages, and event generators", JHEP **07**, 036 (2004), arXiv:hep-ph/0311123 (cit. on p. 168).

[277] B. Allanach et al., "SUSY Les Houches Accord 2", Comput. Phys. Commun. **180**, 8 (2009), arXiv:0801.0045 [hep-ph] (cit. on p. 168).

[278] A. S. Miller, *LesHouches*, (2019) https://github.com/statius/LesHouches (cit. on p. 168).

[279] L. Bartoszek et al. (Mu2e), "Mu2e Technical Design Report", (2014), arXiv:1501.05241 [physics.ins-det] (cit. on p. 176).

[280] V. Andreev et al. (ACME), "Improved limit on the electric dipole moment of the electron", Nature **562**, 355 (2018) (cit. on p. 176).

[281] T. Gherghetta, "A Holographic View of Beyond the Standard Model Physics", in Physics of the large and the small, TASI 09, proceedings of the Theoretical Advanced Study Institute in Elementary Particle Physics, Boulder, Colorado, USA, 1-26 June 2009 (2011), pp. 165–232, arXiv:1008.2570 [hep-ph] (cit. on p. 206).

[282] P. Breitenlohner and D. Z. Freedman, "Positive Energy in anti-De Sitter Backgrounds and Gauged Extended Supergravity", Phys. Lett. **115B**, 197 (1982) (cit. on p. 207).

[283] P. Breitenlohner and D. Z. Freedman, "Stability in Gauged Extended Supergravity", Annals Phys. **144**, 249 (1982) (cit. on p. 207).

[284] A. Watanabe and K. Yoshioka, "Geometry-free neutrino masses in curved spacetime", Phys. Lett. **B683**, 289 (2010), arXiv:0910.0677 [hep-ph] (cit. on p. 215).

[285] E. Shuster, "Killing spinors and supersymmetry on AdS", Nucl. Phys. B **554**, 198 (1999), arXiv:hep-th/9902129 (cit. on p. 257).

[286] J. Scherk and J. H. Schwarz, "How to Get Masses from Extra Dimensions", Nucl. Phys. B **153**, edited by A. Salam and E. Sezgin, 61 (1979) (cit. on p. 259).

[287] J. Scherk and J. H. Schwarz, "Spontaneous Breaking of Supersymmetry Through Dimensional Reduction", Phys. Lett. B **82**, 60 (1979) (cit. on p. 259).

A Spinor Structure in Five Dimensions

This appendix provides the details of the spinor formalism we employ for bulk fermion fields. We first review the structure of the Clifford algebra in curved spacetime, before specializing to five-dimensional AdS. We then discuss the spin-$\frac{1}{2}$ representation of the Lorentz group in five dimensions, constructing both Dirac and symplectic Majorana spinors.

A.1 The Clifford Algebra in Curved Spacetime

In a curved spacetime with metric $g_{\mu\nu}$, the Clifford algebra is

$$\{\Gamma_\mu, \Gamma_\nu\} = 2g_{\mu\nu}\, I_4\,. \tag{A.1}$$

In the absence of curvature, this must reduce to the Lorentzian definition:

$$\{\gamma_a, \gamma_b\} = 2\eta_{ab}\, I_4\,. \tag{A.2}$$

At each point, the spacetime manifold can be considered to be locally flat. Formally, we can define a local change of basis, such that

$$g_{\mu\nu} = e_\mu{}^a\, e_\nu{}^b\, \eta_{ab}\,. \tag{A.3}$$

Here, $e_\mu{}^a$ are the coefficients of a tensor known as the vielbein,

$$e = e_\mu{}^a\, \mathrm{d}x^\mu \otimes \partial_a \tag{A.4}$$

which defines at each spacetime point a mapping to a Lorentzian tangent space:

$$\mathrm{d}x^a = e_\mu{}^a\, \mathrm{d}x^\mu\,, \tag{A.5a}$$

$$\mathrm{d}x^\mu = e^\mu{}_a \, \mathrm{d}x^a \,, \tag{A.5b}$$

We note that the Greek manifold coordinate vielbein indices are raised and lowered by the general metric $g_{\mu\nu}$ and the Roman Lorentzian indices by the flat metric η_{ab}: e.g.,

$$e^\mu{}_a = g^{\mu\nu} \, \eta_{ab} \, e_\nu{}^b \,. \tag{A.6}$$

The Clifford algebra in curved spacetime can therefore be constructed from the flat space algebra (A.2) as

$$\Gamma_\mu = e_\mu{}^a \, \gamma_a \,. \tag{A.7}$$

The local frame transformation (A.3) can be regarded as a gauging of local Lorentz transformations, and accordingly induces a connection for spinor representations of the Lorentz group. To take this into account, we define the spinor covariant derivative

$$D_\mu = \partial_\mu + \omega_\mu = \partial_\mu - \frac{i}{2} \omega_\mu{}^{ab} S_{ab} = \partial_\mu + \frac{1}{8} \omega_\mu{}^{ab} [\gamma_a, \gamma_b] \,, \tag{A.8}$$

where ω_μ is the spin connection and $S_{ab} = \frac{i}{4} [\gamma_a, \gamma_b]$ are the generators of the Lorentz group. Because the vielbein establishes the flat tangent space at each point, it also defines the connection:

$$\omega_\mu{}^{ab} = e_\nu{}^a \partial_{;\mu} \, e^{\nu b} = e_\nu{}^a \, \Gamma^\nu_{\lambda\mu} \, e^{\lambda b} + e_\nu{}^a \, \partial_\mu \, e^{\nu b} \,, \tag{A.9}$$

where $\partial_{;\mu}$ is the gravitational covariant derivative and $\Gamma^\lambda_{\mu\nu}$ are the Christoffel symbols.

A.1.1 Five-dimensional Anti-de Sitter Spacetime

In the specific case of five-dimensional anti-de Sitter spacetime, we see from the metric (3.16) and the definition of the vielbein[1] (A.3) that

$$e^M{}_a = \mathrm{diag}(e^A, e^A, e^A, e^A, 1) \,, \tag{A.10}$$

and the generalized gamma matrices are

$$\Gamma_M = e_M{}^a \gamma_a = \left(e^{-A} \gamma_\mu, \gamma_5\right) . \tag{A.11}$$

[1] In five dimensions, specifically, the fünfbein.

For the metric (3.16), the nonzero Christoffel symbols are

$$\Gamma^5_{\mu\mu} = A' e^{-2A} \eta_{\mu\mu} \,, \tag{A.12a}$$

$$\Gamma^\mu_{5\mu} = -A' \,, \tag{A.12b}$$

$$\Gamma^\mu_{\mu 5} = -A' \,, \tag{A.12c}$$

and thus, the spin connection is

$$\omega_{_M} = \left(-\tfrac{1}{2} A' e^{-A} \gamma_\mu \gamma_5, 0\right) . \tag{A.13}$$

A.2 Dirac Spinors

A convenient representation of the Lorentzian gamma matrices $\gamma^a = (\gamma^\mu, \gamma^5)$ satisfying (A.2) (for the mostly positive metric convention) in five dimensions is given by[2]

$$\gamma^\mu = -i \begin{pmatrix} 0 & \sigma^\mu_{a\dot{c}} \\ \overline{\sigma}^{\mu \dot{a} c} & 0 \end{pmatrix} , \qquad \gamma^5 = -i\gamma_0\gamma_1\gamma_2\gamma_3 = \begin{pmatrix} \delta_a{}^c & 0 \\ 0 & -\delta^{\dot{a}}{}_{\dot{c}} \end{pmatrix} , \tag{A.15}$$

where we have made the spinor indices explicit. Numerically,

$$\sigma^\mu_{a\dot{c}} \equiv \left(I_2, \sigma^i\right) , \tag{A.16a}$$

$$\overline{\sigma}^{\mu \dot{a} c} \equiv \left(I_2, -\sigma^i\right) , \tag{A.16b}$$

[2]Note that in this convention, for a four-vector a_μ,

$$\not{a}\not{a} = a_\mu \gamma^\mu a_\nu \gamma^\nu = \eta^{\mu\nu} a_\mu a_\nu I_4 = a^2 I_4 \,. \tag{A.14}$$

with the Pauli matrices[3]

$$\sigma_1 = \sigma_x = \begin{pmatrix} 0 & 1 \\ 1 & 0 \end{pmatrix}, \qquad \sigma_2 = \sigma_y = \begin{pmatrix} 0 & -i \\ i & 0 \end{pmatrix}, \qquad \sigma_3 = \sigma_z = \begin{pmatrix} 1 & 0 \\ 0 & -1 \end{pmatrix}. \tag{A.18}$$

The fifth gamma matrix acts as the chirality operator, such that Dirac spinor fields can be decomposed as

$$\Psi = \Psi_L + \Psi_R\,, \tag{A.19}$$

where $\Psi_{L,R}$ are chiral eigenstates[4],

$$\gamma^5 \Psi_{L,R} = \pm \Psi_{L,R}\,, \tag{A.21}$$

which can be defined via left and right projection

$$\Psi_{L,R} = \tfrac{1}{2}(I_4 \pm \gamma_5)\Psi \equiv P_{L,R}\Psi\,. \tag{A.22}$$

In terms of Weyl spinors, we identify

$$\Psi = \begin{pmatrix} (\psi_L)_a \\ (\psi_R^\dagger)^{\dot a} \end{pmatrix}, \qquad \Psi_L = \begin{pmatrix} (\psi_L)_a \\ 0 \end{pmatrix}, \qquad \Psi_R = \begin{pmatrix} 0 \\ (\psi_R^\dagger)^{\dot a} \end{pmatrix}. \tag{A.23}$$

The *Dirac conjugate* spinor is defined as

$$\overline{\Psi} = \Psi^\dagger \mathcal{D} = \begin{pmatrix} (\psi_R)^a & (\psi_L^\dagger)_{\dot a} \end{pmatrix}, \tag{A.24}$$

[3]Note that in this convention

$$(\sigma^\mu \overline{\sigma}^\nu + \sigma^\nu \overline{\sigma}^\mu)_a{}^c = -2g^{\mu\nu}\delta_a{}^c\,, \tag{A.17a}$$

$$(\overline{\sigma}^\mu \sigma^\nu + \overline{\sigma}^\nu \sigma^\mu)^{\dot a}{}_{\dot c} = -2g^{\mu\nu}\delta^{\dot a}{}_{\dot c}\,. \tag{A.17b}$$

[4]Note that this is opposite the usual chirality convention,

$$\gamma^5 \Psi_{L,R} = \mp \Psi_{L,R}\,. \tag{A.20}$$

This is due to the definition of γ_5 in (A.15), which reverses the sign of usual convention $\gamma_5 = i\gamma_0\gamma_1\gamma_2\gamma_3$. This usage is historical (see Ref. [94]) and determines the sign convention for parametrization of the localizations of the zero modes of the chiral spinor components in terms of the bulk dirac mass coefficients (B.41).

where

$$\mathcal{D} \equiv \begin{pmatrix} 0 & \delta^{\dot{a}}{}_{\dot{c}} \\ \delta_a{}^c & 0 \end{pmatrix} \tag{A.25}$$

is the Dirac conjugation matrix (numerically, $\mathcal{D} = i\gamma_0$, although the spinor index structure is different), such that products of the form

$$\overline{\Psi}\Psi = \overline{\Psi}_R \Psi_L + \overline{\Psi}_L \Psi_R = \psi_R\, \psi_L + \psi_R^\dagger\, \psi_L^\dagger\,, \tag{A.26}$$

where $\overline{\Psi}_{L,R} \equiv \Psi_{L,R}^\dagger \mathcal{D} = \overline{\Psi} P_{R,L}$, are Lorentz-invariant. Additionally, we can introduce the *charge conjugate* spinor,

$$\Psi^c \equiv \mathcal{C}_5 \overline{\Psi}^{\mathrm{T}} = \begin{pmatrix} -(\psi_R)_a \\ (\psi_L^\dagger)^{\dot{a}} \end{pmatrix}\,, \tag{A.27}$$

where

$$\mathcal{C}_5 \equiv \begin{pmatrix} -\varepsilon_{ac} & 0 \\ 0 & \varepsilon^{\dot{a}\dot{c}} \end{pmatrix} \tag{A.28}$$

is the five-dimensional charge conjugation matrix[5] (numerically, $\mathcal{C}_5 = i\gamma^5\gamma^2\gamma^0 = \gamma^3\gamma^1$, but again the spinor index structure is different) and the antisymmetric invariant is defined as

$$\varepsilon^{12} = \varepsilon^{\dot{1}\dot{2}} = \varepsilon_{21} = \varepsilon_{\dot{2}\dot{1}} = 1\,, \qquad \varepsilon_{12} = \varepsilon_{\dot{1}\dot{2}} = \varepsilon^{21} = \varepsilon^{\dot{2}\dot{1}} = -1\,. \tag{A.32}$$

[5] In five dimensions, the matrices γ_a and their transposes γ_a^{T} both satisfy the Clifford algebra. Accordingly, Shur's lemma implies that these two representations must be connected by a similarity transformation. With the definition (A.28), this is realized by the charge conjugation matrix:

$$\mathcal{C}_5^{-1} \gamma_a\, \mathcal{C}_5 = \gamma_a^{\mathrm{T}}\,. \tag{A.29}$$

Note that this condition does not fix the overall sign of the charge conjugation matrix: we could also take $\mathcal{C}_5 \to -\mathcal{C}_5$.

In four dimensions, the conventional similarity transformation is

$$\mathcal{C}_4^{-1} \gamma_a\, \mathcal{C}_4 = -\gamma_a^{\mathrm{T}}\,, \tag{A.30}$$

with the charge conjugation matrix

$$\mathcal{C}_4 \equiv \begin{pmatrix} \varepsilon_{ac} & 0 \\ 0 & \varepsilon^{\dot{a}\dot{c}} \end{pmatrix}\,. \tag{A.31}$$

Here, products of the form

$$\overline{\Psi}\Psi^c + \text{H.c.} = \overline{\Psi}_L \Psi^c_L + \overline{\Psi}_R \Psi^c_R + \text{H.c.} = \psi_L\,\psi_L + \psi^\dagger_L\,\psi^\dagger_L - \psi_R\,\psi_R - \psi^\dagger_R\,\psi^\dagger_R\,, \tag{A.33}$$

where $\Psi^c_{L,R} \equiv \mathcal{C}_5 \overline{\Psi}^{\mathrm{T}}_{L,R} = P_{R,L}\Psi^c$, are Lorentz-invariant.[6]

Due to the presence of the fifth gamma matrix in the Clifford algebra, left- and right-handed Weyl spinors are not independently Lorentz-covariant (the chirality operator does not commute with the generators of the Lorentz group). The irreducible spin-$\frac{1}{2}$ representation of the Lorentz group in five dimensions is thus a four-component Dirac spinor.

A.3 Majorana Spinors

Majorana spinors do not exist in five dimensions, as it is impossible to enforce the Majorana reality condition:

$$\Psi^c = \Psi \implies \psi_L = \psi_R = -\psi_R\,, \tag{A.36}$$

which has no nontrivial solution. However, a *symplectic Majorana spinor* can be formed out of an even number of Dirac spinors, labeled by $i = 1, 2, \ldots, 2n$, constrained by a symplectic Majorana reality condition

$$\Psi^c_i = \Omega_{ij}\Psi_j\,, \tag{A.37}$$

where Ω is a real antisymmetric matrix in the space of Dirac spinors with $\Omega^2 = -1$. In the specific case $n = 1$, we take two Dirac spinors, Ψ_1 and Ψ_2, and require $\Psi^c_i = \varepsilon_{ij}\Psi_j$, or

$$\left.\begin{aligned}\Psi^c_1 &= -\Psi_2\,,\\ \Psi^c_2 &= \Psi_1\,,\end{aligned}\right\} \implies \left\{\begin{aligned}\psi_{1,L} &= -\psi_{2,R}\,,\\ \psi_{1,R} &= \psi_{2,L}\,,\end{aligned}\right. \tag{A.38}$$

[6] Instead of a charge conjugate spinor, we could have defined an equivalent *Majorana conjugate*:

$$\Psi^{\mathrm{C}} \equiv \Psi^{\mathrm{T}}\mathcal{C}_5 = \begin{pmatrix} (\psi_L)^a & -(\psi^\dagger_R)_{\dot{a}} \end{pmatrix}\,, \tag{A.34}$$

in which case a Lorentz-invariant combination would be

$$\Psi^{\mathrm{C}}\Psi + \text{H.c.} = \overline{\Psi}\Psi^c + \text{H.c.} \tag{A.35}$$

such that we can decompose $\Psi_{1,2}$ in terms of a single set of independent chiral Weyl spinors[7]. Choosing these to be $\psi_{L,R} \equiv \psi_{1\,L,R}$, we find

$$\Psi_1 = \begin{pmatrix} (\psi_L)_a \\ (\psi_R^\dagger)^{\dot{a}} \end{pmatrix}, \qquad \Psi_2 = \begin{pmatrix} (\psi_R)_a \\ -(\psi_L^\dagger)^{\dot{a}} \end{pmatrix}. \tag{A.39}$$

In this case, products of the forms

$$\frac{1}{2}\,(\sigma_3)_{ij}\,\overline{\Psi}_i\Psi_j = \frac{1}{2}\left(\overline{\Psi}_1\Psi_1 - \overline{\Psi}_2\Psi_2\right) = \psi_R\,\psi_L + \psi_R^\dagger\,\psi_L^\dagger \tag{A.40}$$

and

$$\frac{1}{2}\,(\sigma_3)_{ij}\,\overline{\Psi}_i\Psi_j^c = -\frac{1}{2}\left(\overline{\Psi}_1\Psi_2 + \overline{\Psi}_2\Psi_1\right) = \psi_L\,\psi_L + \psi_L^\dagger\,\psi_L^\dagger - \psi_R\,\psi_R - \psi_R^\dagger\,\psi_R^\dagger \tag{A.41}$$

are Lorentz-invariant.

[7] Any of the four sets $(\psi_{1,L}, \psi_{1,R})$, $(\psi_{1,L}, \psi_{2,L})$, $(\psi_{2,L}, \psi_{2,R})$, or $(\psi_{1,R}, \psi_{2,R})$ can be selected as the independent pair.

B Bulk Fields in a Slice of AdS_5

In this appendix we develop the details of field theory in the AdS_5 bulk necessary to construct a supersymmetric extension of the standard model. These results can be found in many places throughout the literature. For two reviews, see Refs. [112, 281].

B.1 Scalars

We consider a bulk complex scalar field $\Phi = \Phi(x^\mu, y)$, with action

$$S_5 = -\int d^5x \sqrt{-g} \left[(\partial^M \Phi^*)(\partial_M \Phi) + m_\Phi^2 \Phi^* \Phi \right] , \tag{B.1}$$

where m_Φ^2 is a bulk mass. In order for the scalar action to be invariant under the $\mathbb{Z}_2$ orbifold symmetry (3.3), the scalar field must be even or odd under the symmetry transformation Z:

$$\Phi(x^\mu, -y) = Z\Phi(x^\mu, y) = \pm\Phi(x^\mu, y) . \tag{B.2}$$

In terms of the parities assigned at the orbifold fixed points,

$$\Phi(x^\mu, 0) = \pm\Phi(x^\mu, 0) , \tag{B.3a}$$

$$\Phi(x^\mu, \pi R) = \pm\Phi(x^\mu, -\pi R) , \tag{B.3b}$$

there are four possible parity profiles for the field, as listed in Table 3.1.

The scalar mass term is even under the $\mathbb{Z}_2$ symmetry and can contain both bulk and boundary components, which we parametrize as

$$m_\Phi^2(y) \equiv ak^2 + k\left[b_{\rm UV}\, 2\delta(y) - b_{\rm IR}\, 2\delta(y - \pi R)\right] , \tag{B.4}$$

where a and $b_{\rm UV,IR}$ are dimensionless real coefficients. In accordance with the Breitenlohner-

Freedman bound for the stability of the AdS spacetime solution [282, 283], we require $a \geq 4$. While the boundary mass terms, on the other hand, are in general unconstrained, four-dimensional $\mathcal{N} = 1$ supersymmetry can only be preserved if they have a special relationship with the bulk mass. With this in mind, we decompose the boundary mass coefficients as

$$b_{\text{UV,IR}} \equiv b \pm \xi_{\text{UV,IR}} \,, \tag{B.5}$$

into a supersymmetric part common to both branes that must be tuned to the bulk mass as

$$b = 2 \pm \sqrt{4 + a} \quad \Longleftrightarrow \quad a = b(b-4) \,, \tag{B.6}$$

and a supersymmetry-breaking deviation $\xi_{\text{UV,IR}}$. Note that in accord with the bound $a \geq 4$, the range of the parameter b is unrestricted: $-\infty \leq b \leq \infty$ (that is, b provides a double cover of the allowed range of a). In the supersymmetric limit $\xi_{\text{UV}} = \xi_{\text{IR}} = 0$, the tuning (B.6) is precisely the condition necessary to allow a zero mode in the Kaluza-Klein spectrum of an even scalar field.

The function $A(y) = k|y|$ is defined in (3.15); its derivatives take the form

$$A'(y) = \frac{d}{dy} A(y) = k \,\text{sgn}(y) \,, \tag{B.7a}$$

$$A''(y) = \frac{d^2}{dy^2} A(y) = 2k\big[\delta(y) - \delta(y - \pi R)\big] \,. \tag{B.7b}$$

With this notation, we can write the scalar mass term (B.4) as

$$m_\Phi^2 = ak^2 + bA'' + \xi_{\text{UV}} k \, 2\delta(y) + \xi_{\text{IR}} k \, 2\delta(y - \pi R) \,. \tag{B.8}$$

B.1.1 Kaluza-Klein theory

The variation of the scalar action (B.1) gives the equations of motion

$$e^{2A} \eta^{\mu\nu} \partial_\mu \partial_\nu \Phi + e^{4A} \partial_5 \left(e^{-4A} \partial_5 \Phi \right) - ak^2 \Phi = 0 \,. \tag{B.9}$$

The boundary conditions are either generalized Neumann (N),[1]

$$\left(\partial_5 - b_{\text{UV,IR}} A'\right) \Phi \big|_{y=0^+,\pi R^-} = \left[\partial_5 - \left(b \pm \xi_{\text{UV,IR}}\right) A'\right] \Phi \big|_{y=0^+,\pi R^-} = 0\,, \tag{B.10}$$

or Dirichlet (D),

$$\Phi \big|_{y=0,\pi R} = 0\,. \tag{B.11}$$

The boundary conditions required on each brane are determined by the scalar's parity profiles according to Table 3.2.

We now assume the field decomposition

$$\Phi(x^\mu, y) = \sum_{n=0}^{\infty} \Phi^{(n)}(x^\mu)\, f_\Phi^{(n)}(y)\,, \tag{B.12}$$

where the Kaluza-Klein eigenmodes $\Phi^{(n)}$ satisfy the Klein-Gordon equations

$$\eta^{\mu\nu}\partial_\mu\partial_\nu\Phi^{(n)} = m_n^2 \Phi^{(n)}\,, \tag{B.13}$$

with mass eigenvalues m_n^2. By convention, we index the eigenmodes in order of increasing mass. The bulk profiles $f_\Phi^{(n)}$ obey the orthonormality conditions

$$\int_{-\pi R}^{\pi R} dy\, e^{-2A(y)} f_\Phi^{(m)}(y)\, f_\Phi^{(n)}(y) = \delta_{mn}\,, \tag{B.14}$$

and the equations of motion

$$\left[-e^{4A}\partial_5\left(e^{-4A}\partial_5\right) + ak^2\right] f_\Phi^{(n)} = e^{2A} m_n^2 f_\Phi^{(n)}\,. \tag{B.15}$$

with generalized Neumann,

$$\left(\partial_5 - b_{\text{UV,IR}} A'\right) f_\Phi^{(n)} \Big|_{y=0^+,\pi R^-} = \left[\partial_5 - \left(b \pm \xi_{\text{UV,IR}}\right) A'\right] f_\Phi^{(n)} \Big|_{y=0^+,\pi R^-} = 0\,, \tag{B.16}$$

[1] These are technically mixed boundary conditions, involving both Neumann and Dirichlet terms. In the terminology of Sec. 3.1, we might define a Neumann boundary condition as one that is compatible with a zero-mode solution. In this case, the Dirichlet contribution is parametrized by $\xi_{\text{UV,IR}}$, which can be varied to interpolate between a Neumann condition.

or Dirichlet,

$$f_\Phi^{(n)}\Big|_{y=0,\pi R} = 0\,, \tag{B.17}$$

boundary conditions.

Massive solutions

For $m_n^2 > 0$, the solutions to (B.15) take the forms:

$$f_\Phi^{(n)}(y) = \begin{cases} f_\Phi^{(n)}(z) & \text{for } \Phi \text{ even}\,, \\ \mathrm{sgn}(y)\, f_\Phi^{(n)}(z) & \text{for } \Phi \text{ odd}\,, \end{cases} \tag{B.18}$$

where

$$f_\Phi^{(n)}(z) = \sqrt{k}\, N_\Phi^{(n)}\, (zk)^2 \left[J_\alpha(m_n z) - C_\Phi^{(n)} Y_\alpha(m_n z)\right] \tag{B.19}$$

are the profiles in terms of the conformal coordinate z. Here, J_α and Y_α are Bessel functions of the first and second kinds, respectively, with index[2]

$$\alpha = \pm\sqrt{4+a} = 2 - b\,. \tag{B.22}$$

The natural argument of the Bessel functions is the dimensionless quantity

$$x_n \equiv m_n z = \frac{m_n}{k e^{-A}}\,. \tag{B.23}$$

For each mode, the dimensionless constant $N_\Phi^{(n)}$ is fixed by the orthonormality condition (B.14). The constant $C_\Phi^{(n)}$ is determined by the boundary conditions: Neumann boundary

[2] In this case, the common boundary mass coefficient b offers a more useful parametrization of the degree of freedom in the KK solutions than the bulk mass coefficient a, as its value is unrestricted ($b \in \mathbb{R}$ as opposed to $a \geq 4$). Note that we could also restrict the index to be positive, writing

$$\alpha = \sqrt{4+a} = |2 - b|\,. \tag{B.20}$$

In this case, the Neumann conditions (B.24) for the constants $C_\Phi^{(n)}$ must be modified [the Dirichlet conditions (B.25) are the same]:

$$C_\Phi^{(n)}\Big|_{y=0,\pi R} = \frac{J_{\alpha-1}(x_n^{\mathrm{UV,IR}}) + (2 - b - \alpha \mp \xi_{\mathrm{UV,IR}})\, J_\alpha(x_n^{\mathrm{UV,IR}})}{Y_{\alpha-1}(x_n^{\mathrm{UV,IR}}) + (2 - b - \alpha \mp \xi_{\mathrm{UV,IR}})\, Y_\alpha(x_n^{\mathrm{UV,IR}})}\,. \tag{B.21}$$

This formulation offers greater stability in numeric evaluation in some regions of the parameter space of b and $\xi_{\mathrm{UV,IR}}$.

conditions (even boundary parity) give rise to the values

$$C_\Phi^{(n)}\Big|_{y=0,\pi R} = \frac{J_{\alpha-1}(x_n^{\rm UV,IR}) \mp \xi_{\rm UV,IR} J_\alpha(x_n^{\rm UV,IR})}{Y_{\alpha-1}(x_n^{\rm UV,IR}) \mp \xi_{\rm UV,IR} Y_\alpha(x_n^{\rm UV,IR})}\,, \tag{B.24}$$

while Dirichlet conditions (odd boundary parity) give

$$C_\Phi^{(n)}\Big|_{y=0,\pi R} = \frac{J_\alpha(x_n^{\rm UV,IR})}{Y_\alpha(x_n^{\rm UV,IR})} \tag{B.25}$$

The eigenmass m_n is determined by ensuring that the boundary conditions on both branes give rise to the same constant:

$$C_\Phi^{(n)} = C_\Phi^{(n)}\Big|_{y=0} = C_\Phi^{(n)}\Big|_{y=\pi R}\,, \tag{B.26}$$

explicitly,

$$C_\Phi^{(n)} = \begin{cases} \dfrac{x_n^{\rm UV} J_{\alpha-1}(x_n^{\rm UV}) - \xi_{\rm UV} J_\alpha(x_n^{\rm UV})}{x_n^{\rm UV}\, Y_{\alpha-1}(x_n^{\rm UV}) - \xi_{\rm UV} Y_\alpha(x_n^{\rm UV})} = \dfrac{x_n^{\rm IR} J_{\alpha-1}(x_n^{\rm IR}) + \xi_{\rm IR} J_\alpha(x_n^{\rm IR})}{x_n^{\rm IR} Y_{\alpha-1}(x_n^{\rm IR}) + \xi_{\rm IR} Y_\alpha(x_n^{\rm IR})} & \text{for } \Phi^{(+,+)}\,, \\ \dfrac{x_n^{\rm UV} J_{\alpha-1}(x_n^{\rm UV}) - \xi_{\rm UV} J_\alpha(x_n^{\rm UV})}{x_n^{\rm UV}\, Y_{\alpha-1}(x_n^{\rm UV}) - \xi_{\rm UV} Y_\alpha(x_n^{\rm UV})} = \dfrac{J_\alpha(x_n^{\rm IR})}{Y_\alpha(x_n^{\rm IR})} & \text{for } \Phi^{(+,-)}\,, \\ \dfrac{J_\alpha(x_n^{\rm UV})}{Y_\alpha(x_n^{\rm UV})} = \dfrac{x_n^{\rm IR} J_{\alpha-1}(x_n^{\rm IR}) + \xi_{\rm IR} J_\alpha(x_n^{\rm IR})}{x_n^{\rm IR} Y_{\alpha-1}(x_n^{\rm IR}) + \xi_{\rm IR} Y_\alpha(x_n^{\rm IR})} & \text{for } \Phi^{(-,+)}\,, \\ \dfrac{J_\alpha(x_n^{\rm UV})}{Y_\alpha(x_n^{\rm UV})} = \dfrac{J_\alpha(x_n^{\rm IR})}{Y_\alpha(x_n^{\rm IR})} & \text{for } \Phi^{(-,-)}\,. \end{cases} \tag{B.27}$$

We discuss the approximate Kaluza-Klein spectrum in Appendix C.

Zero-mode solutions

A solution to (B.15) with zero mass eigenvalue (a Kaluza-Klein zero mode) exists only for $\Phi^{(+,+)}$ (a nontrivial massless solution is only possible with Neumann boundary conditions) when the bulk and boundary masses are tuned according to (B.6) (i.e., when $\xi_{\rm UV} = \xi_{\rm IR} = 0$). This solution, the Kaluza-Klein zero mode, is necessarily the lightest state in the scalar

Kaluza-Klein tower and is accordingly labeled by the index $n = 0$.[3] Its bulk profile takes the form

$$f_\Phi^{(0)}(y) = \sqrt{\frac{(b-1)\,k}{e^{2(b-1)\pi kR}-1}}\, e^{bA(y)} \equiv \sqrt{k}\, N_\Phi^{(0)}\, e^{bA(y)}\,, \tag{B.28}$$

or

$$f_\Phi^{(0)}(z) = \sqrt{\frac{(b-1)\,k}{(z_{\rm IR}k)^{2(b-1)}-1}}\, (zk)^b = \sqrt{k}\, N_\Phi^{(0)}\, (zk)^b\,, \tag{B.29}$$

in terms of the conformal coordinate. If the condition (B.6) is violated (i.e., when $\xi_{\rm UV,IR} \neq 0$), then massless solutions are no longer possible. In this case, the zero mode is said to be *lifted*. and its profile and eigenmass are found as in the general massive case. We present an analytic approximation for the resulting zero-mode mass in Appendix C.

Localization

The localization properties of the KK modes can be extracted by considering the expanded action,

$$\begin{aligned} S_5 &= -\sum_n \int d^5x\, \sqrt{-g}\, \left(f_\Phi^{(n)}\right)^2 \left[g^{\mu\nu}\, \left(\partial_\mu \Phi^{(n)}\right)^*\, \partial_\nu \Phi^{(n)} + e^{2A} m_n^2 \Phi^{(n)*}\, \Phi^{(n)}\right] \\ &= -\sum_n \int d^5x\, \left(f_\Phi^{(n)}\right)^2 e^{-2A} \left[\eta^{\mu\nu}\, \left(\partial_\mu \Phi^{(n)}\right)^*\, \partial_\nu \Phi^{(n)} + m_n^2 \Phi^{(n)*} \Phi^{(n)}\right] \\ &\equiv -\sum_n \int d^5x\, \left(\tilde{f}_\Phi^{(n)}\right)^2 \left[\eta^{\mu\nu}\, \left(\partial_\mu \Phi^{(n)}\right)^*\, \partial_\nu \Phi^{(n)} + m_n^2 \Phi^{(n)*} \Phi^{(n)}\right]\,, \end{aligned} \tag{B.30}$$

where we have absorbed all warp factors from the metric into rescaled profiles:

$$\tilde{f}_\Phi^{(n)}(y) = f_\Phi^{(n)}(y)\, e^{-A(y)}\,. \tag{B.31}$$

Note that for the rescaled profiles the orthonormality relation (B.14) becomes

$$\int_{-\pi R}^{\pi R} dy\, \tilde{f}_\Phi^{(m)}(y)\, \tilde{f}_\Phi^{(n)}(y) = \delta_{mn}\,, \tag{B.32}$$

[3] As there is no zero mode when Φ is has any other parity assignment, we skip $n = 0$ and start the numbering at $n = 1$ in those cases.

and the action can be reduced to a tower of four-dimensional states:

$$S_4 = -\sum_n \int d^4x \left[\eta^{\mu\nu} \left(\partial_\mu \Phi^{(n)}\right)^* \partial_\nu \Phi^{(n)} + m_n^2 \left(\Phi^{(n)}\right)^* \Phi^{(n)} \right] . \tag{B.33}$$

The localization of each mode in the extra dimension with respect to a conformally flat metric is thus determined by the rescaled profiles $\tilde{f}_\Phi^{(n)}$. In particular, the rescaled profiles for the scalar zero modes are

$$\tilde{f}_\Phi^{(0)}(y) = \sqrt{\frac{(b-1)\,k}{e^{2(b-1)\pi kR} - 1}}\, e^{(b-1)\,A(y)} = \sqrt{k}\, N_\Phi^{(0)}\, e^{(b-1)\,A(y)} , \tag{B.34}$$

or

$$\tilde{f}_\Phi^{(0)}(z) = \sqrt{\frac{(b-1)\,k}{(z_{\rm IR}k)^{2(b-1)} - 1}}\, (zk)^{b-1} = \sqrt{k}\, N_\Phi^{(0)}\, (zk)^{b-1} . \tag{B.35}$$

We see that for $b < 1$ ($b > 1$) the zero mode is localized toward the UV (IR) brane, and when $b = 1$, the mode is conformally flat. Because $b \in \mathbb{R}$ is a free parameter, the zero mode may be localized anywhere in the bulk.

B.2 Dirac Fermions

We consider a bulk Dirac fermion $\Psi = \Psi(x^\mu, y)$, with action

$$S_5 = -\int d^5x \sqrt{-g} \left(\frac{1}{2} \overline{\Psi} \Gamma^M D_M \Psi - \frac{1}{2} \left(D_M \overline{\Psi}\right) \Gamma^M \Psi + m_{\rm D} \overline{\Psi} \Psi \right) , \tag{B.36}$$

where $m_{\rm D}$ is a Dirac mass matrix and the kinetic terms have been constructed to be explicitly Hermitian.[4] In order for the fermion action to remain invariant under the $\mathbb{Z}_2$ orbifold symmetry, the fermion field must transform as

$$\Psi(x^\mu, -y) = \pm \gamma^5 \Psi(x^\mu, y) , \tag{B.37}$$

[4] Integration by parts in the AdS geometry generally introduces boundary terms, so we must start with the canonical Dirac operator directly, rather than the right-acting form usual in flat space.

where the overall sign must be determined by the interactions of the fermion with other fields. According to (A.21), the action of γ_5 is

$$\gamma^5\Psi = \gamma^5\Psi_L + \gamma^5\Psi_R = \Psi_L - \Psi_R\,, \tag{B.38}$$

and therefore (B.37) implies that

$$\Psi_L(x^\mu, -y) = \pm\Psi_L(x^\mu, y) \quad \text{and} \quad \Psi_R(x^\mu, -y) = \mp\Psi_R(x^\mu, y)\,. \tag{B.39}$$

That is, the left- and right-handed chiral projections of Ψ must thus be states of definite parity under the orbifold symmetry such that if Ψ_L is even, Ψ_R must be odd and vice versa. In terms of the parities assigned at the orbifold fixed points,

$$\Psi_L(x^\mu, 0) = \pm\Psi_L(x^\mu, 0) \qquad \text{and} \qquad \Psi_R(x^\mu, 0) = \mp\Psi_R(x^\mu, 0)\,, \tag{B.40a}$$

$$\Psi_L(x^\mu, \pi R) = \pm\Psi_L(x^\mu, -\pi R) \quad \text{and} \quad \Psi_R(x^\mu, \pi R) = \mp\Psi_R(x^\mu, -\pi R)\,, \tag{B.40b}$$

there are four possible parity profile configurations for the chiral components, which we list in Table B.1. Because that chiral component with odd parity on a boundary must vanish there, this implies that each boundary is only able to support one fermion chirality. This allows an alternative characterization of the fermion parity configurations in terms of boundary chiralities.

Table B.1: Possible S^1-periodicity and $\mathbb{Z}_2$-parity assignments for bulk Dirac fermions on the orbifold. The left (right) term in the tuples refers to the $\mathbb{Z}_2$ parity or fermion chirality at the $y = 0$ ($y = \pm\pi R$) orbifold fixed point.

boundary chirality	boundary parity		$\mathbb{Z}_2$ parity		S^1 periodicity
	Ψ_L	Ψ_R	Ψ_L	Ψ_R	
(L, L)	$(+, +)$	$(-, -)$	even	odd	periodic
(L, R)	$(+, -)$	$(-, +)$	even	odd	antiperiodic
(R, L)	$(-, +)$	$(+, -)$	odd	even	antiperiodic
(R, R)	$(-, -)$	$(+, +)$	odd	even	periodic

The opposing parity assignments for the chiral components means that the bilinear $\overline{\Psi}\Psi$ is odd and vanishes on the boundaries. Consequently, the Dirac mass matrix $m_{\rm D}$ is only nonzero in the bulk, and we can parametrize it as

$$m_{\rm D}(y) \equiv cA'(y)\,, \tag{B.41}$$

where c is a dimensionless real coefficient. The nontrivial transformation of the bulk mass under the $\mathbb{Z}_2$ symmetry implies that it must arise as the vacuum expectation value of a topological domain wall soliton of an underlying scalar field with odd parity.

On the other hand, using the charge conjugated spinor, we can form an even bilinear such as $\overline{\Psi}\Psi^c$, and therefore, a bulk Majorana mass term of the form

$$S_5 \supset -\int d^5x\,\sqrt{-g}\,\left(\frac{1}{2}m_{\rm M}\overline{\Psi}\Psi^c + \text{H.c.}\right) \tag{B.42}$$

may be added, which we parametrize as

$$m_{\rm M} = \xi k\,, \tag{B.43}$$

where ξ is a dimensionless complex coefficient. We may also add boundary majorana masses, which, because the field theory on the boundaries obeys four-dimensional (rather than five-dimensional) Lorentz symmetry, may be defined separately for each of the chiral components:

$$S_5 \supset -\int d^5x\,\sqrt{-g}\,\left(\frac{1}{2}m_{{\rm M},L}\overline{\Psi}_L\Psi^c_L + \frac{1}{2}m_{{\rm M},R}\overline{\Psi}_R\Psi^c_R + \text{H.c.}\right)\,, \tag{B.44}$$

where

$$m_{{\rm M}\,L,R}(y) + \xi_{{\rm UV}\,L,R}\,2\delta(y) + \xi_{{\rm IR}\,L,R}\,2\delta(y-\pi R)\,. \tag{B.45}$$

with dimensionless complex coefficients $\xi_{{\rm UV}\,L,R}$ and $\xi_{{\rm IR}\,L,R}$. The addition of such a Majorana masses necessarily breaks four-dimensional $\mathcal{N}=1$ supersymmetry and is incompatible with the presence of zero modes in the fermion Kaluza-Klein spectrum. When $m_{\rm M}=0$ and $m_{{\rm M}\,L,R}=0$, the KK spectrum is vectorlike, composed, as we discuss below, of a tower of massive four-dimensional Dirac states along with a single chiral zero-mode solution. When the Majorana mass is included, the KK spectrum instead consists of two towers of massive four-dimensional Majorana fermions. In the following, we will consider both the vectorlike case and the case with boundary Majorana masses (we are not interested in breaking

supersymmetry in the bulk, so we will set $\xi = 0$). For a discussion of bulk Majorana masses in the context of models of a five-dimensional seesaw mechanism, see Refs. [179, 184, 284].

B.2.1 Vectorlike Kaluza-Klein theory

In the absence of any Majorana mass terms,[5] the variation of the action gives for the left- and right-handed components of the fermion the equations of motion:

$$e^A \gamma^\mu \partial_\mu \Psi_R + \partial_5 \Psi_L + (c-2)\, A' \Psi_L = 0\,, \tag{B.46a}$$

$$e^A \gamma^\mu \partial_\mu \Psi_L - \partial_5 \Psi_R + (c+2)\, A' \Psi_R = 0\,. \tag{B.46b}$$

Redefining $\hat{\Psi} = \Psi e^{-2A}$, we can absorb the spin-connection terms:

$$e^A \gamma^\mu \partial_\mu \hat{\Psi}_R + \partial_5 \hat{\Psi}_L + cA' \hat{\Psi}_L = 0\,, \tag{B.47a}$$

$$e^A \gamma^\mu \partial_\mu \hat{\Psi}_L - \partial_5 \hat{\Psi}_R + cA' \hat{\Psi}_R = 0\,. \tag{B.47b}$$

We can decouple these equations by taking further derivatives, finding the second-order equations

$$e^{2A} \eta^{\mu\nu} \partial_\mu \partial_\nu \hat{\Psi}_{L,R} + e^A \partial_5 \left(e^{-A} \partial_5 \hat{\Psi}_{L,R} \right) - c\,(c \pm 1)\, k^2 \hat{\Psi}_{L,R} = 0\,, \tag{B.48}$$

which have a similar form to the scalar equations of motion (B.9). The boundary conditions for each chiral component may be either Neumann (N),

$$\left(\partial_5 + cA'\right) \hat{\Psi}_L \big|_{0^+,\pi R^-} = \left[\partial_5 - (2-c)\, A'\right] \Psi_L \big|_{0^+,\pi R^-} = 0\,, \tag{B.49a}$$

$$\left(\partial_5 - cA'\right) \hat{\Psi}_R \big|_{0^+,\pi R^-} = \left[\partial_5 - (2+c)\, A'\right] \Psi_R \big|_{0^+,\pi R^-} = 0\,, \tag{B.49b}$$

or Dirichlet (D),

$$\hat{\Psi}_{L,R} \big|_{0,\pi R} = \Psi_{L,R} \big|_{0,\pi R} = 0\,, \tag{B.50}$$

depending on the parity assignments, as we list in Table B.2. The correspondence between parity configurations and boundary conditions for Dirac fermions is the natural extension of

[5] In the interacting theory, of course, there may exist additional mass contributions, such as those arising from Yukawa couplings after EWSB, which we also neglect.

the general (scalar) case given in Table 3.2.

Table B.2: Correspondence between parity assignments and boundary conditions for bulk Dirac fermions on the orbifold. The left (right) term in the tuples refers to the $\mathbb{Z}_2$ parity or type of boundary condition at the $y = 0$ ($y = \pm\pi R$) orbifold fixed point

boundary parity		boundary conditions	
Ψ_L	Ψ_R	Ψ_L	Ψ_R
$(+,+)$	$(-,-)$	(N,N)	(D,D)
$(+,-)$	$(-,+)$	(N,D)	(D,N)
$(-,+)$	$(+,-)$	(D,N)	(N,D)
$(-,-)$	$(+,+)$	(D,D)	(N,N)

We now assume the Kaluza-Klein decompositions

$$\Psi_{L,R}(x^\mu, y) = \sum_{n=0}^{\infty} \Psi_{L,R}^{(n)}(x^\mu)\, f_{\Psi_{L,R}}^{(n)}(y) = \sum_{n=0}^{\infty} \Psi_{L,R}^{(n)}(x^\mu)\, e^{2A(y)}\, \hat{f}_{\Psi_{L,R}}^{(n)}(y)\,, \tag{B.51}$$

where the KK eigenmodes $\Psi_{L,R}^{(n)}$ satisfy Dirac equations

$$\eta^{\mu\nu}\gamma_\mu \partial_\nu \Psi_{L,R}^{(n)} = -m_n \Psi_{R,L}^{(n)}\,, \tag{B.52}$$

with mass eigenvalues m_n. The bulk profiles $f_{\Psi_{L,R}}^{(n)}$ obey the orthonormality conditions

$$\int_{-\pi R}^{\pi R} dy\, e^{-3A(y)} f_{\Psi_{L,R}}^{(m)}(y)\, f_{\Psi_{L,R}}^{(n)}(y) = \int_{-\pi R}^{\pi R} dy\, e^{A(y)}\, \hat{f}_{\Psi_{L,R}}^{(m)}(y)\, \hat{f}_{\Psi_{L,R}}^{(n)}(y) = \delta_{mn}\,, \tag{B.53}$$

and equations of motion

$$\partial_5 \hat{f}_{\Psi_L}^{(n)} + cA' \hat{f}_{\Psi_L}^{(n)} = e^A m_n \hat{f}_{\Psi_R}^{(n)}\,, \tag{B.54a}$$

$$-\partial_5 \hat{f}_{\Psi_R}^{(n)} + cA' \hat{f}_{\Psi_R}^{(n)} = e^A m_n \hat{f}_{\Psi_L}^{(n)}\,, \tag{B.54b}$$

or

$$\left[-e^{A}\partial_5\left(e^{-A}\partial_5\right)+c\left(c\pm1\right)k^2\right]\hat{f}^{(n)}_{\Psi_{L,R}}=e^{2A}m_n^2\hat{f}^{(n)}_{\Psi_{L,R}}\,. \tag{B.55}$$

in decoupled, second-order form. The boundary conditions are Neumann,

$$\left(\partial_5+cA'\right)\hat{f}^{(n)}_{\Psi_L}\Big|_{0^+,\pi R^-}=\left[\partial_5-\left(2-c\right)A'\right]f^{(n)}_{\Psi_L}\Big|_{0^+,\pi R^-}=0\,, \tag{B.56a}$$

$$\left(\partial_5-cA'\right)\hat{f}^{(n)}_{\Psi_R}\Big|_{0^+,\pi R^-}=\left[\partial_5-\left(2+c\right)A'\right]f^{(n)}_{\Psi_R}\Big|_{0^+,\pi R^-}=0\,, \tag{B.56b}$$

or Dirichlet,

$$\hat{f}^{(n)}_{\Psi_{L,R}}\Big|_{0,\pi R}=f^{(n)}_{\Psi_{L,R}}\Big|_{0,\pi R}=0\,, \tag{B.57}$$

Note that the four-dimensional Kaluza-Klein spectrum is entirely vectorlike, consisting of a tower of massive Dirac states. The only exception occurs if one of the chiral components of an eigenmode vanishes, in which case the spectrum also contains the remaining component as a massless zero mode. We consider both of these cases below.

Massive solutions

For $m_n^2>0$, the solutions to (B.55) take the forms:

$$f^{(n)}_{\Psi_{L,R}}(y)=e^{2A(y)}\hat{f}^{(n)}_{\Psi_{L,R}}(y)=\begin{cases}f^{(n)}_{\Psi_{L,R}}(z) & \text{for } \Psi_{L,R} \text{ even}\,,\\ \operatorname{sgn}(y)\,f^{(n)}_{\Psi_{L,R}}(z) & \text{for } \Psi_{L,R} \text{ odd}\,,\end{cases} \tag{B.58}$$

where,

$$f^{(n)}_{\Psi_{L,R}}(z)=\sqrt{k}\,N^{(n)}_{\Psi}\,(zk)^{5/2}\left[J_{\alpha_{L,R}}(m_nz)-C^{(n)}_{\Psi}Y_{\alpha_{L,R}}(m_nz)\right] \tag{B.59}$$

and

$$\alpha_{L,R}=c\pm\tfrac{1}{2}\,. \tag{B.60}$$

Here, the constants $N^{(n)}_{\Psi}$ and $C^{(n)}_{\Psi}$ are the same for both components of each mode, a result due ultimately to the fact that each pair of left- and right-handed modes share a common Dirac mass eigenvalue. This is only true in the supersymmetric limit; when Majorana masses are added, we must distinguish separate constants for each component as we discuss below in Sec. B.2.2. For each mode, the dimensionless constant $N^{(n)}_{\Psi}$ is fixed by the orthonormality conditions (B.53). The constant $C^{(n)}_{\Psi}$ is determined by the boundary conditions. Neumann

boundary conditions (even boundary parity) give rise to the values

$$C^{(n)}_{\Psi_L}\Big|_{y=0,\pi R} = \frac{J_{\alpha_L-1}(x_n^{\mathrm{UV,IR}})}{Y_{\alpha_L-1}(x_n^{\mathrm{UV,IR}})} = \frac{J_{\alpha_R}(x_n^{\mathrm{UV,IR}})}{Y_{\alpha_R}(x_n^{\mathrm{UV,IR}})}\,, \tag{B.61a}$$

$$C^{(n)}_{\Psi_R}\Big|_{y=0,\pi R} = \frac{J_{\alpha_R+1}(x_n^{\mathrm{UV,IR}})}{Y_{\alpha_R+1}(x_n^{\mathrm{UV,IR}})} = \frac{J_{\alpha_L}(x_n^{\mathrm{UV,IR}})}{Y_{\alpha_L}(x_n^{\mathrm{UV,IR}})}\,, \tag{B.61b}$$

while Dirichlet conditions (odd boundary parity) give

$$C^{(n)}_{\Psi_L}\Big|_{y=0,\pi R} = \frac{J_{\alpha_L}(x_n^{\mathrm{UV,IR}})}{Y_{\alpha_L}(x_n^{\mathrm{UV,IR}})} = \frac{J_{\alpha_R+1}(x_n^{\mathrm{UV,IR}})}{Y_{\alpha_R+1}(x_n^{\mathrm{UV,IR}})}\,, \tag{B.62a}$$

$$C^{(n)}_{\Psi_R}\Big|_{y=0,\pi R} = \frac{J_{\alpha_R}(x_n^{\mathrm{UV,IR}})}{Y_{\alpha_R}(x_n^{\mathrm{UV,IR}})} = \frac{J_{\alpha_L-1}(x_n^{\mathrm{UV,IR}})}{Y_{\alpha_L-1}(x_n^{\mathrm{UV,IR}})}\,, \tag{B.62b}$$

The Dirac eigenmass m_n is determined by ensuring that the boundary conditions on both branes give rise to the same constant (note that the constants for both chiral components are necessarily the same in each parity configuration):

$$C^{(n)}_{\Psi} = C^{(n)}_{\Psi_{L,R}}\Big|_{y=0} = C^{(n)}_{\Psi_{L,R}}\Big|_{y=\pi R}\,, \tag{B.63}$$

explicitly,

$$C^{(n)}_{\Psi} = \begin{cases} \dfrac{J_{\alpha_R}(x_n^{\mathrm{UV}})}{Y_{\alpha_R}(x_n^{\mathrm{UV}})} = \dfrac{J_{\alpha_R}(x_n^{\mathrm{IR}})}{Y_{\alpha_R}(x_n^{\mathrm{IR}})} & \text{for } \Psi = \Psi_L^{(+,+)} + \Psi_R^{(-,-)}\,, \\ \dfrac{J_{\alpha_R}(x_n^{\mathrm{UV}})}{Y_{\alpha_R}(x_n^{\mathrm{UV}})} = \dfrac{J_{\alpha_L}(x_n^{\mathrm{IR}})}{Y_{\alpha_L}(x_n^{\mathrm{IR}})} & \text{for } \Psi = \Psi_L^{(+,-)} + \Psi_R^{(-,+)}\,, \\ \dfrac{J_{\alpha_L}(x_n^{\mathrm{UV}})}{Y_{\alpha_L}(x_n^{\mathrm{UV}})} = \dfrac{J_{\alpha_R}(x_n^{\mathrm{IR}})}{Y_{\alpha_R}(x_n^{\mathrm{IR}})} & \text{for } \Psi = \Psi_L^{(-,+)} + \Psi_R^{(+,-)}\,, \\ \dfrac{J_{\alpha_L}(x_n^{\mathrm{UV}})}{Y_{\alpha_L}(x_n^{\mathrm{UV}})} = \dfrac{J_{\alpha_L}(x_n^{\mathrm{IR}})}{Y_{\alpha_L}(x_n^{\mathrm{IR}})} & \text{for } \Psi = \Psi_L^{(-,-)} + \Psi_R^{(+,+)}\,. \end{cases} \tag{B.64}$$

We discuss the approximate Kaluza-Klein spectrum in Appendix C.

Zero-mode solutions

A solution to (B.55) with zero mass eigenvalue only exists for chiral components with $(+,+)$ parity, corresponding to Neumann boundary conditions on both branes. For components

with odd parity on any boundary, obeying a Dirichlet condition of the form (B.57), the only massless solution is the trivial one. Only two out of the four parity configurations in Table B.1 support a zero-mode solution.

1. **Left-handed zero mode**

   If $\Psi = \Psi_L^{(+,+)} + \Psi_R^{(-,-)}$, then the left-handed chiral component has a zero-mode solution. The zero-mode profile takes the form

$$f_{\Psi_L}^{(0)}(y) = \sqrt{\frac{(1/2-c)\,k}{e^{2(1/2-c)\pi kR}-1}}\, e^{(2-c)\,A(y)} \equiv \sqrt{k}\, N_{\Psi_L}^{(0)} e^{(2-c)\,A(y)} \tag{B.65}$$

   or

$$f_{\Psi_L}^{(0)}(z) = \sqrt{\frac{(1/2-c)\,k}{(z_{\rm IR}k)^{2(1/2-c)}-1}}\, (zk)^{2-c} = \sqrt{k}\, N_{\Psi_L}^{(0)}\, (zk)^{2-c}\,, \tag{B.66}$$

   in terms of the conformal coordinate.

2. **Right-handed zero mode**

   If $\Psi = \Psi_L^{(-,-)} + \Psi_R^{(+,+)}$, then the right-handed chiral component has a zero-mode solution. The zero-mode profile takes the form

$$f_{\Psi_R}^{(0)}(y) = \sqrt{\frac{(1/2+c)\,k}{e^{2(1/2+c)\pi kR}-1}}\, e^{(2+c)\,A(y)} \equiv \sqrt{k}\, N_{\Psi_R}^{(0)}\, e^{(2+c)\,A(y)} \tag{B.67}$$

   or

$$f_{\Psi_R}^{(0)}(z) = \sqrt{\frac{(1/2+c)\,k}{(z_{\rm IR}k)^{2(1/2+c)}-1}}\, (zk)^{2+c} = \sqrt{k}\, N_{\Psi_R}^{(0)}\, (zk)^{2+c}\,, \tag{B.68}$$

   in terms of the conformal coordinate.

Thus, a bulk Dirac fermion in five-dimensions can either have a left- or right-handed massless mode (but not both), and the resulting KK spectrum consists of a tower of massive four-dimensional Dirac states above a single chiral zero-mode solution. In the case of fermions with twisted boundary conditions, no zero modes are possible, and the spectrum is entirely vectorlike. Therefore, although the five-dimensional bulk is vectorlike, a sense of four-dimensional chirality can be recovered in the fermion zero-mode theory under the appropriate choice of orbifold parity. This chiral zero-mode structure is thus ultimately a result of the orbifold $\mathbb{Z}_2$ symmetry, and hence it is the orbifold compactification that allows chiral theories such as the standard model to be extended into five dimensions.

If Majorana masses are added either in the bulk or on the boundary, then massless solutions are no longer possible. In this case, the zero modes are lifted as we discuss below in Sec. B.2.2. We present an analytic approximation for the resulting zero-mode mass in Appendix C.

Localization

The localization properties of the KK modes can be extracted by considering the expanded action,

$$\begin{aligned}
S_5 &= -\sum_n \int d^5x\, \sqrt{-g} \left[\left(f_{\Psi_L}^{(n)}\right)^2 \left(\overline{\Psi}_L^{(n)} g^{\mu\nu} \Gamma_\mu \partial_\nu \Psi_L^{(n)} + e^A m_n \overline{\Psi}_L^{(n)} \Psi_R^{(n)} \right) \right. \\
&\qquad \left. + \left(f_{\Psi_R}^{(n)}\right)^2 \left(\overline{\Psi}_R^{(n)} g^{\mu\nu} \Gamma_\mu \partial_\nu \Psi_R^{(n)} + e^A m_n \overline{\Psi}_R^{(n)} \Psi_L^{(n)} \right) \right] \\
&= -\sum_n \int d^5x \left[\left(f_{\Psi_L}^{(n)}\right)^2 e^{-3A} \left(\overline{\Psi}_L^{(n)} \eta^{\mu\nu} \gamma_\mu \partial_\nu \Psi_L^{(n)} + m_n \overline{\Psi}_L^{(n)} \Psi_R^{(n)} \right) \right. \\
&\qquad \left. + \left(f_{\Psi_R}^{(n)}\right)^2 e^{-3A} \left(\overline{\Psi}_R^{(n)} \eta^{\mu\nu} \gamma_\mu \partial_\nu \Psi_R^{(n)} + m_n \overline{\Psi}_R^{(n)} \Psi_L^{(n)} \right) \right] \\
&\equiv -\sum_n \int d^5x \left[\left(\tilde{f}_{\Psi_L}^{(n)}\right)^2 \left(\overline{\Psi}_L^{(n)} \eta^{\mu\nu} \gamma_\mu \partial_\nu \Psi_L^{(n)} + m_n \overline{\Psi}_L^{(n)} \Psi_R^{(n)} \right) \right. \\
&\qquad \left. + \left(\tilde{f}_{\Psi_R}^{(n)}\right)^2 \left(\overline{\Psi}_R^{(n)} \eta^{\mu\nu} \gamma_\mu \partial_\nu \Psi_R^{(n)} + m_n \overline{\Psi}_R^{(n)} \Psi_L^{(n)} \right) \right],
\end{aligned} \tag{B.69}$$

where we have absorbed all warp factors from the metric into rescaled profiles:

$$\tilde{f}_{\Psi_{L,R}}^{(n)}(y) = f_{\Psi_{L,R}}^{(n)}(y)\, e^{-(3/2)\,A(y)}\,, \tag{B.70}$$

Note that for the rescaled profiles the orthonormality relation (B.53) becomes

$$\int_{-\pi R}^{\pi R} dy\, \tilde{f}_{\Psi_{L,R}}^{(m)}(y)\, \tilde{f}_{\Psi_{L,R}}^{(n)}(y) = \delta_{mn}\,, \tag{B.71}$$

and the action can be reduced to a tower of four-dimensional states:

$$S_4 = -\sum_n \int d^4x \left(\overline{\Psi}_L^{(n)} \eta^{\mu\nu} \gamma_\mu \partial_\nu \Psi_L^{(n)} + m_n \overline{\Psi}_L^{(n)} \Psi_R^{(n)} + \overline{\Psi}_R^{(n)} \eta^{\mu\nu} \gamma_\mu \partial_\nu \Psi_R^{(n)} + m_n \overline{\Psi}_R^{(n)} \Psi_L^{(n)} \right). \tag{B.72}$$

The localization of each mode in the extra dimension with respect to a conformally flat metric is thus determined by the rescaled profiles $\tilde{f}^{(n)}_{\Psi_{L,R}}$. In particular, the rescaled profiles for the Dirac fermion zero modes are

$$\tilde{f}^{(0)}_{\Psi_{L,R}}(y) = \sqrt{\frac{(1/2 \mp c)\, k}{e^{2(1/2\mp c)\pi k R} - 1}}\, e^{(1/2\mp c)\, A(y)} = \sqrt{k}\, N^{(0)}_{\Psi_{L,R}}\, e^{(1/2\mp c)\, A(y)}\,, \tag{B.73}$$

or

$$\tilde{f}^{(0)}_{\Psi_{L,R}}(z) = \sqrt{\frac{(1/2 \mp c)\, k}{(z_{\text{IR}} k)^{2(1/2\mp c)} - 1}}\, (zk)^{1/2\mp c} = \sqrt{k}\, N^{(0)}_{\Psi_{L,R}}\, (zk)^{1/2\mp c}\,. \tag{B.74}$$

We see that for $\pm c < \frac{1}{2}$ ($\pm c > \frac{1}{2}$) the zero mode is localized toward the IR (UV) brane, and when $c = \pm\frac{1}{2}$, the mode is conformally flat. Because $c \in \mathbb{R}$ is a free parameter, the zero mode may be localized anywhere in the bulk.

B.2.2 Majorana Kaluza-Klein theory

Here, we consider a bulk fermion with Majorana masses on the boundary in form (B.45). Most generally, we include boundary masses for both chiral projections. However, it is important to note that because the boundary theory supports chiral fermions, the right-handed and left-handed boundary masses are independent and may be added separately. (The supersymmetry-breaking couplings for the gauginos in our model, for instance, are only added for the even gaugino components on the IR boundary.) In this case, the variation of the action (B.36) gives for the left- and right-handed components of the fermion the equations of motion:

$$e^A \gamma^\mu \partial_\mu \Psi_R + \partial_5 \Psi_L + (c-2)\, A' \Psi_L + \xi_{\text{UV},R}\, \Psi_R^c\, 2\delta(y) + \xi_{\text{IR},R}\, \Psi_R^c\, 2\delta(y - \pi R) = 0\,, \tag{B.75a}$$

$$e^A \gamma^\mu \partial_\mu \Psi_L - \partial_5 \Psi_R + (c+2)\, A' \Psi_R + \xi_{\text{UV},L}\, \Psi_L^c\, 2\delta(y) + \xi_{\text{IR},L}\, \Psi_L^c\, 2\delta(y-\pi R) = 0 \tag{B.75b}$$

or

$$e^A \gamma^\mu \partial_\mu \hat{\Psi}_R + \partial_5 \hat{\Psi}_L + cA' \hat{\Psi}_L + \xi_{\text{UV},R}\, \hat{\Psi}_R^c\, 2\delta(y) + \xi_{\text{IR},R}\, \hat{\Psi}_R^c\, 2\delta(y-\pi R) = 0\,, \tag{B.76a}$$

$$e^A \gamma^\mu \partial_\mu \hat{\Psi}_L - \partial_5 \hat{\Psi}_R + cA' \hat{\Psi}_R + \xi_{\text{UV},L}\, \hat{\Psi}_L^c\, 2\delta(y) + \xi_{\text{IR},L}\, \hat{\Psi}_L^c\, 2\delta(y-\pi R) = 0\,. \tag{B.76b}$$

The decoupled second-order equations take the same form (B.48) as in the vectorlike case, but the Majorana masses modify the boundary conditions, which may be generalized Neumann (N)

$$\Big[(\partial_5 + cA')\, \hat{\Psi}_L \pm z_{\text{UV,IR}}\, \xi_{\text{UV,IR}\,L}\, A' \eta^{\mu\nu} \gamma_\mu \partial_\nu \hat{\Psi}_L^c\Big]\Big|_{0^+,\pi R^-} = 0\,, \tag{B.77a}$$

$$\Big[(\partial_5 - cA')\, \hat{\Psi}_R \mp z_{\text{UV,IR}}\, \xi_{\text{UV,IR}\,R}\, A' \eta^{\mu\nu} \gamma_\mu \partial_\nu \hat{\Psi}_R^c\Big]\Big|_{0^+,\pi R^-} = 0\,, \tag{B.77b}$$

or generalized Dirichlet (D),

$$\Big(\hat{\Psi}_L \pm \xi_{\text{UV,IR}\,R}\, \hat{\Psi}_R^c\Big)\Big|_{0^+,\pi R^-} = 0\,, \tag{B.78a}$$

$$\Big(\hat{\Psi}_R \mp \xi_{\text{UV,IR}\,L}\, \hat{\Psi}_L^c\Big)\Big|_{0^+,\pi R^-} = 0\,, \tag{B.78b}$$

for each chiral component, depending on the parity assignments (Table B.2). Note that for the components with an odd boundary parity, a coupling to the even component arises in the Dirichlet boundary condition in the even component has a Majorana mass term on the boundary. In order to satisfy such a condition, the odd component must be double-valued on that brane.[6]

We again assume the Kaluza-Klein decomposition

$$\Psi_{L,R}(x^\mu, y) = \sum_{n=0}^{\infty} \Psi_{L,R}^{(n)}(x^\mu)\, f_{\Psi_{L,R}}^{(n)}(y) = \sum_{n=0}^{\infty} \Psi_{L,R}^{(n)}(x^\mu)\, e^{2A(y)}\, \hat{f}_{\Psi_{L,R}}^{(n)}(y)\,. \tag{B.79}$$

We define the four-dimensional charge conjugate spinors $\Psi_{L,R}^{c(n)} \equiv \mathcal{C}_4 \overline{\Psi}_{L,R}^{(n)\text{T}}$ using the four-

[6] This can be resolved if the brane has finite width.

dimensional charge conjugation matrix (A.31), such that

$$\Psi^c_{L,R}(x^\mu, y) = \pm \sum_n \Psi^{c(n)}_{L,R}(x^\mu)\, f^{(n)}_{\Psi_{L,R}}(y)\,. \tag{B.80}$$

The KK eigenmodes then satisfy Majorana equations

$$\eta^{\mu\nu}\gamma_\mu \partial_\nu \Psi^{(n)}_{L,R} = -m_{n\,L,R}\Psi^{c(n)}_{L,R} \quad \Longleftrightarrow \quad \eta^{\mu\nu}\gamma_\mu \partial_\nu \Psi^{c(n)}_{L,R} = -m_{n\,L,R}\Psi^{(n)}_{L,R} \tag{B.81}$$

with separate mass eigenvalues $m_{n\,L,R}$ for the left- and right-handed components. The bulk profiles obey the same orthonormality conditions (B.53) as in the vectorlike case and equations of motion

$$\left[-e^A \partial_5 \left(e^{-A}\partial_5\right) + c\,(c \pm 1)\,k^2\right] \hat{f}^{(n)}_{\Psi_{L,R}} = e^{2A} m^2_{n\,L,R} \hat{f}^{(n)}_{\Psi_{L,R}}\,. \tag{B.82}$$

The boundary conditions are generalized Neumann,

$$\left[\partial_5 + (c \mp m_{n,L}\, z_{\text{UV,IR}}\, \xi_{\text{UV,IR}\,L})\, A'\right] \hat{f}^{(n)}_{\Psi_L}\Big|_{0^+,\pi R^-} = 0\,, \tag{B.83a}$$

$$\left[\partial_5 - (c \pm m_{n,R}\, z_{\text{UV,IR}}\, \xi_{\text{UV,IR}\,R})\, A'\right] \hat{f}^{(n)}_{\Psi_R}\Big|_{0^+,\pi R^-} = 0\,, \tag{B.83b}$$

or generalized Dirichlet,

$$\left(\hat{f}^{(n)}_{\Psi_L} \mp \xi_{\text{UV,IR}\,L}\, \hat{f}^{(n)}_{\Psi_R}\right)\Big|_{0^+,\pi R^-} = 0\,, \tag{B.84a}$$

$$\left(\hat{f}^{(n)}_{\Psi_R} \mp \xi_{\text{UV,IR}\,R}\, \hat{f}^{(n)}_{\Psi_L}\right)\Big|_{0^+,\pi R^-} = 0\,. \tag{B.84b}$$

Massive solutions

Unlike the vectorlike case, there is no massless mode when Majorana mass terms are included. Solutions for $m_{n\,L,R} > 0$ take the vectorlike form (B.58), with

$$f^{(n)}_{\Psi_{L,R}}(z) = \sqrt{k}\, N^{(n)}_{\Psi_{L,R}}\, (zk)^{5/2} \left[J_{\alpha_{L,R}}(m_{n\,L,R} z) - C^{(n)}_{\Psi_{L,R}} Y_{\alpha_{L,R}}(m_{n\,L,R} z)\right]\,, \tag{B.85}$$

where we must now distinguish separate constants and masses for each component of each mode. As before, the dimensionless constants $N^{(n)}_{\Psi_{L,R}}$ are fixed by the orthonormality

conditions (B.53) and the constants $C^{(n)}_{\Psi_{L,R}}$ are determined from the boundary conditions.[7] Neumann boundary conditions (even boundary parity) give rise to the values

$$C^{(n)}_{\Psi_L}\Big|_{y=0,\pi R} = \frac{J_{\alpha_L-1}(x^{\text{UV,IR}}_{n,L}) \mp \xi_{\text{UV,IR}\,L}\, J_{\alpha_L}(x^{\text{UV,IR}}_{n,L})}{Y_{\alpha_L-1}(x^{\text{UV,IR}}_{n,L}) \mp \xi_{\text{UV,IR}\,L}\, Y_{\alpha_L}(x^{\text{UV,IR}}_{n,L})}\,, \tag{B.88a}$$

$$C^{(n)}_{\Psi_R}\Big|_{y=0,\pi R} = \frac{J_{\alpha_R+1}(x^{\text{UV,IR}}_{n,R}) \pm \xi_{\text{UV,IR}\,R}\, J_{\alpha_R}(x^{\text{UV,IR}}_{n,R})}{Y_{\alpha_R+1}(x^{\text{UV,IR}}_{n,R}) \pm \xi_{\text{UV,IR}\,R}\, Y_{\alpha_R}(x^{\text{UV,IR}}_{n,R})}\,. \tag{B.88b}$$

For Dirichlet boundary conditions, however, the dependence on the even profiles in (B.84) results in a set of coupled nonlinear integral equations for $N^{(n)}_{\Psi_{L,R}}$ and $C^{(n)}_{\Psi_{L,R}}$, arising from the conditions

$$C^{(n)}_{\Psi_L}\Big|_{y=0,\pi R} = \frac{J_{\alpha_L}(x^{\text{UV,IR}}_{n,L})}{Y_{\alpha_L}(x^{\text{UV,IR}}_{n,L})} \pm \xi_{\text{UV,IR}\,L}\,\frac{N^{(n)}_{\Psi_R}}{N^{(n)}_{\Psi_L}}\left(\frac{J_{\alpha_R}(x^{\text{UV,IR}}_{n,R})}{Y_{\alpha_L}(x^{\text{UV,IR}}_{n,L})} - C^{(n)}_{\Psi_R}\,\frac{Y_{\alpha_R}(x^{\text{UV,IR}}_{n,R})}{Y_{\alpha_L}(x^{\text{UV,IR}}_{n,L})}\right), \tag{B.89a}$$

$$C^{(n)}_{\Psi_R}\Big|_{y=0,\pi R} = \frac{J_{\alpha_R}(x^{\text{UV,IR}}_{n,R})}{Y_{\alpha_R}(x^{\text{UV,IR}}_{n,R})} \pm \xi_{\text{UV,IR}\,R}\,\frac{N^{(n)}_{\Psi_L}}{N^{(n)}_{\Psi_R}}\left(\frac{J_{\alpha_L}(x^{\text{UV,IR}}_{n,L})}{Y_{\alpha_R}(x^{\text{UV,IR}}_{n,R})} - C^{(n)}_{\Psi_L}\,\frac{Y_{\alpha_L}(x^{\text{UV,IR}}_{n,L})}{Y_{\alpha_R}(x^{\text{UV,IR}}_{n,R})}\right). \tag{B.89b}$$

The Majorana eigenmasses $m_{n\,L,R}$ for the components are determined in the usual way by matching the constants that arise from the boundary conditions on each brane:

$$C^{(n)}_{\Psi_{L,R}} = C^{(n)}_{\Psi_{L,R}}\Big|_{y=0} = C^{(n)}_{\Psi_{L,R}}\Big|_{y=\pi R}\,. \tag{B.90}$$

We discuss the approximate Kaluza-Klein spectrum in Appendix C.

---

[7] As in the scalar case, we can restrict the Bessel function indices to be positive, writing

$$\alpha_{L,R} = \left|c \pm \tfrac{1}{2}\right|\,. \tag{B.86}$$

In this case, the Neumann conditions (B.88) for the constants $C^{(n)}_{\Psi_{L,R}}$ must be modified [the Dirichlet conditions (B.89) are the same]:

$$C^{(n)}_{\Psi_L}\Big|_{y=0,\pi R} = \frac{J_{\alpha_L-1}(x^{\text{UV,IR}}_{n,L}) + (c+1/2-\alpha_L \mp \xi_{\text{UV,IR}\,L})\, J_{\alpha_L}(x^{\text{UV,IR}}_{n,L})}{Y_{\alpha_L-1}(x^{\text{UV,IR}}_{n,L}) + (c+1/2-\alpha_L \mp \xi_{\text{UV,IR}\,L})\, Y_{\alpha_L}(x^{\text{UV,IR}}_{n,L})}\,, \tag{B.87a}$$

$$C^{(n)}_{\Psi_R}\Big|_{y=0,\pi R} = \frac{J_{\alpha_R+1}(x^{\text{UV,IR}}_{n,R}) + (c-1/2-\alpha_R \pm \xi_{\text{UV,IR}\,R})\, J_{\alpha_R}(x^{\text{UV,IR}}_{n,R})}{Y_{\alpha_R+1}(x^{\text{UV,IR}}_{n,R}) + (c-1/2-\alpha_R \pm \xi_{\text{UV,IR}\,R})\, Y_{\alpha_R}(x^{\text{UV,IR}}_{n,R})}\,. \tag{B.87b}$$

This formulation offers greater stability in numeric evaluation in some regions of the parameter space of c and $\xi_{\text{UV,IR}}$.

Localization

The expanded action in this case takes the form

$$\begin{aligned}
S_5 &= -\sum_n \int d^5x\, \sqrt{-g} \left[\left(f_{\Psi_L}^{(n)}\right)^2 \left(\overline{\Psi}_L^{(n)} g^{\mu\nu} \Gamma_\mu \partial_\nu \Psi_L^{(n)} + \frac{1}{2} e^A m_{n,L} \overline{\Psi}_L^{(n)} \Psi_L^{c(n)} + \text{H.c.} \right) \right. \\
&\qquad \left. + \left(f_{\Psi_R}^{(n)}\right)^2 \left(\overline{\Psi}_R^{(n)} g^{\mu\nu} \Gamma_\mu \partial_\nu \Psi_R^{(n)} + \frac{1}{2} e^A m_{n,R} \overline{\Psi}_R^{(n)} \Psi_R^{c(n)} + \text{H.c.} \right) \right] \\
&= -\sum_n \int d^5x \left[\left(f_{\Psi_L}^{(n)}\right)^2 e^{-3A} \left(\overline{\Psi}_L^{(n)} \eta^{\mu\nu} \gamma_\mu \partial_\nu \Psi_L^{(n)} + \frac{1}{2} m_{n,L} \overline{\Psi}_L^{(n)} \Psi_L^{c(n)} + \text{H.c.} \right) \right. \\
&\qquad \left. + \left(f_{\Psi_R}^{(n)}\right)^2 e^{-3A} \left(\overline{\Psi}_R^{(n)} \eta^{\mu\nu} \gamma_\mu \partial_\nu \Psi_R^{(n)} + \frac{1}{2} m_{n,R} \overline{\Psi}_R^{(n)} \Psi_R^{c(n)} + \text{H.c.} \right) \right] \\
&\equiv -\sum_n \int d^5x \left[\left(\tilde{f}_{\Psi_L}^{(n)}\right)^2 \left(\overline{\Psi}_L^{(n)} \eta^{\mu\nu} \gamma_\mu \partial_\nu \Psi_L^{(n)} + \frac{1}{2} m_{n,L} \overline{\Psi}_L^{(n)} \Psi_L^{c(n)} + \text{H.c.} \right) \right. \\
&\qquad \left. + \left(\tilde{f}_{\Psi_R}^{(n)}\right)^2 \left(\overline{\Psi}_R^{(n)} \eta^{\mu\nu} \gamma_\mu \partial_\nu \Psi_R^{(n)} + \frac{1}{2} m_{n,R} \overline{\Psi}_R^{(n)} \Psi_R^{c(n)} + \text{H.c.} \right) \right],
\end{aligned} \tag{B.91}$$

where the rescaled profiles $\tilde{f}_{\Psi_{L,R}}^{(n)}$ are defined in (B.70). We note that using the orthonormality condition (B.53), the action can be reduced to two towers of four-dimensional states:

$$\begin{aligned}
S_5 = -\sum_n \int d^4x \left[\left(\overline{\Psi}_L^{(n)} \eta^{\mu\nu} \gamma_\mu \partial_\nu \Psi_L^{(n)} + \frac{1}{2} m_{n,L} \overline{\Psi}_L^{(n)} \Psi_L^{c(n)} + \text{H.c.} \right) \right. \\
\left. + \left(\overline{\Psi}_R^{(n)} \eta^{\mu\nu} \gamma_\mu \partial_\nu \Psi_R^{(n)} + \frac{1}{2} m_{n,R} \overline{\Psi}_R^{(n)} \Psi_R^{c(n)} + \text{H.c.} \right) \right].
\end{aligned} \tag{B.92}$$

B.3 Symplectic Majorana Fermions

Here, we consider an $n = 1$ bulk symplectic Majorana fermion $\Psi_i = \Psi_i(x^\mu, y)$, with action

$$S_5 = -\int d^5x\, \sqrt{-g} \left(\frac{1}{4} \overline{\Psi}_i \Gamma^M D_M \Psi_i - \frac{1}{4} \left(D_M \overline{\Psi}_i\right) \Gamma^M \Psi_i + \frac{1}{2} m_{\text{D}} \left(\sigma_3\right)_{ij} \overline{\Psi}_i \Psi_j \right), \tag{B.93}$$

where $i = 1, 2$ is the symplectic index labeling the two Dirac spinors. The analysis proceeds parallel to the Dirac case. The orbifold symmetry requires that the left- and right-handed chiral projections of each Dirac spinor Ψ_i must thus be states of definite parity according to (B.39). Further, due to the symplectic Majorana condition (A.38) there are only two

independent chiral projections, such that the parity assignments for each Dirac spinor will be opposite: schematically,

$$\left.\begin{aligned}\Psi_{1,L}(x^\mu,-y) &= \pm\Psi_{1,L}(x^\mu,y)\,,\\ \Psi_{1,R}(x^\mu,-y) &= \mp\Psi_{1,R}(x^\mu,y)\,,\end{aligned}\right\} \Longleftrightarrow \left\{\begin{aligned}\Psi_{2,L}(x^\mu,-y) &= \mp\Psi_{2,L}(x^\mu,y)\,,\\ \Psi_{2,R}(x^\mu,-y) &= \pm\Psi_{2,R}(x^\mu,y)\,.\end{aligned}\right. \tag{B.94}$$

This means that the bilinear $(\sigma_3)_{ij}\overline{\Psi}_i\Psi_j$ is odd, and the Dirac mass must take the form

$$m_{\rm D}(y) = cA'(y)\,, \tag{B.95}$$

where c is a real number. Conversely, the bilinear $\overline{\Psi}_i\Psi_i^c$ is even, and a bulk Majorana mass term of the form

$$S_5 \supset -\int d^5x\,\sqrt{-g}\,\left(\frac{1}{4}m_{\rm M}\,(\sigma_3)_{ij}\,\overline{\Psi}_i\Psi_j^c\right) \tag{B.96}$$

may be added, where

$$m_{\rm M}(y) = \xi k\,, \tag{B.97}$$

for a complex number ξ. Boundary Majorana mass terms may also be added individually for the independent chiral projections:

$$S_5 \supset -\int d^5x\,\sqrt{-g}\,\left(\frac{1}{4}m_{{\rm M},L}\,(\sigma_3)_{ij}\,\overline{\Psi}_{i,L}\Psi_{j,L}^c + \frac{1}{4}m_{{\rm M},R}\,(\sigma_3)_{ij}\,\overline{\Psi}_{i,R}\Psi_{j,R}^c\right) \tag{B.98}$$

where

$$m_{{\rm M}\,L,R}(y) = \xi_{{\rm UV}\,L,R}\,2\delta(y) + \xi_{{\rm IR}\,L,R}\,2\delta(y-\pi R)\,, \tag{B.99}$$

for complex numbers $\xi_{{\rm UV}\,L,R}$ and $\xi_{{\rm IR}\,L,R}$. As before, the addition of such a Majorana masses necessarily breaks $\mathcal{N}=1$ supersymmetry.

If we now define the two independent chiral projections to be $\Psi_{L,R} \equiv \Psi_{1\,L,R}$, then we can represent the symplectic Majorana fermion action (B.93) wholly as an action for the single Dirac fermion $\Psi \equiv \Psi_1$:

$$S_5 \to -\int d^5x\,\sqrt{-g}\left(\frac{1}{2}\overline{\Psi}\Gamma^M D_M\Psi - \frac{1}{2}\left(D_M\overline{\Psi}\right)\Gamma^M\Psi + m_{\rm D}\overline{\Psi}\Psi\right)\,. \tag{B.100}$$

The equations of motion for the chiral projections thus take the same form (B.48) as for a single Dirac fermion. The analysis proceeds identically to that in the preceding section

(Sec. B.2) and we will not repeat it here.

B.4 Gauge Fields

We consider an abelian[8] gauge field $A_M = A_M(x^\mu, y)$. The five-dimensional gauge transformation takes the form

$$A_M(x^\mu, y) \to A_M(x^\mu, y) - \frac{1}{g_5}\partial_M \alpha(x^\mu, y)\,, \tag{B.101}$$

where α is an arbitrary parameter. The gauge-invariant action takes the form

$$S_5 = \frac{1}{g_5^2}\int d^5x\,\sqrt{-g}\left(-\frac{1}{4}F_{MN}F^{MN} - \frac{1}{2\xi}\left[\partial_\mu A^\mu - \xi\, e^{2A}\partial_5\left(e^{-2A}\partial_5 A_5\right)\right]^2\right)\,, \tag{B.102}$$

where g_5 is the five-dimensional gauge coupling and $F_{MN} = \partial_M A_N - \partial_N A_M$ is the field strength tensor. The second term is a gauge-fixing functional [128], with ξ an arbitrary parameter that determines the choice of (R_ξ) gauge. In order for the gauge field action to be invariant under the $\mathbb{Z}_2$ orbifold symmetry (3.3), the components of the gauge fields must transform as[9]

$$A_\mu(x^\mu, -y) = \pm A_\mu(x^\mu, y) \quad \text{and} \quad A_5(x^\mu, -y) = \mp A_5(x^\mu, y)\,. \tag{B.104}$$

That is, the vector and scalar components of the gauge field must thus be states of definite parity under the orbifold symmetry such that if A_μ is even, A_5 must be odd and vice versa. In terms of the parities assigned at the orbifold fixed points,

$$A_\mu(x^\mu, 0) = \pm A_\mu(x^\mu, 0) \qquad \text{and} \qquad A_5(x^\mu, 0) = \mp A_5(x^\mu, 0)\,, \tag{B.105a}$$

$$A_\mu(x^\mu, \pi R) = \pm A_\mu(x^\mu, -\pi R) \quad \text{and} \quad A_5(x^\mu, \pi R) = \mp A_5(x^\mu, -\pi R)\,, \tag{B.105b}$$

[8] The generalization to nonabelian gauge groups is straightforward.

[9] This condition can be seen in two ways. In the absence of the gauge-fixing functional, it arises from the kinetic term, which contains an element of the form

$$S_5 \supset -\int d^5x\,\frac{1}{g_5^2}\left[\partial_5\left(e^{-2A}A_5\right)\right]\left(\eta^{\mu\nu}\partial_\mu A_\nu\right)\,, \tag{B.103}$$

after expansion and integration by parts. This term is canceled by the addition of the gauge-fixing action, but in that case, the requirement that A_μ and A_5 have opposite orbifold parity is necessary to satisfy the boundary conditions resulting from the variation of the action (see Ref. [112]).

there are four possible parity profile configurations, which we list in Table B.3.

Table B.3: Possible S^1-periodicity and $\mathbb{Z}_2$-parity assignments for bulk gauge fields on the orbifold. The left (right) term in the tuples refers to the $\mathbb{Z}_2$ parity at the $y = 0$ ($y = \pm\pi R$) orbifold fixed point.

boundary parity		$\mathbb{Z}_2$ parity		
A_μ	A_5	A_μ	A_5	S^1 periodicity
$(+,+)$	$(-,-)$	even	odd	periodic
$(+,-)$	$(-,+)$	even	odd	antiperiodic
$(-,+)$	$(+,-)$	odd	even	antiperiodic
$(-,-)$	$(+,+)$	odd	even	periodic

B.4.1 Kaluza-Klein theory

Five-dimensional field equations

The variation of the action gives the equations of motion

$$\eta^{\rho\nu}\partial_\rho\partial_\nu A_\mu - \left(1 - \frac{1}{\xi}\right)\eta^{\rho\nu}\partial_\mu\partial_\rho A_\nu + \partial_5\left(e^{-2A}\partial_5 A_\mu\right) = 0\,, \tag{B.106a}$$

$$\frac{1}{\xi}e^{2A}\eta^{\mu\nu}\partial_\mu\partial_\nu A_5 + e^{4A}\partial_5\left(e^{-4A}\partial_5 A_5\right) + 4k^2 A_5 = 0\,, \tag{B.106b}$$

The boundary conditions are either Neumann (N),

$$\partial_5 A_\mu\,\big|_{0^+,\pi R^-} = 0\,, \tag{B.107a}$$

$$\left(\partial_5 - 2A'\right) A_5\,\big|_{0^+,\pi R^-} = 0\,, \tag{B.107b}$$

or Dirichlet (D),

$$A_\mu\,\big|_{0,\pi R} = 0\,, \tag{B.108a}$$

$$A_5\,\big|_{0,\pi R} = 0\,, \tag{B.108b}$$

depending on the parity assignments, as we list in Table B.4. The correspondence between parity configurations and boundary conditions for the gauge field components is the natural extension of the general (scalar) case given in Table 3.2.

Table B.4: Correspondence between parity assignments and boundary conditions for bulk gauge fields on the orbifold. The left (right) term in the tuples refers to the $\mathbb{Z}_2$ parity or type of boundary condition at the $y = 0$ ($y = \pm\pi R$) orbifold fixed point.

boundary parity		boundary conditions	
A_μ	A_5	A_μ	A_5
$(+,+)$	$(-,-)$	(N,N)	(D,D)
$(+,-)$	$(-,+)$	(N,D)	(D,N)
$(-,+)$	$(+,-)$	(D,N)	(N,D)
$(-,-)$	$(+,+)$	(D,D)	(N,N)

Kaluza-Klein decomposition

We now assume the Kaluza-Klein decompositions

$$A_{\mu,5}(x^\mu, y) = \sum_{n=0}^{\infty} A^{(n)}_{\mu,5}(x^\mu)\, f^{(n)}_{A_{\mu,5}}(y)\,, \tag{B.109}$$

where the vector KK eigenmodes $A^{(n)}_\mu$ satisfy the equations[10]

$$\eta^{\rho\nu}\partial_\rho\partial_\nu A^{(n)}_\mu - \left(1 + \frac{1}{\xi}\right)\eta^{\rho\nu}\partial_\mu\partial_\rho A^{(n)}_\nu = m_n^2 A^{(n)}_\mu\,, \tag{B.110}$$

and the scalar eigenmodes $A^{(n)}_5$ satisfy the equations[11]

$$\frac{1}{\xi}\eta^{\mu\nu}\partial_\mu\partial_\nu A^{(n)}_5 = m_n^2 A^{(n)}_5\,, \tag{B.111}$$

[10] In the unitary gauge ($\xi \to \infty$) these are Proca equations.

[11] In the Feynman-'t Hooft gauge ($\xi = 1$) these are Klein-Gordon equations. In the unitary gauge ($\xi \to \infty$), the solutions are trivial: $A^{(n)}_5 = 0$.

both with the same mass eigenvalues m_n^2. The bulk profiles $f^{(n)}_{A_{\mu,5}}$ obey the orthonormality conditions

$$\int_{-\pi R}^{\pi R} dy\, f^{(m)}_{A_\mu}(y)\, f^{(n)}_{A_\mu}(y) = \delta_{mn}\,, \tag{B.112a}$$

$$\int_{-\pi R}^{\pi R} dy\, e^{-2A(y)} f^{(m)}_{A_5}(y)\, f^{(n)}_{A_5}(y) = \delta_{mn}\,, \tag{B.112b}$$

and the equations of motion

$$\left[-e^{2A}\partial_5\left(e^{-2A}\partial_5\right)\right] f^{(n)}_{A_\mu} = e^{2A} m_n^2 f^{(n)}_{A_\mu}\,, \tag{B.113a}$$

$$\left[-e^{4A}\partial_5\left(e^{-4A}\partial_5\right) - 4k^2\right] f^{(n)}_{A_5} = e^{2A} m_n^2 f^{(n)}_{A_5}\,, \tag{B.113b}$$

where the boundary conditions are Neumann

$$\partial_5 f^{(n)}_{A_\mu}\Big|_{0^+,\pi R^-} = 0\,, \tag{B.114a}$$

$$\left(\partial_5 - 2A'\right) f^{(n)}_{A_5}\Big|_{0^+,\pi R^-} = 0\,, \tag{B.114b}$$

or Dirichlet,

$$f^{(n)}_{A_\mu}\Big|_{0,\pi R} = 0\,, \tag{B.115a}$$

$$f^{(n)}_{A_5}\Big|_{0,\pi R} = 0\,. \tag{B.115b}$$

Massive solutions

For $m_n^2 > 0$, the solutions to (B.113) take the forms:

$$f^{(n)}_{A_{\mu,5}}(y) = \begin{cases} f^{(n)}_{A_{\mu,5}}(z) & \text{for } A_{\mu,5} \text{ even}\,, \\ \mathrm{sgn}(y)\, f^{(n)}_{A_{\mu,5}}(z) & \text{for } A_{\mu,5} \text{ odd}\,, \end{cases} \tag{B.116}$$

where

$$f^{(n)}_{A_\mu}(z) = \sqrt{k}\, N^{(n)}_A z k \left[J_1(m_n z) - C^{(n)}_A Y_1(m_n z)\right]\,, \tag{B.117a}$$

$$f_{A_5}^{(n)}(z) = \sqrt{k}\, N_A^{(n)}\, (zk)^2 \left[J_0(m_n z) - C_A^{(n)} Y_0(m_n z) \right] , \tag{B.117b}$$

are the profiles in terms of the conformal coordinate z. Here, the constants $N_A^{(n)}$ and $C_A^{(n)}$ are the same for both the vector and scalar components of each mode, a result due ultimately the gauge symmetry, which requires that both components of each mode share a common mass eigenvalue; if the gauge symmetry is spontaneously broken, we must distinguish separate constants for each component. For each mode, the dimensionless constant $N_A^{(n)}$ is fixed by the orthonormality conditions (B.112) and the constant $C_A^{(n)}$ is determined by the boundary conditions. Neumann boundary conditions (even boundary parity) give rise to the values

$$C_{A_\mu}^{(n)}\Big|_{y=0,\pi R} = \frac{J_0(x_n^{\mathrm{UV,IR}})}{Y_0(x_n^{\mathrm{UV,IR}})} , \tag{B.118a}$$

$$C_{A_5}^{(n)}\Big|_{y=0,\pi R} = \frac{J_1(x_n^{\mathrm{UV,IR}})}{Y_1(x_n^{\mathrm{UV,IR}})} , \tag{B.118b}$$

while Dirichlet conditions (odd boundary parity) give

$$C_{A_\mu}^{(n)}\Big|_{y=0,\pi R} = \frac{J_1(x_n^{\mathrm{UV,IR}})}{Y_1(x_n^{\mathrm{UV,IR}})} , \tag{B.119a}$$

$$C_{A_5}^{(n)}\Big|_{y=0,\pi R} = \frac{J_0(x_n^{\mathrm{UV,IR}})}{Y_0(x_n^{\mathrm{UV,IR}})} , \tag{B.119b}$$

The eigenmass m_n is determined by ensuring that the boundary conditions on both branes give rise to the same constant (note that the constants for both the vector and scalar components are necessarily the same in each parity configuration):

$$C_A^{(n)} = C_{A_{\mu,5}}^{(n)}\Big|_{y=0} = C_{A_{\mu,5}}^{(n)}\Big|_{y=\pi R} , \tag{B.120}$$

explicitly,

$$C_A^{(n)} = \begin{cases} \dfrac{J_0(x_n^{\rm UV})}{Y_0(x_n^{\rm UV})} = \dfrac{J_0(x_n^{\rm IR})}{Y_0(x_n^{\rm IR})} & \text{for } A_M = \left(A_\mu^{(+,+)}, A_5^{(-,-)}\right), \\ \dfrac{J_0(x_n^{\rm UV})}{Y_0(x_n^{\rm UV})} = \dfrac{J_1(x_n^{\rm IR})}{Y_1(x_n^{\rm IR})} & \text{for } A_M = \left(A_\mu^{(+,-)}, A_5^{(-,+)}\right), \\ \dfrac{J_1(x_n^{\rm UV})}{Y_1(x_n^{\rm UV})} = \dfrac{J_0(x_n^{\rm IR})}{Y_0(x_n^{\rm IR})} & \text{for } A_M = \left(A_\mu^{(-,+)}, A_5^{(+,-)}\right), \\ \dfrac{J_1(x_n^{\rm UV})}{Y_1(x_n^{\rm UV})} = \dfrac{J_1(x_n^{\rm IR})}{Y_1(x_n^{\rm IR})} & \text{for } A_M = \left(A_\mu^{(-,-)}, A_5^{(+,+)}\right). \end{cases} \tag{B.121}$$

We discuss the approximate Kaluza-Klein spectrum in Appendix C.

We note that there is a redundancy in this Kaluza-Klein description related to presence of the gauge symmetry: for $m_n^2 > 0$, the solutions to (B.113a) are also solutions to (B.113b) as

$$f_{A_5}^{(n)} = \frac{1}{m_n}\,\partial_5 f_{A_\mu}^{(n)}\,. \tag{B.122}$$

Evidently, the massive fields $A_5^{(n)}$ provide the longitudinal polarizations of the associated massive fields $A_\mu^{(n)}$. This is a result of the compactification, which spontaneously breaks the five-dimensional gauge invariance. At each KK level a Higgs mechanism operates in which the scalar modes $A_5^{(n)}$ are eaten by the vector modes $A_\mu^{(n)}$, such that the physical KK spectrum consists only of a tower of massive spin-one fields with three physical polarizations each.

Zero-mode solutions

Massless Kaluza-Klein solutions can arise only for the components of the gauge field with $(+,+)$ parity, corresponding to Neumann boundary conditions on both branes. For components with odd parity on any boundary, obeying a Dirichlet condition of the form (B.115), the only massless solution is the trivial one. Only two out of the four parity configurations in Table B.3 support a zero-mode solution.

1. **Vector zero mode**

   When $A = A_\mu^{(+,+)} + A_5^{(-,-)}$, a solution to (B.113a) with zero mass eigenvalue exists. Such solutions offer the only possibility of recovering the four-dimensional standard model gauge fields from the five-dimensional bulk, and accordingly, realistic theories of physics on the orbifold require that the gauge fields of the standard model have even

parities on both boundaries. The zero-mode solutions have constant profiles of the form

$$f^{(0)}_{A_\mu}(y) = \sqrt{\frac{k}{2\pi kR}} \equiv \sqrt{k}\, N^{(0)}_{A_\mu}\,. \tag{B.123}$$

These massless solutions only exist when the four-dimensional gauge symmetry is unbroken, or equivalently, when the action (B.102) contains no bulk or boundary mass terms. If it does, the zero mode is lifted and the profiles take the form (B.116) as in the massive case, where the masses are found by simultaneously satisfying (B.120) for Neumann boundary conditions on both branes, appropriately modified to account for the extra mass terms. Although we do not consider it explicitly, a UV-brane mass term will arise for the standard model SU(2) gauge fields after the Higgs acquires a VEV in EWSB, lifting the corresponding tower of KK masses.

2. Scalar zero mode

Conversely, when $A = A_\mu^{(-,-)} + A_5^{(+,+)}$, a solution to (B.113b) with zero mass eigenvalue exists with a profile of the form

$$f^{(0)}_{A_5}(y) = \sqrt{\frac{2k}{e^{2\pi kR}-1}}\, e^{2A(y)} \equiv \sqrt{k}\, N^{(0)}_{A_5}\, e^{2A(y)}\,, \tag{B.124}$$

or

$$f^{(0)}_{A_5}(z) = \sqrt{\frac{2k}{(z_{\rm IR}k)^2-1}}\, (zk)^2 = \sqrt{k}\, N^{(0)}_{A_5}\, (zk)^2\,, \tag{B.125}$$

in terms of the conformal coordinate. Again, this zero mode can be lifted if bulk or brane mass terms are added to the gauge field action (B.102).

Localization

The localization properties of the KK modes can be extracted by considering the expanded action. The vector part takes the form

$$S_5 = \sum_n \frac{1}{g_5^2} \int d^5x\, \sqrt{-g}\, \left(f^{(n)}_{A_\mu}\right)^2 \Big(-\frac{1}{4} g^{\mu\nu} g^{\rho\sigma} F^{(n)}_{\mu\rho} F^{(n)}_{\nu\sigma} \\ - \frac{1}{2\xi} g^{\mu\nu} g^{\rho\sigma} \left(\partial_\mu A^{(n)}_\nu\right) \left(\partial_\rho A^{(n)}_\sigma\right) + \frac{1}{2} e^{2A} m_n^2\, g^{\mu\nu} A^{(n)}_\mu A^{(n)}_\nu \Big)$$

$$= \sum_n \frac{1}{g_5^2} \int d^5x \, (f^{(n)}_{A_\mu})^2 \Big(-\frac{1}{4}\eta^{\mu\nu}\eta^{\rho\sigma} F^{(n)}_{\mu\rho} F^{(n)}_{\nu\sigma} \tag{B.126}$$
$$- \frac{1}{2\xi}\eta^{\mu\nu}\eta^{\rho\sigma} \left(\partial_\mu A^{(n)}_\nu\right)\left(\partial_\rho A^{(n)}_\sigma\right) + \frac{1}{2} m_n^2 \eta^{\mu\nu} A^{(n)}_\mu A^{(n)}_\nu \Big) ,$$

while the scalar part takes the form

$$\begin{aligned} S_5 &= -\sum_n \frac{1}{g_5^2} \int d^5x \, \sqrt{-g} \, (f^{(n)}_{A_5})^2 \left(\frac{1}{2} g^{\mu\nu} \left(\partial_\mu A^{(n)}_5\right)\left(\partial_\nu A^{(n)}_5\right) - \frac{\xi}{2} e^{2A} m_n^2 \left(A^{(n)}_5\right)^2 \right) \\ &= -\sum_n \frac{1}{g_5^2} \int d^5x \, (f^{(n)}_{A_5})^2 \, e^{-2A} \left(\frac{1}{2} \eta^{\mu\nu} \left(\partial_\mu A^{(n)}_5\right)\left(\partial_\nu A^{(n)}_5\right) - \frac{\xi}{2} m_n^2 \left(A^{(n)}_5\right)^2 \right) \\ &= -\sum_n \frac{1}{g_5^2} \int d^5x \, (\tilde{f}^{(n)}_{A_5})^2 \left(\frac{1}{2} \eta^{\mu\nu} \left(\partial_\mu A^{(n)}_5\right)\left(\partial_\nu A^{(n)}_5\right) - \frac{\xi}{2} m_n^2 \left(A^{(n)}_5\right)^2 \right) , \end{aligned} \tag{B.127}$$

where we have absorbed all warp factors from the metric into the rescaled scalar profile:

$$\tilde{f}^{(n)}_{A_5}(y) = f^{(n)}_{A_5}(y) \, e^{-A(y)} . \tag{B.128}$$

Note that for the rescaled scalar profiles the orthonormality relation (B.112b) becomes

$$\int_{-\pi R}^{\pi R} dy \, \tilde{f}^{(m)}_{A_5}(y) \, \tilde{f}^{(n)}_{A_5}(y) = \delta_{mn} . \tag{B.129}$$

Using this and the vector relation (B.112a), we can reduce the actions to two towers of four-dimensional states:

$$S_4 = \sum_n \frac{1}{g_5^2} \int d^4x \, \Big(-\frac{1}{4}\eta^{\mu\nu}\eta^{\rho\sigma} F^{(n)}_{\mu\rho} F^{(n)}_{\nu\sigma} \tag{B.130}$$
$$- \frac{1}{2\xi}\eta^{\mu\nu}\eta^{\rho\sigma} \left(\partial_\mu A^{(n)}_\nu\right)\left(\partial_\rho A^{(n)}_\sigma\right) + \frac{1}{2} m_n^2 \eta^{\mu\nu} A^{(n)}_\mu A^{(n)}_\nu \Big) ,$$

and

$$S_4 = -\sum_n \frac{1}{g_5^2} \int d^5x \, \left(\frac{1}{2} \eta^{\mu\nu} \left(\partial_\mu A^{(n)}_5\right)\left(\partial_\nu A^{(n)}_5\right) - \frac{\xi}{2} m_n^2 \left(A^{(n)}_5\right)^2 \right) . \tag{B.131}$$

The localization of each vector mode $A^{(n)}_\mu$ in the extra dimension with respect to a conformally flat metric is thus determined directly by the original profiles $f^{(n)}_{A_\mu}$ and the

localization of each scalar mode $A_5^{(n)}$ by the rescaled profiles $\tilde{f}_{A_5}^{(n)}$. In particular, the vector zero mode is conformally flat, while the rescaled scalar zero mode is

$$\tilde{f}_{A_5}^{(0)}(y) = \sqrt{\frac{2k}{e^{2\pi kR}-1}}\, e^{A(y)} = \sqrt{k}\, N_{A_5}^{(0)}\, e^{A(y)}\,, \tag{B.132}$$

or

$$\tilde{f}_{A_5}^{(0)}(z) = \sqrt{\frac{2k}{(z_{\rm IR}k)^2-1}}\, zk = \sqrt{k}\, N_{A_5}^{(0)}\, zk\,, \tag{B.133}$$

which is IR-localized.

B.5 Gravitino

We next consider the gravitino, which, in five-dimensions is described by a spin-$\frac{3}{2}$ symplectic Majorana fermion Ψ_M^i, with action

$$S_5 = -\frac{M_5^3}{2}\int d^5x\,\sqrt{-g}\left(\frac{1}{2}\overline{\Psi}_M^i\,\Gamma^{MNR}D_N\Psi_R^i - \frac{1}{2}\left(D_N\overline{\Psi}_M^i\right)\Gamma^{MNR}\Psi_R^i \right.$$
$$\left. - \frac{3}{2}A'\,(\sigma_3)_{ij}\,\overline{\Psi}_M^i\,\Gamma^{MN}\Psi_N^j\right), \tag{B.134}$$

where the symplectic index $i = 1, 2$ labels the fundamental representation of the $\mathrm{SU}(2)_R$ automorphism group (R symmetry) of the $\mathcal{N} = 1$ supersymmetry algebra in five dimensions and

$$\Gamma^{M_1M_2\ldots M_n} \equiv \frac{1}{n!}\Gamma^{[M_1}\Gamma^{M_2}\cdots\Gamma^{M_n]} \tag{B.135}$$

are the antisymmetrized products of gamma matrices. Like the spin-$\frac{1}{2}$ symplectic majorana fermion considered in Sec. B.3, there are only two independent chiral projections for each spacetime component of the graviton. Choosing these to be $\Psi_{ML,R} \equiv \Psi^1_{ML,R}$, invariance under the orbifold $\mathbb{Z}_2$ symmetry requires the parity assignments

$$\left.\begin{aligned}\Psi_{\mu,L}(x^\mu,-y) &= \pm\Psi_{\mu,L}(x^\mu,y)\\ \Psi_{\mu,R}(x^\mu,-y) &= \mp\Psi_{\mu,R}(x^\mu,y)\end{aligned}\right\} \quad\text{and}\quad \left\{\begin{aligned}\Psi_{5,L}(x^\mu,-y) &= \mp\Psi_{5,L}(x^\mu,y)\\ \Psi_{5,R}(x^\mu,-y) &= \pm\Psi_{5,R}(x^\mu,y)\end{aligned}\right., \tag{B.136}$$

In terms of the parities assigned at the orbifold fixed points there are four possible parity profile configurations for the chiral components, which we list in Table B.5.

Table B.5: Possible S^1-periodicity and $\mathbb{Z}_2$-parity assignments for a bulk gravitino on the orbifold. The left (right) term in the tuples refers to the $\mathbb{Z}_2$ parity at the $y = 0$ ($y = \pm\pi R$) orbifold fixed point.

boundary parity				$\mathbb{Z}_2$ parity				
$\Psi_{\mu,L}$	$\Psi_{\mu,R}$	$\Psi_{5,L}$	$\Psi_{5,R}$	$\Psi_{\mu,L}$	$\Psi_{\mu,R}$	$\Psi_{5,L}$	$\Psi_{5,R}$	S^1 periodicity
$(+,+)$	$(-,-)$	$(-,-)$	$(+,+)$	even	odd	odd	even	periodic
$(+,-)$	$(-,+)$	$(-,+)$	$(+,-)$	even	odd	odd	even	antiperiodic
$(-,+)$	$(+,-)$	$(+,-)$	$(-,+)$	odd	even	even	odd	antiperiodic
$(-,-)$	$(+,+)$	$(+,+)$	$(-,-)$	odd	even	even	odd	periodic

B.5.1 Kaluza-Klein theory

Due to the gauging of local supersymmetry in supergravity, not all of the degrees of freedom of the gravitino are physical. In five-dimensional $\mathcal{N} = 1$ supergravity on the orbifold, the effective $\mathcal{N} = 2$ four-dimensional supersymmetries are nonlinearly realized. This is a result of compactification over the orbifold, which spontaneously breaks local five-dimensional supergravity, leaving a residual 4D $\mathcal{N} = 1$ or $\mathcal{N} = 0$ supersymmetry, depending on whether the compactification is periodic or antiperiodic [94, 95, 208]. The breaking occurs order-by-order in the Kaluza-Klein theory. If we take the Kaluza-Klein decompositions for the gravitino components to be of the forms

$$\Psi_{\mu\, L,R}(x^\mu, y) = \sum_{n=0}^{\infty} \Psi^{(n)}_{\mu\, L,R}(x^\mu)\, f^{(n)}_{\Psi_{\mu\, L,R}}(y)\,, \tag{B.137a}$$

$$\Psi_{5\, L,R}(x^\mu, y) = \sum_{n=0}^{\infty} \Psi^{(n)}_{5\, L,R}(x^\mu)\, f^{(n)}_{\Psi_{5\, L,R}}(y)\,, \tag{B.137b}$$

then the Kaluza-Klein modes for the fifth components of the gravitino $\Psi^{(n)}_{5\, L,R}$ each act as the goldstino of a 4D $\mathcal{N} = 1$ supersymmetry at the nth level. A super-Higgs mechanism operates at each level, such that they are eaten by the $\Psi^{(n)}_{\mu\, L,R}$ modes, which thereby acquire

masses. In the unitary gauge, this takes the form

$$\Psi^{(n)}_{\mu,L} \to m_n \Psi^{(n)}_{\mu,L} - \partial_\mu \Psi^{(n)}_{5,L} + m_n \gamma_\mu \sum_{n=0}^{\infty} a_{nk} \frac{\Psi^{(k)}_{\mu,R}}{m_k} \,, \tag{B.138a}$$

$$\Psi^{(n)}_{\mu,R} \to m_n \Psi^{(n)}_{\mu,R} - \partial_\mu \Psi^{(n)}_{5,R} \,, \tag{B.138b}$$

where

$$a_{mn} \equiv \int_{-\pi R}^{\pi R} dy\, e^{-2A(y)} f^{(m)}_{\Psi_{\mu,L}}(y)\, f^{(n)}_{\Psi_{\mu,R}}(y) \,, \tag{B.139}$$

such that the gravitino modes $\Psi^{(n)}_{\mu\, L,R}$ obey the four-dimensional Rarita-Schwinger equations

$$\gamma^{\mu\nu\rho} \partial_\nu \Psi^{(n)}_{\rho\, L,R} = m_n \gamma^{\mu\rho} \Psi^{(n)}_{\rho\, L,R} \,, \tag{B.140}$$

with eigenmasses m_n, while the goldstino modes $\Psi^{(n)}_{5\, L,R}$ are eliminated.

Because of the super-Higgs mechanism, the bulk profiles for the gravitino and goldstino components are related by

$$f^{(n)}_{\Psi_{5\, L,R}} = \frac{1}{m_n} \left(\frac{1}{2} A' \pm \partial_5 \right) f^{(n)}_{\Psi_{\mu\, L,R}} \,. \tag{B.141}$$

The gravitino profiles themselves obey the orthonormality conditions

$$\int_{-\pi R}^{\pi R} dy\, e^{-A} f^{(m)}_{\Psi_{\mu\, L,R}}(y)\, f^{(n)}_{\Psi_{\mu\, L,R}}(y) = \delta_{mn} \,, \tag{B.142}$$

and the equations of motion

$$\partial_5 f^{(n)}_{\Psi_{\mu,L}} + \frac{1}{2} A' f^{(n)}_{\Psi_{\mu,L}} = e^A m_n f^{(n)}_{\Psi_{\mu,R}} \,, \tag{B.143a}$$

$$-\partial_5 f^{(n)}_{\Psi_{\mu,R}} + \frac{5}{2} A' f^{(n)}_{\Psi_{\mu,R}} = e^A m_n f^{(n)}_{\Psi_{\mu,L}} \,. \tag{B.143b}$$

Redefining $\hat{f}^{(n)}_{\Psi_{\mu\,L,R}} = e^{-A} f^{(n)}_{\Psi_{\mu\,L,R}}$, these are

$$\partial_5 \hat{f}^{(n)}_{\Psi_{\mu,L}} + \frac{3}{2} A' \hat{f}^{(n)}_{\Psi_{\mu,L}} = e^{A} m_n \hat{f}^{(n)}_{\Psi_{\mu,R}} \,, \tag{B.144a}$$

$$-\partial_5 \hat{f}^{(n)}_{\Psi_{\mu,R}} + \frac{3}{2} A' \hat{f}^{(n)}_{\Psi_{\mu,R}} = e^{A} m_n \hat{f}^{(n)}_{\Psi_{\mu,L}} \,. \tag{B.144b}$$

or

$$\left[-e^{A} \partial_5 \left(e^{-A} \partial_5 \right) + \frac{3}{2} \left(\frac{3}{2} \pm 1 \right) k^2 \right] \hat{f}^{(n)}_{\Psi_{\mu\,L,R}} = e^{2A} m_n^2 \hat{f}^{(n)}_{\Psi_{\mu\,L,R}} \,. \tag{B.145}$$

in decoupled, second-order form. The boundary conditions are Neumann,

$$\left(\partial_5 + \frac{3}{2} A' \right) \hat{f}^{(n)}_{\Psi_{\mu,L}} \Big|_{0^+,\pi R^-} = \left(\partial_5 + \frac{1}{2} A' \right) f^{(n)}_{\Psi_{\mu,L}} \Big|_{0^+,\pi R^-} = 0 \,, \tag{B.146a}$$

$$\left(\partial_5 - \frac{3}{2} A' \right) \hat{f}^{(n)}_{\Psi_{\mu,R}} \Big|_{0^+,\pi R^-} = \left(\partial_5 - \frac{5}{2} A' \right) f^{(n)}_{\Psi_{\mu,R}} \Big|_{0^+,\pi R^-} = 0 \,, \tag{B.146b}$$

or Dirichlet,

$$\hat{f}^{(n)}_{\Psi_{\mu\,L,R}} \Big|_{0,\pi R} = f^{(n)}_{\Psi_{\mu\,L,R}} \Big|_{0,\pi R} = 0 \,, \tag{B.147}$$

depending on the parity assignments, which take the same form as those in Table B.2 a Dirac fermion. In fact, the equations of motion (B.145) for each spacetime component of the gravitino profiles are exactly the same as those of a Dirac fermion with bulk mass parameter $c = \frac{3}{2}$. The rest of the Kaluza-Klein theory follows directly from this correspondence.

Massive solutions

For $m_n^2 > 0$, the solutions to (B.145) take the forms:

$$f^{(n)}_{\Psi_{\mu\,L,R}}(y) = e^{A(y)} \hat{f}^{(n)}_{\Psi_{\mu\,L,R}}(y) = \begin{cases} f^{(n)}_{\Psi_{\mu\,L,R}}(z) & \text{for } \Psi_{\mu\,L,R} \text{ even} \,, \\ \operatorname{sgn}(y)\, f^{(n)}_{\Psi_{\mu\,L,R}}(z) & \text{for } \Psi_{\mu\,L,R} \text{ odd} \,, \end{cases} \tag{B.148}$$

where,

$$f^{(n)}_{\Psi_{\mu,L}}(z) = \sqrt{k}\, N^{(n)}_{\Psi_\mu} (zk)^{3/2} \left[J_2(m_n z) - C^{(n)}_{\Psi} Y_2(m_n z) \right] \,, \tag{B.149a}$$

$$f^{(n)}_{\Psi_{\mu,R}}(z) = \sqrt{k}\, N^{(n)}_{\Psi_\mu} (zk)^{3/2} \left[J_1(m_n z) - C^{(n)}_{\Psi} Y_1(m_n z) \right] \,. \tag{B.149b}$$

Here, the constants $N^{(n)}_{\Psi_\mu}$ and $C^{(n)}_{\Psi_\mu}$ are the same for both components of each mode. This is only true in the supersymmetric limit; if Majorana masses are added, we must distinguish separate constants for each component (just as what happens for a Dirac fermion as we discuss in Sec. B.2.2). For each mode, the dimensionless constant $N^{(n)}_{\Psi_\mu}$ is fixed by the orthonormality conditions (B.142). The constant $C^{(n)}_{\Psi_\mu}$ is determined by the boundary conditions:

$$C^{(n)}_{\Psi_\mu} = \begin{cases} \dfrac{J_1(x_n^{\rm UV})}{Y_1(x_n^{\rm UV})} = \dfrac{J_1(x_n^{\rm IR})}{Y_1(x_n^{\rm IR})} & \text{for } \Psi_\mu = \Psi^{(+,+)}_{\mu,L} + \Psi^{(-,-)}_{\mu,R}\,, \\ \dfrac{J_1(x_n^{\rm UV})}{Y_1(x_n^{\rm UV})} = \dfrac{J_2(x_n^{\rm IR})}{Y_2(x_n^{\rm IR})} & \text{for } \Psi_\mu = \Psi^{(+,-)}_{\mu,L} + \Psi^{(-,+)}_{\mu,R}\,, \\ \dfrac{J_2(x_n^{\rm UV})}{Y_2(x_n^{\rm UV})} = \dfrac{J_1(x_n^{\rm IR})}{Y_1(x_n^{\rm IR})} & \text{for } \Psi_\mu = \Psi^{(-,+)}_{\mu,L} + \Psi^{(+,-)}_{\mu,R}\,, \\ \dfrac{J_2(x_n^{\rm UV})}{Y_2(x_n^{\rm UV})} = \dfrac{J_2(x_n^{\rm IR})}{Y_2(x_n^{\rm IR})} & \text{for } \Psi_\mu = \Psi^{(-,-)}_{\mu,L} + \Psi^{(+,+)}_{\mu,R}\,. \end{cases} \tag{B.150}$$

The eigenmass m_n is found as the solution to this equation. We discuss the approximate Kaluza-Klein spectrum in Appendix C.

Zero-mode solutions

A solution to (B.145) with zero mass eigenvalue only exists for chiral components with $(+,+)$ parity, corresponding to Neumann boundary conditions on both branes. Only two out of the four parity configurations in Table B.5 support a zero-mode solution.

1. Left-handed zero mode

If $\Psi_\mu = \Psi^{(+,+)}_{\mu,L} + \Psi^{(-,-)}_{\mu,R}$, then the left-handed chiral component has a zero-mode solution. The zero-mode profile takes the form

$$f^{(0)}_{\Psi_{\mu,L}}(y) = \sqrt{\frac{k}{1-e^{-2\pi kR}}}\, e^{-(1/2)\,A(y)} \equiv \sqrt{k}\, N^{(0)}_{\Psi_{\mu,L}} e^{-(1/2)\,A(y)} \tag{B.151}$$

or

$$f^{(0)}_{\Psi_L}(z) = \sqrt{\frac{k}{1-(z_{\rm IR}k)^{-2}}}\,(zk)^{-1/2} = \sqrt{k}\, N^{(0)}_{\Psi_L}\,(zk)^{-1/2}\,, \tag{B.152}$$

in terms of the conformal coordinate.

2. Right-handed zero mode

If $\Psi = \Psi_L^{(-,-)} + \Psi_R^{(+,+)}$, then the right-handed chiral component has a zero-mode solution. The zero-mode profile takes the form

$$f_{\Psi_R}^{(0)}(y) = \sqrt{\frac{2k}{e^{4\pi kR}-1}}\, e^{(5/2)\,A(y)} \equiv \sqrt{k}\, N_{\Psi_R}^{(0)}\, e^{(5/2)\,A(y)} \tag{B.153}$$

or

$$f_{\Psi_R}^{(0)}(z) = \sqrt{\frac{2k}{(z_{\rm IR}k)^4-1}}\, (zk)^{5/2} = \sqrt{k}\, N_{\Psi_R}^{(0)}\, (zk)^{5/2}\,, \tag{B.154}$$

in terms of the conformal coordinate.

If Majorana masses are added either in the bulk or on the boundary, then massless solutions are no longer possible. In this case, the zero modes are lifted as in the Dirac fermion case discussed in Sec. B.2.2. An analytic approximation for the resulting zero-mode mass is given in Appendix C.

Localization

In this case, a conformal rescaling of the bulk profiles gives:

$$\tilde{f}_{\Psi_{\mu\,L,R}}^{(n)}(y) = f_{\Psi_{\mu\,L,R}}^{(n)}(y)\, e^{-(1/2)\,A(y)}\,, \tag{B.155}$$

such that the orthonormality relation (B.142) becomes

$$\int_{-\pi R}^{\pi R} dy\, \tilde{f}_{\Psi_{\mu\,L,R}}^{(m)}(y)\, \tilde{f}_{\Psi_{\mu\,L,R}}^{(n)}(y) = \delta_{mn}\,. \tag{B.156}$$

In particular, the rescaled profiles for the gravitino zero modes are

$$\tilde{f}_{\Psi_{\mu,L}}^{(0)}(y) = \sqrt{\frac{k}{1-e^{-2\pi kR}}}\, e^{-A(y)} = \sqrt{k}\, N_{\Psi_{\mu,L}}^{(0)}\, e^{-A(y)}\,, \tag{B.157a}$$

$$\tilde{f}_{\Psi_{\mu,R}}^{(0)}(y) = \sqrt{\frac{2k}{e^{4\pi kR}-1}}\, e^{2A(y)} = \sqrt{k}\, N_{\Psi_{\mu,R}}^{(0)}\, e^{2A(y)}\,, \tag{B.157b}$$

or

$$\tilde{f}^{(0)}_{\Psi_{\mu,L}}(z) = \sqrt{\frac{k}{1-(z_{\rm IR}k)^{-2}}}\,(zk)^{-1} = \sqrt{k}\,N^{(0)}_{\Psi_{\mu,L}}\,(zk)^{-1}\,, \tag{B.158a}$$

$$\tilde{f}^{(0)}_{\Psi_{\mu,R}}(z) = \sqrt{\frac{2k}{(z_{\rm IR}k)^4-1}}\,(zk)^2 = \sqrt{k}\,N^{(0)}_{\Psi_{\mu,R}}\,(zk)^2 \tag{B.158b}$$

We see that the left-handed (right-handed) gravitino zero mode is UV-localized (IR-localized).

B.6 Graviton

We consider tensor fluctuations of the AdS$_5$ metric of the form

$$ds^2 = g_{MN}(x^\mu, y)\,\mathrm{d}x^M\mathrm{d}x^N = e^{-2A(y)}\left[\eta_{\mu\nu} + h_{\mu\nu}(x^\mu, y)\right]\mathrm{d}x^\mu\mathrm{d}x^\nu + dy^2\,, \tag{B.159}$$

where $h_{\mu\nu}$ is the graviton field. In the transverse-traceless (TT) gauge,[12] where $\partial_\mu h^{\mu\nu} = 0$ and $h_\mu{}^\mu = 0$, the linearized gravitational action in the bulk is

$$\begin{aligned} S_5 &= -\int d^5x\,\sqrt{-g}\left(\frac{1}{2}M_5^3\mathcal{R}_5 + \Lambda_5\right) \\ &\to -\frac{M_5^3}{2}\int d^5x\,e^{-2A}\left(\frac{1}{2}\left(\partial_\rho h_{\mu\nu}\right)\left(\partial^\rho h^{\mu\nu}\right) + \frac{1}{2}e^{-2A}\left(\partial_5 h_{\mu\nu}\right)\left(\partial_5 h^{\mu\nu}\right)\right)\,, \end{aligned} \tag{B.161}$$

where all indices are contracted with the Minkowski metric $\eta_{\mu\nu}$. In order for the graviton action to be invariant under the $\mathbb{Z}_2$ orbifold symmetry (3.3), the graviton fields must be either even or odd:

$$h_{\mu\nu}(x^\mu, -y) = \pm h_{\mu\nu}(x^\mu, y)\,. \tag{B.162}$$

In terms of the parities assigned at the boundaries, there are the same four possible parity configurations as in the general scalar case (see Table 3.1).

[12] More formally, we could parametrize the tensor fluctuations as

$$ds^2 = g_{MN}(x^\mu, y)\,\mathrm{d}x^M\mathrm{d}x^N = \left[g_{MN}(y) + h_{MN}(x^\mu, y)\right]\mathrm{d}x^M\mathrm{d}x^N\,, \tag{B.160}$$

where $g_{MN}(y)$ is the unperturbed metric (3.16). In this case we employ the Randall-Sundrum (RS) gauge, which combines the constraints $h_{M5} = 0$ with the TT conditions.

B.6.1 Kaluza-Klein theory

The variation of the action gives the equations of motion

$$\eta^{\rho\sigma}\partial_\rho\partial_\sigma h_{\mu\nu} + e^{2A}\partial_5\left(e^{-4A}\partial_5 h_{\mu\nu}\right) = 0\,, \tag{B.163}$$

where the boundary conditions may be either Neumann (N),

$$\partial_5 h_{\mu\nu}\,\big|_{0,\pi R} = 0\,, \tag{B.164}$$

or Dirichlet (D),

$$h_{\mu\nu}\,\big|_{0,\pi R} = 0\,, \tag{B.165}$$

depending on the parity assignments (the correspondence is the same as for the general scalar case shown in Table 3.2).

We now assume the Kaluza-Klein decompositions

$$h_{\mu\nu}(x^\mu, y) = \sum_{n=0}^{\infty} h_{\mu\nu}^{(n)}(x^\mu)\, f_h^{(n)}(y)\,, \tag{B.166}$$

where the KK eigenmodes $h_{\mu\nu}^{(n)}$ satisfy the equations

$$\eta^{\rho\sigma}\partial_\rho\partial_\sigma h_{\mu\nu}^{(n)} = m_n^2 h_{\mu\nu}^{(n)}\,, \tag{B.167}$$

with mass eigenvalues m_n^2. The bulk profiles $f_h^{(n)}$ obey the orthonormality conditions

$$\int_{-\pi R}^{\pi R} dy\, e^{-2A(y)} f_h^{(m)}(y)\, f_h^{(n)}(y) = \delta_{mn}\,, \tag{B.168}$$

and the equations of motion

$$-e^{4A}\partial_5\left(e^{-4A}\partial_5 f_h^{(n)}\right) = e^{2A} m_n^2 f_h^{(n)}\,, \tag{B.169}$$

with Neumann,

$$\partial_5 f_h^{(n)}\,\Big|_{0,\pi R} = 0\,, \tag{B.170}$$

or Dirichlet,

$$f_h^{(n)}\Big|_{0,\pi R} = 0\,, \tag{B.171}$$

boundary conditions.

Massive solutions

For $m_n^2 > 0$, the solutions to (B.169) take the forms:

$$f_h^{(n)}(y) = \begin{cases} f_h^{(n)}(z) & \text{for } h_{\mu\nu} \text{ even}\,, \\ \operatorname{sgn}(y)\, f_h^{(n)}(z) & \text{for } h_{\mu\nu} \text{ odd}\,, \end{cases} \tag{B.172}$$

where

$$f_h^{(n)}(z) = \sqrt{k}\, N_h^{(n)}\, (zk)^2 \left[J_2(m_n z) - C_h^{(n)} Y_2(m_n z) \right] \tag{B.173}$$

is the profile in terms of the conformal coordinate z. For each mode, the dimensionless constant $N_h^{(n)}$ is fixed by the orthonormality conditions (B.168) and the constant $C_h^{(n)}$ is determined by the boundary conditions. Neumann boundary conditions (even boundary parity) give rise to the values

$$C_h^{(n)}\Big|_{y=0,\pi R} = \frac{J_1(x_n^{\mathrm{UV,IR}})}{Y_1(x_n^{\mathrm{UV,IR}})}\,, \tag{B.174}$$

while Dirichlet conditions (odd boundary parity) give

$$C_h^{(n)}\Big|_{y=0,\pi R} = \frac{J_2(x_n^{\mathrm{UV,IR}})}{Y_2(x_n^{\mathrm{UV,IR}})}\,, \tag{B.175}$$

The eigenmass m_n is determined by ensuring that the boundary conditions on both branes give rise to the same constant:

$$C_h^{(n)} = C_h^{(n)}\Big|_{y=0} = C_h^{(n)}\Big|_{y=\pi R}\,, \tag{B.176}$$

explicitly,

$$C_h^{(n)} = \begin{cases} \dfrac{J_1(x_n^{\rm UV})}{Y_1(x_n^{\rm UV})} = \dfrac{J_1(x_n^{\rm IR})}{Y_1(x_n^{\rm IR})} & \text{for } h_{\mu\nu}^{(+,+)}\,, \\ \dfrac{J_1(x_n^{\rm UV})}{Y_1(x_n^{\rm UV})} = \dfrac{J_2(x_n^{\rm IR})}{Y_2(x_n^{\rm IR})} & \text{for } h_{\mu\nu}^{(+,-)}\,, \\ \dfrac{J_2(x_n^{\rm UV})}{Y_2(x_n^{\rm UV})} = \dfrac{J_1(x_n^{\rm IR})}{Y_1(x_n^{\rm IR})} & \text{for } h_{\mu\nu}^{(-,+)}\,, \\ \dfrac{J_2(x_n^{\rm UV})}{Y_2(x_n^{\rm UV})} = \dfrac{J_2(x_n^{\rm IR})}{Y_2(x_n^{\rm IR})} & \text{for } h_{\mu\nu}^{(-,-)}\,. \end{cases} \tag{B.177}$$

We discuss the approximate Kaluza-Klein spectrum in Appendix C.

Zero-mode solutions

A solution to (B.169) with zero mass eigenvalue exists only for $h_{\mu\nu}^{(+,+)}$. Such solutions offer the only possibility of recovering the four-dimensional graviton fields from the five-dimensional bulk, and accordingly, realistic theories of gravitation on the orbifold require that the graviton field has even parity on both boundaries. The zero-mode solutions have constant profiles of the forms

$$f_h^{(0)}(y) = \sqrt{\frac{k}{1 - e^{-2\pi kR}}} \equiv \sqrt{k}\, N_h^{(0)}\,, \tag{B.178}$$

or

$$f_h^{(0)}(z) = \sqrt{\frac{k}{1 - (z_{\rm IR}k)^{-2}}} = \sqrt{k}\, N_h^{(0)}\,, \tag{B.179}$$

in terms of the conformal coordinate.

Localization

In this case, a conformal rescaling of the bulk profiles gives

$$\tilde{f}_h^{(n)}(y) = f_h^{(n)}(y)\, e^{-A(y)}\,, \tag{B.180}$$

such that the orthonormality relation (B.168) becomes

$$\int_{-\pi R}^{\pi R} dy\, \tilde{f}_h^{(m)}(y)\, \tilde{f}_h^{(n)}(y) = \delta_{mn}\,. \tag{B.181}$$

In particular, the rescaled profiles for the graviton zero mode is

$$\tilde{f}_h^{(0)}(y) = \sqrt{\frac{k}{1 - e^{-2\pi kR}}}\, e^{-A(y)} = \sqrt{k}\, N_h^{(0)} e^{-A(y)}\,, \tag{B.182}$$

or

$$\tilde{f}_h^{(0)}(z) = \sqrt{\frac{k}{1 - (z_{\rm IR}k)^{-2}}}\, (zk)^{-1} = \sqrt{k}\, N_h^{(0)}\, (zk)^{-1}\,. \tag{B.183}$$

Thus, we see that the zero mode is localized toward the UV brane.

C Approximate Kaluza-Klein Spectra

The basic formalism for bulk fields in a slice of AdS_5 with arbitrary boundary masses is discussed in Appendix B. In this appendix, we present analytical expressions for the approximate Kaluza-Klein mass spectra for bulk fields with such boundary masses.

C.1 Scalar Zero-Mode Mass

When a bulk scalar field has even parity on both branes (i.e., $\Phi^{(+,+)}$) and boundary masses of the form (B.4), where a and b are related according to (B.6), the mass of its lightest Kaluza-Klein state (the lifted zero mode) has an analytic approximation:[1]

$$m_0 \simeq \sqrt{\frac{C_1^{\mathrm{UV}}\xi_{\mathrm{UV}} + C_1^{\mathrm{IR}}\xi_{\mathrm{IR}} + C_2\xi_{\mathrm{UV}}\xi_{\mathrm{IR}}}{C_3 + C_4^{\mathrm{UV}}\xi_{\mathrm{UV}} - C_4^{\mathrm{IR}}\xi_{\mathrm{IR}} + C_5\xi_{\mathrm{UV}}\xi_{\mathrm{IR}}}}\, k_{\mathrm{IR}} \tag{C.1}$$

where

$$C_1^{\mathrm{UV,IR}} \equiv 4\alpha\,(1+\alpha)\,(1-\alpha)\,e^{(1\pm\alpha)\pi kR}\,, \tag{C.2a}$$

$$C_2 \equiv 4\,(1+\alpha)\,(1-\alpha)\sinh(\alpha\pi kR)\,e^{\pi kR}\,, \tag{C.2b}$$

$$C_3 \equiv 4\alpha\,(1+\alpha)\sinh\big[(1-\alpha)\,\pi kR\big]\,, \tag{C.2c}$$

$$C_4^{\mathrm{UV,IR}} \equiv 2\,(1+\alpha)\,(1-\alpha)\sinh(\pi kR)\,e^{\pm\alpha\pi kR} - 2\,(1+\alpha)\sinh\big[(1-\alpha)\,\pi kR\big]\,, \tag{C.2d}$$

$$C_5 \equiv (1+\alpha)\sinh\big[(1-\alpha)\,\pi kR\big] - (1-\alpha)\sinh\big[(1+\alpha)\,\pi kR\big]\,. \tag{C.2e}$$

To unpack this expression, we consider separately the limits in which a mass term is added on only one of the two branes.

[1] This can be derived by expanding the quantization condition (B.26) with Neumann boundary conditions on both branes up to second order for small m_n.

C.1.1 UV-brane boundary mass

When $\xi_{\text{IR}} = 0$, the scalar zero-mode mass (C.1) reduces to

$$m_0 \simeq \sqrt{\frac{C_1^{\text{UV}}\xi_{\text{UV}}}{C_3 + C_4^{\text{UV}}\xi_{\text{UV}}}}\, k e^{-\pi kR} \tag{C.3}$$

In the limit $\xi_{\text{UV}} \ll \xi^*_{\text{UV}}$, where

$$\xi^*_{\text{UV}} = \frac{C_3}{C_4^{\text{UV}}} \sim \begin{cases} -2\alpha & \alpha \ll 0\,, \\ 2\left(\frac{\alpha}{\alpha-1}\right) e^{-2\pi kR} & \alpha \gg 1\,, \end{cases} \tag{C.4}$$

this becomes

$$m_0 \simeq \sqrt{\xi_{\text{UV}}k^2}\sqrt{\frac{2\,(1-\alpha)}{e^{2(1-\alpha)\pi kR}-1}} \sim \begin{cases} \sqrt{2\,(1-\alpha)}\,\sqrt{\xi_{\text{UV}}k^2}\, e^{-(1-\alpha)\pi kR} & \alpha < 1\,, \\ \frac{1}{\sqrt{\pi kR}}\,\sqrt{\xi_{\text{UV}}k^2} & \alpha \sim 1\,, \\ \sqrt{2\,(\alpha-1)}\,\sqrt{\xi_{\text{UV}}k^2} & \alpha > 1\,, \end{cases} \tag{C.5}$$

which coincides precisely with the mass obtained in the *zero-mode approximation*,[2] while in the limit $\xi_{\text{UV}} \gg \xi^*_{\text{UV}}$ it approaches a constant:

$$m_0 \simeq \sqrt{\frac{4\alpha\,(\alpha-1)}{e^{-2\alpha\pi kR} - (1-\alpha) - \alpha e^{-2\pi kR}}}\, k_{\text{IR}}$$

[2] In the zero-mode approximation, the five-dimensional fields are expanded using the Kaluza-Klein basis for the massless ($\xi_{\text{UV}} = 0$) case. The Kaluza-Klein mass matrix is not diagonal in this basis when $\xi_{\text{UV}} \neq 0$ (the states are no longer orthogonal), but provided the additional boundary masses represent a small perturbation (compared to the scale of the heavier Kaluza-Klein masses) the diagonal entries are a good approximation of the true mass eigenvalues. For the zero mode, the effective four-dimensional mass in this approximation arises entirely from its overlap with the boundary mass:

$$S_5 \supset -\int d^5x\, \xi_{\text{UV}} k e^{-2A} (\tilde{f}_\Phi^{(0)})^2\, (\Phi^{(0)})^*\, \Phi^{(0)}\, 2\delta(y) \implies m_0^2 \simeq 2\,(N_\Phi^{(0)})^2\, \xi_{\text{UV}} k^2\,. \tag{C.6}$$

$$\sim \begin{cases} \sqrt{4\alpha\,(\alpha-1)}\,k e^{-(1-\alpha)\pi kR} & \alpha < 0\,, \\ \sqrt{\frac{2}{\pi kR}}\,k_{\rm IR} & \alpha \sim 0\,, \\ \sqrt{4\alpha}\,k_{\rm IR} & \alpha > 0\,. \end{cases} \tag{C.7}$$

This is same mass that obtains in the *twisted limit* when the scalar field has a Dirichlet boundary condition on the UV brane and a Neumann boundary condition on the IR brane ($\Phi^{(+,+)} \to \Phi^{(-,+)}$). The large boundary mass has the effect of repelling the wave function from the brane [it dominates in the Neumann boundary condition (B.10)], introducing a kink in the profile of the field in the extra dimension.

C.1.2 IR-brane boundary mass

When $\xi_{\rm UV} = 0$, the zero-mode mass (C.1) reduces to

$$m_0 \simeq \sqrt{\frac{C_1^{\rm IR}\xi_{\rm IR}}{C_3 - C_4^{\rm IR}\xi_{\rm IR}}}\,k_{\rm IR} \tag{C.8}$$

In the limit $\xi_{\rm IR} \ll \xi_{\rm IR}^*$, where

$$\xi_{\rm IR}^* = \frac{C_3}{C_4^{\rm IR}} \sim \begin{cases} 2 & \alpha \leq 1\,, \\ 2\alpha & \alpha > 1\,, \end{cases} \tag{C.9}$$

this becomes

$$\begin{aligned} m_0 &\simeq \sqrt{\xi_{\rm IR}k_{\rm IR}^2}\sqrt{\frac{2\,(1-\alpha)}{e^{2(1-\alpha)\pi kR}-1}}\,e^{(1-\alpha)\pi kR} \\ &\sim \begin{cases} \sqrt{2\,(1-\alpha)}\,\sqrt{\xi_{\rm IR}k_{\rm IR}^2} & \alpha < 1\,, \\ \frac{1}{\sqrt{\pi kR}}\,\sqrt{\xi_{\rm IR}k_{\rm IR}^2} & \alpha \sim 1\,, \\ \sqrt{2\,(\alpha-1)}\,\sqrt{\xi_{\rm UV}k_{\rm IR}^2}\,e^{(1-\alpha)\pi kR} & \alpha > 1\,, \end{cases} \end{aligned} \tag{C.10}$$

which also coincides precisely with the mass obtained in the zero-mode approximation,[3] while in the limit $\xi_{\rm IR} \gg \xi_{\rm IR}^*$ it takes the form

$$m_0 \simeq \sqrt{\frac{4\alpha\,(\alpha-1)}{e^{-2(1-\alpha)\pi kR} - \alpha - (1-\alpha)\,e^{-2\pi kR}}}\,k_{\rm IR}$$
$$\sim \begin{cases} \sqrt{4\,(1-\alpha)}\,k_{\rm IR} & \alpha < 1\,, \\ \sqrt{\frac{2}{\pi kR}}\,k_{\rm IR} & \alpha \sim 1\,, \\ \sqrt{4\alpha\,(\alpha-1)}\,k e^{-\alpha\pi kR} & \alpha > 1\,. \end{cases} \tag{C.13}$$

This again corresponds to the mass obtained in the twisted limit, when the scalar field has a Neumann boundary condition on the UV brane and a Dirichlet boundary condition on the IR brane ($\Phi^{(+,+)} \to \Phi^{(+,-)}$).

C.2 Fermion Zero-Mode Mass

When a chiral component of a bulk Dirac fermion field[4] has even parity on both branes (i.e., $\Psi_{L,R}^{(+,+)}$) and Majorana boundary masses of the form (B.45), the mass of its lightest Kaluza-Klein state (the lifted zero mode) has an analytic approximation:[5]

$$m_{0\,L,R} \simeq \frac{C_1 - C_2\xi_{\rm UV}\xi_{\rm IR}}{C_4^{\rm UV}\xi_{\rm UV} + C_4^{\rm IR}\xi_{\rm IR}} \mp \sqrt{\frac{\left(C_1 + C_2\xi_{\rm UV}\xi_{\rm IR}\right)^2 + C_3^{\rm UV}\xi_{\rm UV}^2 + C_3^{\rm IR}\xi_{\rm IR}^2}{\left(C_4^{\rm UV}\xi_{\rm UV} + C_4^{\rm IR}\xi_{\rm IR}\right)^2}} \tag{C.14}$$

where

$$C_1 = \alpha_{L,R}\sinh\left[\left(1 \mp \alpha_{L,R}\right)\pi kR\right]\,e^{(1\pm\alpha_{L,R})\pi kR}\,, \tag{C.15a}$$

[3] In this case:

$$S_5 \supset -\int d^5x\,\xi_{\rm IR} k e^{-2A} (\tilde{f}_\Phi^{(0)})^2\,(\Phi^{(0)})^*\,\Phi^{(0)}\,2\delta(y-\pi R)\,, \tag{C.11}$$

such that

$$m_0^2 \simeq 2\,(N_\Phi^{(0)})^2\,e^{2(\alpha-1)\pi kR}\xi_{\rm IR}k_{\rm IR}^2\,. \tag{C.12}$$

[4] These approximations can also be used for a bulk gravitino.

[5] This can be derived by expanding the quantization condition (B.90) with Neumann boundary conditions on each brane up to second order for small m_n.

$$C_2 = (1 \mp \alpha_{L,R}) \sinh(\alpha_{L,R}\pi kR)\, e^{(1\pm\alpha_{L,R})\pi kR}\,, \tag{C.15b}$$

$$C_3^{\rm UV} = 2\alpha_{L,R}\,(1 \mp \alpha_{L,R}) \left(C_1 + C_2 e^{\pi kR}\right) e^{\pm 2\alpha_{L,R}\pi kR}\,, \tag{C.15c}$$

$$C_3^{\rm IR} = 2\alpha_{L,R}\,(1 \mp \alpha_{L,R}) \left(C_1 - C_2 e^{-\pi kR}\right) e^{2\pi kR}\,, \tag{C.15d}$$

$$C_4^{\rm UV} = C_1 e^{-\pi kR} - C_2\,, \tag{C.15e}$$

$$C_4^{\rm IR} = C_2 e^{-\pi kR} - C_1\,, \tag{C.15f}$$

and the upper (lower) sign corresponds to the left-handed (right-handed) case. When the boundary masses are sufficiently small that they may be treated as perturbations, $\xi_{\rm UV,IR} \ll \xi^*_{\rm UV,IR}$, where

$$\xi^*_{\rm UV} = \sqrt{\frac{C_1^2}{C_3^{\rm UV}}} \sim \begin{cases} \dfrac{1}{2\,|\alpha_{L,R}|}\, e^{(1\mp\alpha_{L,R})\pi kR} & \pm\alpha_{L,R} \ll 0\,, \\ \dfrac{1}{2\,|\alpha_{L,R} \mp 1|}\, e^{-\pi kR} & \pm\alpha_{L,R} \gg 1\,, \end{cases} \tag{C.16}$$

and

$$\xi^*_{\rm IR} = \sqrt{\frac{C_1^2}{C_3^{\rm IR}}} \sim \begin{cases} \dfrac{1}{\sqrt{4\,(1 \mp \alpha_{L,R})}} & \pm\alpha_{L,R} \ll 1\,, \\ \dfrac{1}{2}\, e^{\pm(\alpha_{L,R}\mp 1)\pi kR} & \pm\alpha_{L,R} \gg 1\,, \end{cases} \tag{C.17}$$

a first-order expansion of the quantization condition is sufficient, giving the simpler form[6]

$$m_{0\,L,R} \simeq \left[\frac{\alpha_{L,R}\,(1 \mp \alpha_{L,R}) \left(\xi_{\rm UV} e^{\pm\alpha_{L,R}\pi kR} + \xi_{\rm IR} e^{(1\mp\alpha_{L,R})\pi kR}\right)}{\alpha_{L,R} \sinh\left[(1 \mp \alpha_{L,R})\,\pi kR\right] - (1 \mp \alpha_{L,R})\,\xi_{\rm UV}\xi_{\rm IR} \sinh(\alpha_{L,R}\pi kR)}\right] k_{\rm IR}\,. \tag{C.18}$$

To unpack these expressions, we consider separately the limits in which a mass term is added on only one of the two branes.

[6] We note that this limit does *not* correspond to the first-order term in an expansion of (C.14) for small $\xi_{\rm UV,IR}$.

C.2.1 UV-brane boundary mass

When $\xi_{\rm IR} = 0$, the fermion zero-mode mass (C.14) reduces to

$$m_{0\,L,R} \simeq \frac{C_1}{C_4^{\rm UV}\xi_{\rm UV}} \mp \sqrt{\left(\frac{C_1}{C_4^{\rm UV}\xi_{\rm UV}}\right)^2 + \frac{C_3^{\rm UV}}{(C_4^{\rm UV})^2}} \tag{C.19}$$

In the limit $\xi_{\rm UV} \gg \xi_{\rm UV}^*$ this approaches a constant:[7]

$$\begin{aligned} m_{0\,L,R} &\simeq \sqrt{\frac{4\alpha_{L,R}\,(\alpha_{L,R} \mp 1)}{e^{\mp 2\alpha_{L,R}\pi kR} - (1 \pm \alpha_{L,R}) \mp \alpha_{L,R}\, e^{-2\pi kR}}}\, k_{\rm IR} \\ &\sim \begin{cases} \sqrt{4\alpha_{L,R}\,(\alpha_{L,R} \mp 1)}\, k e^{-(1\mp\alpha_{L,R})\pi kR} & \pm\alpha_{L,R} < 0\,, \\ \sqrt{\frac{2}{\pi kR}}\, k_{\rm IR} & \pm\alpha_{L,R} \sim 0\,, \\ \sqrt{4\,|\alpha_{L,R}|}\, k_{\rm IR} & \pm\alpha_{L,R} > 0\,. \end{cases} \end{aligned} \tag{C.20}$$

This is same mass that obtains in the twisted when the even component of the fermion field has a Dirichlet boundary condition on the UV brane and a Neumann boundary condition on the IR brane ($\Psi_{L,R}^{(+,+)} \to \Psi_{L,R}^{(-,+)}$). The large boundary mass has the effect of repelling the wave function from the brane [it dominates in the Neumann boundary condition (B.77)], introducing a kink in the profile of the even component in the extra dimension.

In the limit $\xi_{\rm UV} \ll \xi_{\rm UV}^*$, we use the lower-order result (C.18), finding

$$\begin{aligned} m_0 &\simeq \xi_{\rm UV} k \left[\frac{2\,(1 \mp \alpha_{L,R})}{e^{2(1\mp\alpha_{L,R})\pi kR} - 1}\right] \\ &\sim \begin{cases} 2\,(1 \mp \alpha_{L,R})\, e^{-2(1\mp\alpha_{L,R})\pi kR}\xi_{\rm UV} k & \pm\alpha_{L,R} < 1\,, \\ \frac{1}{\pi kR}\,\xi_{\rm UV} k & \pm\alpha_{L,R} \sim 1\,, \\ 2\,|1 \mp \alpha_{L,R}|\,\xi_{\rm UV} k & \pm\alpha_{L,R} > 1\,, \end{cases} \end{aligned} \tag{C.21}$$

[7] Note that when $\alpha \gg 1$ (the field is UV-localized) this reduces to the same form as (C.7).

which coincides precisely with the mass obtained in the zero-mode approximation.[8]

C.2.2 IR-brane boundary mass

When $\xi_{\text{UV}} = 0$, the zero-mode mass (C.14) reduces to

$$m_{0\,L,R} \simeq \frac{C_1}{C_4^{\text{IR}}\xi_{\text{IR}}} \mp \sqrt{\left(\frac{C_1}{C_4^{\text{IR}}\xi_{\text{IR}}}\right)^2 + \frac{C_3^{\text{IR}}}{(C_4^{\text{IR}})^2}} \tag{C.23}$$

In the limit $\xi_{\text{IR}} \gg \xi_{\text{IR}}^*$ this approaches a constant:[9]

$$\begin{aligned} m_{0\,L,R} &\simeq \sqrt{\frac{4\alpha_{L,R}\,(\alpha_{L,R} \mp 1)}{e^{-2(1\mp\alpha_{L,R})\pi kR} \mp \alpha_{L,R} - (1 \mp \alpha_{L,R})\, e^{-2\pi kR}}}\, k_{\text{IR}} \\ &\sim \begin{cases} \sqrt{4\,(1 \mp \alpha_{L,R})}\, k_{\text{IR}} & \pm\alpha_{L,R} < 1\,, \\ \sqrt{\frac{2}{\pi kR}}\, k_{\text{IR}} & \pm\alpha_{L,R} \sim 1\,, \\ \sqrt{4\alpha_{L,R}\,(\alpha_{L,R} \mp 1)}\, k e^{\mp\alpha_{L,R}\pi kR} & \pm\alpha_{L,R} > 1\,. \end{cases} \end{aligned} \tag{C.24}$$

This again corresponds to the mass obtained in the twisted limit, when the even component of the fermion field has a Neumann boundary condition on the UV brane and a Dirichlet boundary condition on the IR brane ($\Psi_{L,R}^{(+,+)} \to \Psi_{L,R}^{(+,-)}$).

In the limit $\xi_{\text{IR}} \ll \xi_{\text{IR}}^*$ we use the lower-order result (C.18), finding

$$\begin{aligned} m_{0\,L,R} &\simeq (\xi_{\text{UV}} k_{\text{IR}}) \left[\frac{2\,(1 \mp \alpha_{L,R})}{e^{2(1\mp\alpha_{L,R})\pi kR} - 1}\right] e^{2(1\mp\alpha_{L,R})\pi kR} \\ &\sim \begin{cases} 2\,(1 \mp \alpha_{L,R})\,(\xi_{\text{UV}} k_{\text{IR}}) & \pm\alpha_{L,R} < 1\,, \\ \frac{1}{\pi kR}\,(\xi_{\text{UV}} k_{\text{IR}}) & \pm\alpha_{L,R} \sim 1\,, \\ 2\,|1 \mp \alpha_{L,R}|\, e^{2(1\mp\alpha_{L,R})\pi kR}\,(\xi_{\text{UV}} k_{\text{IR}}) & \pm\alpha_{L,R} > 1\,, \end{cases} \end{aligned} \tag{C.25}$$

[8] Here, this looks like:

$$S_5 \supset -\int d^5x\, \xi_{\text{UV}} e^{-A} (\tilde{f}^{(0)}_{\Psi_{L,R}})^2 \left(\frac{1}{2}\overline{\Psi}^{(0)}_{L,R}\Psi^{c(0)}_{L,R} + \text{H.c.}\right) 2\delta(y) \implies m_0 \simeq 2\,(N^{(0)}_{\Psi_{L,R}})^2\, \xi_{\text{UV}} k\,. \tag{C.22}$$

[9] Note that this is the same as (C.13).

which also coincides precisely with the mass obtained in the zero-mode approximation.[10]

C.3 Heavy Kaluza-Klein Masses

For the heavy eigenmasses, we can employ a variety of asymptotic expansions.

C.3.1 Cross-product expansion

Neglecting any supersymmetry-breaking boundary masses,[11] the quantization conditions for bulk fields take the forms of cross products of Bessel functions:

$$J_{\alpha-1}(x_n^{\mathrm{UV}})\,Y_{\alpha-1}(x_n^{\mathrm{IR}}) = J_{\alpha-1}(x_n^{\mathrm{IR}})\,Y_{\alpha-1}(x_n^{\mathrm{UV}}) \quad \text{for } (+,+) \text{ parity}\,, \tag{C.28a}$$

$$J_{\alpha-1}(x_n^{\mathrm{UV}})\,Y_{\alpha}(x_n^{\mathrm{IR}}) = J_{\alpha}(x_n^{\mathrm{IR}})\,Y_{\alpha-1}(x_n^{\mathrm{UV}}) \quad \text{for } (+,-) \text{ parity}\,, \tag{C.28b}$$

$$J_{\alpha}(x_n^{\mathrm{UV}})\,Y_{\alpha-1}(x_n^{\mathrm{IR}}) = J_{\alpha-1}(x_n^{\mathrm{IR}})\,Y_{\alpha}(x_n^{\mathrm{UV}}) \quad \text{for } (-,+) \text{ parity}\,, \tag{C.28c}$$

$$J_{\alpha}(x_n^{\mathrm{UV}})\,Y_{\alpha}(x_n^{\mathrm{IR}}) = J_{\alpha}(x_n^{\mathrm{IR}})\,Y_{\alpha}(x_n^{\mathrm{UV}}) \quad \text{for } (-,-) \text{ parity}\,. \tag{C.28d}$$

These admit asymptotic expansions for large arguments.[12] As $n \to \infty$,

$$m_n \simeq \left(\pi s + \frac{p}{8\pi s} + \frac{4\,(q-3p^2)}{3\,(8\pi s)^3} + \frac{32\,(3r-10pq+60p^3)}{15\,(8\pi s)^5} + \cdots\right) k_{\mathrm{IR}} \tag{C.30}$$

[10] In this case:

$$S_5 \supset -\int d^5x\,\xi_{\mathrm{IR}} e^{-A} (\tilde{f}^{(0)}_{\Psi_{L,R}})^2 \left(\frac{1}{2}\overline{\Psi}^{(0)}_{L,R}\Psi^{c(0)}_{L,R} + \mathrm{H.c.}\right) 2\delta(y-\pi R)\,, \tag{C.26}$$

such that

$$m_0 \simeq 2\,(N^{(0)}_{\Psi_{L,R}})^2\, e^{2\left(1\mp\alpha_{L,R}\right)\pi k R} \xi_{\mathrm{IR}} k_{\mathrm{IR}}\,. \tag{C.27}$$

[11] The following results generally hold even when such terms are included.

[12] For fields with twisted boundary conditions, we expand the cross products

$$J'_{\alpha}(x_n^{\mathrm{UV}})\,Y_{\alpha}(x_n^{\mathrm{IR}}) = J_{\alpha}(x_n^{\mathrm{IR}})\,Y'_{\alpha}(x_n^{\mathrm{UV}}) \quad \text{for } (+,-) \text{ parity}\,, \tag{C.29a}$$

$$J_{\alpha}(x_n^{\mathrm{UV}})\,Y'_{\alpha}(x_n^{\mathrm{IR}}) = J'_{\alpha}(x_n^{\mathrm{IR}})\,Y_{\alpha}(x_n^{\mathrm{UV}}) \quad \text{for } (-,+) \text{ parity}\,. \tag{C.29b}$$

where the expansion parameter is

$$s \equiv \begin{cases} n & \text{for } (+,+) \text{ and } (-,-) \text{ parity}\,, \\ n - \frac{1}{2} & \text{for } (+,-) \text{ parity}\,, \\ n + \frac{1}{2} & \text{for } (-,+) \text{ parity}\,, \end{cases} \tag{C.31}$$

and

$$p \equiv \begin{cases} (\mu - 1) & \text{for } (+,+) \text{ and } (-,-) \text{ parity}\,, \\ (\mu + 3)\, e^{\pi k R} - (\mu - 1) & \text{for } (+,-) \text{ parity}\,, \\ (\mu - 1)\, e^{\pi k R} - (\mu + 3) & \text{for } (-,+) \text{ parity}\,, \end{cases} \tag{C.32a}$$

$$q \equiv \begin{cases} (\mu - 1)\,(\mu - 25)\, e^{3\pi k R} & \text{for } (+,+) \text{ and } (-,-) \text{ parity}\,, \\ (\mu^2 + 46\mu - 63)\, e^{3\pi k R} \\ \qquad - (\mu^2 + 46\mu - 63) & \text{for } (+,-) \text{ parity}\,, \\ (\mu^2 + 46\mu - 63)\, e^{3\pi k R} \\ \qquad - (\mu^2 + 46\mu - 63) & \text{for } (-,+) \text{ parity}\,, \end{cases} \tag{C.32b}$$

$$r \equiv \begin{cases} (\mu - 1)\,(\mu^2 - 114\mu + 1073)\, e^{5\pi k R} & \text{for } (+,+) \text{ and } (-,-) \text{ parity}\,, \\ (\mu^3 + 185\mu^2 + 2053\mu + 1899)\, e^{5\pi k R} \\ \qquad - (\mu - 1)\,(16\mu^2 - 114\mu + 1073) & \text{for } (+,-) \text{ parity}\,, \\ (\mu - 1)\,(16\mu^2 - 114\mu + 1073)\, e^{5\pi k R} \\ \qquad - (\mu^3 + 185\mu^2 + 2053\mu + 1899) & \text{for } (-,+) \text{ parity}\,, \end{cases} \tag{C.32c}$$

with

$$\mu = \begin{cases} 4\,(\alpha - 1)^2 & \text{for } (+,+) \text{ parity}\,, \\ 4\alpha^2 & \text{otherwise}\,. \end{cases} \tag{C.33}$$

As $n \to \infty$, we see that the masses are approximately

$$m_n \simeq \begin{cases} n\pi k_{\text{IR}} & \text{for } (+,+) \text{ and } (-,-) \text{ parity}\,, \\ \left(n - \frac{1}{2}\right)\pi k_{\text{IR}} & \text{for } (+,-) \text{ parity}\,, \\ \left(n + \frac{1}{2}\right)\pi k_{\text{IR}} & \text{for } (-,+) \text{ parity}\,; \end{cases} \tag{C.34}$$

that is, integer multiples of the *Kaluza-Klein mass scale*

$$m_{\text{KK}} \equiv \pi k_{\text{IR}}\,. \tag{C.35}$$

In general, these expansions are only valid for $n \geq 1$. When the lowest KK mass is light ($m_1 \lesssim m_{\text{KK}}$), as can occur for twisted boundary conditions, it may be necessary to adjust the index of the expansion to account for the light mass that is not captured in the approximation.

C.3.2 Large Bessel-zero expansion

The cross-product asymptotic expansion series (C.30) converges for $n \to \infty$, but that convergence can be slow (particularly for $\pi kR \gg 1$). For smaller n, the quantization conditions (C.28) are satisfied approximately at the zeros of Bessel functions of the first kind evaluated on the IR brane:

$$m_n \simeq \left(\pi s - \frac{\mu - 1}{8\pi s} - \frac{4\,(\mu-1)\,(7\mu - 31)}{3\,(8\pi s)^3} - \frac{32\,(\mu-1)\,(83\mu^2 - 982\mu + 3779)}{15\,(8\pi s)^5} - \cdots\right) k_{\text{IR}}\,, \tag{C.36}$$

where,

$$\mu = \begin{cases} 4\,(\alpha - 1)^2 & \text{for } (+,+) \text{ and } (-,+) \text{ parity}\,, \\ 4\alpha^2 & \text{for } (+,-) \text{ and } (-,-) \text{ parity}\,. \end{cases} \tag{C.37}$$

and the expansion parameter is

$$s = n + \frac{\sqrt{\mu}}{8} - \frac{1}{4}\,. \tag{C.38}$$

The convergence of this approximation is asymptotic. The point of closest convergence occurs at larger n for larger πkR. At first order,

$$m_n \simeq \begin{cases} \left(n + \frac{|\alpha-1|}{2} - \frac{1}{4}\right)\pi k_{\mathrm{IR}} & \text{for } (+,+) \text{ and } (-,+) \text{ parity}\,, \\ \left(n + \frac{|\alpha|}{2} - \frac{1}{4}\right)\pi k_{\mathrm{IR}} & \text{for } (+,-) \text{ and } (-,-) \text{ parity}\,, \end{cases} \tag{C.39}$$

and hence the masses are again approximately integer multiples of the Kaluza-Klein mass scale m_{KK}.

D Supersymmetry in a Slice of AdS_5

In this appendix we describe the supergravity multiplet of five-dimensional supersymmetry in a slice of AdS_5 and organize bulk gauge and matter fields into vector supermultiplets and hypermultiplets and consider their behavior and Kaluza-Klein mass spectra. A similar analysis is presented in Ref. [94]. The supermultiplet mass-spectrum for uncompactified AdS_5 is derived in Ref. [285].

D.1 Supergravity Multiplet

The on-shell supergravity multiplet consists of the vielbein $e^a{}_M$, the graviphoton B_M, and an $n = 1$ symplectic Majorana gravitino spinor Ψ^i_M. The gravitational action is given by[1]

$$S = -\int d^5x\,\sqrt{-g}\left(\frac{1}{2}M_5^3\mathcal{R}_5 + \Lambda_5 - \frac{1}{2}\Lambda_5 A''\right)\,, \tag{D.1}$$

while the gravitino action takes the form (B.134). In our analysis, we are primarily interested in the gravitino. Arising from the possible parity assignments, there are three classes of spectra. We summarize the results in Table D.1.

1. Left-handed zero modes

When the parity assignments of the fields are chosen so that the left-handed fields have positive parity on both boundaries and the right-handed field negative parity, i.e.,

$$\Psi_{\mu,L} \to \Psi^{(+,+)}_{\mu,L}\,, \quad \Psi_{5,R} \to \Psi^{(+,+)}_{5,R}\,, \quad \Psi_{\mu,R} \to \Psi^{(-,-)}_{\mu,R}\,, \quad \Psi_{5,L} \to \Psi^{(-,-)}_{5,L}\,, \tag{D.2}$$

the even fields $\Psi_{\mu,L}$ and $\Psi_{5,R}$ have zero-mode solutions, but otherwise the Kaluza-Klein

[1] Note that in the AdS_5 background we set $B_M = 0$.

masses for all modes are identical and determined by the condition

$$\frac{J_1(x_n^{\rm UV})}{Y_1(x_n^{\rm UV})} = \frac{J_1(x_n^{\rm IR})}{Y_1(x_n^{\rm IR})}\,. \tag{D.3}$$

The higher Kaluza-Klein modes for all states therefore have identical masses, given approximately by

$$m_n \simeq \left(n + \frac{1}{4}\right)\pi k_{\rm IR}\,. \tag{D.4}$$

The massless sector forms a four-dimensional $\mathcal{N} = 1$ supersymmetric gravity supermultiplet. In this case $\Psi^{(0)}_{5,R}$ is identified as the radino, the supersymmetric partner of the radion of the 5D geometry.

2. Right-handed zero modes

When the parity assignments of the fields are chosen so that the right-handed fields have positive parity on both boundaries and the left-handed field negative parity, i.e.,

$$\Psi_{\mu,L} \to \Psi^{(-,-)}_{\mu,L}\,, \quad \Psi_{5,R} \to \Psi^{(-,-)}_{5,R}\,, \quad \Psi_{\mu,R} \to \Psi^{(+,+)}_{\mu,R}\,, \quad \Psi_{5,L} \to \Psi^{(+,+)}_{5,L}\,, \tag{D.5}$$

the even fields $\Phi_{\mu,R}$ and $\Psi_{5,L}$ have zero-mode solutions, but otherwise the Kaluza-Klein masses for all modes are identical and determined by the condition

$$\frac{J_2(x_n^{\rm UV})}{Y_2(x_n^{\rm UV})} = \frac{J_2(x_n^{\rm IR})}{Y_2(x_n^{\rm IR})}\,. \tag{D.6}$$

The higher Kaluza-Klein modes for all states therefore have identical masses, given approximately by

$$m_n \simeq \left(n + \frac{3}{4}\right)\pi k_{\rm IR}\,. \tag{D.7}$$

The massless sector forms a four-dimensional $\mathcal{N} = 1$ supersymmetric gravity supermultiplet.

3. Twisted boundary conditions

When the parity assignments of the fields are twisted, i.e.,

$$\Psi_{\mu,L} \to \Psi^{(+,-)}_{\mu,L}\,, \quad \Psi_{5,R} \to \Psi^{(+,-)}_{5,R}\,, \quad \Psi_{\mu,R} \to \Psi^{(-,+)}_{\mu,R}\,, \quad \Psi_{5,L} \to \Psi^{(-,+)}_{5,L}\,, \tag{D.8a}$$

or

$$\Psi_{\mu,L} \to \Psi_{\mu,L}^{(-,+)}\,, \quad \Psi_{5,R} \to \Psi_{5,R}^{(-,+)}\,, \quad \Psi_{\mu,R} \to \Psi_{\mu,R}^{(+,-)}\,, \quad \Psi_{5,L} \to \Psi_{5,L}^{(+,-)}\,, \tag{D.8b}$$

the boundary conditions completely break supersymmetry and no massless modes exist in the spectrum.[2] In the first case, the Kaluza-Klein masses are given approximately by

$$m_n \simeq \left(n + \frac{3}{4}\right) \pi k_{\text{IR}}\,. \tag{D.9}$$

and in the second case by

$$m_n \simeq \left(n + \frac{1}{4}\right) \pi k_{\text{IR}}\,. \tag{D.10}$$

Compared to the result for untwisted boundary conditions, the twisted Kaluza-Klein mass spectra are shifted by a value that asymptotically approaches $\frac{1}{2}\pi k_{\text{IR}}$.[3]

Table D.1: Boundary parity configurations for the gravitino of an on-shell gravity supermultiplet. The left (right) term in the tuples refers to the $\mathbb{Z}_2$ parity at the $y = 0$ ($y = \pm\pi R$) orbifold fixed point.

boundary parity					
$\Psi_{\mu,L}$	$\Psi_{\mu,R}$	$\Psi_{5,L}$	$\Psi_{5,R}$	zero modes	residual supersymmetry
$(+,+)$	$(-,-)$	$(+,+)$	$(-,-)$	left-handed	4D $\mathcal{N} = 1$
$(+,-)$	$(-,+)$	$(-,+)$	$(+,-)$	none	4D $\mathcal{N} = 0$
$(-,+)$	$(+,-)$	$(+,-)$	$(-,+)$	none	4D $\mathcal{N} = 0$
$(-,-)$	$(+,+)$	$(+,+)$	$(-,-)$	right-handed	4D $\mathcal{N} = 1$

[2] Note that these boundary conditions break supersymmetry but preserve a $\text{U}(1)_R$ symmetry. This mechanism is usually called *Scherk-Schwarz supersymmetry breaking* [286, 287].

[3] This can also be seen from the cross-product mass approximations (C.30) in the $n \to \infty$ limit.

D.2 Matter Hypermultiplet

The on-shell hypermultiplet consists of two complex scalars Φ_i $(i = 1, 2)$ and one Dirac fermion Ψ with action

$$S_5 = -\int d^5x\,\sqrt{-g}\left[(\partial^M\Phi_i^*)(\partial_M\Phi_i) + m_{\Phi_i}^2\Phi_i^*\Phi_i \right. \\ \left. + \frac{1}{2}\overline{\Psi}\Gamma^M D_M\Psi - \frac{1}{2}\left(D_M\overline{\Psi}\right)\Gamma^M\Psi + m_\Psi\overline{\Psi}\Psi\right]. \tag{D.11}$$

We recall that in order for the Dirac fermion action to be invariant under the orbifold $\mathbb{Z}_2$ symmetry, its chiral components must have opposite parity assignments, as listed in Table B.1. These parity assignments must be shared by the scalar superpartners, which suggests that a more natural way of identifying the scalar fields is by the chirality of the fermion component with the same parity: $\Phi_{1,2} \to \Phi_{L,R}$. Invariance under supersymmetric transformations (see Ref. [94]) requires that the five-dimensional masses of the scalars and fermions are related, taking the forms

$$m_{\Phi_{L,R}}^2 = \left(c^2 \pm c - \frac{15}{4}\right)k^2 + \left(\frac{3}{2} \pm c\right)A'', \tag{D.12a}$$

$$m_\Psi = cA', \tag{D.12b}$$

where c is an arbitrary dimensionless *hypermultiplet localization parameter*.[4] In the notation of Sec. B.1, we identify

$$a = c^2 \pm c - \frac{15}{4}, \tag{D.13a}$$

$$b = \frac{3}{2} \pm c, \tag{D.13b}$$

which satisfy the supersymmetric condition (B.6). As a result, the Bessel function index of the bulk Kaluza-Klein profiles is the same for each pair of fields with the same parity:

$$\alpha = \begin{cases} \alpha_L = c + \frac{1}{2} & \text{for } \Phi_L \text{ and } \Psi_L, \\ \alpha_R = c - \frac{1}{2} & \text{for } \Phi_R \text{ and } \Psi_R. \end{cases} \tag{D.14}$$

[4] We choose to use the bulk mass parameter of the hypermultiplet fermion fields.

This implies that the bulk profiles of the fields with the same parity have the same form, differing only in conformal scaling:

$$f^{(n)}_{\Phi_{L(R)}}(y) = e^{-(1/2)\,A(y)} f^{(n)}_{\Psi_{L(R)}}(y)\,. \tag{D.15}$$

There are three classes of spectra arising from the possible parity assignments. We summarize the results in Table D.2.

1. Left-handed zero modes

When the parity assignments of the fields are chosen so that the left-handed fields have positive parity on both boundaries and the right-handed field negative parity, i.e.,

$$\Psi_L \to \Psi_L^{(+,+)}\,, \quad \Phi_L \to \Phi_L^{(+,+)}\,, \quad \Psi_R \to \Psi_R^{(-,-)}\,, \quad \Phi_R \to \Phi_R^{(-,-)}\,, \tag{D.16}$$

the even fields Φ_L and Ψ_L have zero-mode solutions, but otherwise the Kaluza-Klein masses for all modes are identical and determined by the condition

$$\frac{J_{c-1/2}(x_n^{\rm UV})}{Y_{c-1/2}(x_n^{\rm UV})} = \frac{J_{c-1/2}(x_n^{\rm IR})}{Y_{c-1/2}(x_n^{\rm IR})}\,. \tag{D.17}$$

The higher Kaluza-Klein modes for all states therefore have identical masses, given approximately by

$$m_n \simeq \left(n + \frac{|c-1/2|}{2} - \frac{1}{4}\right)\pi k_{\rm IR}\,. \tag{D.18}$$

The massless sector of the hypermultiplet $(\Phi_L^{(0)}, \Psi_L^{(0)})$ forms a four-dimensional $\mathcal{N}=1$ supersymmetric chiral multiplet.

2. Right-handed zero modes

When the parity assignments of the fields are chosen so that the right-handed fields have positive parity on both boundaries and the left-handed field negative parity, i.e.,

$$\Psi_L \to \Psi_L^{(-,-)}\,, \quad \Phi_L \to \Phi_L^{(-,-)}\,, \quad \Psi_R \to \Psi_R^{(+,+)}\,, \quad \Phi_R \to \Phi_R^{(+,+)}\,, \tag{D.19}$$

the even fields Φ_R and Ψ_R have zero-mode solutions, but otherwise the Kaluza-Klein

masses for all modes are identical and determined by the condition

$$\frac{J_{c+1/2}(x_n^{\rm UV})}{Y_{c+1/2}(x_n^{\rm UV})} = \frac{J_{c+1/2}(x_n^{\rm IR})}{Y_{c+1/2}(x_n^{\rm IR})}\,. \tag{D.20}$$

The higher Kaluza-Klein modes for all states therefore have identical masses, given approximately by

$$m_n \simeq \left(n + \frac{|c+1/2|}{2} - \frac{1}{4}\right)\pi k_{\rm IR}\,. \tag{D.21}$$

The massless sector of the hypermultiplet $(\Phi_R^{(0)}, \Psi_R^{(0)})$ forms a four-dimensional $\mathcal{N}=1$ supersymmetric chiral multiplet.

3. Twisted boundary conditions

When the parity assignments of the fields are twisted, i.e.,

$$\Psi_L \to \Psi_L^{(+,-)}\,, \quad \Phi_L \to \Phi_L^{(+,-)}\,, \quad \Psi_R \to \Psi_R^{(-,+)}\,, \quad \Phi_R \to \Phi_R^{(-,+)}\,, \tag{D.22a}$$

or

$$\Psi_L \to \Psi_L^{(-,+)}\,, \quad \Phi_L \to \Phi_L^{(-,+)}\,, \quad \Psi_R \to \Psi_R^{(+,-)}\,, \quad \Phi_R \to \Phi_R^{(+,-)}\,, \tag{D.22b}$$

the boundary conditions completely break supersymmetry and no massless modes exist in the spectrum. In the first case, the Kaluza-Klein masses are given approximately by

$$m_n \simeq \left(n + \frac{|c+1/2|}{2} - \frac{1}{4}\right)\pi k_{\rm IR}\,. \tag{D.23}$$

and in the second case by

$$m_n \simeq \left(n + \frac{|c-1/2|}{2} - \frac{1}{4}\right)\pi k_{\rm IR}\,. \tag{D.24}$$

As with the graviton case, compared to the results for untwisted boundary conditions, the twisted Kaluza-Klein mass spectra are shifted by a value that asymptotically approaches $\frac{1}{2}\pi k_{\rm IR}$.

Table D.2: Boundary parity configurations for the field content of an on-shell hypermultiplet. The left (right) term in the tuples refers to the $\mathbb{Z}_2$ parity at the $y = 0$ ($y = \pm\pi R$) orbifold fixed point.

boundary parity					
Ψ_L	Ψ_R	Φ_L	Φ_R	zero modes	residual supersymmetry
$(+,+)$	$(-,-)$	$(+,+)$	$(-,-)$	left-handed	4D $\mathcal{N}=1$
$(+,-)$	$(-,+)$	$(+,-)$	$(-,+)$	none	4D $\mathcal{N}=0$
$(-,+)$	$(+,-)$	$(-,+)$	$(+,-)$	none	4D $\mathcal{N}=0$
$(-,-)$	$(+,+)$	$(-,-)$	$(+,+)$	right-handed	4D $\mathcal{N}=1$

D.3 Vector Supermultiplet

The on-shell vector supermultiplet consists of a gauge field A_M^a, an $n = 1$ symplectic Majorana spinor Λ_i^a, and a real scalar Σ^a in the adjoint representation with action

$$\begin{aligned} S_5 = -\frac{1}{g_5^2}\int d^5x\,\sqrt{-g}\,\Big[&\frac{1}{4}F^a_{MN}F^{MNa} \\ &+\frac{1}{2}\left(\partial^M\Sigma^a\right)\left(\partial_M\Sigma^a\right)+\frac{1}{2}m_\Sigma^2\left(\Sigma^a\right)^2 \\ &+\frac{1}{4}\overline{\Lambda}^a_i\Gamma^M D_M\Lambda^a_i-\frac{1}{4}\left(D_M\overline{\Lambda}^a_i\right)\Gamma^M\Lambda^a_i+\frac{1}{2}m_\Lambda\left(\sigma_3\right)_{ij}\overline{\Lambda}^a_i\Lambda^a_j\Big]\,. \end{aligned} \tag{D.25}$$

where a is a gauge group index. In order for four-dimensional gauge symmetry to be preserved, A_μ^a must have even parity on both branes and A_5^a odd parity, i.e.,

$$A_\mu^a \to A_\mu^{a(+,+)}\,, \tag{D.26a}$$

$$A_5^a \to A_5^{a(-,-)}\,. \tag{D.26b}$$

Then, if we take for the two independent fermion components

$$\Lambda^a_{1,L} \to \Lambda^{a(+,+)}_{1,L}\,, \tag{D.26c}$$

$$\Lambda^a_{2,L} \to \Lambda^{a(-,-)}_{2,L}\,, \tag{D.26d}$$

supersymmetry dictates that Σ^a is odd:

$$\Sigma^a \to \Sigma^{a(-,-)}\,. \tag{D.26e}$$

Given these assignments, it is convenient to identify the independent fermion components by their parity: $\Lambda^a_{1,2\,L} \to \Lambda^a_\pm$.

Invariance under supersymmetric transformations (see Ref. [94]) requires that the five-dimensional masses of the scalars and fermions are related, taking the forms

$$m^2_\Sigma = -4k^2 + 2A''\,, \tag{D.27a}$$

$$m_\Lambda = \frac{1}{2}A'\,. \tag{D.27b}$$

In the notation of Secs. B.1 and B.2, we identify[5]

$$a = -4\,, \qquad b = 2\,, \qquad c = \frac{1}{2}\,. \tag{D.28}$$

As a result, the Bessel function index of the bulk Kaluza-Klein profiles is the same for each set of fields with the same parity:

$$\alpha = \begin{cases} 1 & \text{for } A^a_\mu \text{ and } \Lambda^a_+\,, \\ 0 & \text{for } A^a_5,\ \Lambda^a_-, \text{ and } \Sigma^a\,. \end{cases} \tag{D.29}$$

This implies that the bulk profiles of the fields with the same parity have the same form, differing only in conformal scaling:

$$f^{(n)}_{A_\mu}(y) = e^{-(3/2)\,A(y)} f^{(n)}_{\Lambda_+}(y)\,, \tag{D.30a}$$

$$f^{(n)}_{A_5}(y) = e^{-(1/2)\,A(y)} f^{(n)}_{\Lambda_-}(y) = f^{(n)}_\Sigma(y)\,. \tag{D.30b}$$

In particular, we note that the even gaugino component is conformally flat like the gauge

[5]Note that a and b satisfy the supersymmetric condition (B.6).

field.

The even fields A_μ^a and Λ_+^a have zero-mode solutions, but otherwise the Kaluza-Klein masses for all modes are identical and determined by the condition

$$\frac{J_0(x_n^{\rm UV})}{Y_0(x_n^{\rm UV})} = \frac{J_0(x_n^{\rm IR})}{Y_0(x_n^{\rm IR})}\,. \tag{D.31}$$

The higher Kaluza-Klein modes for all states therefore have identical masses, given approximately by

$$m_n \simeq \left(n - \frac{1}{4}\right)\pi k_{\rm IR}\,. \tag{D.32}$$

The massless sector of the hypermultiplet $(A_\mu^{a(0)}, \Lambda_+^{a(0)})$ forms an $\mathcal{N} = 1$ supersymmetric vector multiplet.